ANALYSIS OF THE PRODUCTS FROM MIXED PLASTIC WASTE PYROLYSIS

By

Bradlee Kevin Naidoo

BSc.Eng. (Chemical Engineering)

University of KwaZulu-Natal, South Africa

Submitted in fulfilment of the academic requirements for the degree of Master of Science in Engineering in the College of Agriculture, Engineering and Science, University of KwaZulu-Natal

January 2024

Supervisor: Prof. K. Moodley

Co-Supervisor(s): Prof. P. Naidoo, Dr. M. H. Durski

DECLARATION ON-PLAGIARISM

I, Bradlee Kevin Naidoo, declare that:

1. The research reported in this thesis, except where otherwise indicated, is my original research.

2. This thesis has not been submitted for any degree or examination at any other university.

3. This thesis does not contain other persons' data, pictures, graphs, or other information, unless specifically acknowledged as being sourced from other persons.

4. This thesis does not contain other persons' writing, unless specifically acknowledged as being sourced from other researchers. Where other written sources have been quoted, then:

a. Their words have been re-written, but the general information attributed to them has been referenced.

b. Where their exact words have been used, then their writing has been placed in italics and inside quotation marks and referenced.

5. This thesis does not contain text, graphics or tables copied and pasted from the Internet, unless specifically acknowledged, and the source being detailed in the thesis and in the References sections.

_____

Mr BK Naidoo

As the candidate's supervisor, I, Prof. K. Moodley, agree to the submission of this thesis.

_____

Prof K Moodley

As the candidate's co-supervisor, I, Prof. P. Naidoo, agree to the submission of this thesis.

_____

Prof P Naidoo

As the candidate's co-supervisor, I, Dr M. Durski, agree to the submission of this thesis.

_____

Dr MH Durski

ACKNOWLEDGEMENTS

I acknowledge the following individuals who have contributed greatly to the progression of this study:

i. My supervisor, Professor K. Moodley (Associate Professor at the University of KwaZulu-Natal) for his continuous guidance in all aspects of this work.

ii. My co-supervisor, Dr M.H. Durski (Postdoctoral researcher at the University of KwaZulu-Natal), for providing assistance and guidance with the experiments performed in this work.

iii. Professor P. Naidoo (Professor at Stellenbosch University), for her guidance on the project.

iv. Mr Ayanda Khanyile and Mrs Nomthandazo Hadebe (laboratory staff at the University of KwaZulu-Natal) for their assistance with the use of laboratory equipment.

v. The Council of Scientific and Industrial Research (CSIR) for their funding towards my studies through the Waste RDI Grant (CSIR/BEI/WRIU/2020/034).

ABSTRACT

The utilization of plastic products has grown significantly in the last several decades and consequently expanded the production rate of plastic products, as well as increased pollution rates of waste plastic globally. Pyrolysis processes may be a feasible alternative for the management of non-recyclable plastic waste such as mixed plastic. During this process, plastics (individual or mixed types) are reacted at high temperatures (generally from 300˚C to 900˚C) to crack and breakdown. Products such as pyrolysis liquid, wax, gas, and char result from the process. South African legislation on pyrolysis emissions has caused several pyrolysis facilities in KwaZulu-Natal to halt operations due to non-compliance. Hence, pyrolysis technologies for the treatment of plastics needs to be analysed and redesigned/optimized to reduce emissions such that it complies with legislation.

This work falls under a broader research project with the goal of developing an optimized pyrolysis process with novel aspects to manage mixed waste plastic through catalytic pyrolysis. This dissertation focuses specifically on the analysis of components generated from catalyzed lab-scale plastic pyrolysis. Plastic pyrolysis experiments were conducted using a feedstock of compounded low-density polyethylene (LDPE), high-density polyethylene (HDPE), and polypropylene (PP) and mixtures of these plastics at 450˚C and vacuum of approximately 42 kPa. Zinc oxide powder was used as the catalyst, and its effect was investigated in comparison to the thermal (uncatalysed) pyrolysis process. The selection of the conditions and catalyst used are described in detail within this dissertation. Product yields of the pyrolysis liquid, wax, char, and gas were determined through weighing and mass balance. Gas chromatography-mass spectrometry (GC-MS) was used to perform chemical analyses on the liquid and wax to determine the types of components constituting these products. Additionally, the emissions were analysed to identify the volatile organic compounds (VOCs) present.

The results indicated that the zinc oxide catalyst effectively enhanced the pyrolysis experiments and increased the combined liquid and wax product yields, which are the desirable products. Pure LDPE and HDPE pyrolysis with catalyst to feed ratios of 5:100 produced 78.3 wt % and 78.2 wt % of combined liquid and wax yields respectively. This was relatively high compared to the other pure plastic experiments with and without catalyst. However, uncatalysed HDPE pyrolysis produced a combined liquid and wax yield of 85.4 % but required a longer reaction time. The use of zinc oxide catalyst (5:100 ratio) in LDPE pyrolysis experiments reduced

reaction times by approximately 14 hours compared to the uncatalyzed experiment. Reaction times of catalysed (5:100) HDPE and PP pyrolysis experiments were reduced by 1 hour 30 minutes (HDPE) and 15 minutes (LDPE) compared to their respective uncatalyzed experiments. Pure PP pyrolysis produced the highest gas yields (ranging from 17.7 wt % to 19.2 wt %).

Mixed plastic feed experiments with higher proportions of compounded LDPE produced the highest combined liquid and wax yields. The usage of catalyst caused a reduction of gas yields in many of the mixed plastic pyrolysis experiments. According to the GC-MS analyses, the use of 5:100 zinc oxide catalyst to feed ratio produced the lowest total VOC peak area percentages for many of the pure plastic feed types, however it seems the catalyst caused greater fractions of VOCs to form in the mixed plastic experiments. Many of the liquid and wax analysis results indicated a large proportion of components within the C_{12} to C_{27} range. This indicates that the liquid products potentially had similar properties to diesel fuel and correlates with the results of similar studies in the literature. Furthermore, the 5:100 zinc oxide catalyst to feed specification produced the highest combined liquid and wax yields in many of the experiments. A catalysed (5:100) experiment using a feedstock of 32.3 wt % LDPE, 34.52 wt % HDPE, and 33.18 wt % PP indicated a trade-off between high liquid + wax yields, reasonable VOC content in emissions, lower gas yields, and lower energy usage per gram of product formed relative to experiments with other feed compositions.

A preliminary life cycle gate to gate analysis was conducted for the laboratory scale process, and it was determined that the major power consuming units, heating mantle, condensing circulator and vacuum pump contribute approximately equally to the indirect CO_2 emissions for the process, assuming they are operating at capacity. Pure LDPE pyrolysis had the highest CO_2 emissions per gram of desirable product obtained (3.83 $\frac{kg\ CO_2}{g}$) while PP pyrolysis with a catalyst ratio of 10:100 had the lowest CO_2 emissions (0.31 $\frac{kg\ CO_2}{g}$). In the mixed plastic experiments, the CO_2 emissions increased as the amount of LDPE in the feed was increased.

The proportion of gas product streams that would be considered volatile organic compounds (VOCs) constituted between 32-83 % for each experiment. The total VOCs was lowest in mixed plastic pyrolysis experiments where approximately equal proportions of compounded LDPE, HDPE and PP was used as the feed, compared to the other sets. It was observed that the use of catalyst (5:100) generally increased the total VOCs and the carbon number of the most abundant VOCs in the gas stream in the mixed plastic experiments.

TABLE OF CONTENTS

LIST OF FIGURES

LIST OF TABLES

NOMENCLATURE

Symbol/Term	Definition	Unit
IP	Pure plastic pyrolysis experiments	Dimensionless
m	Mass	g
MP	Mixed plastic pyrolysis experiments	Dimensionless
P	Pressure	kPa
Peak Area %	Proportion of specific component in the pyrolysis product	%
Pyrolysis Product Yield	Mass percentage of pyrolysis product out of total feedstock mass	wt %
T	Temperature	°C
VOCs	Volatile organic compound	Dimensionless
wt %	Weight percentage	%

Subscript	Description
final	Upon completion of reaction
initial	Before reaction has commenced
product	Product of pyrolysis (liquid, wax, char, or gas)
uncatalysed	Reaction without zinc oxide powder catalyst

CHAPTER ONE: INTRODUCTION

1.1 Background

Municipalities, process industries and other large businesses are aiming to become more sustainable by maximizing outputs while simultaneously minimizing wastage and environmental impact (Phakedi et al., 2021). This aligns with the UN Climate Change Conference of the Parties (COP26) (United Nations, 2021) and UN Sustainable Development Goals (SDG) (United Nations, 2022) goals that target cleaner production, and reduction in emissions by 2030 with an aim to net zero by 2050. Such stringent measures have been put in place due to the surge in engineering activities over recent decades. With the world's population growth increase by almost 2 billion people within the past decade (United Nations, 2022), such drastic changes affect factors such as the demand for goods and services and consequently the management of the resulting waste generated in meeting these demands.

Due to its low cost and ease of production, plastic products have become a vital material for modern society. The vast use of plastic includes its use in food and beverage containers, fragile goods packaging for transportation, appliances, vehicle manufacturing, and even in the construction of buildings (Núñez-Cacho et al., 2020).

Table 1.1 shows the waste production figures from South Africa for common plastic types such as low-density polyethylene (LDPE), polystyrene (PS) polyethylene terephthalate (PET), and high-density polyethylene (HDPE). There is a continuous increase in the application and use of plastic-containing products and the wastage rates of plastic are therefore increasing.

Table 1.1: Common waste plastic types and their annual production rates in South Africa.

Plastic Type	Waste Produced (tonnes/year)[1]
Low-density polyethylene	120 000
Polystyrene	1100
Polyethylene terephthalate	250 000
High-density polyethylene	500 000

[1] (SAWIC, 2021)

Plastic waste deposition into landfills is one of the most basic waste-handling practices, but this does not align with a low environmental impact future, and hence is not a sustainable

solution. More sustainable plastic waste management initiatives aim to recycle plastics such as polystyrene, polyethylene terephthalate, high-density polyethylene, and polyvinyl chloride (PVC) to name a few (SAPRO, 2015).

Polystyrene (PS) is widely used in South Africa as packaging for fragile goods, food and beverage containers, and even in thermal insulation of buildings. The material has been recycled through several recycling initiatives in South Africa such as the Polystyrene Association of South Africa, Polyco, and New Earth Recycling (Averda, 2022). Literature indicates that more than 6500 tonnes of polystyrene were reprocessed in the year 2019 in South Africa (Averda, 2022). There are however issues that arise with the recycling process. Polystyrene is expensive to collect and transport to recycling centres due to its low density and bulky shape. This factor can delay the entire recycling process and may cause major throughput issues (AIPE, 2019). The solvent purification method involves the use of a suitable solvent to selectively dissolve polystyrene (Salisu & Maigari, 2021). This leaves behind contaminants in a solid phase. Thereafter, the solvent can be recovered from the solution. Mechanical recycling of polystyrene may involve firstly washing the material to remove contaminants. Thereafter, the polystyrene may be dried, granulated, or compressed (Salisu & Maigari, 2021).

Polyethylene terephthalate (PET) is used to manufacture products such as beverage bottles. Statistics show that the recycling rate of all PET bottles produced in South Africa increased from 55 % to more than 60 % from the years 2016 to 2018 (Plastics SA, 2019). Recycling rates of 70 % were projected for the year 2022 in South Africa. The reuse of PET products is also possible. PETCO is a South African organization which facilitates the collection, separation, and recycling processes of waste plastics such as PET (PETCO, 2018). PETCO has stated that consumers should ensure that PET bottles are washed properly and cleaned with detergents as this allows the bottles to be safely reused (PETCO, 2018). Commonly used PET recycling methods consist of mechanical processes. PET plastic may be shredded, washed, and melted to form new products. Additionally, chemical recycling of PET could be another option. PET plastic may be broken down into valuable raw materials such as monoethylene glycol and terephthalic acid (Muringayil Joseph et al., 2024).

Low-density polyethylene (LDPE) is another important plastic which is widely used in South Africa. The plastic finds application in products such as consumer carry bags, refuse bags, machine parts, cling-wrap, and pipes (Slimani et al., 2021). Being one of the most abundant plastics in South Africa, efficient waste management strategies are required for the handling of

used LDPE products. The LDPE recycling process is relatively simple and may allow a large throughput. Companies such as Rebox Recycling implement automated feeding and extrusion processes to efficiently recycle LDPE waste into pellets (Rebox Recycling, 2022). LDPE recycling processes generally beginning with sorting of the plastic. The waste LDPE may be reduced to a small particle size with the use of a grinder. Contaminants can be removed from the plastic using the appropriate cleaning solvents. The cleaned and granulated LDPE can thereafter be melted and moulded into new products (EDL, 2021).

High-density polyethylene (HDPE) is a commonly used plastic in South Africa and has application in products such as milk bottles and crates (Plastics SA, 2019). Sources indicate that over 70 % of all HDPE bottles which are produced in South Africa are recycled (Polyco, 2020). Polyco is one of the waste management initiatives which contributes to HDPE recycling. Similar recycling processes are seen with HDPE compared to LDPE. Waste HDPE plastic can be washed to remove dirt and impurities. The washed plastic can thereafter be shredded, melted, and moulded into useful products (Infinita Lab, 2024).

Polypropylene (PP) is another plastic that is used abundantly in South Africa. The low cost of the flexible material makes it ideal for packaging items such as beverage containers, packaging for food, and bottles. The material also has applications in the medical sector such as packaging for pharmaceuticals. In the mechanical plastic recycling process, the waste plastics undergo processes (such as grinding and re-granulating) which do not alter the chemical nature of the plastics (Circular Asia, 2022). Extruders can be used to melt and cut polypropylene plastic into granulated material. This material can be used in larger industrial operations to form new LDPE products (Plastics SA, 2019).

The plastic recycling sector in South Africa has been growing over the past decade. According to statistics, almost 350 000 tons of plastic were recycled in 2021. This was an increase of 10 % compared to the previous year. South Africa’s plastic recycling industry showed a growth of 4.7 % in 2022 as compared to the previous year (Plastics SA, 2022). This slight dip may be attributed to the effects of the COVID-19 pandemic on recycling initiatives from a health and safety perspective.

While there are plastic recycling companies such as PETCO, Rhino Recycling, Mpact Limited, Polyco, and New Earth Recycling that were responsible for the 46.3 % recycling rate (Averda, 2022) for all plastic products in South Africa in 2018, there remains a significant amount of plastic waste that is not attended to. Sources indicate that almost 110 000 tonnes of plastic are

still disposed (wilfully and unwilfully) into the ocean every year in South Africa (Ryan, 2020). Again, this is not a viable, sustainable waste management strategy.

Issues such as poorly managed/ill-equipped collection facilities reduce the effectiveness of the treatment and disposal initiatives in South African waste management. Lancet Planet Health reported that 55 % of waste is sent to landfills or improperly disposed in nature (Lancet Planet Health, 2022). Considering single-use plastic, that does not readily biodegrade, increased waste production rates contribute to an increase and persistence in plastic waste in landfill deposits.

The adoption of a single waste management technique such as recycling will not be comprehensive enough to treat all plastic waste types in the most sustainable manner. Different plastic waste materials require appropriate techniques such as thermal or chemical treatment, and recycling/repurposing, which necessitates extensive research to optimize their efficiencies and effectiveness. Therefore, the stages observed in waste management research has focused on waste types with high abundance (Osman et al., 2020) that have significantly destructive impacts on the environment. These factors would make unique management techniques operationally viable and impactful.

Constraints to recycling include collection, sorting, and cleaning of the waste plastic as these are labour intensive and expensive tasks. Presently, the proper disposal of plastic into designated plastic recycling bins pose a challenge in South Africa (Department of Environment, Forestry and Fisheries, 2020). Furthermore, many different types of plastics may be mixed together and end up in landfills. Since the plastic recycling processes are generally different for each plastic type, it is often necessary that mixed plastic be sorted into different categories (often manually) prior to recycling. Informal waste pickers play an important role as they manually sift through the waste, collecting and sorting the materials into different types of plastic waste products (SAWPA, 2022), however it is not always viable to do so. Additionally, items comprised of different plastic types generally cannot be recycled directly by conventional means.

In these cases, recycling is often not the viable management route of mixed plastic waste. Plastic pyrolysis processes may be a viable alternative to handle the abundant mass of mixed plastic waste that is improperly disposed of. The pyrolysis process involves applying high temperatures to a feedstock (with or without catalyst) in an oxygen free environment (de Freitas Costa et al., 2023). An oxygen free environment can be achieved in a few ways including applying vacuum to a closed system or maintaining an inert atmosphere in the closed system

using a component such as nitrogen gas (Gowrishankar et al., 2021). The work by (Osman et al., 2020), described that plastic waste with a high abundance (such as PET) can be managed with the use of techniques such as pyrolysis. In other research such as the work of (Tekade et al., 2020), common plastics (in high abundance) such as LDPE and HDPE were pyrolyzed. It was mentioned that pyrolysis processes could significantly decrease the amount of plastic waste which is usually improperly disposed of.

The pyrolysis process for mixed plastic waste has a few advantages over other methods of plastic waste management such as recycling and incineration. As mentioned, plastic recycling processes are designed for a specific plastic type and often requires collection and sorting which is performed by informal waste pickers (DOING Holdings, 2022). In a single product facility, one type of plastic would be processed for a batch of waste plastic. In comparison to the recycling process, the plastic pyrolysis could be implemented simultaneously for a feed stock of more than one type of plastic. Literature has indicated studies in which mixed waste plastic pyrolysis has been compared to processes using just one feed type. In Kumar et al. (2017), a laboratory-scale plastic pyrolysis process was carried out using a round bottom flask reactor. A feed of only polystyrene produced a valuable liquid product with a yield of 80 % (mass basis). In comparison, a feed of mixed plastics (polyethylene, polypropylene, and polystyrene) was used in a separate reaction which produced a liquid product with a yield of almost 96 %. Unlike a recycling process in which performance may be hindered by a mixed feed, plastic pyrolysis processes may be enhanced by using variations of mixed plastics. Implementation of a plastic pyrolysis process does not require rigorous cleaning methods and solvents as required in numerous recycling processes (Baena-González et al., 2020). This minimizes not only the cost of cleaning, but also the time for the handling of the plastic waste (DOING Holdings, 2022).

The emission of gases from the waste plastic pyrolysis process is much lower than from the waste plastic incineration processes however the emissions must be considered carefully. The plastic pyrolysis process may produce a variety of emissions such as CO_2, CO, ethane, and propane. Many volatile organic compounds (VOCs) and semi-VOCs such as benzene, toluene, xylene, other aromatics, and alkenes are also produced. Issues arise due to the many regulations that are placed on the type of emissions that can be produced and their respective quantities in a jurisdiction. Various energy industries have had challenges with adhering to the regulations of the South African government (Engineering News, 2019). Apart from the challenges with regulations, there is also the impact on health and the environment that these emissions impose.

Research has shown that high exposure to VOCs could cause many health issues such as a damaged central nervous system and various organ damage. Furthermore, many VOCs such as benzene are known to be carcinogenic (American Lung Association, 2022). Analysis of the emissions from the plastic pyrolysis process will allow one to determine the quantity of emissions produced, the composition of these emissions, and whether it would be manageable in a commercial pyrolysis operation.

The benefits derived from pyrolysis treatment of plastics is the fuel oil product and energy rich emission stream. Literature has shown that fuel oils with similar properties to motor oil, diesel fuel, and gasoline can be produced from plastic pyrolysis (Senthil Kumar et al., 2017). The pyrolysis oil has many applications such as providing a fuel source to boilers for steam turbines. Refining and upgrading the pyrolysis oil may provide a product suitable for use in a transportation fuel blend (Van De Beld et al., 2013).

The process does have a few drawbacks and extensive research on the technical feasibility is required before widespread implementation can be considered. This work aims to contribute to this assessment.

The heating requirements for the pyrolysis process is one of the major factors due to the high temperatures that are associated with thermal cracking reactions. Both the operational temperature and the duration of the process affects the heating requirements. Numerous authors (as reviewed later) have shown that catalysts such zeolites and zinc oxide could be used to reduce process temperature and energy requirements significantly in the pyrolysis of plastics such as PE, PP, PS, PET, and PVC. Catalyst usage and cost may therefore be a vital factor in assessing the feasibility of mixed plastic pyrolysis.

1.2 Motivation for research

One of the major drawbacks of the plastic pyrolysis process considered in this work are the VOC emissions from the process. The South African government places minimum emission standards as to the type of emissions which can be produced, and the maximum quantities that can be emitted from any processing industry. The plastic pyrolysis processes may produce volatile organic compounds such as benzene, toluene, and xylene (BTX) in significant quantities (Conesa et al., 2009), which is regulated under South African law. According to the Air Quality Act of 2004, thermal processes are not to emit more than 10 mg of VOCs per cubic metre of total gaseous emissions. For this reason, it is important to research into the possible quantity of emissions which are produced from these plastic pyrolysis processes. Such research

and developments can be performed using laboratory experiments and can thereafter be upscaled to determine the impact of emissions from a commercial plastic pyrolysis plant in future work. Determining the emissions of the process will provide information as to whether the pyrolysis plant could operate within the emissions regulations of the South African government.

1.3 Aim & objectives

The aim of this study is to perform pyrolysis experiments at laboratory scale using a catalysed process of mixed waste plastic feed with subsequent analysis of the product streams and emissions. This required plastic pyrolysis experiments are performed using mixtures of low-density polyethylene, high density polyethylene, and polypropylene using a laboratory-scale reactor. Based on the analyses of the products, a preliminary assessment of the pyrolysis process technology is conducted. The following objectives were considered:

1. Determine which combination of operational parameters produces the lowest quantity of VOCs and maximizes the production of the products of value.
2. Investigate the effect of zinc oxide catalyst with regards to the enhancement of product yields and the effect on product fractions (liquid and wax, gas), VOC emission compositions, and reactions times.
3. Provide insight to the current government regulations on VOC emissions in relation to plastic pyrolysis gas composition.
4. Determine the emissions composition of the lab-scale process by analysis for use in future work to develop a sustainable and environmentally compliant pyrolysis process at scale.
5. Perform a preliminary gate-to-gate analysis on the lab-scale pyrolysis process to identify key parameters that would be translatable to a potential life cycle analysis on the future to-scale process.

The results of this work address a few key questions which is critical to the implementation of pilot and commercial mixed plastic waste pyrolysis processes. Optimum operational parameters (temperature (in the range of 400-500 °C), pressure (sub-atmospheric to atmospheric), duration of process (to completion) which can be used for a catalysed pyrolysis process based on a synthetic mixed plastic feed are to be determined. Results such as the pyrolysis product fractions, more specifically the combined liquid and wax yields, will provide

information as to the specific set of operational parameters which could produce large quantities of desirable products. The effect of these operational parameters on the emissions and waste will be analysed.

Thesis overview

This thesis is presented in six chapters. A comprehensive literature review of plastic pyrolysis equipment, procedures, and catalyst usage was performed and compiled in Chapter 2. Chapter 3 presents the experimental equipment, and methodology used in the present work. The results from the current plastic pyrolysis experiments are presented and discussed in Chapter 4. The chapter presents pyrolysis product yields, emission analysis results, and the effect of the catalyst selected on the pyrolysis experiments. Conclusions made from the results of the study and recommendations for future work were described in Chapters 5 and 6. References for the relevant literature are presented in Chapter 7, followed by Appendices.

CHAPTER TWO: LITERATURE REVIEW

This chapter presents a review of plastic pyrolysis processes which can be found in relevant literature. It is important to take note of the operational parameters and usage of catalyst as this information provides a guideline for further research into the topic of plastic pyrolysis. This provides an understanding of the mechanisms occurring in the reactions and the reasons as to why certain operational parameters may significantly alter the yields of products. Information of products such as the amount and composition of emissions produced will indicate whether it is possible to implement plastic pyrolysis processes in South Africa that align with current governmental regulations.

2.1 Overview of the pyrolysis process for pure and mixed plastic waste

To implement a plastic pyrolysis process, the plastic feed is initially placed within a reactor vessel in batch or continuous mode. The system is isolated, and an inert atmosphere or vacuum is applied. The reactor is exposed to high temperatures (generally 300°C to 900°C) (Miandad et al., 2019). The high temperatures are required for the thermal decomposition of the plastic material. The oxygen free environment is required to prevent combustion reactions from occurring (Aladin et al., 2021). Common feed plastic types are polyolefins such as low-density polyethylene and high-density polyethylene. The term polyolefin refers to polymers that have a molecular formula of $(CH_2CHR)_n$, where 'R' represents the alkyl functional group (LibreTexts, 2022). The reactive decomposition of the polymers is known as a cracking reaction.

As mentioned, products such as fuel oil, gas, and char can be obtained from the plastic pyrolysis process. Pyrolysis studies such as that by (Miandad et al., 2019) have indicated that pyrolysis fuel oil may have similar chemical properties to fuels such as diesel. However, the properties of the fuel oil are dependent on the operational parameters used during the process. Pyrolysis gas is continuously released during the reaction and may be combustible. However, many volatile organic compounds may be present in the gas, which is a safety and stability concern. Literature have also reported the formation of a wax product which is usually comprised of molecules with long branched carbon chains (Gebre et al., 2021). The wax products can be converted to a liquid oil product by further fluid catalytic cracking. This is a process whereby heavy hydrocarbons (high-boiling point) are converted to lighter hydrocarbons (low-boiling

point) with the addition of heat and catalyst (Sulzer, 2023). In effect, this produces a large fraction of useable fuel oils. The pyrolysis char is formed inside the reactor and may be observed as a dry black residue. According to (Jamradloedluk and Lertsatitthanakorn, 2014), the pyrolysis char could possibly be briquetted and used as a fuel source for cooking.

2.2 The role of catalyst in pure and mixed plastic pyrolysis

The usage of catalyst is a critical aspect of plastic pyrolysis experiments. The catalyst may be able to decrease the pyrolysis process duration, reduce the temperatures required for a given yield of liquid oil or wax, and improve the quality and composition of pyrolysis products including the types and quantities of the gaseous emissions (López et al., 2011b). As part of process optimization, the type of catalyst and quantity must be varied to determine the resultant effect on the process outcomes. A major factor associated with the incorporation of catalyst in plastic pyrolysis is the catalyst effectiveness (generally quantified by its selectivity toward producing liquid oil over wax at a lower temperature), lifecycle and reuse, and catalyst cost.

The use of catalysts in plastic pyrolysis may assist the thermal degradation of plastic feedstock, thereby allowing effective decomposition at lower temperatures when compared to uncatalyzed pyrolysis (Papuga et al., 2022). Studies such as Fadillah et al., (2021), Sivagami et al., (2022), and Rehan et al., (2017) indicate that the use of zeolite catalysts could be used to reduce plastic pyrolysis reaction times and improve the quality of the pyrolysis products (hydrocarbon liquids of commercial value). However, there are several catalyst types apart from zeolites that offer similar benefits. In a recent work, Tekade et al., (2020) employed the more economical zinc oxide catalyst in LDPE and HDPE pyrolysis experiments. The use of this catalyst increased pyrolysis liquid yields significantly when compared to the uncatalysed processes. Comprehensive studies documenting the effects of catalyst on the pyrolysis process is limited in the literature. Recent work focuses on catalyst morphology and size which is beyond the scope of this work. A brief review of the performance of pyrolysis catalysts reported in key recent studies in the literature follows. For a more detailed review on the literature of catalytic pyrolysis of plastic, the reader is referred to the comprehensive work of Miandad et al., (2016).

2.2.1 Catalyst usage in LDPE pyrolysis experiments

Tekade et al., (2020) performed LDPE pyrolysis experiments under vacuum. A pressure of 50 kPa and a heating rate of 10°C per minute were used in these experiments. Zinc oxide catalyst

was used to enhance the oil product yields (increase of 12.0 to 20.8 wt % compared to the uncatalyzed reaction). Wax and char residue amounted to less than 10 % for the catalysed experiments. Reaction temperatures were not reported in the study. The results from literature are presented in Figure 2.1 below.

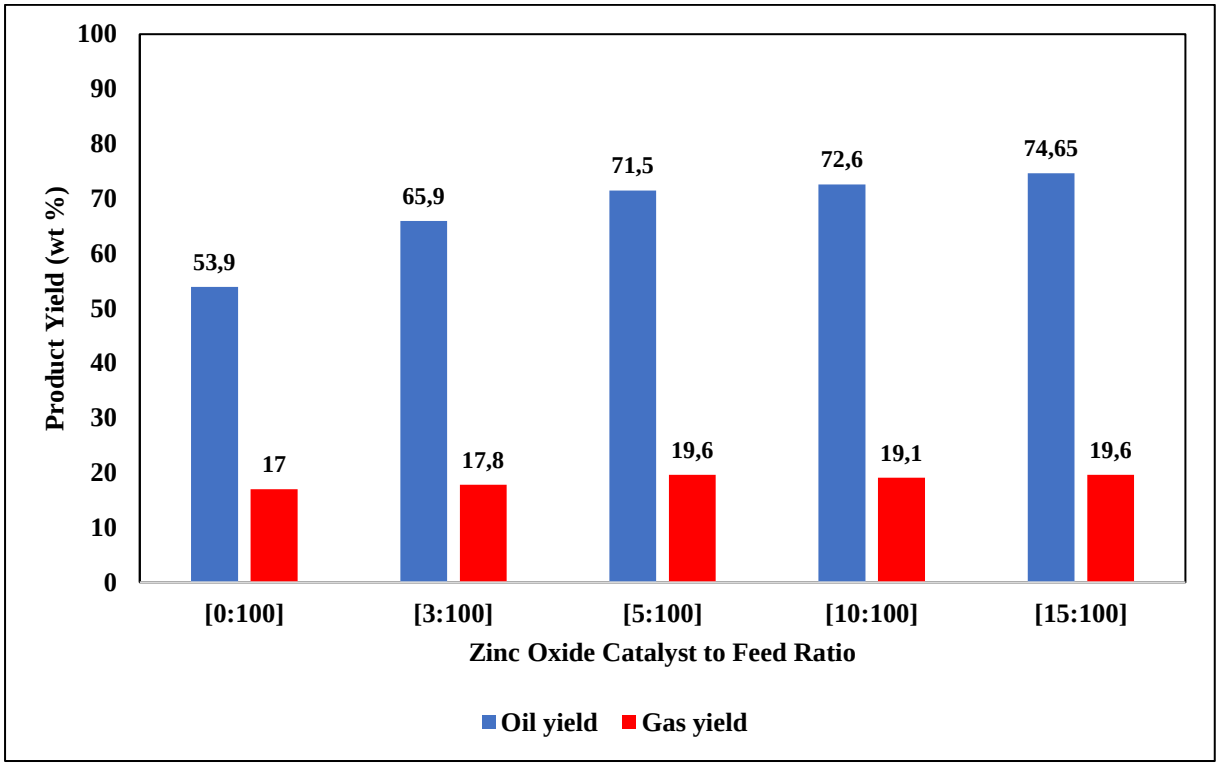

Figure 2.1: The effect of zinc oxide catalyst on LDPE pyrolysis under vacuum at 50 kPa (replotted) (Tekade et al., 2020).

In the work of Lee et al., (2021), LDPE plastic pyrolysis experiments were performed using H-ZSM-11 catalyst. Product yields were compared to that of the uncatalysed experiments. Temperatures ranged from 500°C to 900°C. A heating rate of 10°C per minute was utilized. The reactions took place in a nitrogen (inert) atmosphere. The uncatalysed and catalysed experiments results are presented in Figures 2.2 and 2.3 respectively.

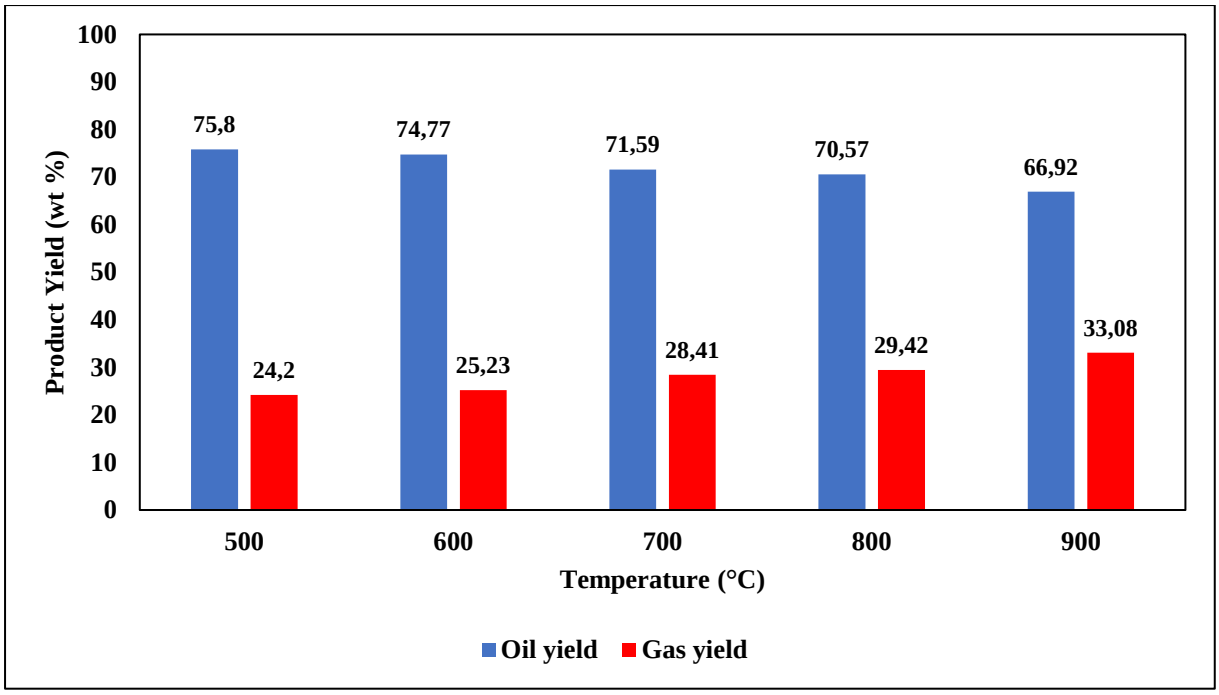

Figure 2.2: Uncatalysed LDPE pyrolysis in the presence of nitrogen (replotted) (Lee et al., 2021).

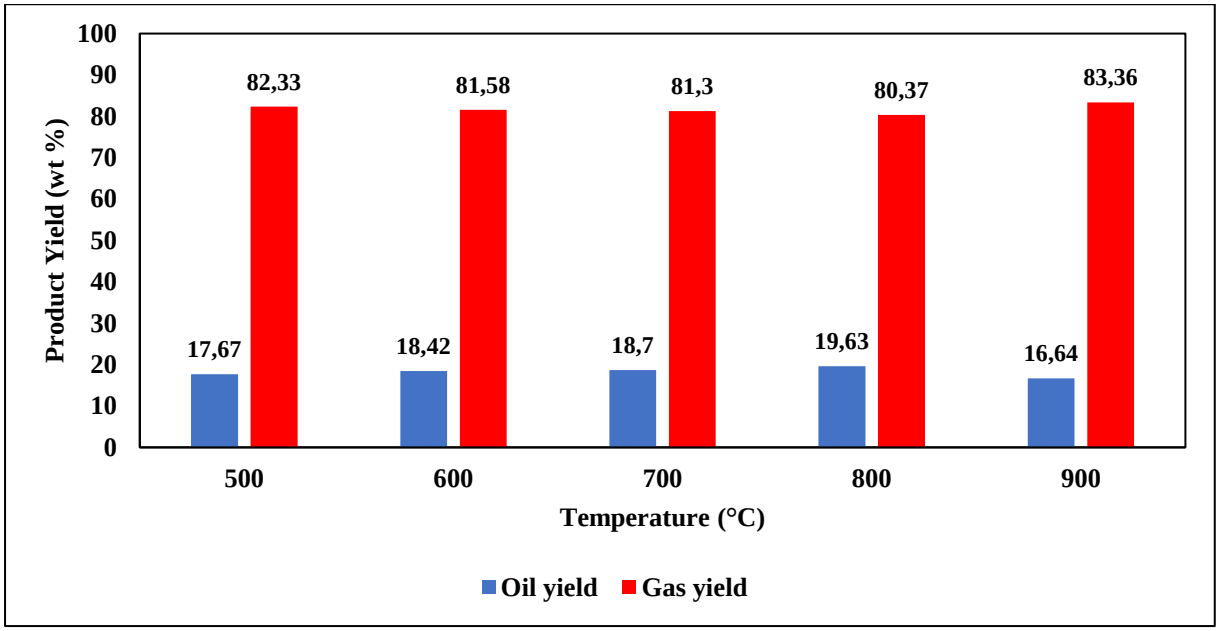

Figure 2.3: The effect of H-ZSM-11 catalyst on LDPE pyrolysis in the presence of nitrogen (replotted) (Lee et al., 2021).

Batool et al., (2016) implemented LDPE pyrolysis experiments using POM (polyoxometalate) and ZSM-5 catalysts in a nitrogenous environment. A heating rate of 5°C/min was applied. Table 2.1 indicates the product yield data extracted from the respective literature.

Table 2.1: The effect of ZSM-5 and POM catalyst on LDPE pyrolysis in the presence of nitrogen (Batool et al., 2016).

Feed	Reactor	Catalyst	Heating rate (°C/min)	Process duration (min)	Oil yield (wt %)	Gas yield (wt %)
LDPE	Stainless Steel Furnace	POM	5	90	73	19
		ZSM-5	5	90	49	44
		None	5	90	42	14

Further details for LDPE pyrolysis experiments using catalyst are summarized in Appendix C.

In summary, in the work of Tekade et al., (2020) the liquid yields increased with an increase in amount of zinc oxide catalyst used. Lee et al., (2021) showed that the H-ZSM-11 catalyst resulted in high pyrolysis gas yields and a minor proportion of liquid product. Uncatalysed experiments (Figure 2.2) resulted in major proportions of liquid products. This indicates that it could be possible to lower the catalysed process temperatures to produce more liquid than gas. Batool et al., (2016) indicated that the POM catalyst produced significantly larger liquid yields than the ZSM-5 catalysed experiment and the uncatalysed experiment. It is clear that the liquid yields using zinc oxide catalyst is competitive with those experiments using zeolite and POM catalyst.

2.2.2 Catalyst usage in HDPE pyrolysis experiments

Similar to the LDPE pyrolysis, Tekade et al., (2020) utilized identical zinc oxide catalyst to feed ratios for pyrolysis experiments using a feed plastic of HDPE. The product yield results are presented in Figure 2.4. It is evident that higher oil yields are achievable with the zinc oxide catalyst.

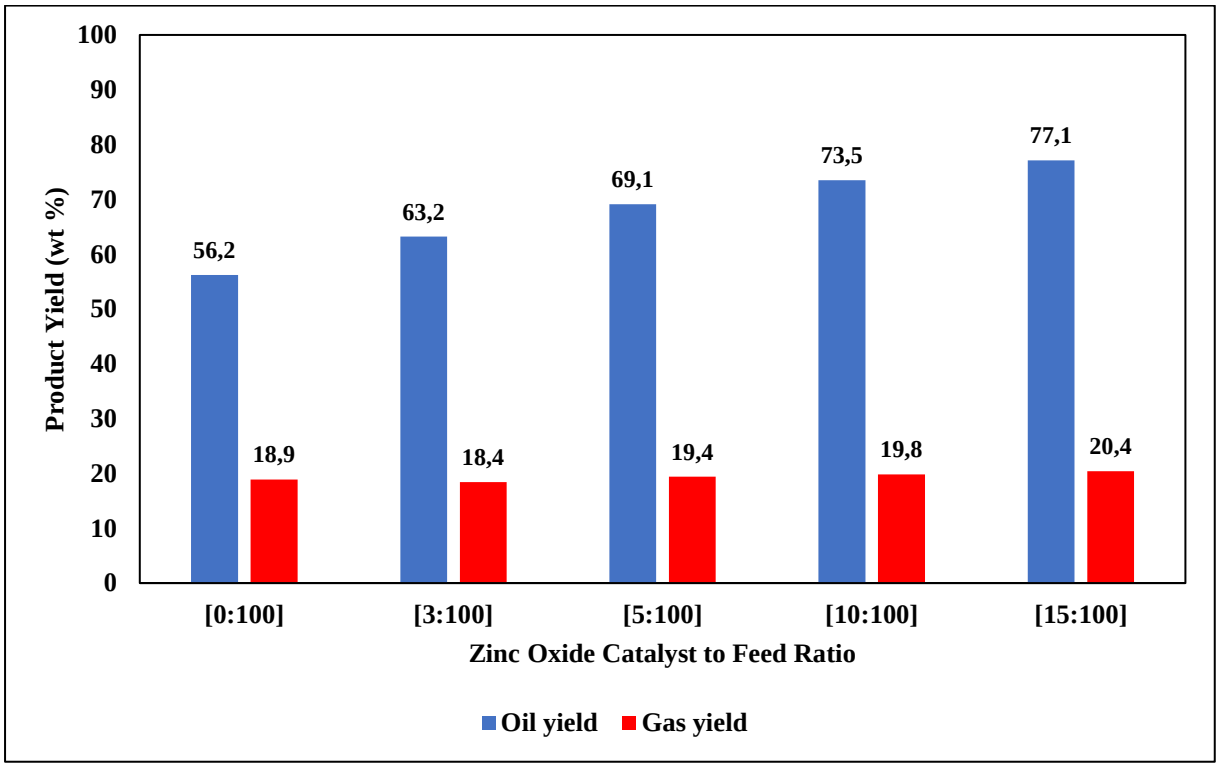

Figure 2.4: The effect of zinc oxide catalyst on HDPE pyrolysis under vacuum (replotted) (Tekade et al., 2020).

Raveh-Amit et al., (2022) investigated the catalysed pyrolysis of HDPE under temperatures of 450°C and 525°C in a quartz tubular reactor. Nitrogen gas was used to eliminate the oxygen from the environment. A heating rate of 20°C per minute was used. The product yields of catalysed processes were compared to that of the uncatalysed processes. The results are presented in Figures 2.5 and 2.6. These results showed that higher oil yields are achievable with the uncatalysed process using the higher temperatures. It may be likely that a lower reaction hold temperature (below 450°C) would have resulted in higher liquid yields in the catalysed experiments.

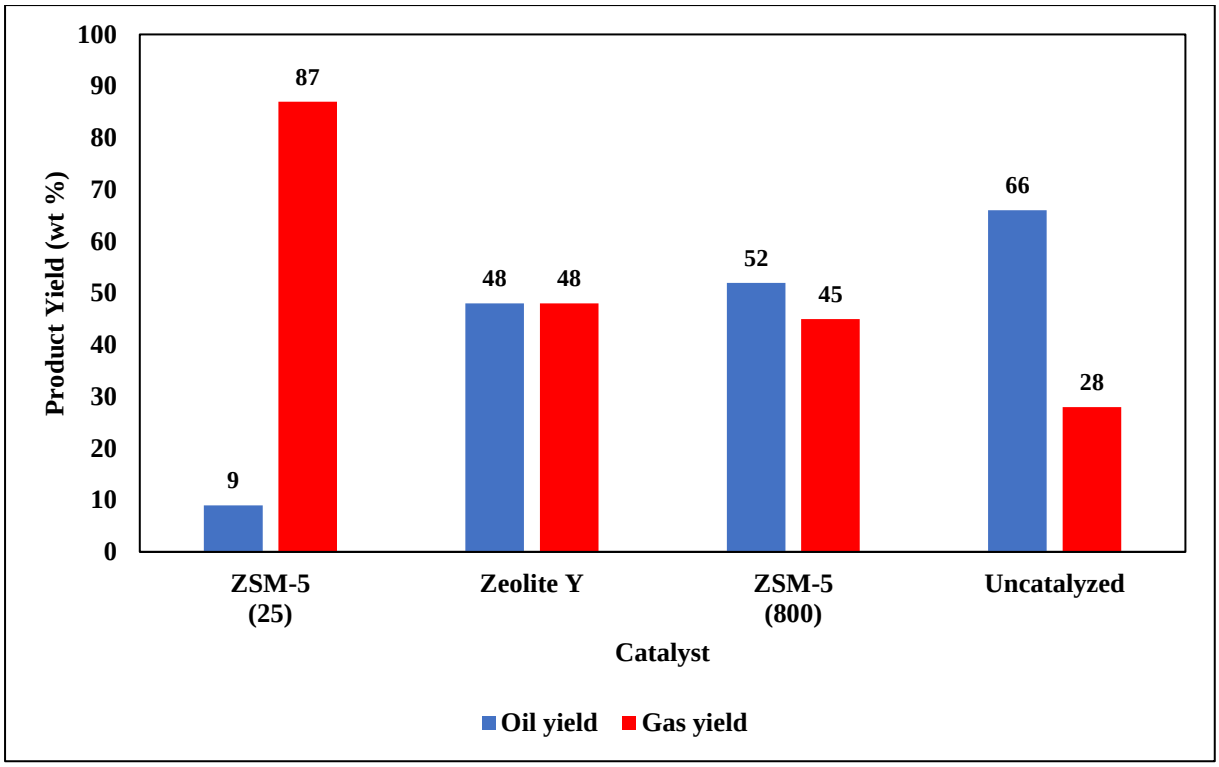

Figure 2.5: The effect of zeolite catalysts on HDPE pyrolysis at 450°C (replotted) (Raveh-Amit et al., 2022).

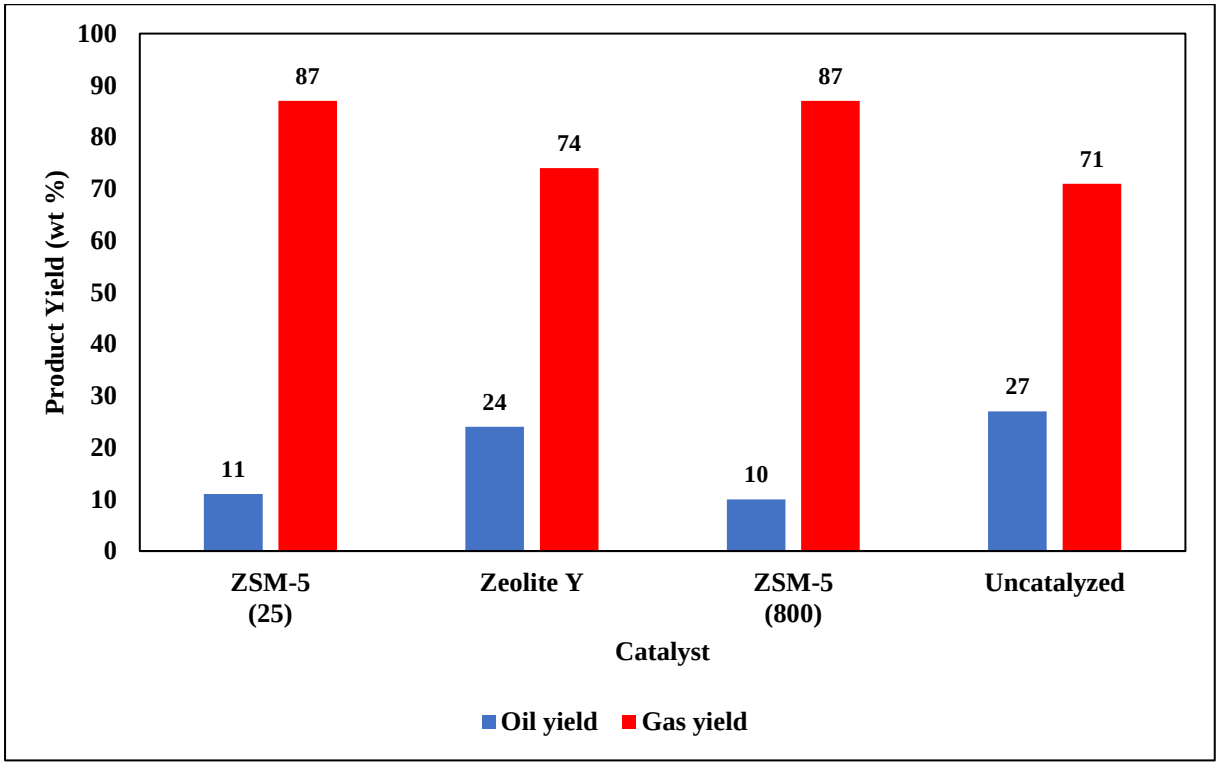

Figure 2.6: The effect of zeolite catalysts on HDPE pyrolysis at 525°C (replotted) (Raveh-Amit et al., 2022).

HDPE pyrolysis in article published by Tekade et al., (2020) showed an increase in liquid yield with an increase in the zinc oxide catalyst to feed ratio (Figure 2.4). Raveh-Amit et al., (2022) indicated that uncatalysed HDPE pyrolysis produced a higher liquid yield than experiments using zeolite catalysts. Again, the conversion to liquid products is higher in the zinc oxide experiments than when zeolite catalysts or no catalysts are used.

2.2.3 Catalyst usage in PP pyrolysis experiments

Gaurh and Pramanik, (2020) investigated the pyrolysis of polypropylene plastic at temperatures ranging 500°C to 800°C in a stainless-steel reactor. The effect of ZSM-5 catalyst was compared to the uncatalysed experiments. The process duration of each experiment was 35 minutes. The product yield results are presented in Figure 2.7.

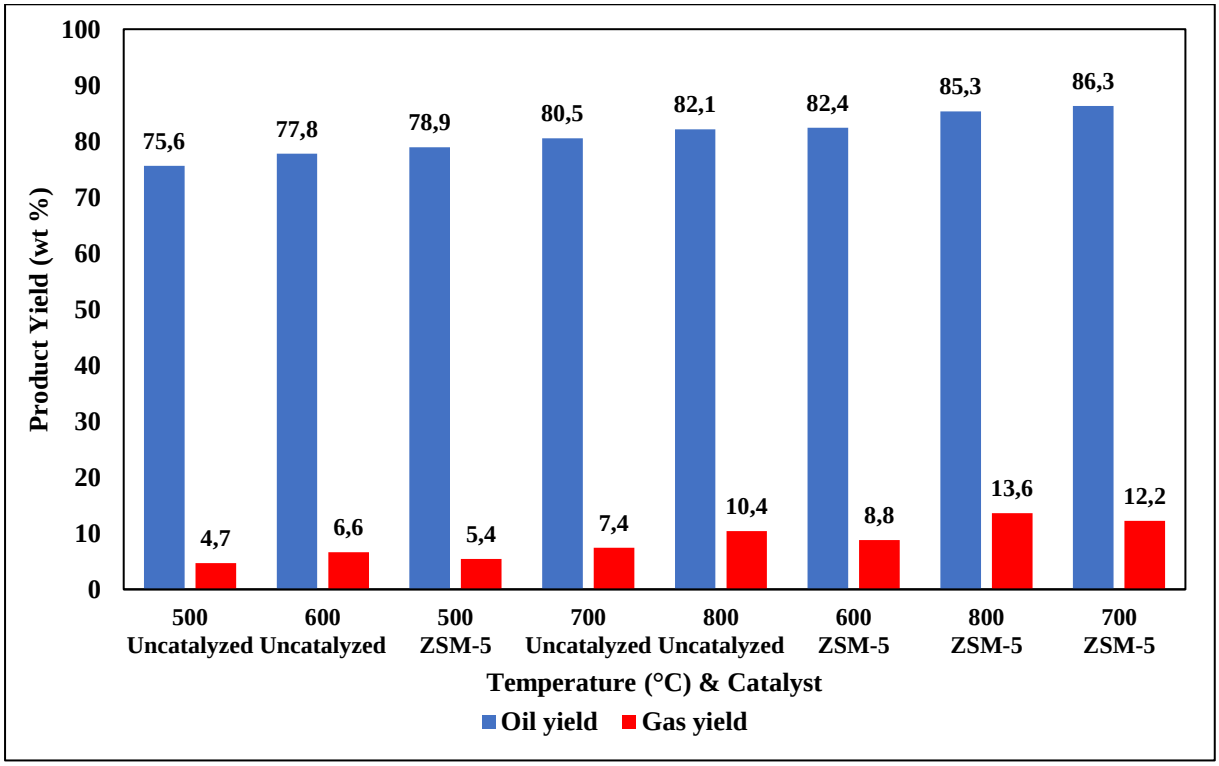

Figure 2.7: The effect of ZSM-5 catalyst on PP pyrolysis at 500°C to 800°C (replotted) (Gaurh and Pramanik, 2020).

The work of Gaurh and Pramanik, (2020) showed that the ZSM-5 catalyst resulted in higher liquid and gas yields in the pyrolysis of polypropylene compared to the uncatalysed

experiments. The effect of zinc oxide catalyst on the pyrolysis of PP has not been studied sufficiently in the literature to the authors knowledge.

2.2.4 Cost considerations for catalyst usage in the plastic pyrolysis process

In addition to the catalyst performance and longevity, the overall economic impact of the process is affected by the cost of operation and the cost of essential materials such as catalysts. Hence catalyst cost needs to also be considered when selecting a suitable catalyst for plastic pyrolysis. The cost of operation will vary depending on the amount of catalyst used in the pyrolysis process. Although higher catalyst ratios may have positive effects such as increased liquid oil yields and improved oil quality, the cost of the process may increase. Table 2.2 indicates the relative cost of different commercially available catalysts that are similar to those used in the plastic pyrolysis laboratory studies reported above.

Table 2.2: Cost of catalyst used in plastic pyrolysis processes.

Catalyst	Pricing	Reference
ZSM-5 Pellets [Si/Al2O3 Molar Ratio of 38]	336 USD per kg (R 6535)	ACS Material, (2022e)
ZSM-5 Powder [Si/Al203 Molar Ratio of 38]	402 USD per kg (R 7819)	ACS Material, (2022b)
ZSM-11	264 USD per 50 g (R 5135)	ACS Material, (2022d)
Zeolite Y [Si/Al203 Molar ratio of 5.1:1]	400 USD per 500 g (R 7780)	Alfa Aesar, (2022)
Zeolite Y [Si/Al203 Molar Ratio >5.3]	186 USD per 200g (R 3618)	ACS Material, (2022c)
Zinc Oxide	10.3 USD per kg (R 200)	Masiye Labs, (2022)

Conversion rate of R 19.45 to 1 USD taken on 20-05-2023.

The catalyst costs were obtained from their respective suppliers. According to Table 2.2, the ZSM-5 pellets (R 6535 per kg) are relatively lower in cost among the zeolite class. However, the different zeolites listed have significantly different effects on the plastic pyrolysis processes. The cost of zinc oxide catalyst was compared from different suppliers and found to be similar in price. Zinc Oxide catalyst was found to be R 200 per kg (Masiye Labs). Zinc oxide may therefore be significantly less expensive (more economical) than catalysts such as the zeolites. This supports the use of zinc oxide in plastic pyrolysis research from an economic perspective.

2.3 Impacts and challenges associated with pure and mixed plastic pyrolysis

A significant drawback to the plastic pyrolysis process is the production of very volatile, volatile and semi-volatile organic emissions (VOCs) which are now regulated in South Africa. Very volatile organic compounds have a normal boiling point between 0-100°C, volatile organic compounds between 100-260°C and semi-volatile compounds between 260-400 °C (US EPA, 2014). In this work, the general term "VOC" will be used for the three subcategories.

The volume and type of emissions released is an important factor which needs to be controlled and managed. VOCs are a safety hazard as many of these components are toxic and carcinogenic. The production of emissions such as carbon dioxide and carbon monoxide are also possible during pyrolysis as a degree of oxidation is often unavoidable. The release of CO_2 directly into the atmosphere increases the carbon footprint of a process. Additional regulations and carbon tax laws apply to processes which release significant amounts of CO_2. For a plastic pyrolysis process to be viable, the volume and composition of the emissions produced needs to fall within the range specified in government approved regulations. According to the Air Quality Act of 2004, thermal processes are not to emit more than 10 mg of VOCs per cubic metre of total gaseous emissions. Carbon monoxide emissions are governed at 75 mg per cubic metre of gaseous emissions (Juta & Company Limited, 2018). In 2022, the tax rate for carbon dioxide emissions was approximately R 144 per tonne of CO_2 produced (Global Compliance News, 2022). According to Grewan and Trois, (2023), plastic waste pyrolysis is considered a long-term waste management strategy in South Africa due to the infancy of application in South Africa to date.

2.3.1 Carbon dioxide production during pyrolysis

The gas product of the pyrolysis process may contain components which are useful as a fuel however there are some undesirable products which may be formed. Components such as

carbon dioxide may be formed if there is a small amount of oxygen present within the pyrolysis equipment. The implementation of a commercial scale pyrolysis plant could therefore be hindered if the emissions produced are not acceptable according to CO_2 emissions regulations. It is therefore important to consider these emissions in plastic pyrolysis research.

Carbon dioxide emission data from various plastic pyrolysis processes were extracted from literature and are listed in Tables 2.3 to Tables 2.9. The availability of this data is limited, so various plastic types were considered to form a broad understanding of the effect of process parameters on the CO_2 production rates.

Jin et al., (2019) implemented pyrolysis experiments using a feed of polyurethane (PU) in a fluidized bed reactor at temperatures ranging from 800°C to 1100°C. Kaminsky, (2021a) compiled pyrolysis literature data which involved the use of fluidized bed reactors and a variation of plastic feeds. Table 2.3 indicates CO_2 emission data collected from the work of Jin et al., (2019) and Kaminsky, (2021b) which used a feed of polyurethane. Lower CO_2 emissions were observed at higher temperatures.

Table 2.3: CO_2 emissions from polyurethane pyrolysis (FB=Fixed Bed Reactor, FLB=Fluidized Bed Reactor).

Feed	Reactor	T (°C)	Process duration (min)	Heating rate (°C/min)	CO_2 Production (w = wt %, v = vol %)	Reference
PU	FB	800	40	20	24 v	(Jin et al., 2019)
		900	Not	Not	17.3 v	
		1000	Not	Not	14.9 v	
		1100	Not	Not	8.9 v	
PU	FLB	750	Not	Not	0.8 w	(Kaminsky, 2021b)

Osman et al., (2020) reported the emissions released from PET pyrolysis processes in a fixed bed reactor. PET pyrolysis data from Osman et al., (2020) and Kaminsky, (2021a) are presented in Table 2.4. In this case, CO_2 emissions decrease with temperature.

Table 2.4: CO_2 emissions from PET pyrolysis (FB=Fixed Bed Reactor, FLB=Fluidized Bed Reactor).

Feed	Reactor	T (°C)	Heating rate (°C/min)	CO_2 Production (wt %)	Reference
PET	FB	500	8	42.8	(Osman et al., 2020)
	FLB	505	-	15	(Kaminsky, 2021b)
		458	-	15	
		451	-	13	
		401	-	11	

Tables 2.5 lists CO_2 emission data in poly(methyl methacrylate) (PMMA) pyrolysis from the work of Kaminsky, (2021a). The literature also contained data from pyrolysis experiments using a feed of polyamides. This data has been presented in Table 2.6 with lower emissions observed at lower temperatures for both types.

Table 2.5: CO_2 emissions from PMMA pyrolysis (FLB=Fluidized Bed Reactor).

Feed	Reactor	T (°C)	CO_2 Production (wt %)	Reference
PMMA	FLB	490	0.4	(Kaminsky, 2021b)
PMMA	FLB	590	13.6	

Table 2.6: CO_2 emissions from pyrolysis of polyamides (FLB=Fluidized Bed Reactor).

Feed	Reactor	T (°C)	CO_2 Production (wt %)	Reference
Polyamides	FLB	630	4.5	(Kaminsky, 2021b)
Polyamides	FLB	510	0.5	

Pires et al., (2021) investigated plastic pyrolysis experiments using various feed plastics such as PE, PP, styrene, and PVC. Operation temperatures ranged from 750°C to 950°C. The

emissions of CO_2 per kg of product formed were recorded. The results are presented in Table 2.7. The lowest CO_2 emissions were observed for LDPE feed.

Table 2.7: CO_2 emissions from pyrolysis of polyethylene, polypropylene, and styrene.

Feed	T (°C)	CO_2 Production (kg CO_2/kg product formed)	Reference
PP		0.04	(Pires et al., 2021)
HDPE		0.03	
LDPE	700 to 950	0.002	
LLDPE		0.08	
Styrene		0.11	
PVC		0.01	

López et al. (2011b) investigated the use of catalysts such as ZSM-5 and Red Mud and their effect on the pyrolysis of mixed plastics (PE, PP, PET, and PVC). Kaminsky, (2021a) investigated uncatalysed mixed plastic pyrolysis. Both literature sources provided CO_2 emission data which has been summarized in Table 2.9. These results indicate that CO_2 - emissions were lower at high pyrolysis operating temperatures for the mixed plastic waste.

Table 2.8: CO_2 emissions from the pyrolysis of mixed plastic feedstocks (aA/bB/cC/dD/eE = a wt % A/b wt % B/c wt % C/d wt % D/e wt % E, where the upper-case and lower-case letters indicate numerical values and plastic feed types respectively).

Feed	Reactor	T (°C)	Process duration after heating (min)	Catalyst	Heating rate (°C/min)	CO_2 Production (gcw= product gas wt%, gcy=yield of total products)	Reference
40PE/35PP/18PS/4PET/3PVC	SB Unstirred	440	30	Red Mud	20	8.5 gcw	(López et al., 2011b)
		500	30	Red Mud		7.5 gcw	
		440	30	ZSM-5		4.9 gcw	
		500	30	-		2.9 gcw	
		440	30	-		2.7 gcw	
		500	30	ZSM-5		1.9 gcw	
		500	0	-		5.4 gcw	
		500	15	-		4.6 gcy	
		500	30	-		2.9 gcy	
		500	120	-		2.7 gcy	
		600	30	-		2 gcy	
		460	30	-		2 gcy	
PE and PP	FLB	700	-	-	-	1.3 gcy	(Kaminsky, 2021b)
65polyolefin/25PS/1.2PVC/1.5polyester/7.3 water, filler, and metals	FLB	740	-	-	-	0.6 gcy	

In summary, the pyrolysis of polyurethane produced emissions with 24 % CO_2 (by volume) at 800°C. The CO_2 volume percent decreased as the temperature was increased in the work of Jin et al., (2019) (Table 2.3). Literature showed CO_2 emissions were much higher in the PET pyrolysis compared to the pyrolysis results of other plastics such as PMMA (Table 2.5), and polyamides (Table 2.6). Osman et al., (2020) showed significantly high CO_2 emissions in PET pyrolysis (42.8 wt %) compared to the results from Kaminsky, (2021b) (CO_2 emissions ranging from 11 wt % to 15 wt %). Table 2.7 listed CO_2 emission results from the pyrolysis of LDPE, HDPE, and LLDPE. Data published by Pires et al., (2021) are related the CO_2 emissions to the amount of liquid product formed. LLDPE produced higher CO_2 emissions per unit mass of product formed compared to LDPE and HDPE.

Figure 2.8 illustrates the CO_2 production data for the previously mentioned mixed pyrolysis experiments in the work of López et al., (2011b) as reported in Table 2.8.

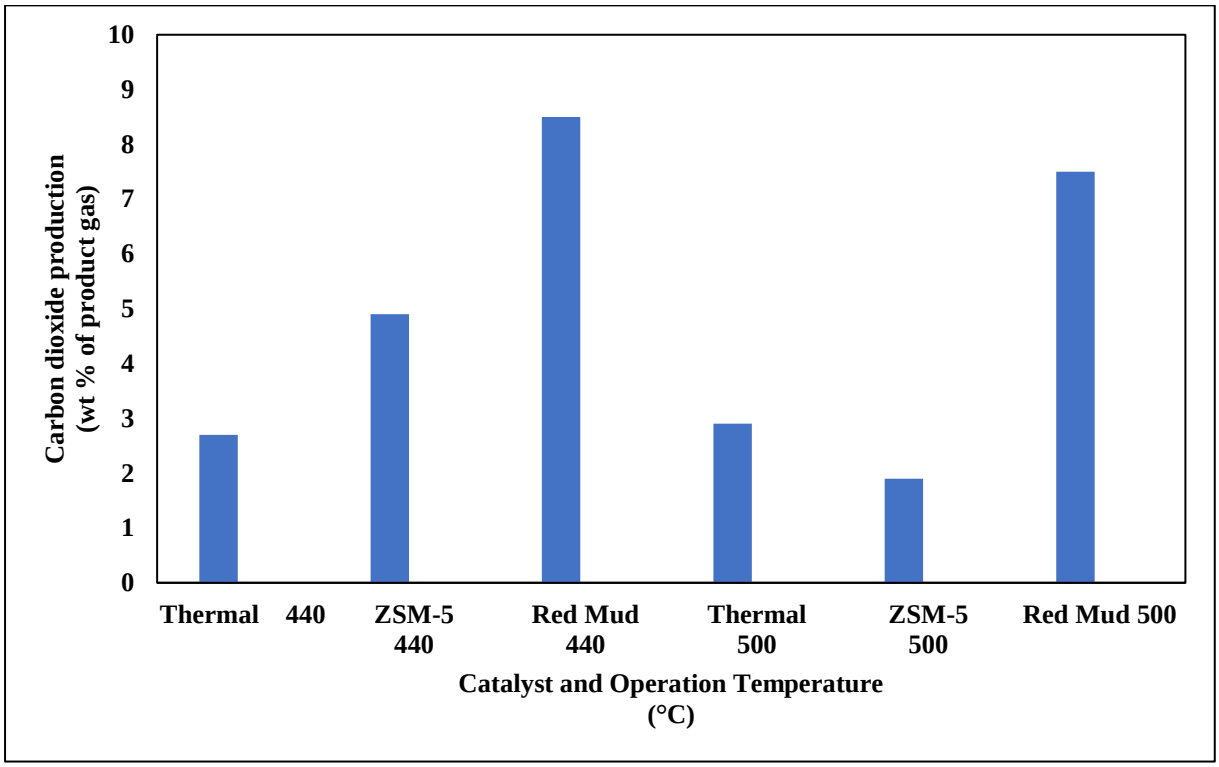

Figure 2.8: Comparison of CO_2 production for mixed plastic pyrolysis experiments with various operating temperatures and catalysts (replotted) (López et al., 2011b).

According to Figure 2.8, the lowest CO_2 concentration (1.9 wt %) of the product gas was observed when using a catalyst of ZSM-5 at a temperature of 500°C. This indicates that with

respect to the CO_2 output from the plastic pyrolysis process, the ZSM-5 catalyst (a commercial catalyst) is superior in reducing CO_2 emissions in comparison to the other pseudo-catalyst materials considered. López et al., (2011a) do however indicate that for these parameters, the liquid yield was approximately 39.8 wt %, which is the lowest yield recorded. The highest CO_2 concentration (8.9 wt %) was observed using the Red Mud catalyst at 440°C. Literature indicated that for this set of parameters, the liquid yield was relatively high (76.2 wt %). Trends such as those observed in the work of López et al., (2011b) indicate that a trade-off could possibly exist between liquid yield and CO_2 gas-phase concentration. This implies that liquid production is favoured when the reactor is maintained under true inert conditions such that oxidation is prevented.

2.3.2 The contribution of plastic pyrolysis processes to the production of volatile organic compounds (VOCs)

The design of the plastic pyrolysis process needs to consider all significant negative effects on the environment to assess whether the impact would be acceptable according to national regulations. The emission of VOCs is not only limited to the plastic pyrolysis process, but also to some plastic recycling processes where the melting step is employed. Yamashita et al., (2007) proposed a study which analysed the melting process of plastics such as low-density polyethylene, high-density polyethylene, polypropylene, polystyrene, which is analogous to the first step of the reaction mechanism within the pyrolysis reactor. Experiments were carried out in different atmospheres including nitrogen. According to Yamashita et al., (2007), heating the LDPE plastic to temperatures above 250°C in air produced more VOCs as compared to heating at lower temperatures (approximately 150°C). The higher melting temperatures (in the presence of air) cause the plastic polymer chains to degrade at a faster rate. The fast degradation rate produces more oxidative compounds. In effect, the production of VOCs substantially increases with the increase in temperature. The nitrogen atmosphere has also been used for the purpose of plastic pyrolysis research and was discussed in the work of Luo et al., (2000). According to Luo et al., (2000), HDPE and PP pyrolysis experiments were performed using SA (consisting of SiO_2 and Al_2O_3) and F9 (consisting of SiO_2, Al_2O_3, and Na_2O) catalysts. The experiments utilized an operation temperature of 500°C and a nitrogen atmosphere. Due to the inert atmosphere, shorter chain compounds that are gaseous at ambient conditions are formed.

Figure 2.9 indicates the type and quantity of emissions released in the LDPE melting experiments at 200°C in air and nitrogen atmospheres (Yamashita et al., 2007b). The “Other”

category included butylated hydroxytoluene, siloxanes, limonene, and several nitrogen containing compounds.

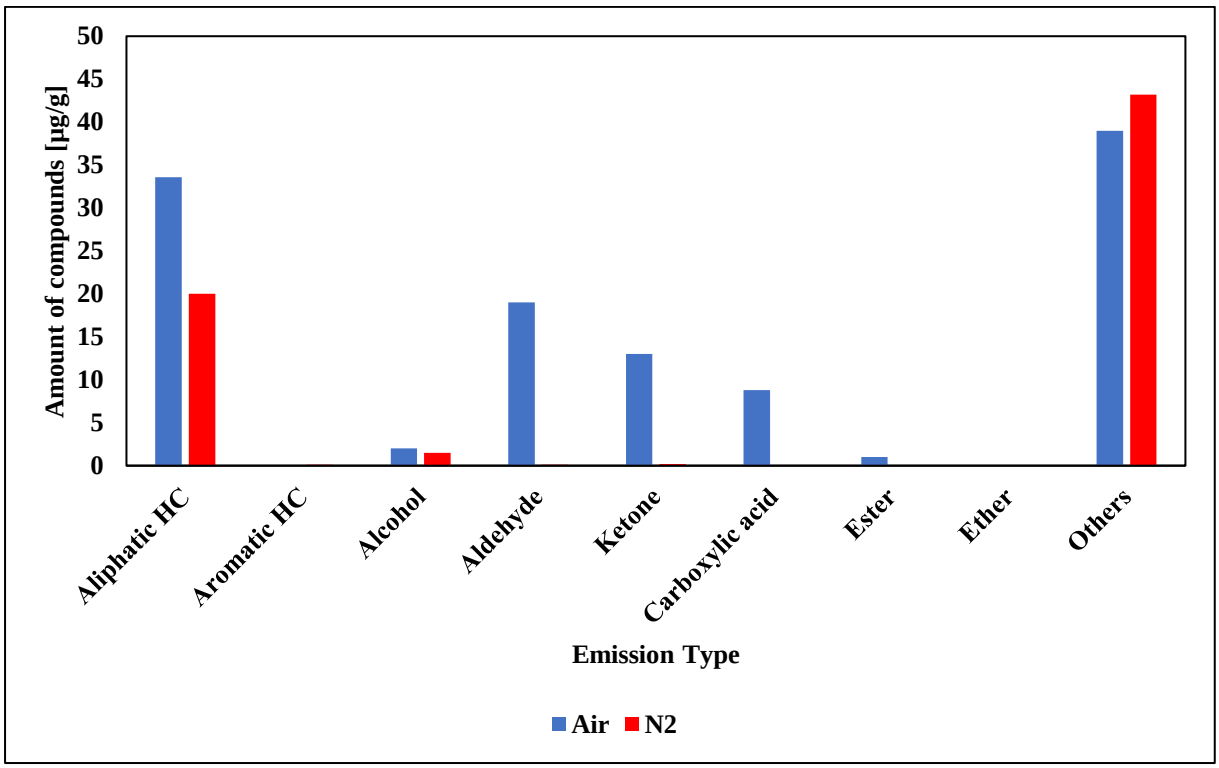

Figure 2.9: Plot showing VOC emissions for the melting process of LDPE plastic at 200°C in different atmospheres (replotted) (Yamashita et al., 2007b).

According to the Figure 2.9, the emissions of all compounds were reduced significantly in a nitrogen atmosphere as compared to the experiments performed in the presence of air. According to Yamashita et al., (2007), this trend is observed because the nitrogen hinders the degradation process and reduces the amount of low-molecular weight oxygenated components forming, which usually result in VOCs.

VOC emission data were extracted from plastic pyrolysis process results available in literature. Kaminsky, (2021b) provided VOC emission data for pyrolysis processes using a variation of plastic feeds such as poly(methyl methacrylate), polyurethane, polyamides, polystyrene, polyethylene, polypropylene, and mixtures of the plastics. VOC emission data from individual plastic pyrolysis processes found in article published by Kaminsky, (2021b) are presented in Tables 2.9. The product gas components were summarized as a mass percentage of the total product gas stream mass. Lee et al., (2021) reported the VOC emissions from LDPE pyrolysis experiments with the use of H-ZSM-11 catalyst.

Table 2.9 shows mixed plastic pyrolysis emissions from (Kaminsky, 2021b). Cho et al., (2010) implemented pyrolysis experiments using a mixed plastic feedstock consisting of PE, PP, PS, PMMA, and PET. The experiments were conducted at temperatures ranging 677°C to 722°C. Veksha et al., (2018) utilized a Ni-Ca catalytic sorbent in pyrolysis reactions using a mixed feed of LDPE, PP, PS, and PVC. The operation temperatures ranged from 500°C to 700°C.

Table 2.9: VOC emission data from various pyrolysis processes using pure and mixed plastic feedstocks.

Feed	Reactor	T (°C)	Catalyst	VOC Emissions	Reference
PMMA	FLB[1]	490	-	0.3 me/0.6 et/0.2 pr/0.2 bu[2]	(Kaminsky, 2021b)
		590	-	3.9 me/0.9 et/7 pr/1.2 bu	
		490	-	0.8 me/0.2 et/0.5 pr/0.6 bu	
Polyurethane-I	FLB	750	-	0.8 hc/0.5 am/15 me/1.5 et/8.5 ethy/1.4 pr[3]	(Kaminsky, 2021b)
Polyurethane-II	FLB	750	-	2.3 hc/0.1 am/17.4 me/0.9 et/5.6 ethy/0.2 pr	
Polyamides	FLB	510	-	0.4 me/0.9 ethy/0.6 pr/0.3 et[4]	(Kaminsky, 2021b)
		630	-	0.2 am/6.4 me/3.2 et/7.8 ethy/3.9 pr	
PS	FLB	515	-	0.2 me/0.3 ethy/0.1 et/0.2 pr[5]	(Kaminsky, 2021b)

[1] FLB=Fluidized Bed Reactor.
[2] wt %, me=methane, et=ethane, pr=propene, bu=butane.
[3] wt %, hc=hydrogen cyanide, am=ammonia, me=methane, et=ethane, ethy=ethylene, pr=propene
[4] wt %, me=methane, ethy=ethylene, pr=propene, et=ethane, am=ammonia
[5] wt %, me=methane, ethy=ethylene, pr=propene, et=ethane, am=ammonia

		540	-	0.5 me/0.6 ethy/0.2 et/0.3 pr	
LLDPE	FLB	510	-	0.4 me/0.8 ethy/0.8 pr/0.5 bu/0.05 BTX[6]	(Kaminsky, 2021b)
		450	-	0.2 pr/0.1 me/0.2 bu/0.2 ethy/0.03 BTX	
HDPE	FLB	530	-	2 ethy/1.1 bu/1.8 pr/0.8 me/0.3 BTX[7]	(Kaminsky, 2021b)
		510	-	0.7 pr/0.6 ethy/0.3 me/0.3 bu/0.05 BTX	
PP	FLB	740	-	20.6 me/13.3 ethy/18.1 ben/6.7 to[8]	(Kaminsky, 2021b)
		510	-	0.6 me/0.5 ethy/3 pr/0.7 bu/0.02 BTX	
		500	-	0.8 me/1.9 et/9.6 pr/2.6 bu	
		400	$AlCl_3$	0.1 me/0.2 et/2 pr/0.2 bu	
		400	$TiCl_3$	1.2 me/2.2 et/10.3 pr/3.8 bu	
		400	$TiCl_4$	0.6 me/0.6 et/3.4 pr/0.5 bu	
LDPE	Split-hinge	500	-	8.77 me/15.94 ethy/20 et/24.81 py/31.14 pa[9]	(Lee et al., 2021)

[6] wt %, me=methane, ethy=ethylene, pr=propene, bu=butenes, BTX=BTX aromatics
[7] wt %, me=methane, ethy=ethylene, pr=propene, bu=butenes, BTX=BTX aromatics
[8] wt %, me=methane, ethy=ethylene, be=benzene, to=toluene, BTX=BTX aromatics, pr=propene, bu=butenes, et=ethane
[9] gas composition %, me=methane, ethy=ethylene, et=ethane, py=propylene, pa=propane, h=hydrogen gas

		600	-	8 8.10 me/16.45 ethy/18.22 et/26.83 py/30.4 pa	
		700	-	8.11 me/18.22 ethy/16.45 et/28.10 py/29.12 pa	
		800	-	1.26 h/8.35 me, 31.89 ethy/12.65 et/25.82	
		900	-	1.3 h/9.36 me/42.02 ethy/8.87 et/24.55 py/13.9	
		500	H-ZSM-11	1.64 me/37.53 ethy/2.46 et/14.24 py/44.13 pa	
		600	H-ZSM-11	1.09 me/21.36 ethy/2.46 et/51.23 py/23.86 pa	
		700	H-ZSM-11	1.09 me/22.46 ethy/2.19 et/50.68 py/23.58 pa	
		800	H-ZSM-11	1.15 me/16.75 ethy/1.62 et/62.97 py/17.51 pa	
		900	H-ZSM-11	1.64 me/19.45 ethy/1.36 et/62.46 py/15.09 pa	
PE and PP	FLB	700	-	30 ethy/8.8 me/7.4 be/2.4 to[10]	(Kaminsky, 2021b)
PE, PP, PS, PMMA, PET	FLB	677	-	30.31 me/22.8 ethy/10.35 et/19.05 pr/2.37 by[11]	(Cho et al., 2010)
		710	-	35.42 me/25.92 ethy/9.26 et/15.26 pr/2.36 by	
		735	-	41.72 me/27.56 ethy/10.35 et/7.75 pr/1.98 by	
		773	-	49.05 me/28.33 ethy/5.7 et/5.93 pr/1.77 by gc%	
		690	CaO	18.4 me/14.6 ete/7.8 pr/7.5 be/6.5 to/1.6 xy	
		711	CaO	20.9 me/16 ete/9.7 pr/8.5 be/5.7 to/1.3 xy wt%	

[10] gas composition %, me=methane, ethy=ethylene, et=ethane, py=propylene, pa=propane, h=hydrogen gas
[11] gc %=gas composition %, wt%=weight %, me=methane, ethy=ethylene, et=ethane, pr=propene, by=butyne, ete=ethene, xy=xylene, to=toluene

		712	$Ca(OH)_2$	21.4 me/15.8 ete/9.2 pr/8.6 be/5.9 to/1.4 xy	
		719	$Ca(OH)_2$	22.5 me/15.3 ete/7.3 pr/9.9 be/6.5 to/1.4 xy	
		711	Oyster	20.6 me/14.7 ete/7.7 pr/8.7 be/6.2 to/1.4 xy	
		722	Rice Straw	23.7 me/15.7 ete/7.4 pr/8.7 be/6.1 to/1.4 xy	
15LLDPE/45HDPE/40PP	FLB	510	-	0.4 me/0.6 ethy/1.5 pr/1 bu/0.1 BTX[12]	(Kaminsky, 2021b)
40LDPE/40PP/ 10PS/10PVC	Two reactors: Horizontal and vertical quartz reactor	500	-	45.20 me/18.35 et/44.93 ethy/4.93 pa/39.73[13] py/0.96 C4A/ 14.24 C4E/3.56 C5A/2.46 C5E/2.33 di/2.46 ay	(Veksha et al., 2018)
		600	-	62.19 me/21.9 et/61.37 ethy/4.38 pa/47.39 py/1.36 C4A/	
		700	-	87.39 me/16.43 et/83.83 ethy/1.92 pa/35.06 py/0.14 C4A/	

[12] wt %, me=methane, ethy=ethylene, pr=propene, bu=butenes, BTX=BTX aromatics
[13] volume in ml, et=ethane, ethy=ethylene, pa=propane, py=propylene, C4A=C4 alkenes, C4E=C4alkenes, C5A=C5 alkenes, C5E=C5alkenes, di=dienes, ay=alkynes

		500	Ni-Ca catalytic sorbent	52.32 me/20.01 et/40.27 ethy/4.93 pa/35.61 py/1.5 C4A/ 14.52 C4E/3.56 C5A/2.46 C5E/0.27 di/2.19 ay	
		600	Ni-Ca catalytic sorbent	67.12 me/18.63 et/7.93 ethy/3.01 pa/4.65 py/0.54 C4A/ 1.09 C4E/2.19 C5A/0.01 C5E/0.01 di/0.02 ay	
40LDPE/40PP/ 10PS/10PVC	Two reactors: Horizontal and vertical quartz	700	Ni-Ca catalytic sorbent	86.02 me/16.99 et/49.31[14] ethy/3.01/pa/19.17/py/0.27 C4A/4.38 C4E/0.82 C5A/0.01 C5E/0.02 di/0.01 ay	(Veksha et al., 2018)
65Polyolefin/25PS/1.2PVC/1.5PET	FLB	740		20.5 me/10.3 ethy/17.4 be/3.9 to	(Kaminsky, 2021b)

[14] volume in ml, et=ethane, ethy=ethylene, pa=propane, py=propylene, C4A=C4 alkenes, C4E=C4alkenes, C5A=C5 alkenes, C5E=C5alkenes, di=dienes, ay=alkynes

In summary, according to the results from article published by Kaminsky, (2021b), components such as methane, ethylene, and benzene were produced in large quantities for all plastic types. Emissions such as ethylene and benzene are significant because these fall into the categories of volatile organic compounds. The mixed plastic pyrolysis data indicated that the use of various plastic types in one feed mixture could significantly lower the production rate of VOC emissions compared to pure plastic pyrolysis experiments.

After an examination of the data presented in Table 2.9, it is evident that the trend in VOC emissions is complex, especially in cases of mixed plastic pyrolysis, and is dependent on the type of plastic, operating conditions and catalyst used. Hence, increasing the temperature in pyrolysis of mixed plastics may not necessarily increase the quantity of emissions produced. Consider for example the work of Lee et al., (2021), the thermal pyrolysis experiments showed a drastic increase in emissions such as C2 emissions (ethylene) when the temperature was increased from 500°C to 900°C. According to the data, the amount of ethylene increased from 15.9 % to 42 %. Addition of the H-ZSM-11 catalyst caused the emissions of ethylene to decrease with an increase in temperature. According to the data, the amount of ethylene decreased from 37.5 % to 19.45 % when the temperature was increased from 500°C to 900°C (Lee et al., 2021). Hence emissions data must be collected carefully for any proposed pyrolysis operation for specific quantification and subsequent management of the emissions.

2.4 Optimization of the lab-scale pyrolysis process for pure and mixed plastic

2.4.1 Laboratory scale plastic pyrolysis experiments carried out in a Borosil round bottom flask reactor under vacuum pressures

Laboratory scale studies can be used to collect data which can provide preliminary estimates regarding the environmental impact of a large-scale pyrolysis processes. A study performed by Senthil Kumar et al. (2017), investigated the pyrolysis process for different feedstocks such as HDPE, LDPE, PS, PP, and PET. The experimental setup, which similar versions have been used by numerous authors, is shown below in Figure 2.10. Further review of the equipment used in literature is reviewed in work by Anuar Sharuddin et al., (2016).

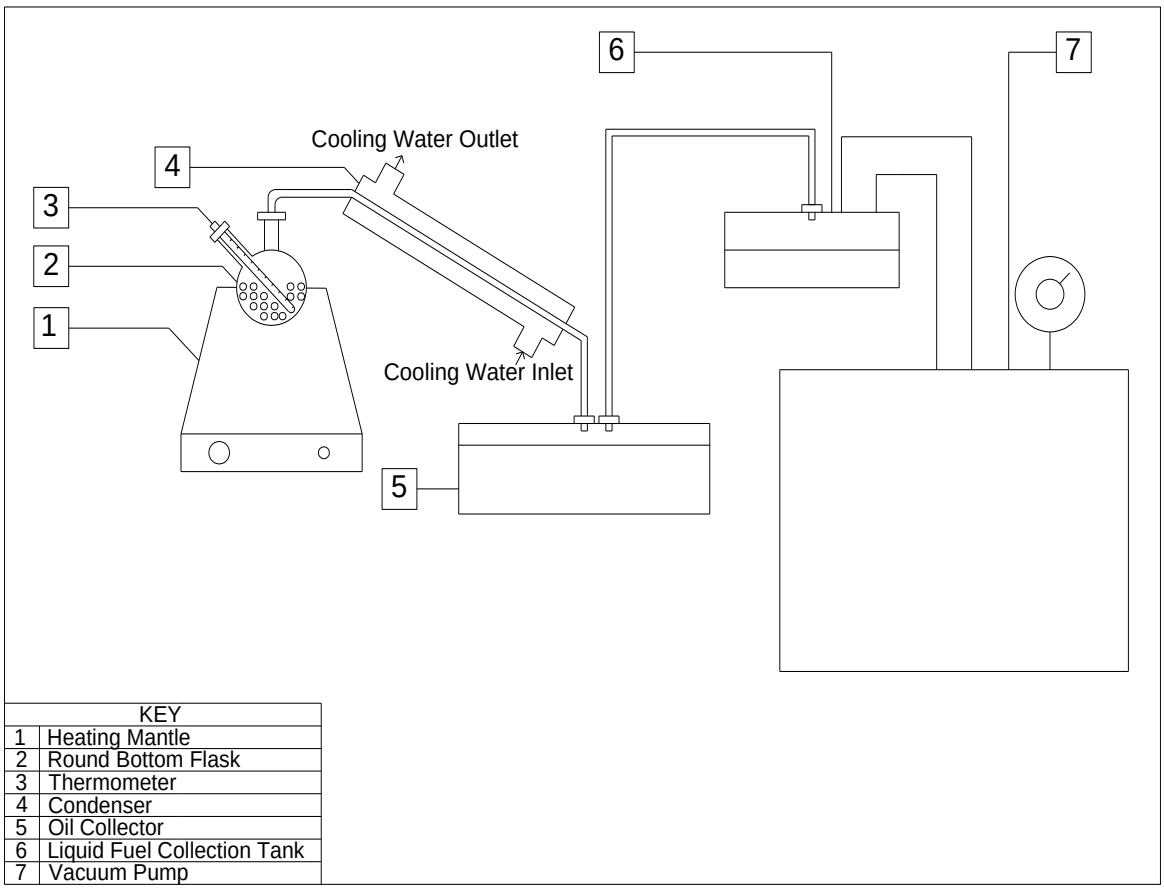

Figure 2.10: Diagram showing the plastic pyrolysis experimental setup using a round bottom flask reactor according to literature redrawn from Senthil Kumar et al., (2017).

Initially, a fixed mass of plastic (between 10-20 g) was placed in the round bottom flask. The flask served as a reactor for the process. The flask was placed within a heating mantle. The flask opening was connected to a condenser. The oil produced was condensed in a condensing tube and thereafter transferred to an oil collector. The oil from the oil collector was

subsequently distilled in a separate apparatus. Analysis of the products were performed with a gas chromatograph equipped with flame ionization detector (FID).

The pyrolysis product yield results from Senthil Kumar et al., (2017) are presented in Table 2.10.

Table 2.10: Laboratory scale plastic pyrolysis results from experiments under vacuum pressure Senthil Kumar et al., (2017).

Feed	T (°C)	P (kPa)	Catalyst	Reaction Time (min)	Liquid Yield (wt %)	Residue (wt %)
PS	240	73.3	-	30	80	13.3
PP	240	66.7	-	35	60.7	34.4
PE	240	40	-	45	75	22.4
PE, PP, PS	240	46.7	-	45	66.9	25.9
	240	40	Activated Carbon	45	82.4	15.2
	240	40	Charcoal	35	95.5	2.3
PE, PP, PS, PET	240	40	CaO + Activated Carbon	45	75.5	20.3

2.4.2 Laboratory scale pyrolysis experiments carried out in a fluidized bed reactor

The large-scale pyrolysis processes (commercial) are more likely to use more flow and heat transfer efficient reactors such as a fluidized bed reactor. Literature has however shown that pyrolysis experiments from laboratory-scale reactors can be scaled to large-scale commercial processes. This is evident in the work of Kulas et al., (2022). Since the operation on the laboratory-scale can closely relate to that of the large-scale processing plant equipment, laboratory-scale experiments are employed as one has more control over these experiments and has more flexibility with respect to the multiple permutations of the different experimental parameters. Unlike with glass equipment, which is not meant for high pressure applications, pilot-scale reactors fabricated specifically for laboratory from steel can withstand a variation of pressure. Utilizing this equipment could provide a wide range of experimental data which is

critical to the upscaling of a laboratory-scale pyrolysis process to the commercial scale. One case study using this design type is detailed below as an example, with more detailed reviews provided by Anuar Sharuddin et al., (2016) for example.

The work of Luo et al., (2000) provided information on the plastic pyrolysis of high-density polyethylene and polypropylene using a laboratory-scale bubbling fluidized bed reactor (FLB). The experimental setup (Figure 2.11) consisted of a fluidized bed reactor which was heated by an electric furnace. Plastic particles are continuously transferred to the FLB using a micro-feeder. A designated amount of catalyst was initially loaded into the FLB. The fluidized bed reactor was connected to a cylinder of nitrogen which was used as the fluidization gas. The pyrolysis gas which was formed passed through a micro-cyclone and filter which was connected to the FLB. The pyrolysis gas was quenched, and the traps collected the pyrolytic oil. The gas phase product passed through the traps and were collected by a gas bag. Wet gas meters were used to measure the gas phase product. The mass of the solid residue and the mass of gas was measured. Using this data and a material balance, yields of the liquid product were obtained. The results from the pyrolysis experiments were extracted from literature and are shown in Figure 2.12.

The above description indicates an example of how a laboratory-scale fluidized bed pyrolysis process could be achieved. Analysis of the pyrolysis products require a few tools such as gas chromatography with mass spectrometry. This can be used to obtain the compositions of the products.

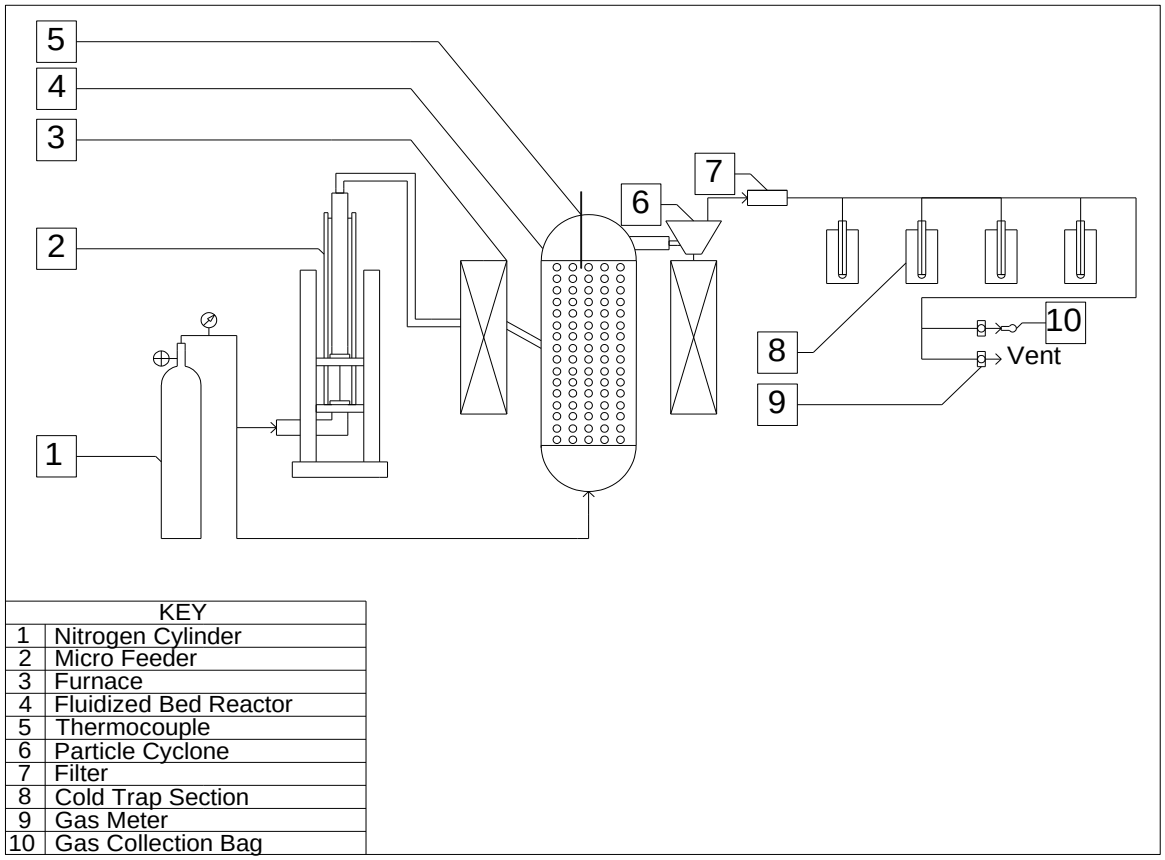

KEY	
1	Nitrogen Cylinder
2	Micro Feeder
3	Furnace
4	Fluidized Bed Reactor
5	Thermocouple
6	Particle Cyclone
7	Filter
8	Cold Trap Section
9	Gas Meter
10	Gas Collection Bag

Figure 2.11: Diagram showing the plastic pyrolysis experimental setup using a bubbling fluidized bed reactor redrawn from Luo et al., (2000).

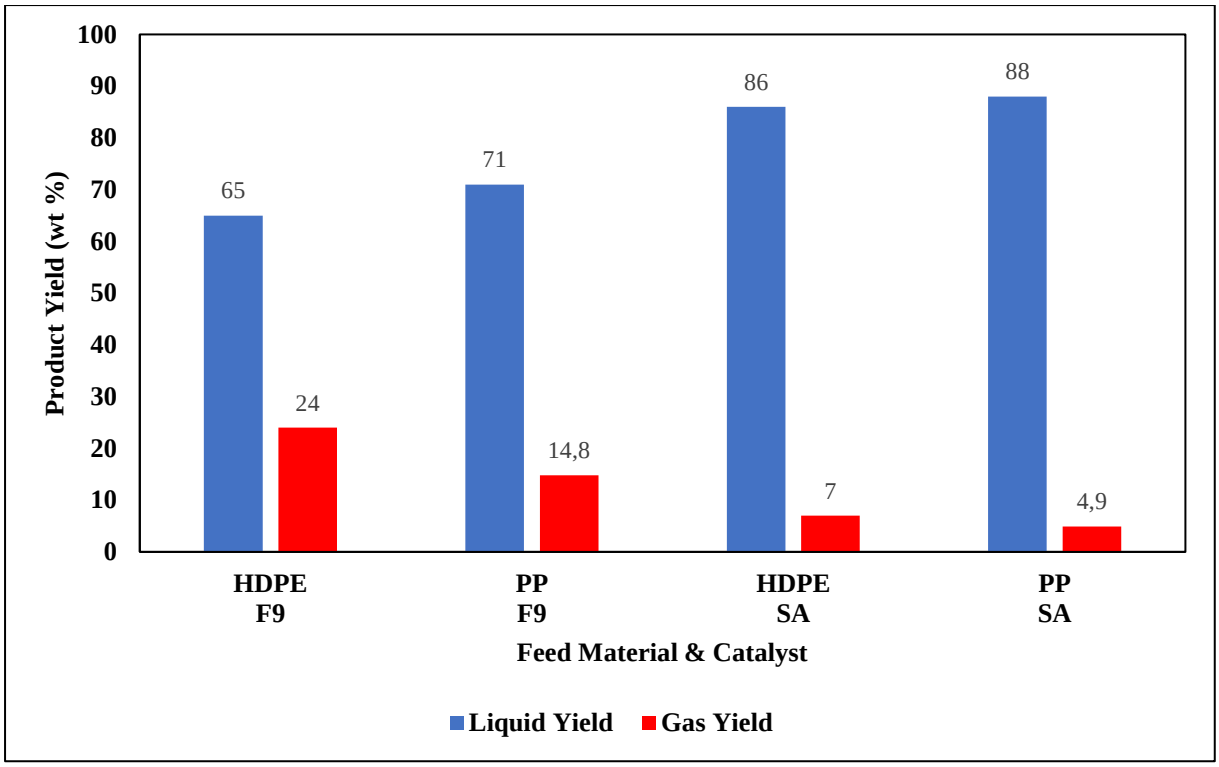

Figure 2.12: Plot showing the liquid and gas product yields for HDPE and PP plastic pyrolysis experiments at 500°C performed in an atmosphere of nitrogen (replotted) (Luo et al., 2000) [SA=SiO_2 and Al_2O_3. F9=SiO_2, Al_2O_3, and Na_2O].

2.4.3 The effect of operational parameters on product yields

The selection of operational parameters (such as temperature, pressure, process duration, and catalyst usage) are essential in the optimization of plastic pyrolysis processes. The purpose of changing these parameters is to maximize the yields of desirable products (pyrolysis oil). One of the limiting factors include the type of plastic feed for the pyrolysis process. There are specific plastics which may produce higher yields compared to other plastic feedstocks. Within a commercial scale pyrolysis plant, the process may utilize feedstock which is obtained from areas such as landfills. Consequently, there is less control on the composition of plastics in the feed. For this reason, the commercial scale pyrolysis process plant may not always achieve maximum yields of liquid oil due to the constant variation of the plastic feed composition. A possible solution to this is the variation of temperature or the usage of catalyst. Both factors significantly affect the distribution of products in a plastic pyrolysis process. To further understand these trends, the results of various pyrolysis experiments in literature have been

reviewed and essential data such as pyrolysis product yields have been recorded. The data from literature has been listed in Table 2.11 below.

Table 2.11: The effect of operational parameters on pyrolysis product yields.

Feed	Reactor [15]	T (°C)	Catalyst (A:B=AZinc Oxide to BFeed)	P (kPa)	Heating rate (°C/min)	Duration (min)	Oil Yield (wt %)	Gas Yield (wt %)	Reference
LDPE	FB	500	BC[16]	-	10	10	84.9	-	(Budsaereechai et al., 2019b)
		-	BC	-	15	-	75.6	-	
	RBF	-	10:100	50	10	-	72.6	19.1	(Tekade et al., 2020)
		-	5:100	50	-	-	71.5	19.6	
		-	3:100	50	-	-	65.9	17.8	
	FB	500	BC	-	20	10	64.9	-	(Budsaereechai et al., 2019b)
	RBF	-	-	47	10	-	54.2	16.7	(Tekade et al., 2020)
		-	-	50	-	-	53.9	17.0	
		-	-	60	-	-	52.3	17.5	
	FB	500	BC	-	25	10	51.8	-	(Budsaereechai et al., 2019b)
	RBF	-	-	73	10	-	48.1	13.2	(Tekade et al., 2020)

[15] FB=Fixed Bed Reactor, RBF= Round Bottom Flask Reactor, FLB=Fluidized Bed Reactor
[16] BC=Bentonite Clay

		-	-	88	-	-	44.7	8.67	
		-	-	101	-	-	42.1	6.22	
HDPE	FB	500	BC	-	10	10	86.9	-	(Budsaereechai et al., 2019b)
		-	BC	-	15	-	76.7	-	
	RBF	-	10:100	50	10	-	73.5	19.8	(Tekade et al., 2020)
		-	5:100	-	-	-	69.1	19.4	
	FB	500	BC	-	20	10	63.6	-	(Budsaereechai et al., 2019b)
	RBF	-	3:100	50	10	-	63.2	18.4	(Tekade et al., 2020)
		-	-	-	-	-	56.2	18.9	
		-	-	47	-	-	55.1	19.3	
		-	-	-	-	-	55.1	19.3	
		-	-	60	-	-	52.9	18.1	
HDPE	FB	500	BC	-	25	10	5	-	(Budsaereechai et al., 2019b)
	RBF	-	-	73	10	-	49	13.8	(Tekade et al., 2020)
		-	-	88	-	-	43.6	8.3	
		-	-	101	-	-	43.1	5.8	
	FLB	530	-	-	-	-	-	7.6	(Kaminsky, 2021b)
		510	-	-	-	-	-	2.6	

PP	FB	500	BC	10	10	89.5[17]	-	(Budsaereechai et al., 2019b)
			-	15	-	79.5	-	
			-	20	-	70.72	-	
			-	25	-	55.6	-	
	FLB	400	$AlCl_3$	-	-	45.4 LO/49.7 HO	4.9	(Kaminsky, 2021b)
		500	-	-	-	42.7 LO/37.5 HO	19.8	
		400	$TiCl_4$	-	-	41.5 LO/49.4 HO	7.9	
			$TiCl_3$	-	-	37.3 LO/41.6 HO	22.1	
		510	-	-	-	-	6.3	
PET	FLB	458					0.9	(Kaminsky, 2021b)
		401					0.8	
		505					0.3	
		451					2	

[17] LO=light oil, HO=heavy oil

PS	FLB	515	-		-	-	98.9	0.8	(Kaminsky, 2021b)
		540	-		-	-	97.8	2	
		-	-		20	-	68.3	-	
	FB	500	BC		25	10	53.5	-	(Kaminsky, 2021b)
		-	-		15	-	78	-	(Kaminsky, 2021b)
	FB	500	BC		10	10	87	-	(Budsaereechai et al., 2019b)
PU	FLB	750	-	-	-	-	14.2 HB[18]	-	(Kaminsky, 2021b)
	FB	1100	-	-	20	40	-	40	(Jin et al., 2019)
		1000	-	-	-	-	-	39	
		900	-	-	-	-	-	38.5	
		800	-	-	-	-	-	36	
LLDPE	FLB	510						3.4	(Kaminsky, 2021b)
		450						1.1	

[18] HB=high boiling oil

40PE/35 PP/18PS/ 4PET/3P VC	Unstirred Semi-batch	400	ZSM-5	20	30	40.4	31.8	(López et al., 2011b)
		500				39.8	58.4	
		460				54.3	43.6	
		425				61.2	31.3	
		500	Red Mud			57	41.3	
40PE/35 PP/18PS/ 4PET/3P VC	Unstirred Semi-batch	440	ZSM-5	20	30	56.9	40.4	(López et al., 2011b)
		500	-	20	30	65.2	34	(López et al., 2011b)
		440	Red Mud	20	30	76.2	21.6	(López et al., 2011b)
		440	-	20	30	79.3	17.7	(López et al., 2011b)
15LLDP E/45HD PE/40PP	FLB	510	-	-	-	-	4.7	(Kaminsky, 2021b)

PA[19]	FLB	510		50.8 HB[20]	-	(Kaminsky, 2021b)

[19]PA=Polyamides
[20] HB=high boiling oil

Apart from the work of Tekade et al., (2020) which did not specify pyrolysis processes durations, majority of the pyrolysis experiments from other literature reported run times under 40 minutes. The use of bentonite clay as a catalyst in a fixed bed reactor allowed a lower process duration of 10 minutes, and a high yield of 89.6 % pyrolysis oil (HDPE feedstock) to be produced Budsaereechai et al., (2019b). According to Table 2.11, zeolite catalysts such as ZSM-5 may be used for mixed plastic pyrolysis processes, although the liquid product yield is moderate.

2.4.4 Considerations for the uses of char produced from waste plastic pyrolysis.

A less desirable product which usually remains in the reactor after completion of the pyrolysis reaction is char. Char has a rich carbon content and could be used for application such as combustion and gasification. The work of Jamradloedluk and Lertsatitthanakorn, (2014) included plastic pyrolysis experiments performed on HDPE waste plastics at temperatures ranging 400°C-450°C. The effects of pyrolysis temperatures on char yields were investigated. A general trend observed is that as the process temperature increases, the yield of char decreases but the yield of oil and gas increases. Proximate analysis of the products revealed that the char had a moisture content of 2.4 %, 51.4 % volatile matter, 46.0 % fixed carbon, and 0.16 % ash. The work indicated that the char could be briquetted and used as a fuel source for cooking. Consideration of char is important as this is one of the outputs of the plastic pyrolysis process and hence affects the environmental impact of the process. The handling and utilization of the char would need to be considered in a comprehensive Environmental Impact Assessmemt.

Martín-Lara et al., (2021) performed a study which investigated the char produced from a mixed plastic pyrolysis process. The work used a feedstock of polypropylene, polystyrene, and polyethylene. According to authors, the application most suitable for the char produced depends on the properties of the feedstock such as the composition of plastics available. To investigate the char properties, an elemental analysis was performed. This allows one to analyse the weight composition of carbon, hydrogen, nitrogen, and sulphur. Thermogravimetric analysis also allows the analysis of moisture, composition of volatile components, ash content, and fixed carbon content on a weight basis. For the plastic waste mixture, a pyrolysis temperature of 450°C produced a solid product (char and some wax) yield of 4.56 %. However, a temperature of 550°C generated only 2.38 % char. This aligns with the trend in which the yield of char decreases as the pyrolysis temperature increases.

The work by Martín-Lara et al., (2021) also investigated the application of solid char in the adsorption of heavy metals such as lead from aqueous solutions. The results showed that the char produced at 450°C removed 37.79 % of lead from the aqueous solutions. In comparison, the char produced 550°C removed 73.48 % lead. The adsorption capacity therefore increases as the temperature increases. If the char product were to be used as an adsorbent, a trade-off would be made between the value of the char as an adsorbent and the liquid product yield. That is, a low pyrolysis temperature with lower energy requirements maximizing char production, vs. a higher energy requirement process maximizing liquid yields. In effect, the environmental impact caused by the process (energy requirement) could be reduced if the market for char adsorbents was available.

Harussani et al., (2022) performed a review which indicates the yields of char that could be obtained from various plastic pyrolysis feeds and process conditions. The results of which were reproduced in Table 2.12.

Table 2.12: Production of char from plastic pyrolysis processes published by Harussani et al. (2022).

Feed Plastic	Reactor	T (°C)	Process Duration (min)	Catalyst	P(MPa)	Heating Rate (°C/min)	Yield of Char (wt%)
PP	Microwave-assisted semi-batch reactor	500	30	-	-	20	33.5
HDPE	Fixed bed	500	330	-	-	5	20
	Batch	450	60	HZM-5	-	-	19.7
	Batch	440	120	-	-	-	17
PVC	Wire mesh	500	-	-	-	60	16
PP	Horizontal steel	250	30	-	-	20	13.7
	Batch	380	-	-	0.1	3	13.3
LDPE	Batch	300	360	-	-	5	10.80
	Semi-batch	300	-	-	-	5	10.12
PET	-	500	-	-	0.1	6	9
PP	Fluidized bed	703	-	-	-	-	6.9
HDPE	Batch autoclave	490	60	-	-	-	6.5
PP	Semi-batch	450	-	FCC	0.1	25	3.6
	Fixed bed	900	21	-	-	-	2.8
	Fixed bed	400	45	-	-	5	2.5
HDPE	Semi-batch	300	-	-	-	5	2.3
PP	Batch	740	-	-	-	10	1.6
PS	Batch	425	-	-	1.6	10	0.5

The char yields in the review by Harussani et al., (2022) showed a few significant trends with similarities for plastics of the same type. HDPE pyrolysis produced char yields of 17 wt % at 440°C. In another experiment at 500°C and more than a 3.5 hour longer process duration, the char yield only increased by 3 wt % when compared to the experiment at 440°C. Additionally, polypropylene pyrolysis experiments at 400°C, 450°C, and 900°C produced char yields ranging from 2.5 wt % to 3.6 wt %. There was a significant difference between the PP and HDPE char yields. The reason for this may be due to the weaker intermolecular structures of PP (and lower density) as compared to HDPE. Cracking reactions may take place more easily in the PP molecules. Consequently, more liquid or gas product could be formed which results

in a lower char yield as compared to HDPE pyrolysis. Evidence of weak intermolecular forces are also indicated by the lower process duration times of PP pyrolysis (ranging from 21 minutes to 45 minutes) compared to HDPE pyrolysis (ranging from 60 minutes to 330 minutes).

2.4.5 Evaluation of product quality in plastic pyrolysis process

Although high desirable product (liquid) yields are important, the quality of liquid (chemical composition) is required to determine the nature and marketability of the product. Determining the chemical composition of the product will allow one to match the liquids properties to similar types of fuels. Chemical analysis methods such as gas chromatography with mass spectroscopy (GC-MS) have become an efficient way of determining the chemical composition of plastic pyrolysis oil.

In work published by Miandad et al., (2019), catalytic pyrolysis experiments were performed using different types of plastics wastes such as PS, PE, PP, and PET. The experiments utilized natural zeolite catalysts. GC-MS was used to determine the composition of products such as the liquid oil. The pyrolysis oil for each plastic feed contained mainly hydrocarbon compounds such as a aromatics and aliphatic components. Comparing the product qualities from different pyrolysis experiments may also allow one to further understand the mechanisms of the cracking reactions. According to Miandad et al., (2019), the number of aromatic components in the polystyrene and polypropylene experiments increased when an acidic activated catalyst was used. In comparison, the use of the acidic activated catalyst reduced the aromatic composition in the pyrolysis of polyethylene. According to the literature, the acidic catalyst influenced a production of hydrocarbons with shorter chains as an effect of the high-cracking ability. The liquid product of the catalytic pyrolysis experiments using different plastic feedstocks contained olefins and naphthalene components which are generally found in petroleum products. Furthermore, the liquid oil produced using a feedstock of PS with an acid activated natural zeolite catalyst has similar chemical properties to that of diesel. Simultaneously running experiments and chemical analyses is a technique which could help optimize the product quality in the plastic pyrolysis process.

Tekade et al., (2020) utilized GC-MS for the chemical analysis of plastic pyrolysis products. Similarly, to Miandad et al., (2019), the liquid oil composition described by Tekade et al., (2020) for the LDPE experiment contained a large number of hydrocarbons. Carbon numbers ranged from C_6 to C_{54}. The major constituents in the liquid oil were components such as 1-tridecene, 1-undecene, and eicosane. In comparison, the oil produced by HDPE contained

relatively short-chained molecules with carbon numbers ranging from C_{13} to C_{28}. In this case, there were similar major constituents to that of the LDPE oil such as eicosane and 1-tridecene. However, there were also large proportions of components such as hexadecene, 1-pentadecene, and pentacosane.

The comprehensive environmental impact assessment for the plastic pyrolysis experiment could be supported by a chemical analysis of the products and emissions. As mentioned before, there could be various components in the pyrolysis gas such as carbon dioxide, carbon monoxide, and VOCs. The chemical analysis of emissions on a laboratory scale could therefore be used to find optimum process parameters so that the emissions fall within regulations (with the aim of implementing pilot and commercial scale pyrolysis processes).

2.5 Introduction to the preliminary Gate to Gate Assessment (GGA) for pure and mixed plastic pyrolysis

When considering a relatively new process in large-scale operation, there are many factors that need to be accounted for. Information on the impact that the process may have on the environment/life cycle of materials is essential to determine if the process could possibly be environmentally friendly and sustainable. Additionally, this information on the processes impact could indicate whether the operational parameters of the process fall within the regulations stipulated by the government. The data obtained in this laboratory-scaled study can be used to inform the preliminary factors that would be considered in a comprehensive life cycle analysis for a to-scale process for plastic pyrolysis using some of the processing methods developed in this work.

A life cycle analysis (LCA) considers the environmental impact of products or services throughout the life cycle (BPF, 2022) and can also be used in a broader scope to analyse the economic impact of the process and material life cycle through quantifying resource consumption and product generation. The LCA may consider steps from the beginning, such as the collection of raw materials. Processing steps and conversion of raw materials to finished products are involved. The final steps associated with the LCA generally include the disposal of the product after use.

The ISO 14044 standards provide guidelines for the appropriate accepted methodology for an LCA.

The first step in a life cycle assessment is to identify the scope of the project (PRé Sustainability, 2023). In this step, the boundaries of the projects are defined. This determines what is included and excluded in the LCA (determines the depth of the LCA). In the next step the inventory analysis is conducted which is where the inputs and outputs which affect the environment/economics of the process are analysed. This includes areas such as raw materials, waste streams, emissions, etc. Using the process input and outputs, a life cycle impact assessment (LCIA) can be drawn up. The LCIA is used to organize the relevant data from the inputs and outputs. The LCIA can thereafter be interpreted, reviewed and conclusions (whether the process has an acceptable environmental and economic impact) may be drawn. Sensitivities of the selected inputs can also be assessed, along with peer review (Curran, 2012).

There are many variables when considering an LCA and conducting a comprehensive LCA on the proposed to-scale pyrolysis process based on the data measured in this work, is beyond the scope of this work. The use of tools such as computer programmes (designed for LCA) may be useful to simplify the process. These programmes could be used to identify all the variables associated with the process for which the LCA is performed. Using these programmes will therefore minimize the time taken for the LCA since manual identification of these variables (time consuming) is not required.

A gate-to-gate assessment (GGA) is a component of the process LCA that focuses on the environmental impacts and resource consumption within a particular defined stage of a process. The system boundary in this case (as shown in Figure 2.13) is the gate of the process operation, hence only inputs to and outputs from the process gate are considered. Estimating the life cycle inventory (LCI) for chemical substances at the gate-to-gate stage using chemical engineering process design methods is a viable and credible alternative when there is a lack of factual or literature-based information for a study (Jiménez-González et al., 2000).

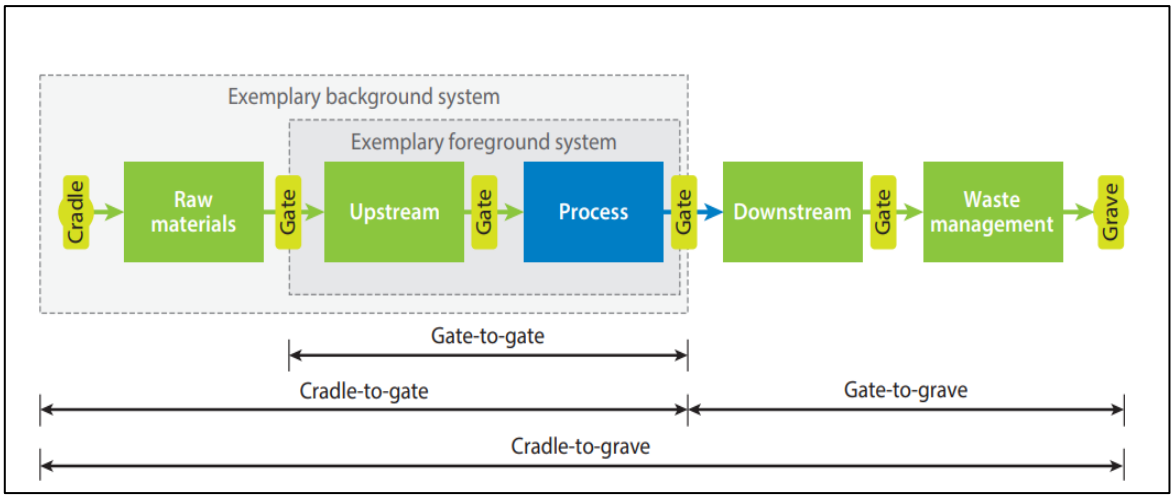

Figure 2.13: System boundaries of different categories of LCA assessments (replotted) (Kleinekorte et al., 2020).

The GGA includes the input of raw materials up until the conversion into products (Cao, 2017). The assessment excludes processes beyond processing plant gate but forms part of the comprehensive LCA/LCIA. The steps of the gate-to-gate assessment are similar to those of the general ISO 14044 LCA process as outlined above, but are typically characterized by a narrow focus, a specific functional unit based on a particular process feed, is informed by data, limited in scope and used for decision support for optimization or consideration of process alternatives (Jiménez-González et al., 2000). Using the methodology outlined by Jiménez-González et al, (2000), the identification of scope requires the selection of the appropriate specific process under study, with the subsequent definition of the process such as the reactions, process conditions, flow diagram and estimation of stream properties. Thereafter, the inventory analysis is conducted to identify the mass and energy balances. Jiménez-González et al. (2000) highlight the need for high quality process details and stream property data for LCIA, as this directly affects the precision of the analysis. Numerous authors have applied a similar methodology to that described by Jiménez-González et al. (2000), however the method has not been used specifically for plastic pyrolysis as part of an LCA/GGA for the process conditions studied in this work. Fichana, (2005), Van der Vorst et al. (2011), Parvatker et al. (2019), and Güneş and Şengül, (2022) have applied the methodology to production in the pharmaceutical industry to develop processes for novel active pharmaceutical ingredients. Capello et al. (2009) and Wernet et al. (2012) adapted the methodology for the production of process chemicals to reduce energy use. Zhang et al. (2023) and Al Rayaan (2022) used the gate-to-gate analysis approach to compare process scenarios in the textile industry and ground water purification

respectively, considering water use and contamination. Mahath et al. (2019) used gate-to-gate assessment to assess the environmental impacts of dairy processing products to identify cleaner production opportunities. In these studies, the gate-to-gate assessment identified environmental impacts of the various process routes considered which allowed for robust design decision making.

In the plastic pyrolysis processes, a crude fuel oil is being produced. Further refining and upgrading is required. However, the exact processes required will depend on the actual product obtained. In this case, a gate-to-gate assessment is useful since processes beyond the plant gate are not currently well-defined limiting the option of a comprehensive LCA for the process being developed in this work. Since the South African government places regulations on major process outputs such as the emission of VOCs and carbon dioxide, the GGA can be used to identify and quantity the VOCs released for a section in the pyrolysis process with specific operational parameters. In effect, the GGA would indicate whether the specific process falls within regulations. The implementation of a GGA should be considered as VOC emissions from the pyrolysis process is an important focus of this study.

The preliminary gate-to-gate analysis based on the lab scale process implemented in this work, will identify the major factors for consideration that can be used in a comprehensive LCA for the scaled-up plastic pyrolysis plant that forms part of the broader research project that is supported by the Council for Scientific and Industrial Research (South Africa), which this work forms a component of. For the scaled-up process, comprehensive LCAs, reviews and methodologies for various plastic pyrolysis process alternatives have been reported in the literature, to which the reader is referred for further reading: (Roy and Dutta, 2019), (Davidson et al., 2021), (Xayachak et al., 2022), (Andooz et al., 2023), (Almadhi et al., 2023) and (Yadav et al., 2023).

CHAPTER THREE: MATERIALS AND METHODOLOGY

3.1 Introduction

The plastic pyrolysis process requires an efficient control of parameters such as the operation temperature, operation pressure, and catalyst usage. Laboratory scale plastic pyrolysis experiments may be used to obtain valuable data such as product yields, emission compositions, and effects of operational parameters on the pyrolysis process. The experiments in this study were performed under low pressures induced by a vacuum pump to create an inert environment for the reaction. The following chapter discusses the research methodology, experimental procedures, and equipment used to perform these experiments in a vacuum environment. The preparation of the equipment and type of feedstock used is discussed. The rigorous procedures for the analysis of gas emissions from the pyrolysis experiments are also described in this chapter. The procedures used to analyse the desirable pyrolysis products are also discussed. This is essential to determine the quality of the plastic pyrolysis products.

The methodological approach was developed using the following outline:

- Literature review
- Equipment, feed and catalyst selection and modifications
- Testing measurements, GC-MS preparation
- Non-catalytic and catalytic experimental runs for pure and mixed plastics
- Analysis of emissions
- Data collection, processing and reporting
- Gate to gate analysis

3.2 Equipment

A summary of the equipment and materials are presented.

- Ohaus PA423C Pioneer Analytical Balance
- Laboratory Spatula
- Weighing boat
- Flask cork stand
- 20 ml vials with caps
- 10 ml disposable syringes
- Pyrolyzer cups (4 mm o.d x 8 mm, 80 µL) and cup holder
- PY1-ES20F Eco-Stick (80 mm), used to secure pyrolyzer cup prior to injector.
- PY1-1020 Double-shot pyrolyzer sampler (suitable for 80 mm Eco-Stick)
- 500 ml Stuart Heating Mantle
- Temperature probe and display
- 250 ml single neck round bottom flask
- 250 ml Duran Schott triple neck flask
- Spiral condenser
- VIVO RT4 circulator (maximum operating temperature of 85°C, pumping rate of 10 litres per minute)
- Edwards RV5 vacuum pump (ultimate pressure of 1.5 $x10^{-3}$ Torr, pump speed displacement of 4.1 CFM at 60 Hz)
- Sensotec pressure transducer and reader (max pressure 25 psi)
- Shimadzu GC-MS-QP2010 Plus - gas chromatograph equipped with mass spectrometer.
- Shimadzu AOC-20i auto injector
- Frontier Lab EGA/PY-3030D Multi-Shot Pyrolyzer (10°C to 1050°C operating temperature range)

3.3 Materials

The plastic materials and other chemicals used in the experiments are listed.

- Low-density polyethylene (LDPE) plastic pellets
- High-density polyethylene (HDPE) plastic pellets
- Polypropylene (PP) plastic pellets
- Zinc Oxide powder catalyst (99.99 % trace metals basis)
- Vacuum grease
- Hexane (≥99 % purity) Supplier: Sigma-Aldrich
  Impurities: <0.001 % water
  <0.005 % water
- Acetone
- Helium (GC-MS carrier gas)

To obtain uniform results for research purposes, purchased plastic pellets was used as the plastic feed in this work, as a substitute for waste plastic. The plastic pellets were difficult to procure at the quantity and quality required for this work, but were ultimately sourced from Potch Plastic (Potchefstroom, North West Province, South Africa) after an extensive and lengthy search. Table 3.1 presents the particle size (measured with a vernier) and densities (calculated using measured mass and volume of pellets) of the LDPE, HDPE, and PP plastic pellets used in this experiment. Note that these pellets have likely undergone compounding during processing by the supplier, hence their physical properties may differ from average values. Table 3.2 presents the specifications of the zinc oxide catalyst powder.

Table 3.1: Measured particle size and density of LDPE, HDPE, and PP cylindrical plastic pellets used in pyrolysis experiments.

Plastic type	**LDPE**	**HDPE**	**PP**
Particle dimensions (mm)	4.5L x 2.5D	3.5Lx 3D	4.5L x 2.5D
Density ($\frac{kg}{m^3}$) at 25°C	1367.18	1378.34	1367.18

Table 3.2: Zinc oxide catalyst specifications.

Supplier	Sigma-Aldrich
Product Number	205532
CAS-No.	1314-13-2
Product Name	Zinc oxide
Appearance (colour, form)	White, powder
Formula Weight ($\frac{g}{mol}$)	81.39
Particle size (micron)	<5
Purity (wt %)	99.9

3.4 Experimental Procedures

3.4.1 Plastic pyrolysis carried out in a round bottom flask reactor under vacuum pressures

The experimental procedure consisted of the pyrolysis of LDPE, HDPE, PP, and mixed plastic at approximately 42 kPa (uncertainty due to repeatability and stability u_P equal to 2 kPa). Test experiments utilized a feed plastic of LDPE and process temperatures ranging from 240°C to 420°C (uncertainty due to repeatability and stability u_T equal to 2°C). Additionally, LDPE, HDPE, PP, and mixed plastic pyrolysis experiments were performed at 450°C to completion. Pyrolysis products such as liquid, wax, and char were collected, and their respective yields were calculated. The pyrolysis gas yields were calculated using a mass balance. A microlitre syringe was used to draw gas samples while the process was in operation. GC-MS was used to analyse the gas samples. A complete run with analysis took 1.5 to 2 weeks to complete. The schematic of the apparatus used for the pyrolysis measurements is presented in Figure 3.1.

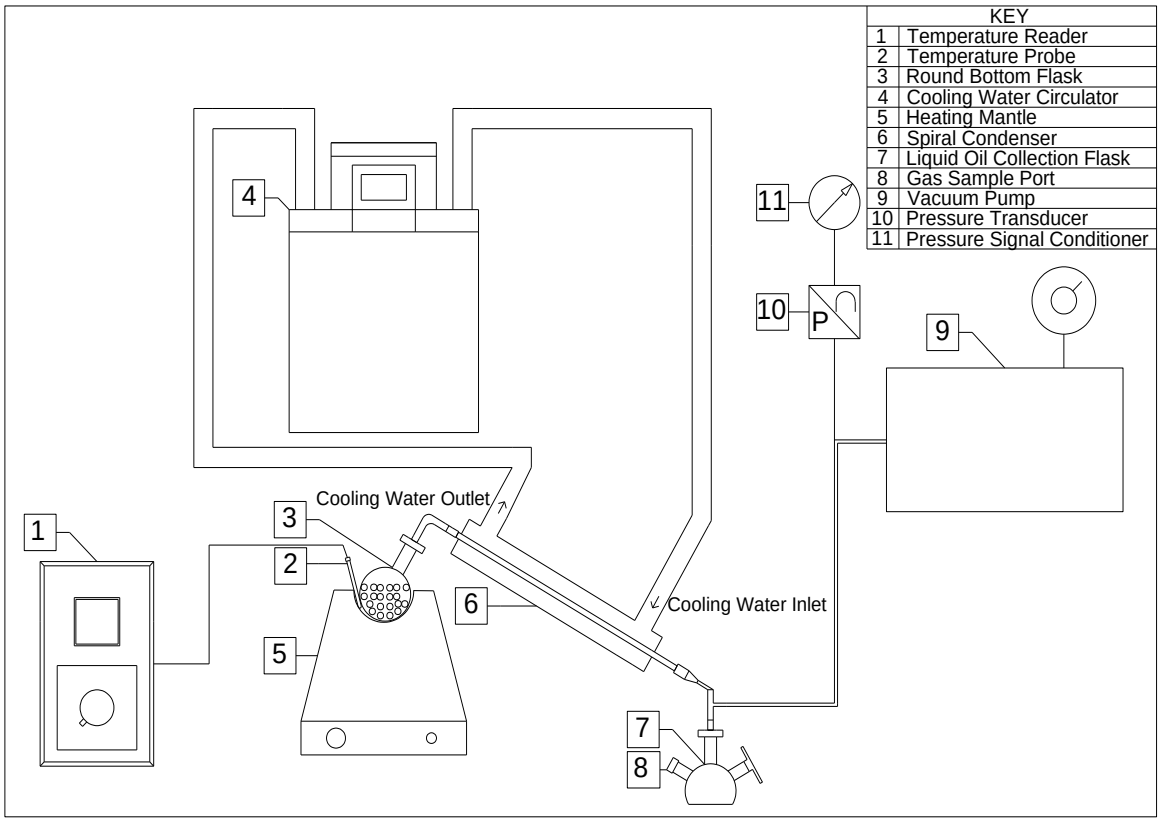

Figure 3.1: Diagram of plastic pyrolysis experimental setup used in this study.

Table 3.3: Operational conditions for pyrolysis experiments using 15g LDPE refuse bags at system pressure of 42 kPa.

Experiment Label	Plastic	Catalyst to Feed Ratio	Operation Temperature (°C)
RB-01	LDPE	Uncatalysed	420
RB-02		3:100	350
RB-03		3:100	350
RB-04		3:100	300
RB-05		10:100	280
RB-06		3:100	300
RB-07		Uncatalysed	240
RB-08		Uncatalysed	280

Table 3.4: Operational conditions for pyrolysis experiments using LDPE, HDPE, and PP plastic pellets at 450°C and 42 kPa.

Experiment Label	Plastic	Catalyst to Feed Ratio
IP-01	LDPE	Uncatalysed
IP-02		5:100
IP-03		10:100
IP-04	HDPE	Uncatalysed
IP-05		5:100
IP-06		10:100
IP-07	PP	Uncatalysed
IP-08		5:100
IP-09		10:100

Table 3.5: Operational conditions for pyrolysis experiments using a mixed plastic feed at 450°C and 42 kPa.

Experiment Label	Plastic Composition (wt %)			Catalyst to Feed Ratio
	LDPE	HDPE	PP	
MP-01	15	45	40	Uncatalysed
MP-02				5:100
MP-03				10:100
MP-04	32.3	34.52	33.18	Uncatalysed
MP-05				5:100
MP-06				10:100
MP-07	65	20	15	Uncatalysed
MP-08				5:100
MP-09				10:100

The preliminary experiments utilized a feedstock of LDPE refuse bags. Experiments were conducted using operational conditions stated in Table 3.3. These reactions were used to validate the experimental method. Thereafter plastic pellets (LDPE, HDPE, PP, and mixed feeds) were used in pyrolysis experiments. The plastic pellets decomposed much slower in pyrolysis experiments compared to the LDPE refuse bags. For this reason, a constant temperature of 450°C was used in experiments using plastic pellet feedstocks based on literature averages. Conditions for the pure plastic and mixed plastic pyrolysis experiments were listed in Table 3.4 and 3.5 respectively. Using a factorial design for conditions based on ranges recommended in literature, the desired yields were optimized.

The experimental setup consisted of a 250 ml round bottom flask which served as the reactor for the experiments. A vacuum pump (Edwards RV5 Rotary Vane-A65301906) was used to reduce the pressure in the closed system of apparatus and the pressure was measured by a Sensotec STJE/1833-02 pressure transducer. A Sensotec Model HM pressure signal conditioner was used to output the pressure reading. A 500 ml Stuart heating mantle served as the heat source for the pyrolysis reaction and temperature was measured using a Pt100 probe. The microlitre litre syringe was placed into the gas sample port of the collection flask to extract pyrolysis gas samples.

Method:

The spiral condenser was weighed using the analytical balance and the mass was recorded. The 250 ml triple neck flask was weighed on the analytical balance and recorded. A flask cork stand was placed on the analytical balance and its mass was tared. The 250ml round bottom flask was placed on the cork stand. The mass for the round bottom flask was recorded. A total of 15 g of plastic was weighed into the round bottom flask. A weighing boat was used to measure the required mass of zinc oxide catalyst (uncatalysed, 5:100, 10:100) for a particular run. The zinc oxide catalyst was placed in the reactor flask. The reactor flask was shaken to evenly distribute the catalyst with the feed plastic pellets. Vacuum grease was applied to the connections of all glassware. The apparatus was assembled according to the diagram in Figure 3.1. The water circulator was switched on and the temperature was set to 25°C. The temperature was allowed 10-20 minutes to stabilize. The vacuum pump was switched on. The pressure was allowed 10-20 minutes to stabilize. The reactor was insulated with aluminium foil and fibreglass lagging wool.

The heating mantle was switched on and adjusted to the lowest level of heating. The temperature of the cooling water and the reactor temperature were recorded at five-minute intervals. The heating mantle heating level was adjusted to allow an average heating rate of 10°C per minute until the desired operation temperature was obtained. The reactor was then held at this temperature. This required rigorous control of the heating mantle. The progressing reaction was observed in the reactor. The time of initial visible gas formation and formation of liquid and wax products were recorded for each experiment.

The analysis of the emissions from the pyrolysis process required gas samples to be taken using a microliter syringe during the experiment, followed by instantaneous analysis. The reaction was deemed complete when the bubbling and formation of visible gas in the reactor stopped, and when the plastic feed had depleted. Upon completion, the process duration was recorded. The heating mantle was switched off and the reactor was left to cool. Once the reactor temperature dropped well below 50°C, the vacuum pump was switched off. The water circulator was thereafter switched off.

Upon completion of the pyrolysis reaction, the glassware used in the experiment were disassembled. The reactor, spiral condenser, and collection flask were individually weighed using the analytical balance.

The product masses were calculated with mass by difference calculations. The mass of liquid in the collection flask was calculated as follows:

$$m_{liquid} = m_{collection\ flask,\ final} - m_{collection\ flask,\ initial} \quad (3.1)$$

The wax product of the pyrolysis process builds up in the spiral condenser. The mass of wax produced is calculated as follows:

$$m_{wax} = m_{spiral\ condenser,\ final} - m_{spiral\ condenser,\ initial} \quad (3.2)$$

All the residue in the reactor may be referred to as char. However, careful consideration is needed depending on the usage of catalyst in the process. For an uncatalysed pyrolysis reaction (only plastic feed is present in reactor at beginning of experiment), the mass of char is calculated as follows:

$$m_{char,\ uncatalysed} = m_{reactor,\ final} - m_{reactor,\ initial} \quad (3.3)$$

For a catalysed plastic pyrolysis reaction, the quantity of catalyst used needs to be considered. During the plastic pyrolysis reaction, it is assumed that all catalyst remains in the reactor as solids were not observed to entrain out of the top of the vessel. For this reason, the mass of catalyst is deducted from the mass of residue in the reactor. The mass of char for a catalysed reaction is calculated as follows:

$$m_{char,\ catalysed} = m_{reactor,\ final} - m_{reactor,\ initial} - m_{catalyst} \quad (3.4)$$

The calculation of the mass of gas formed requires the mass balance of the entire plastic pyrolysis process. The main input into the reaction was the feed plastic. The main outputs of the reaction are the liquid, wax, char, and gas. The feed mass is known. The liquid, wax, and char masses are calculated using equations (3.1) to (3.4). The overall mass balance is represented by the following equation:

$$m_{feed} = m_{liquid} + m_{wax} + m_{char} + m_{gas} \quad (3.5)$$

Using equation (3.5), the mass of gas formed during the plastic pyrolysis process can be calculated.

The calculation of product yields is an essential step to determine the overall effect of operational parameters (temperatures, pressures, catalyst usage, plastic composition) on the plastic pyrolysis reaction. Product yields can give an indication of the relative proportions of desirable and undesirable products formed. Many literature sources such as Tekade et al., (2020) have reported plastic pyrolysis yields as the mass of product divided by the mass of feed plastic used. The results have been reported in weight percentage (wt %). In this work, plastic pyrolysis yields are calculated in wt % to efficiently form comparisons with product yields reported in literature. The product yields are calculated as follows:

$$\text{Pyrolysis Product Yield (wt \%)} = \frac{m_{product}}{m_{feed}} \text{ x } 100 \quad (3.6)$$

Equation (3.6) above can be used to calculate yields for the liquid, wax, gas, and char.

The liquid, wax, and char samples were stored in 20 ml vials. In the cleaning procedure, the spiral condenser was heated using the water circulator. This was done to melt the residue of wax in the condenser. Thereafter, the condenser was rinsed with hexane to dissolve the residue. Acetone was used to rinse the condenser. The collection flask was rinsed with hexane and

acetone. The inside of the reactor flask was scrubbed using a brush and hexane solvent. The flask was thereafter rinsed with acetone.

3.4.2 Analysis of products using GC-MS

Figure 3.2 provides a simplified illustration of the GC-MS analysis set-up used in this study.

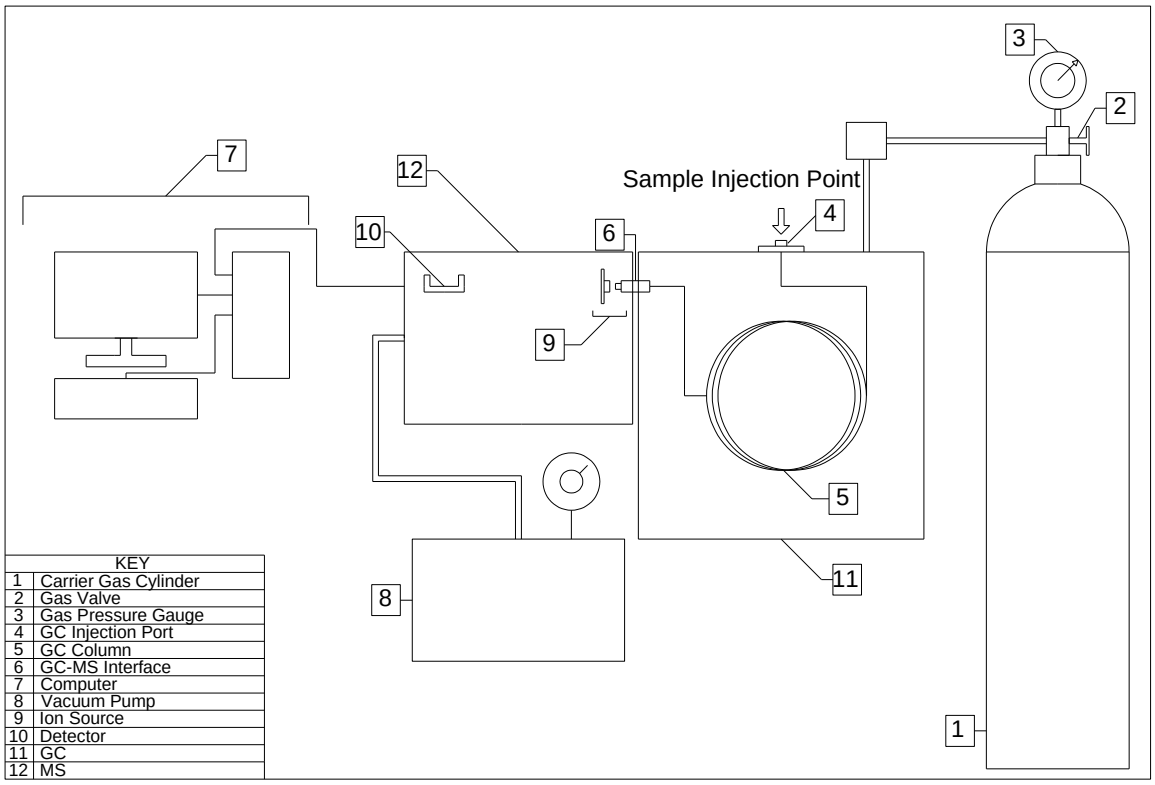

Figure 3.2: Diagram of GC-MS setup used in this study.

Gas chromatography-mass spectrometry (GC-MS) was used to perform chemical analyses on the pyrolysis products. Samples of generated chromatographs are shown in Figures A1 and A2 in Appendix A.

The analysis set-up consisted of the Shimadzu GCMS-QP2010 Plus. Helium was the selected carrier gas for the GCMS analyses. Gas samples drawn from the collection flask (Figure 3.1) during experimental runs were manually injected into the GC via the sample injection port (shown in Figure 3.2). The GCMS also included the Shimadzu AOC-20i autoinjector which was used to inject the liquid and wax produced from each pyrolysis experiment after the completed run.

Due to the observed high viscosity of the liquid and the solid properties of the wax, the pyrolysis products needed to be diluted with a suitable solvent so that the GC-MS detector would not become saturated (providing unusable results). To find an appropriate solvent, a small mass of the wax was placed into 20 ml vials. Solvents such as acetone, cyclohexane, hexane, heptane were dispensed into the vials. The vials were shaken and observed to determine if the wax dissolved in the solvent and remained in solution for an extended period. From observation, hexane was the optimum solvent to completely dissolve the wax. For this reason, hexane was selected for the dilution of the liquid and wax products.

The following procedure was used in the operation of the GC-MS to analyse the pyrolysis products:

Firstly, the valve to the carrier gas was opened and the optimum pressure levels were selected as 700 kPa to 800 kPa for the carrier gas vessel. The pressure gauge on the carrier gas vessel was observed to see if the pressure fell within these bounds. The power switch on the gas chromatography machine (GC) and mass spectrometer (MS) was switched on. Next, the computer connected to the GC-MS was switched on. The vacuum pump oil level was inspected to verify that a suitable amount of oil was present in the pump for sufficient lubrication and control. The vacuum pump was started using the GC-MS software. After this step, the GC-MS was allowed to stabilize for up to 2 hours. This was an important step for the GC-MS to produce reliable results. The GC-MS was tuned for a consistent baseline for analysis results. The method file was used to input the analysis parameters such as column temperatures, detector temperatures, analysis duration, etc. The same analysis parameters were used for the wax and liquid samples. The gas samples required different parameters to ensure clear peak formations. This is due to the range of constituents that are generally unique to each phase. The parameters used in the method file for analysis of the gas samples are listed in Table 3.6. The liquid and wax analysis parameters are listed in Table 3.7.

Table 3.6: Chemical analysis parameters used for the gas samples.

Constant Parameters	
Interface temperature	250^0C
Ion source temperature	250^0C
Equilibrium time	3.00 min

Split ratio	-
Start time	0.00 min
End time	60.00 min

Temperature Profile

Rate	Temperature (°C)	Hold Time (min)
-	50.00	5.00
5.00	250.00	15.00

Table 3.7: Chemical analysis parameters used for the liquid oil and wax samples.

Constant Parameters	
Interface temperature	250^0C
Ion source temperature	250^0C
Equilibrium time	3.00 min
Split ratio	150
Start time	16.00 min
End time	76.67 min

Temperature Profile

Rate	Temperature (°C)	Hold Time (min)
-	50.00	5.00
5.00	250.00	5.00
3.00	300.00	10.00

The method file was downloaded which set the required parameters. The next step was the injection of the product samples. For the liquid and wax samples, the vials with diluted liquid and wax (hexane solvent) were placed in the autosampler. Injection of the samples were automatic once the run was initialized. For the gas samples, manual injection was necessary using a microlitre syringe. After downloading the parameters, the microlitre syringe was used to draw a gas sample from the collection flask sample port using the microlitre syringe. The sample was thereafter injected directly into the GC-MS injection port. The analysis was initialized a few seconds after the injection of the sample. Upon completion of the analysis, the

chromatograph peaks were integrated automatically by the software to determine the composition of the pyrolysis products.

Before switching off the GC-MS, the vacuum control shutdown option was selected using the GC-MS software. This process took approximately 45 minutes to complete (including shutdown of the vacuum pump). The GC-MS was switched off after the shutdown was complete and the carrier gas valve was closed.

3.4.3 Plastic Pyrolysis via the GC-MS pyrolyzer

As a comparison for the emission data being collected from the bench-top lab-scale unit, the plastic pellets pyrolysis experiments were replicated using a 20 ml GC-MS pyrolyzer (Frontier Lab EGA/PY-3030D). This was done so that pyrolysis products and emissions could be sampled online from the pyrolyzer chamber. The following procedure was used to perform the pyrolyzer experiments:

Plastic pellets were cut into small pieces using a side-cutter and a retractable utility knife. The pyrolyzer cup holder was placed on the analytical balance using a pair of tweezers. A pyrolyzer cup was placed into the holder. The mass of the holder and cup was tared and a total of 1 mg of plastic was weighed into the pyrolyzer cup. Zinc oxide catalyst was weighed and loaded into the pyrolyzer cup. The amount of catalyst was dependent on the catalyst to feed ratio (uncatalyzed, 5:100, 10:100). The pyrolyzer cup was secured onto the falling sampler injector device. The main pyrolyzer unit was then switched on and the falling sampler injector device was secured onto the pyrolyzer unit. The pyrolyzer chamber temperature and interface temperature were set to 450°C and 250°C respectively. The sample time was set to 1 min. These parameters formed part of the analysis method file. The analysis method file was downloaded, and the initial parameters were set. Once the GC-MS and pyrolyzer temperatures stabilized, the run was initialized using the pyrolyzer software. After observing the prompt on screen for injection, the falling sampler injector device was used to release the pyrolyzer cup.

The GC-MS sampled the gas from the pyrolyzer temperature for 1 minute. Thereafter, the GC-MS performed the analysis using the temperature profile in Table 3.8.

Table 3.8: Chemical analysis parameters used for the GC-MS pyrolyzer experiments.

Constant Parameters

Interface temperature (°C)	250
Ion source temperature (°C)	250
Equilibrium time (min)	3.00
Split ratio	-
Start time (min)	0.00
End time (min)	78.00

Temperature Profile

Rate	Temperature (°C)	Hold Time (min)
-	60.00	0.00
5.00	105.00	1.00
3.00	280.00	15.00
10.00	300.00	10.00

The analysis continued for an additional 77 minutes. Thereafter, the chromatograph peaks were integrated to determine the composition of the gas. The cup with the residual char was removed.

3.5 Gate-to-gate analysis to consider circular data in the plastic pyrolysis process

The comprehensive life cycle analysis (LCA) for the future scaled-up pyrolysis process requires a thorough analysis and evaluation of the environmentally relevant input and outputs. In the LCA, the technical aspects of the main process would be analysed. With the current lab scale experimental work, there were many limitations regarding the availability of data (inputs and outputs). Factors such as the true composition of VOC emissions could not be determined since a gas chromatograph calibration would be required for each of the hundreds of components in the pyrolysis gas phase. Hence, only relative volumes could be determined. The comprehensive LCA scope was therefore too broad for the current work. There are however many important inputs and outputs that could be determined to further understand the processes impact on the environment. These inputs and outputs form the subset of the Life Cycle Inventory Analysis (LCIA) for the scaled-up process, and these lab-scale factors are translatable and can hence be used in future work in the development of an LCA of the scaled-up process. The gate-to-gate analysis (GGA) methodology as described in detail by Jiménez-

González et al, (2000) was used to determine the relevant input and outputs/inventory factors for the process, which include water usage, usage of solvents and other cleaning agents, electricity usage, and carbon dioxide and VOC emissions. The methodology used is summarized below. Information from Morgan et al., (2021) and Skone et al., (2013) was also used to develop the methodology for a preliminary GGA as used in this work.

Stage 1: Search and Selection of the Process

Investigation of Processes:

a. Research processes with industrial significance. In this work, the proposed process was the semi-batch pyrolysis of mixed plastic using zinc oxide catalyst.

b. Collect information from various sources like patents, articles, databases, and industrial contacts. This constitutes the literature review and experimental methodology used to select the lab-scale process. However, by reviewing the literature, the inventory factors were confirmed to be transferable to the scaled-up process.

Selection of the Process:

a. Choose a process based on information availability, relevance, and regional prevalence.

b. Consider factors like information quantity, age, scale, and regional applicability.

The process selected for the lab scale tests is commonly applied in the literature.

Stage 2: Definition of the Process

Description of the Process:

a. Define chemical reactions, including reactants and products with structural formulae. Because of the complex nature of the reactions and vastness of products from plastic pyrolysis, only generic chemical reactions could be feasibly identified. These are Plastic - > Gas, Plastic - > Liquid, Plastic -> Wax, Plastic-> Char.

b. Identify temperature, pressure, and composition conditions for each operation.

Flow Diagram and Properties:

i. Create a flow diagram of the process with temperature and pressure indications.
ii. Search or estimate physical and chemical properties for all chemicals involved.

In this work, only relevant properties were determined experimentally where possible.

Mass

Mass Balance Calculation:

a. Perform a mass balance for a chosen basis This was varied during the experimental process based on the different feed mixtures considered. Hence unique bases were used for the process permutations.

b. Consider inputs not in the product as process emissions and estimate chemical losses including catalyst use.

Factors for Emission Estimation:

a. Consider process emissions based on conversion, by-products, separation efficiency, and more.

b. Utilize Material Safety Data Sheets (MSDS) for impurity assessment and estimate fugitive losses.

Energy

Energy consumption calculation:

a. Calculate energy requirements for steam, fuel or electricity.

b. Consider heat of reaction (endothermic in this case), and energy for separation units such as condensers etc.

Energy Recovery:

a. Evaluate potential energy recovery by analysing heating requirements and energy losses due to cooling.

b. Estimate recoverable energy based on efficiency rules.

Energy recovery estimation was considered to be beyond the scope of the present study as it was not possible to accurately measure any relevant data on waste heat/cooling recycling with the semi-batch set-up used. This would have to be considered when the pilot scale continuous unit is examined.

Using this methodology, the essential input and outputs for the process is described in Figure 3.3. Attempts were made to relate lab-scale operational factors to to-scale operation to ensure that a more comprehensive inventory was created.

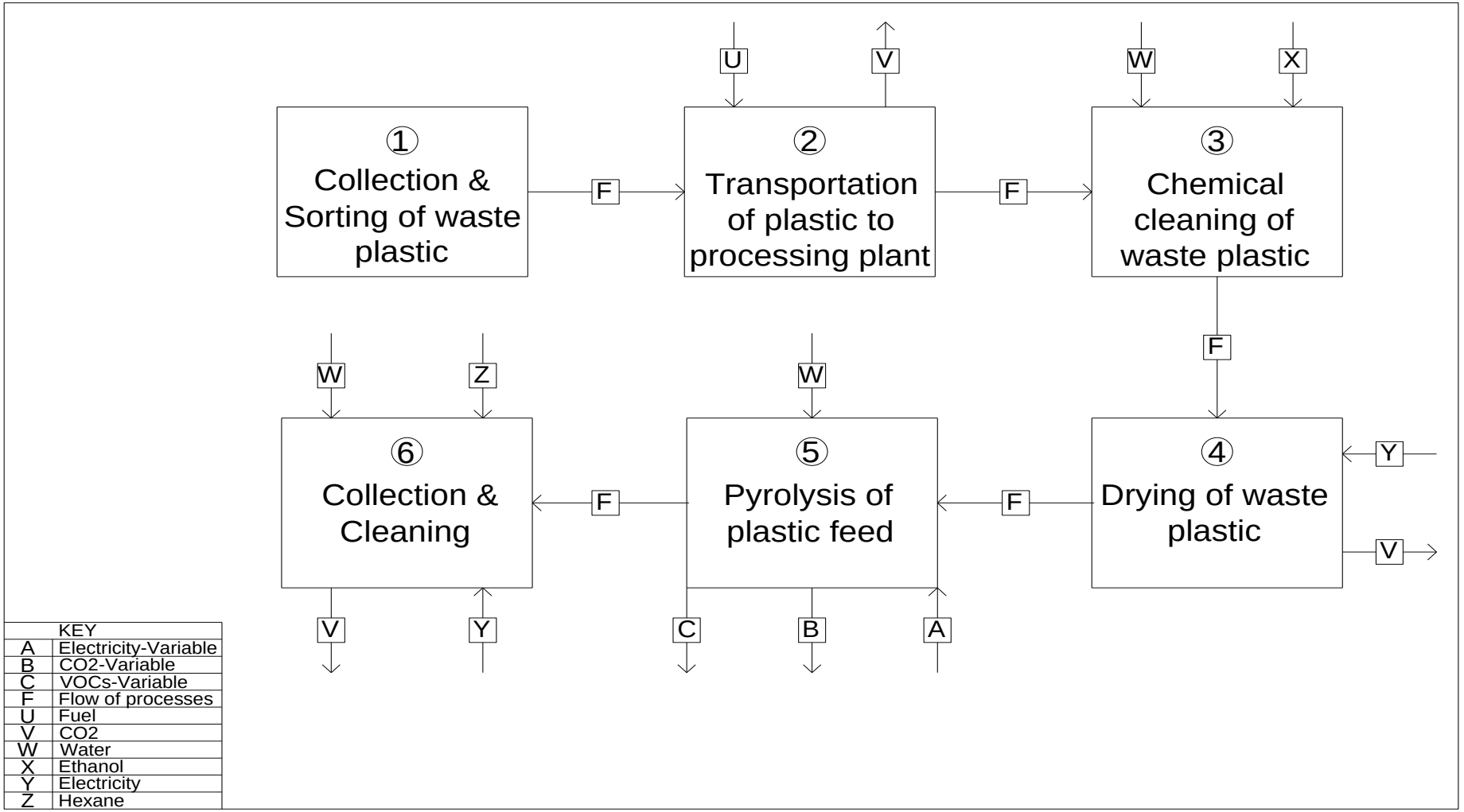

Figure 3.3: Analysis of essential inputs and outputs in the plastic pyrolysis process.

Table 3.3: Gate to gate analysis terminology

Symbol/Term	Definition	Unit
Amount of fuel used	Fuel used by light duty truck	litres
CO_2 Emission Factor	Amount of CO_2 indirectly emitted from producing the same amount of electricity which is used by pyrolysis equipment	$\frac{kg\ CO_2}{kWh}$
Distance Travelled	Distance travelled to and from plant with light duty truck	km
Duration	Time taken to complete pyrolysis reaction	h
Electricity Usage	Total amount of electricity used by equipment	kWh
Energy Requirement	Power rating of equipment	kW
Fuel Consumption	Possible distance that can be travelled per litre of fuel	$\frac{km}{litre}$
Transport CO_2 Emissions	CO_2 emissions from combustion of fuel from engine of light duty truck	kg
Vehicle CO_2 Emission Factor	Amount of CO_2 emitted from vehicle engine combustion of a litre of diesel	$\frac{kg\ CO_2}{litre}$

Depending on the nature of the to-scale pyrolysis processes (individual plastic or mixed plastic), the waste plastic will be sorted and organized (as per step 1 in Figure 3.3.) according to the plastic type (low-density polyethylene, high-density polyethylene, and polypropylene). This is a labour-intensive step and would require the assistance of waste pickers.

After collection and sorting of the waste plastic, the material would be loaded into transportation vehicles. The second is the transportation of the plastic to the processing plant. Transportation of the plastic generally involves shipping of the plastic in suitable combustion engine vehicles. The one key input is the usage of fuel by the vehicle. Consequently, this causes an emission of carbon dioxide which is an output in this sub-process. The amount of carbon dioxide released during transportation is proportional to the amount of fuel consumed by the vehicle. The emissions can be calculated as follows:

$$\text{Transportation } CO_2 \text{ Emissions} = \frac{Distance\ Travelled\ (km)}{Fuel\ Efficiency\ (km\ per\ litre)} \text{ x Vehicle } CO_2 \text{ Emission Factor (kg } CO_2 \text{ per litre of fuel consumed)} \quad (3.7)$$

The quantity of plastic waste collected, sorted and transported is variable, however the vehicle emission factor would scale based on the delivery size.

The third and fourth subprocesses are the plastic preparation steps. The third step involves the chemical cleaning of the waste plastic. This subprocess utilizes cleaning agents such as water and ethanol to remove dirt present on the plastic. Therefore, the major key inputs for this subprocess are these chemicals per kg washed.

The drying (fourth) process is required to remove traces of the cleaning agents left on the plastic after chemical cleaning. This subprocess involves a usage of electricity by the drying equipment. The process indirectly contributes to the carbon dioxide emissions. This is primarily because of the coal-burning activities that are used to produce this electricity. The amount of indirect carbon dioxide emissions can be calculated using carbon emission factors found in literature:

$$CO_2 \text{ Emissions from Electricity Usage (kg } CO_2) = \text{Electricity Usage (kWh) x } CO_2 \text{ Emission Factor (kg } CO_2 \text{ per kWh)} \quad (3.8)$$

The 5th subprocess deals with the actual pyrolysis of the plastic feed. The process utilizes many pieces of equipment such as a heating mantle, vacuum pump, and water circulator which draws electricity. These items would have analogous versions in the scaled-up process, such as electrically heated jacket, large vacuum pump or ejector, and condenser. Therefore, indirect contributions to carbon dioxide emissions are present. Figure 3.3 also includes the output of VOCs which is released during the pyrolysis reaction. In this work, this is estimated experimentally. The calculation of the electricity usage for a specific piece of equipment depends on the energy requirement of that equipment and the duration that the equipment was used. The electricity usage is calculated as follows:

Electricity Usage (kWh) = Energy Requirement (kW) x Duration (h) (3.9)

The cost of electricity used can be calculated using the kilowatt unit cost and the total amount of electricity used:

Cost of Electricity (Rands) = Electricity Usage (kWh) x Unit Cost of Electricity (Rands per kWh) (3.10)

It is important to note that CO_2 emissions, electricity usage, and VOC emissions in step 5 are dependent on the pyrolysis process duration and the quantity processed.

The final subprocess, as specified in Figure 3.3, is the collection and cleaning step. In this step, pyrolysis products such liquid and wax are collected from the equipment. Cleaning of the equipment requires heating of the condensing tube with the water circulator. Indirect contributions to carbon dioxide emissions are present. Additionally, water and solvents are required to clean the apparatus.

CHAPTER FOUR: RESULTS & DISCUSSION

This chapter presents the pyrolysis experimental results with the major focus on product yields, liquid and wax chemical compositions, and VOC emissions. The results from test experiments using black LDPE refuse bags are presented and compared with literature to verify the method. The experiments using single-plastic types (LDPE, HDPE, and PP pellets) are thereafter discussed. The results from the final set of experiments utilizing mixed plastic feed of the three mentioned types are also discussed. The chapter concludes with comments on the plastic feed types which produced the highest product yields and the lowest total VOC peak area percentages, as well as the preliminary gate to gate analysis.

4.1 Test experiments using LDPE refuse bags

Table 4.1 provides a description of operational parameters for the LDPE refuse bag pyrolysis experiments. The LDPE plastic pyrolysis experiments utilizing a feed of refuse bags were given an 'RB' label.

Table 4.1: Operational conditions for pyrolysis experiments using 15g LDPE refuse bags at system pressure of 42 kPa.

Experiment Label	Plastic	Catalyst to Feed Ratio	Operation Temperature (°C)	Reaction Time (h:min)
RB-01	LDPE	Uncatalysed	420	2:17
RB-02		3:100	350	1:45
RB-03		3:100	350	1:48
RB-04		3:100	300	1:50
RB-05		10:100	280	1:35
RB-06		3:100	300	3:57
RB-07		Uncatalysed	240	7:08
RB-08		Uncatalysed	280	6:12

Experiments runs labelled RB-01 to RB08 refer to the varying catalyst to feed ratios, operating temperatures and reaction times. The specified catalyst to feed ratios aligned with the work of

Tekade et al. (2020). The specific catalyst to feed ratios were used to allow for comparison with literature data and verification of the experimental method. The apparatus mass changes for RB-08 are shown in Table A1 in Appendix A. Sample calculation B1 (Appendix B) indicates the calculation procedure for the product mass and yields. Table A2 in Appendix A presents this data. Figure 4.1 and 4.2 shows product yield data for the refuse bag pyrolysis experiments.

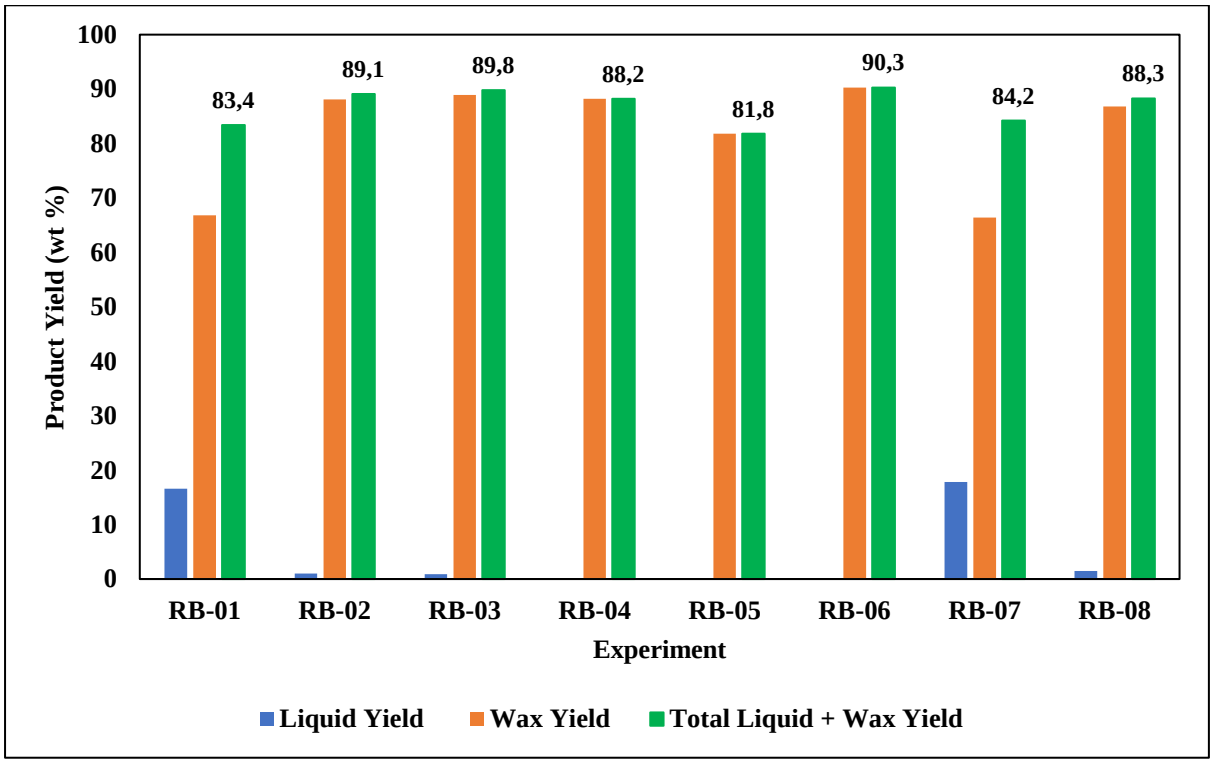

Figure 4.1: Comparison of liquid, wax, and total liquid + wax product yields for uncatalysed and catalysed plastic pyrolysis experiments using feedstock of LDPE refuse bags at temperatures ranging from 240°C to 420°C and a pressure of 42 kPa.

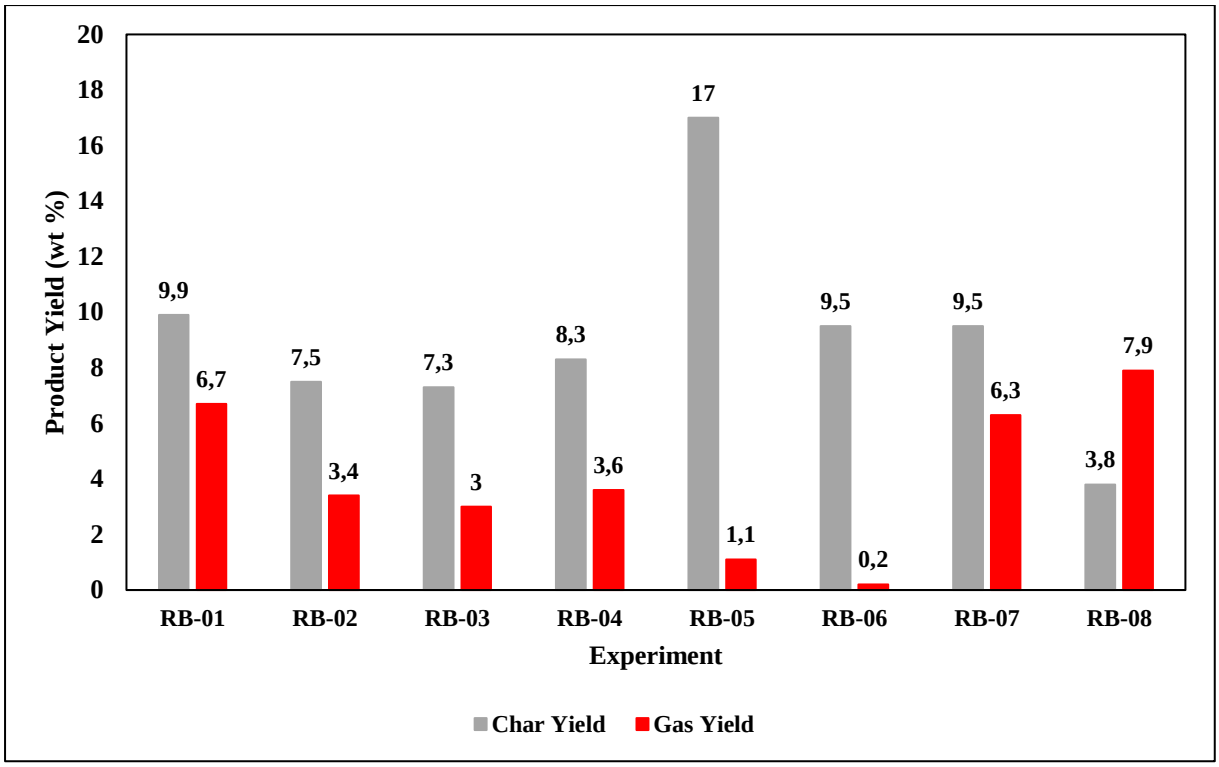

Figure 4.2: Comparison of char and gas yields for uncatalysed and catalysed plastic pyrolysis experiments using feedstock of LDPE refuse bags at temperatures ranging from 240°C to 420°C and a pressure of 42 kPa.

The general trend in the literature for plastic pyrolysis experiments is to designate the waxy dense product as a 'liquid', indistinct from the low density, viscous liquid product Miandad et al., (2019). For this reason, additional data is shown in Figure 4.1 (total liquid + wax yield). In the current plastic pyrolysis work, a similar experimental set-up was used to that of the research performed by Senthil Kumar et al. (2017). Due to the similarities with the experiments (such as temperatures, plastic type, and operational pressure), the test experiments may be compared to the data found in the literature by Senthil Kumar et al., (2017). The uncatalysed LDPE experiment from literature was performed at 240°C with a heating rate of 10°C per minute and a subsequent hold. This can be compared to RB-07 which was also performed at 240°C. According to the literature, a 75 wt % yield of liquid product was formed. The experiment in the current work at 240°C produced a total yield of 84.2 wt %. By comparing the data, while the results are similar, a 12.3 % increase in this work was obtained. Reasons for the difference may be due to the possible difference in density between the experimental and literature feed plastic as the refuse bag thickness may be different based on the manufacturer. The precise degree of vacuum applied was approximately 42 kPa in this work; however, no pressure value

was reported in the literature study. The precision of the heating rate may also affect the yield. The effectiveness of the insulation for the heating mantle used in both studies could also affect the yield.

Figure 4.1 indicates that all LDPE refuse bag pyrolysis experiment yields measured in this work, ranged between 80 wt % and 90 wt %, which indicates consistency. A few changes in yields between the experiments are expected since changes were made to the operational parameters. To ensure that the experimental methods were being performed consistently, RB-02 and RB-03 were performed with virtually identical operational conditions. Figure 4.1 indicates that RB-02 and RB-03 produced a total liquid and wax yield of 89.1 wt % and 89.8 wt % respectively. The error between the results was only 0.78 %. The experimental method is therefore consistent, and repeatability of experiments is obtainable.

The change in operational parameters had significant effects on the reaction time to completion. Reaction times for the LDPE refuse bag pyrolysis experiments were listed in Table 4.1. RB-07 at 240°C took the longest to complete (7h 8m). The fastest experiment was RB-05 with the highest catalyst ratio, at a temperature of 280°C. The process duration was 2h 17m for RB-01 and 7h 8m for RB-07. The reason for this is due to the difference in the quantity and rate of the energy supplied to the reacting plastic. In RB-01, a larger quantity of energy is supplied to the plastic as compared to RB-07. Due to the increase in energy, the plastic polymer molecules can break down more easily. The rate at which these polymer chains break down increase. Since more chains break per unit time, the overall process duration decreases. Similar results were observed by Harussani et al. (2022).

The char and gas yields for RB-01 to RB-08 are plotted in Figure 4.2 due to scale. This data helps to further understand the effects of operational parameters on the pyrolysis reaction and the products obtained. The use of catalyst played a significant role regarding the production of emissions. According to Figure 4.2, RB-01, RB-07, and RB-08 produced the highest yields of gas emissions (6.7 wt %, 6.3 wt %, and 7.9 wt % respectively). Importantly, these experiments were performed without the use of catalyst.

The zinc oxide catalyst was used for all other refuse bag pyrolysis experiments. RB-02 and RB-03 used a catalyst to feed ratio of 3:100 (mass basis) and produced a gas yield of 3.4 wt % and 3 wt % respectively. Increasing the catalyst to feed ratio to 10:100 (experiment RB-05) produced a low gas yield 1.1 wt %. These results indicate that the zinc oxide catalyst caused a decrease in the production of emissions. Figure 4.1 shows that increasing the amount of catalyst

in an LDPE pyrolysis experiment does not guarantee an increase in the liquid and wax yield. Figure 4.2 shows that RB-08 produced the lowest char yield (3.8 wt %). Char is not necessarily an undesirable product. However, having a large quantity of char would imply that the maximum possible yield of liquid and wax will decrease. It is important to identify catalyst to feed ratios which produce both low gas yields and high desirable product yields (liquid/wax).

Although higher temperatures may decrease the pyrolysis reaction time (Harussani et al., 2022), the faster reactions do not guarantee high liquid and wax yields. This is evident in Figure 4.1. RB-01 was performed at one of the highest temperatures considered for this class of experiments, however the liquid and wax yield was one of the lowest (83.4 wt %). According to Figure 4.2, the experiment RB-01 also produced the second highest yield of char (9.9 wt %). A few comments could also be made on the influence of temperature. According to Papuga et al. (2016), high temperatures may certainly promote high rates of polymer degradation. A high conversion of reactant plastic to desirable products (liquid and wax) may be obtained with higher temperatures. However, increasing the processes temperatures too high may cause a significant production of gas phase molecules. This is due to the large quantity of energy being supplied which breaks down the polymer chains more easily. Apart from forming liquid and wax products, the polymer chains may have enough energy to decompose into gas phase products (Papuga et al., 2016). This trend from literature was observed in this work as in Figure 4.2 which shows that RB-01 (at high temperatures of 420°C) produced a relatively higher gas yield than the other reactions.

Figure 4.3 shows the results from the chemical composition analysis of the liquid product from RB-01. These analyses were conducted in triplicate for each product sample with variations in peak percentages not exceeding 0.1-0.5 %. The results from Figure 4.3 were compared to chemical analysis results of LDPE pyrolysis liquid from Tekade et al. (2020). The comparison of results indicated that the current chemical analysis detected many similar components reported in literature. The alkanes detected both in current results and literature were undecane, octadecane, dodecane, tetrapentacontane, and tridecane. The alkenes detected in this study and in literature were 1-pentadecene, nonadecene, 1-tridecene (Tekade et al., 2020).

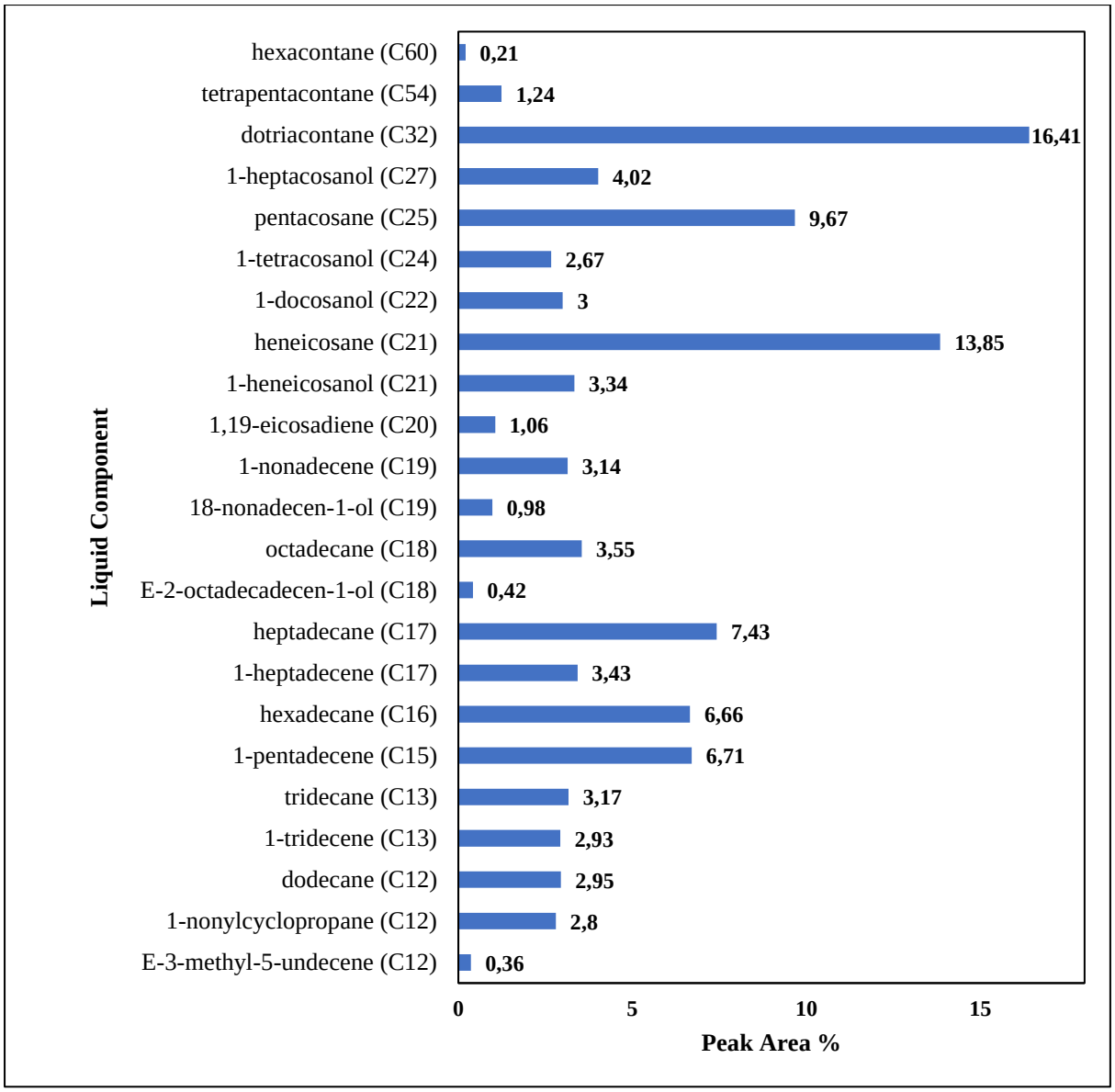

Figure 4.3: Comparison of peak area % of different components in liquid product for uncatalysed plastic pyrolysis of LDPE refuse bags at 420°C and 42 kPa (RB-01).

Due to the nature of the liquid product (high viscosity), one would expect hydrocarbon molecules with high carbon number molecular chains. Figure 4.3 does show that many components formed which have high carbon numbers. Components such as dotriacontane (C_{32}), and 1-heptacosanol (C_{27}) possess similar chain lengths to components in literature such as hexatriacontane (C_{36}) and 1-heneicosanol (C_{21}) (Tekade et al., 2020). Since the experiments were not identical to literature and differences were present (such as feed mass), some differences regarding the chemical analysis results should be expected. That is, similar product classes to literature would be expected as opposed to identical compositions. Nevertheless, many components detected in the current work either matched with literature or had similar

chain lengths to the components from literature. The results of the chemical analysis test experiments therefore validate the experimental method used in the GC-MS analysis.

4.2 Product yields of pyrolysis experiments using a feedstock of pure LDPE, HDPE, or PP pellets

Table 4.2 provides a description of the pyrolysis experiments which utilized a feedstock of 15g of pure LDPE, HDPE, or PP plastic pellets. The product yield results are presented in Figures 4.4 and 4.5.

Table 4.2: Operational conditions for pyrolysis experiments using LDPE, HDPE, and PP plastic pellets at 450°C and 42 kPa.

Experiment Label	Plastic	Catalyst to Feed Ratio	Reaction Time (h:min)
IP-01	LDPE	Uncatalysed	27:40
IP-02		5:100	13:45
IP-03		10:100	10:50
IP-04	HDPE	Uncatalysed	4:50
IP-05		5:100	3:20
IP-06		10:100	3:10
IP-07	PP	Uncatalysed	2:55
IP-08		5:100	2:45
IP-09		10:100	2:20

The equipment used for these experiments is similar to that of Tekade et al. (2020). Upon review of the literature, it was found that both uncatalysed and catalysed pyrolysis experiments were performed in that study. A zinc oxide catalyst was used in the literature in various catalyst to feed ratios such as 3:100, 5:100, 10:100, and 15:100 (Tekade et al., 2020). Vacuum pressures ranging from atmospheric pressure to 47 kPa were implemented, with improved product yields obtained at lower vacuum pressures. For the current work, a zinc oxide catalyst was readily available. The vacuum pressures for this work were approximately 42 kPa. This work builds

on the study of Tekade et al. (2020), with the addition of the emissions testing and with variations in the feed material.

Pyrolysis temperatures were not provided in Tekade et al. (2020). However, the literature mentioned that a 300 W heating mantle was used. Heating mantles with a 300 W power rating generally have a maximum temperature between 450°C and 500°C (LabFriend, 2022). For this reason, all plastic pyrolysis experiments in this work were performed at 450°C to align with the common literature. The heating rate of 10°C per min was also selected to match the general literature. For the pure plastic pyrolysis experiments, the catalyst to feed ratios were varied according to Table 4.2.

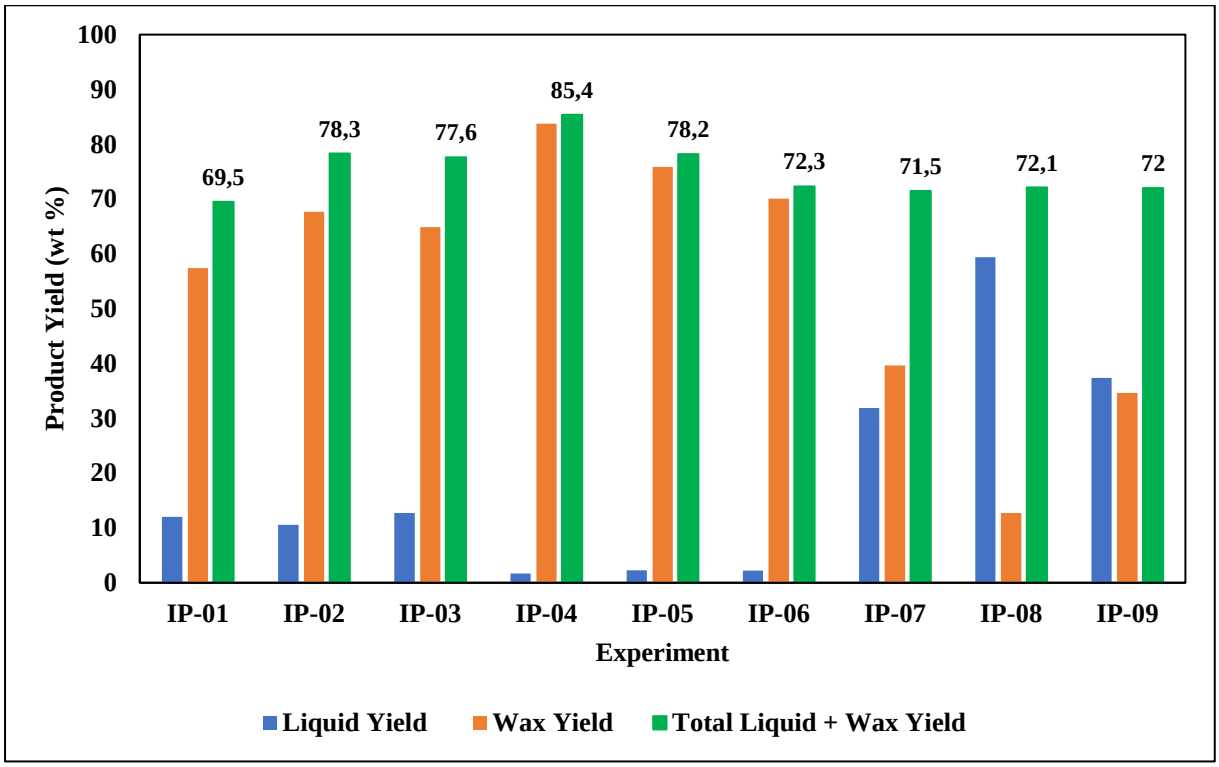

Figure 4.4: Comparison of low-density liquid, wax, and total liquid + wax product yields for uncatalysed and catalysed plastic pyrolysis experiments using feedstock of LDPE, HDPE, and PP pellets at 450°C and 42 kPa.

The results shown in Figure 4.4 indicate a few significant trends. IP-01 to IP-03 refer to the uncatalysed and catalysed LDPE pyrolysis experiments. The low-density liquid yield for these three experiments showed consistencies and ranged from 10.5 wt % (IP-02) to 12.7 wt % (IP-03). IP-01 (uncatalysed) produced a total liquid + wax yield of 69.5 wt %. According to the data shown, the addition of the zinc oxide catalyst (5:100 catalyst to feed ratio) increased the total liquid + wax yield by 8.8 wt %. Moreover, the low-density liquid yield decreased, and the waxy liquid yield increased. In this case, the use of the zinc oxide catalyst lowered the energy requirements for the conversion of plastic polymer to liquid and wax products. However, the wax product is the intermediate between the plastic polymers and the low-density liquid product. Therefore, by lowering the energy requirement, a higher conversion to wax was achieved instead of an increase in the low-density liquid yield. The use of a 10:100 catalyst ratio for the LDPE pyrolysis experiments (IP-03) produced a slightly lower total liquid and wax yield (77.6 wt %) as compared to IP-02 (78.3 wt %). As mentioned before, simply adding a higher quantity of catalyst does not guarantee a higher total liquid and wax yield.

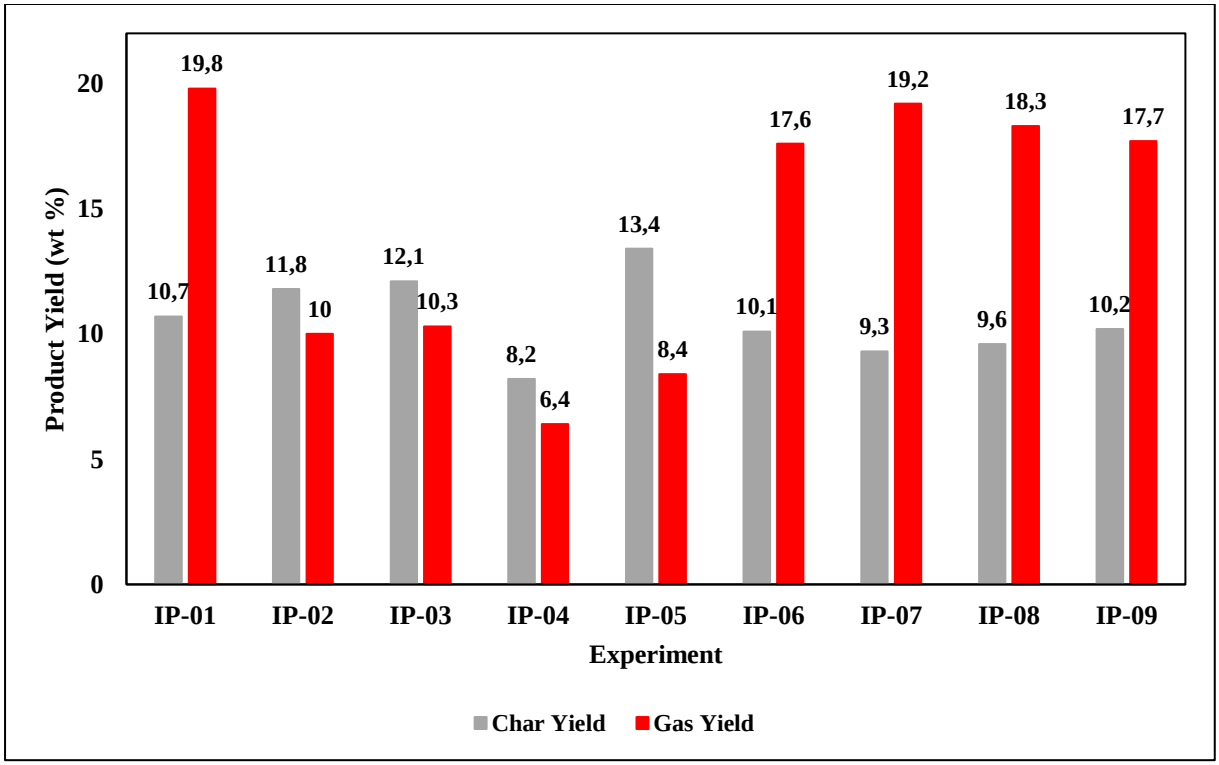

Figure 4.5: Comparison of char and gas yields for uncatalysed and catalysed plastic pyrolysis experiments using feedstock of LDPE, HDPE, and PP pellets at 450°C and 42 kPa.

According to Figure 4.5, the usage of a 10:100 ratio (IP-03) caused a 0.3 wt % increase in the production of gas which is virtually insignificant. Figure 4.5 also shows that the use of zinc oxide catalyst caused a decrease in the yield of emissions from 19.8 wt % (IP-01) to 10 wt % and 10.3 wt % (IP-02 and IP-03 respectively). This trend aligns with the results from the refuse bag pyrolysis experiments in the test measurements. The data from Tekade et al. (2020) shows that the total liquid + wax yields at approximately 50 kPa, increases with the addition of the 5:100 catalyst to feed ratio to the LDPE pyrolysis experiment as compared to the thermal pyrolysis experiment at 50 kPa. Thereafter, the literature shows that the total liquid + wax yield does not increase drastically. A similar trend was observed for the LDPE pellets pyrolysis experiments. This reinforces that an optimum catalyst to feed ratio is required to both lower gas emissions and increase desirable product yields.

In the HDPE experiments, the total liquid + wax yield of 85.4 wt % (IP-04) was similar to the results from the work of Budsaereechai et al. (2019b) where plastic pyrolysis of HDPE using bentonite clay was implemented (yielding 86.9 wt % liquid in a fixed bed reactor at 500°C). The high yields obtained in the current work indicate that lower temperatures without catalyst may be as effective as other catalytic experiments at high temperatures (specifically for HDPE). Lower operation temperatures decrease the energy requirement of the pyrolysis process thereby reducing the energy costs incurred. Figure 4.4 shows that unlike the LDPE pyrolysis experiments in which the total liquid + wax yield increases as the catalyst to feed ratio was increased to 5:100, the HDPE total liquid + wax yields decrease with an increase in catalyst to feed ratio. According to literature, LDPE has a high abundance of branched molecules whereas HDPE is composed of linear hydrocarbon chains with a low occurrence of branching. Generally, energy requirements for pyrolysis of the LDPE pellets is lower due to these branches in the molecules (Sogancioglu et al., 2017). Molecular bonds both in the branches (easier to breakdown) and in the straight chains need to be broken in order for the LDPE polymer to decompose. Comparatively, the molecular bonds in the straight chains need to be broken in the thermal degradation of HDPE. This would imply that LDPE would pyrolyze faster than HDPE. However, this trend was not observed in the current experiments. In this study, HDPE pyrolyzed faster in comparison to LDPE. This may be attributed to the particle (pellet) size of HDPE (3.5 mm x 3 mm) compared to that of LDPE (4.5 mm x 2.5 mm) available, although this is a small difference. Luo et al. (2010) indicates that relatively higher gas yields are formed with feed plastics of small particle sizes. Evidence for this occurrence in this work is presented in Figure 4.5. Additionally, the plastic pellets used in this work had likely undergone

compounding, which may increase their heat resistance, and resistance to pyrolysis. The degree of compounding used by the supplier is assumed to be more significant for the LDPE pellets, as it would generally be more critical to improve its property stability in specific applications.

Analysing IP-04 to IP-06, it can be observed that the gas product fraction increases significantly as the catalyst to feed ratio is increased. Since a higher rate of degradation was observed for HDPE, the energy requirement of the HDPE plastic is lower as compared to that of LDPE. Increasing the catalyst to feed ratio lowers the pyrolysis energy requirement even further. This contributes to more gas product being formed. The trend is evident for IP-04 to IP-06 in Figure 4.4 and 4.5 since the total liquid + wax yield decreases while the gas yield increases. When using a catalyst to feed ratio of 10:100, higher gas yields were observed for HDPE pyrolysis (17.6 wt %) as compared to LDPE pyrolysis (10.3 wt %). The process duration of HDPE pyrolysis (less than 5 h) is consequently much shorter compared to LDPE pyrolysis (10 h to 28 h). It may be possible that the pyrolysis of HDPE to liquids with high yields could be effectively conducted at temperatures lower than 450°C using catalyst.

Unlike the HDPE and LDPE reactions, significant yields of low-density liquid were produced in PP pyrolysis (Figure 4.4). In IP-08 and IP-09, the liquid yields form the major portion of the total liquid + wax yield. Low-density liquid yields increased to 54.4 wt % (IP-08) in PP experiments as compared to the maximum of 12.7 wt % (IP-03) and 2.3 wt % (IP-05) for LDPE and HDPE respectively. This clearly shows that the polymer molecules in polypropylene were able to crack more easily into low-density liquid instead of forming the intermediate wax. The PP pyrolysis experiments show a similar trend to the LDPE pyrolysis where the total liquid and wax yield increase when a catalyst ratio of 5:100 is used and thereafter decreases slightly when 10:100 is used.

The total liquid + wax yields for the polypropylene did not vary significantly between runs. The PP polymer chains were able to crack more easily and form a significant amount of gas molecules. This is evident in Figure 4.5 as the gas yields for PP experiments were higher than most of the gas yields for the LDPE and HDPE experiments.

4.3 Product yields of pyrolysis experiments using a feedstock of mixed LDPE, HDPE, and PP pellets

Since plastic waste is seldom sorted into specific plastic types (such as LDPE, HDPE, and PP), plastic pyrolysis processes which only deal with singular plastic types are limited. For this reason, it is important to research into the area of mixed plastic pyrolysis processes. Hence, in addition to the pure plastic pyrolysis experiments, mixed plastic pyrolysis experiments were performed. The operational parameters for each experiment are listed in Table 4.3. Three composition variations of the mixed plastic waste totalling 15g per run were used. Compositions such as 15 wt % LDPE, 45 wt % HDPE, and 40 wt % PP are typical to feedstocks in plastic pyrolysis processes according to literature (Kaminsky, 2021). Plastic compositions for experiment sets MP-04 to MP-06 and MP-07 to MP-09 were unique to this work. Using various compositions not found in literature provides novel and useful data on plastic pyrolysis experiments to observe the effect of composition changes on the pyrolysis process.

The product yield results from the mixed plastic waste experiments are presented in Figure 4.6 and 4.7.

Table 4.3: Operational conditions for pyrolysis experiments using a mixed plastic feed at 450°C and 42 kPa.

Experiment Label	Plastic Composition (wt %)			Catalyst to Feed Ratio	Reaction Time (h:min)
	LDPE	HDPE	PP		
MP-01	15	45	40	Uncatalysed	13:54
MP-02				5:100	7:50
MP-03				10:100	7:10
MP-04	32.3	34.52	33.18	Uncatalysed	15:57
MP-05				5:100	12:45
MP-06				10:100	12:24
MP-07	65	20	15	Uncatalysed	17:45
MP-08				5:100	15:40
MP-09				10:100	15:25

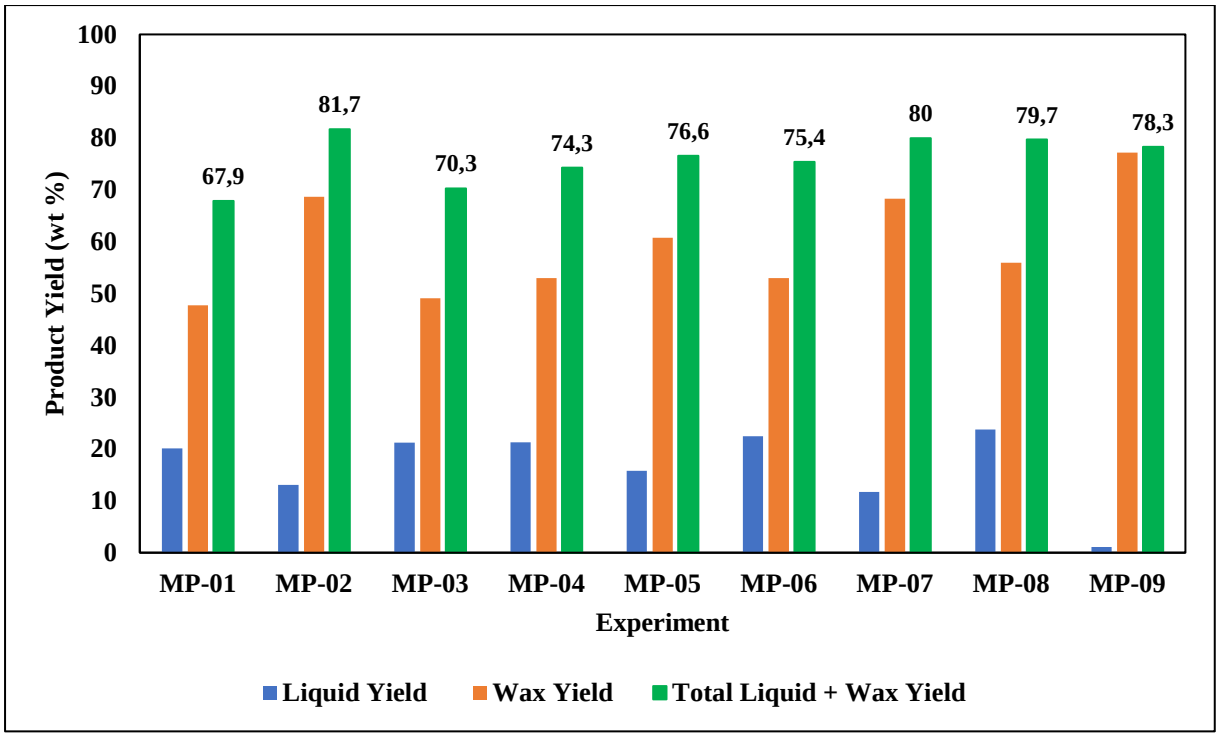

Figure 4.6: Comparison of liquid, wax, and total liquid + wax product yields for uncatalysed and catalysed plastic pyrolysis experiments using feedstock of mixed plastic (MP) comprising LDPE, HDPE, and PP pellets at 450°C and 42 kPa.

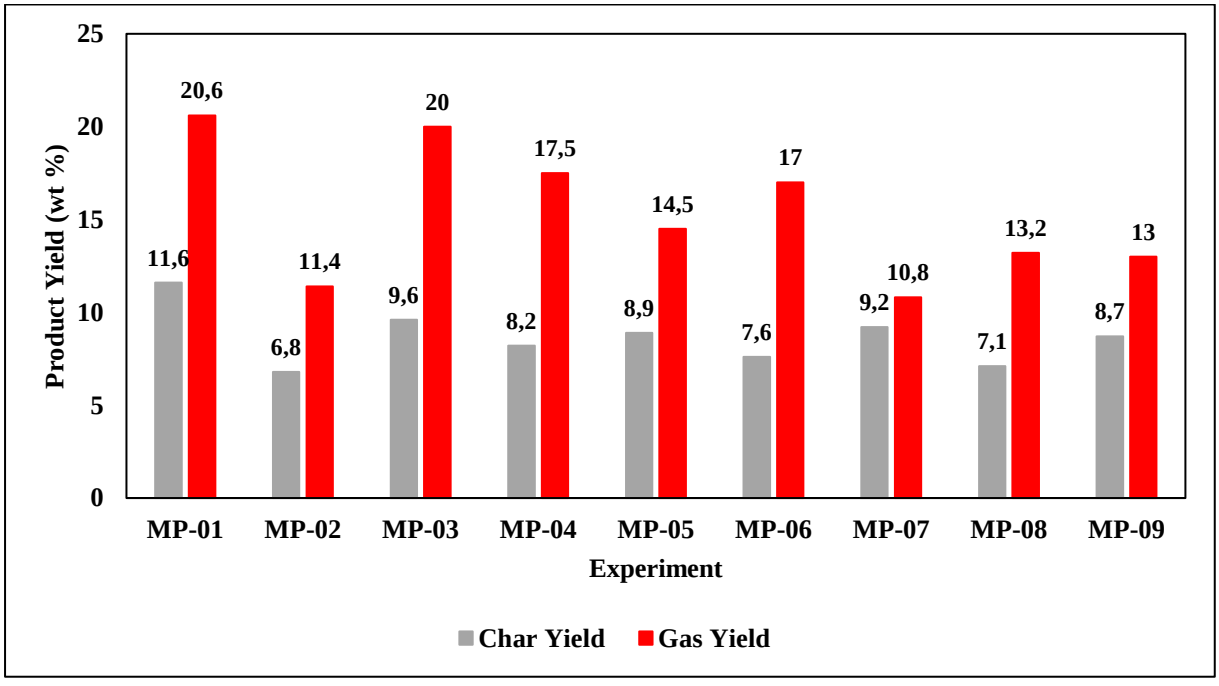

Figure 4.7: Comparison of char and gas yields for uncatalysed and catalysed plastic pyrolysis experiments using feedstock of mixed plastic MP comprising LDPE, HDPE, and PP pellets at 450°C and 42 kPa.

The mixed plastic pyrolysis experiments (indicated in Table 4.3) were performed using similar operational parameters (catalyst to feed ratio, temperature, pressure) compared to the pure plastic pyrolysis experiments presented in Table 4.2. The liquid, wax, and total liquid + wax yields for the mixed plastic pyrolysis experiments have been calculated and are present in Figure 4.6. Compositions included LDPE proportions such as 15 wt % (MP-01 to MP-03) and 65 wt % (MP-07 to MP-09). The large difference in wt % was so that the effects of plastics being both the minor and major proportion in a mixture of plastic could be observed.

MP-01 to MP-03 were the uncatalysed and catalysed pyrolysis experiments performed for a plastic composition of 15 wt % LDPE, 45 wt % HDPE, and 40 wt % PP. There are a few significant observations indicated in Figure 4.6. Similar to the pure plastic pyrolysis experiments (Figure 4.4), MP-01 to MP-03 show a significant change in total liquid + wax yield when zinc oxide catalyst was used as compared to the uncatalysed process (MP-01). Using a 5:100 ratio yielded a 13.8 wt % increase in total liquid (81.7 wt % total liquid + wax) when compared to MP-01 (67.9 wt % total liquid + wax). The addition of the zinc oxide catalyst reduces the energy requirement for the plastic pyrolysis cracking. Therefore, a higher conversion of plastic polymer to desirable products (total liquid + wax) is obtained as compared to the uncatalysed process.

In addition to MP-02 (15 wt % LDPE, 45 wt % HDPE, 40 wt % PP) exhibiting the highest total liquid + wax yield for the specific composition (MP-01 to MP-03), it also exhibits the highest yield when compared to the entire set of compositions. This is quite significant and highlights another trend which is also observed in the pure plastic pyrolysis experiments. For the pure plastic experiments (Figure 4.4), the highest total liquid and wax yield was obtained for IP-04 (85.4 wt %). This was an HDPE plastic pyrolysis experiment. The liquid + wax yields for the HDPE experiments (IP-04 to IP-06) were also relatively high as shown in Figure 4.4.

The HDPE pyrolysis energy requirement may be higher than that of the polypropylene plastic. For this reason, the HDPE plastic pyrolysis experiments may be able to form higher liquid + wax yields while simultaneously minimizing the gas yields produced. This was evident from MP-02 in Figure 4.7 since the gas yield is the second lowest in the set (11.4 wt %). The high gas yields in MP-01 may be caused by the significant quantity of PP in the plastic (lower energy requirements for polymer to crack into the gas phase). In experiments found in the literature (Kaminsky, 2021b), a similar composition set was used in plastic pyrolysis experiments (15 wt % LLDPE, 45 wt % HDPE, 40 wt % PP). The experiments were implemented in a

fluidized bed reactor at 510°C with an inert nitrogen atmosphere. Total gas yields of 4.7 wt % were observed (Kaminsky, 2021b). This is significantly lower compared to the current work. The use of the LLDPE (in literature) instead of the LDPE (current work) may be a factor in the lower yield of emissions, as well as the reactor dynamic differences and temperature differences. The total liquid + wax yield of the literature experiment (95 wt %) was also significantly higher than the current experiment. Apart from LDPE, HDPE, and PP, LLDPE would be a suitable plastic to investigate in plastic pyrolysis experiments in future work.

Experiments MP-03 to MP-04 a composition of 32.3 wt % LDPE, 34.52 wt % HDPE, and 33.18 wt % PP was employed. The proportions of each plastic were similar (1-2 % differences). According to Figure 4.6, MP-06 to MP-06 produced relatively similar total liquid + wax yields ranging from 74.3 wt % to 76.6 wt %. The total liquid + wax yield increased with an addition of catalyst (MP-05 yielded 76.6 wt %). The 5:100 zinc oxide to feed ratio generally produced the highest total liquid + wax yield in experiments for a certain plastic type/composition. The 10:100 ratio generally produced a lower yield compared to the 5:100 ratio which may still be higher than the uncatalysed experiment. Although the 10:100 ratio reduces the energy requirement, a higher conversion is observed. However, more gas phase molecules may form. Therefore, the liquid + wax yield may still be higher than the uncatalysed experiment, but lower than the 5:100 experiment due to the formation of gas molecules. This is also evident in Figure 4.5.

According to Figure 4.6, the gas yield increases to 17 wt % in MP-06 (10:100) from 14.5 wt % in MP-05 (5:100). The feed composition of 32.3 wt % LDPE, 34.52 wt % HDPE, and 33.18 wt % PP was chosen since a similar composition type was found in literature. In Senthil Kumar et al. (2017), 32.3 wt % LDPE, 33.18 wt % PP, and 34.52 wt % polystyrene was used. The proportions of LDPE and PP are identical to the current work however polystyrene was used in the literature compared to the HDPE in the current work. The experiments in literature were also performed under vacuum with a similar experimental setup (Figure 2.10 in chapter 2) to that of the current work. The literature experiments performed at 240°C yielded 66.7 wt % total liquid + wax compared to the current work uncatalysed experiment (74.3 wt %) (Senthil Kumar et al., 2017). The residue in the literature experiment was also much higher (25.85 wt % char) as compared to MP-04 (8.2 wt % char). The current mixture with HDPE therefore produced a higher yield of desirable products as compared to the literature experiment with polystyrene.

MP-07 to MP-09 represented plastic pyrolysis experiments using a feed composition of 65 wt % LDPE, 20 wt % HDPE, and 15 wt % polypropylene. The use of a major proportion of LDPE is significant. The process duration (Table 4.3) for MP-07 to MP-09 is relatively longer than that of MP-04 to MP-06 (32.3 wt % LDPE used). In this work LDPE is the component that requires the longest time to pyrolyze. The liquid + wax yields for MP-07 to MP-09 were relatively similar. However, the yield decreased insignificantly from MP-07 to MP-08. by 0.3 wt %. Nevertheless, relatively high liquid + wax yields were observed in all the experiments with this composition. The high proportion of LDPE would explain the similarities in comparison to the LDPE refuse bag experiments. Relatively low gas yields were present in MP-07 and MP-09 (ranging from 10.8 wt % to 13 wt %). These values are similar to the pure LDPE plastic pyrolysis experiment gas yields for IP-02 and IP-03.

4.4 Chemical analysis of liquid and wax products obtained from pure plastic pyrolysis of LDPE, HDPE, and PP

Tables 4.2. and 4.3 provided a list of experiments that were performed using the plastic pyrolysis process. During the pyrolysis process, two condensed products were formed (low-density liquid and wax product). Figures 4.8 and 4.9 show the GC-MS peak area % for various components in the liquid and wax products of IP-01 (uncatalysed LDPE feed). As mentioned previously, this work did not include the standard sample calibration of each emission component on the GC-MS as this would require the purchase of hundreds of standardised solutions of various chemicals. Therefore, absolute concentrations of the components could not be determined. In this case, the peak percentage area method is used (Shimadzu, 2022). In this method for chemical analysis using GC-MS, identifying the peak area percentage of a specific component in the chemical analysis runs is used to indicate the relative changes of the amount of the component. The analyses were run in triplicate and GC-MS peak area % was estimated within a repeatability of 0.1-0.5 %.

The GC-MS peak area data provides an indication of the carbon numbers of components expected from the plastic pyrolysis experiments at the conditions used in this work. The chromatograms for the liquid and wax analysis from IP-01 are presented in Figures A1 and A2 in Appendix A.

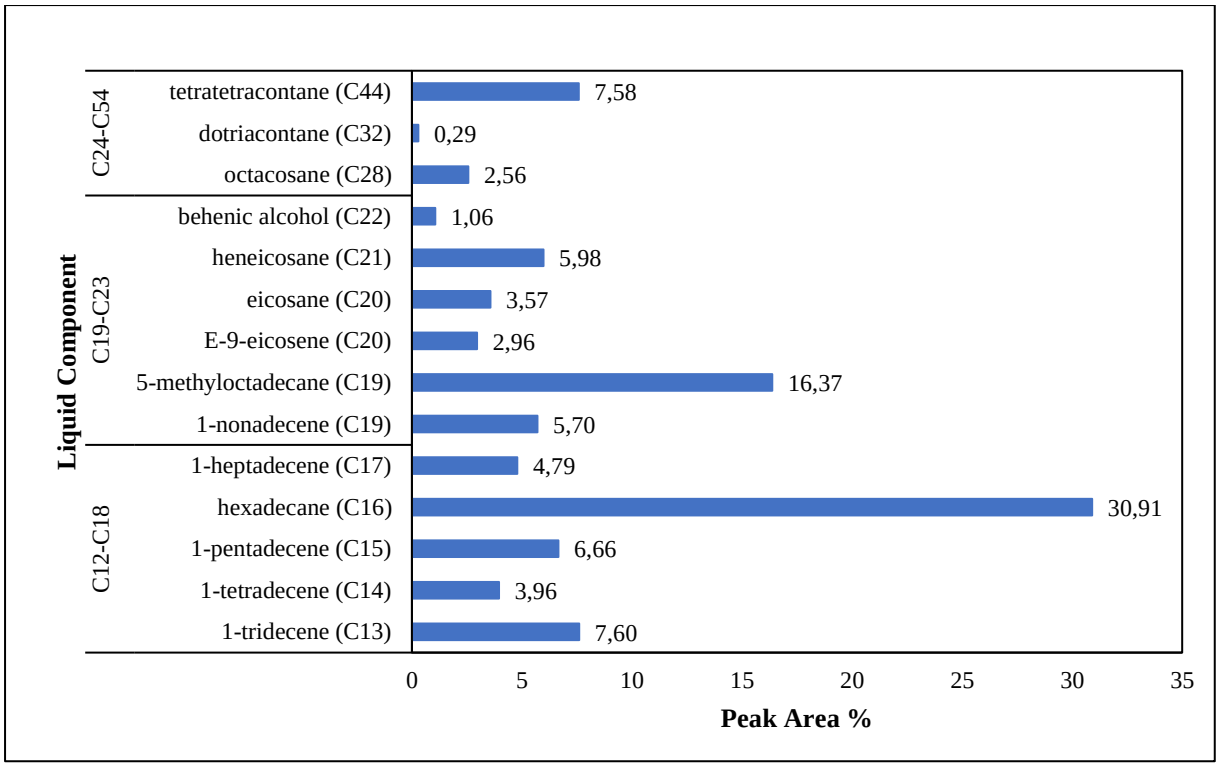

Figure 4.8: Comparison of peak area % of various components in the liquid product from uncatalyzed LDPE pyrolysis at 450°C and 42 kPa (IP-01).

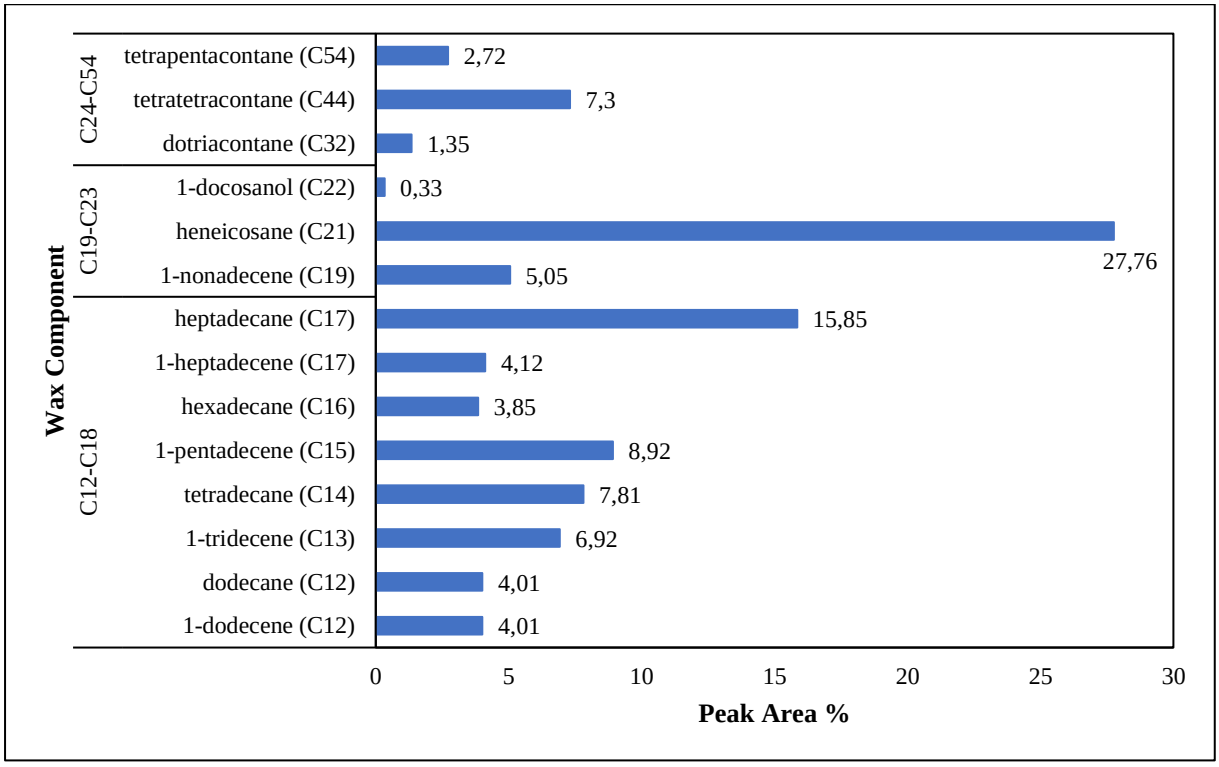

Figure 4.9: Comparison of peak area % of various components in the wax product from uncatalyzed LDPE pyrolysis at 450°C and 42 kPa (IP-01).

The liquid products contain hydrocarbon components with carbon numbers ranging from C_{13} to C_{44}. Many components present in Figure 4.8 such as 1-pentadecene, 1-tetradecene, and 1-tridecene were present in literature chemical analyses of LDPE pyrolysis products (Tekade et al., 2020). This was expected since the experiments were performed using similar operating conditions. Figure 4.8 indicates that many of the components had a carbon number less than C_{20} (C7-C15 alkanes fall approximately into the VOC range, with larger molecules falling in the semi-VOC range). However, the wax analysis results (Figure 4.9) indicate larger proportions of long chain hydrocarbons. According to the data, heneicosane (C21) has a peak area percentage of 5.98 % in the liquid product (likely dissolved in lighter liquids). In the wax product, this value increased to 27.76 %. Furthermore, high carbon number components such as tetrapentacontane (C54) were present in the wax product but not the liquid product. The chain length of the components affects the volatility of products within the pyrolysis process. From the experiments, it was observed that the wax product condensed more easily (built up in the condensing tube) than the liquid product (condensed in the collection flask). The process of the wax product condensing more easily would imply that the wax has a relatively lower volatility as compared to the liquid.

With hydrocarbons such as the alkanes present in the chemical analysis results, boiling points generally increase with an increase in molecular size and chain length (LibreTexts, 2022). This would explain why a larger proportion of higher chain length components are present in the wax product as compared to the liquid product. The chromatogram for the liquid product (Figure A1 in Appendix A) indicates relatively lower peak intensities towards the end of the analysis as compared to the wax product chromatogram. This is because of the ramp temperature analysis method used for the GC-MS. The oven temperature increases to higher temperatures (above 250°C) towards the end of the analysis. This allowed the less volatile components to reach the detector. In effect, the peaks of low volatility components are produced towards the end of the chromatogram. Since the wax product had fewer volatile components compared to the liquid product, the wax chromatogram would be expected to contain higher intensity peaks towards the end of the analysis period. This is evident since high carbon-number molecules such as tetrapentacontane (C_{54}) were detected at a retention time of approximately 69 minutes (Figure A2 in Appendix A).

One of the important reasons for chemical analysis of the liquid and wax products is to determine if these products have similarities to certain fuel types. This would provide an indication of how useful the products are. Fuel types may be classified based on the

composition of components in the fuel. Fuel classifications may be done according to the chain length (carbon number) indicated by these components. Fuels such as gasoline generally have carbon numbers ranging from C_4 to C_{12} (Altin and Eser, 2004). Since the liquid and wax products generally have components with carbon numbers ranging from C_{13} and upwards, the products may not have properties representing that of the gasoline fuel. According to the literature, diesel has been defined to have many different hydrocarbons such as alkanes, naphthene, and aromatics which have carbon numbers ranging from 9 to 27 (Kar et al., 2018). From the GC-MS results for the liquid product, molecules ranging from 1-tridecene (C_{13}) to 1-docosanol (C_{22}) may fall into this category. The data shows that more than 89 % of the liquid components has carbon numbers ranging from C_9 to C_{27}. This may indicate that the plastic pyrolysis products may have similar properties to that of diesel or biodiesel. Further thermophysical property analysis of these components was not possible due to the small sample size generated per run.

Figures 4.10 and 4.11 show the peak area % for various components in the liquid and wax products of IP-02. In comparison to IP-01 (uncatalysed), IP-02 was performed using a 5:100 zinc oxide catalyst to feed ratio. The results for IP-03 where a 10:100 zinc oxide catalyst to feed ratio are presented in Appendix A Figures A3 - A4.

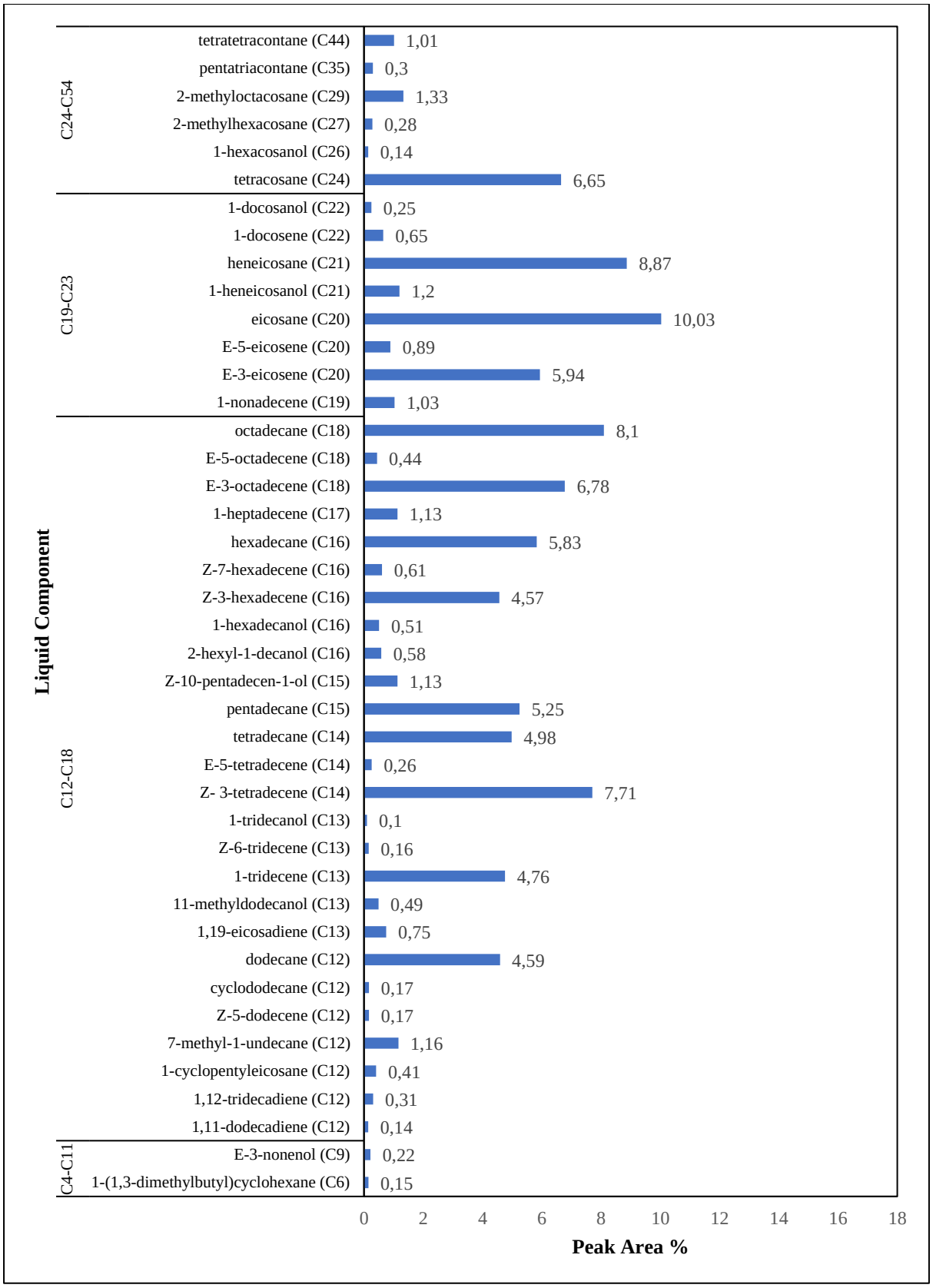

Figure 4.10: Comparison of peak area % of various components in the liquid product from LDPE pyrolysis using a 5:100 zinc oxide catalyst to feed ratio at 450°C and 42 kPa (IP-02).

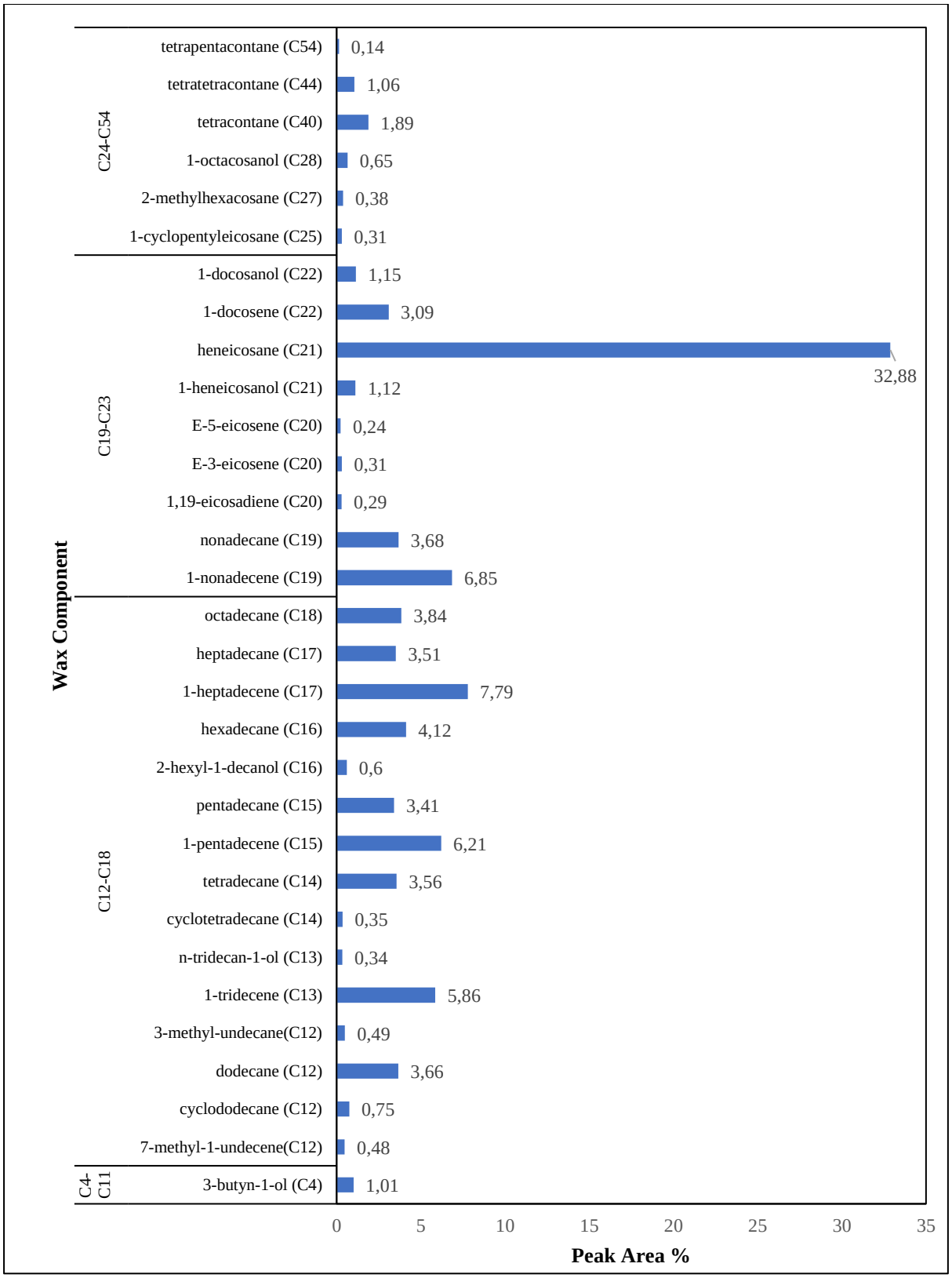

Figure 4.11: Comparison of peak area % of various components in the wax product from LDPE pyrolysis using a 5:100 zinc oxide catalyst to feed ratio at 450°C and 42 kPa (IP-02).

According to the data in Figure 4.10, the peak area % of high carbon number (C24-C54) components such as tetratetracontane in the liquid product reduced from 7.58 % (IP-01) to 1.01 % (IP-02) and to 2.01 % (IP-03) when a catalyst of zinc oxide was used as compared to the uncatalysed reaction (IP-01). dotriacontane (C_{32}), which is one of the higher carbon number components, was not detected in the liquid product of both catalysed experiments. Moreover, the relative proportions of lower carbon number components increased. According to the data, the use of catalyst influenced the production of many hydrocarbons ranging from carbon numbers C_6 to C_{44}. Data shows that components such as eicosane (C_{20}) increased from 3.57 % to 10.03 % when compared to the uncatalysed experiment, and C21s were most abundant in IP-03. Hence, the production of these low carbon number components is greatly influenced by the catalyst. The catalyst reduces the required process temperature and duration for certain reactions in the pyrolysis process (Serrano et al., 2012). Pyrolysis products which could only form at higher temperatures (such as low carbon number components) may therefore form at lower temperatures due to the use of catalysts such as zinc oxide. This is also evident in the wax GC-MS results in Figures 4.9 and 4.11 and Table A4.

Similar to the liquid analysis results, the wax product in the catalysed reactions (Figure 4.11 and Table A4) was composed of a large variety of components but with higher carbon number components, such as tetrapentacontane (C_{54}) and tetracontane (C_{40}) present.

The chemical analysis results for the liquid and wax product of IP-04, IP-05 and IP-06 (uncatalysed, 5:100 catalyst and 10:100 catalyst HDPE experiments respectively) are listed in Tables A5 to A10 in Appendix A. Tables 4.4 to 4.9 provide a summary of the major constituents in these products.

Table 4.4: Peak area % of major components in the liquid product from uncatalysed HDPE pyrolysis at 450°C and 42 kPa (IP-04).

Liquid Component	Peak Area %
hexadecane (C16)	14.98
eicosane (C20)	13.03
1-docosene (C22)	11.57

Table 4.5: Peak area % of major components in the liquid product from HDPE pyrolysis using a 5:100 zinc oxide catalyst to feed ratio at 450°C and 42 kPa (IP-05).

Liquid Component	Peak Area %
eicosane (C20)	8.15
1-docosene (C22)	12.25

Table 4.6: Peak area % of major components in the liquid product from HDPE pyrolysis using a 10:100 zinc oxide catalyst to feed ratio at 450°C and 42 kPa (IP-06).

Liquid Component	Peak Area %
hexadecane (C16)	18.4
1-docosene (C22)	11.48

Table 4.7: Peak area % of major components in the wax product from uncatalysed HDPE pyrolysis at 450°C and 42 kPa (IP-04).

Liquid Component	Peak Area %
hexadecane (C16)	12.8
1-docosene (C22)	11.77
octacosane (C28)	8.76

Table 4.8: Peak area % of major components in the wax product from HDPE pyrolysis using a 5:100 zinc oxide catalyst to feed ratio at 450°C and 42 kPa (IP-05).

Liquid Component	Peak Area %
hexadecane (C16)	15.55
hexacosane (C26)	10.06

Table 4.7: Peak area % of major components in the wax product from HDPE pyrolysis using a 10:100 zinc oxide catalyst to feed ratio at 450°C and 42 kPa (IP-06).

Liquid Component	Peak Area %
10-methyleicosane, (C21)	9.82
hexacosane (C26)	13.91

There were a few trends observed in the HDPE experimental analysis results that were similar to the analysis results of the LDPE pyrolysis products. Components such as triacontane, 11,20-didecyl- (C_{50}) (found in uncatalysed HDPE pyrolysis) were not detected in the liquid product of the catalysed HDPE experiment (Table A6). The catalysed experiment (IP-05) with a 5:100 catalyst ratio also produced a larger variation of components with relatively lower carbon numbers such as 1-tridecene (C_{13}), 1,15-pentadecandiol (C_{15}), and E-14-hexadecanal (C_{16}) in significant proportions (4.32 %, 0.6 %, and 4.18 % respectively). Similar results were observed in the liquid analysis from IP-06. This supports the argument that the catalyst influences the production of a large variety of low carbon number components as compared to the uncatalysed reactions which contains a larger proportion of high carbon number components.

The analysis of IP-05 and IP-06 liquid indicated high peak area percentages for components with carbon numbers C_{16} to C_{26}. The peak area % of eicosane (C_{20}) in the liquid decreased (Table 4.5) in the catalysed experiment since a higher variation of components were produced. However, eicosane and 1-docosene still remained as the major components in the liquid (similar to the uncatalysed experiment liquid). Many of the high carbon number components were broken down to smaller components in the catalysed reactions. For this reason, components such as octacosane (Table 4.6) was not found in the catalysed pyrolysis wax.

The chemical analysis results for the liquid and wax product of IP-07 and IP-08 (uncatalysed,5:100 catalysed and 10:100 catalysed PP experiment respectively) are listed in Tables A11 to A16 in Appendix A. Tables 4.10 to 4.15 provide a summary of the major constituents of these products.

Table 4.8: Peak area % of major components in the liquid product from uncatalyzed PP pyrolysis at 450°C and 42 kPa (IP-07).

Liquid Component	Peak Area %
7-methyl-1-undecene (C12)	40.47
11-methyldodecanol (C13)	11.65

Table 4.9: Peak area % of major components in the liquid product from PP pyrolysis using a 5:100 zinc oxide catalyst to feed ratio at 450°C and 42 kPa (IP-08).

Liquid Component	Peak Area %
7-methyl-1-undecene (C12)	40.98
11-methyldodecanol (C13)	9.46

Table 4.10: Peak area % of major components in the liquid product from PP pyrolysis using a 10:100 zinc oxide catalyst to feed ratio at 450°C and 42 kPa (IP-09).

Liquid Component	Peak Area %
7-methyl-1-undecene (C12)	35.54
2-hexyl-1-decanol (C16)	20.95

Table 4.11: Peak area % of major components in the wax product from uncatalyzed PP pyrolysis at 450°C and 42 kPa (IP-07).

Liquid Component	Peak Area %
1,2,3,5-tetraisopropylcyclohexane (C18)	10.64
E-3-eicosene (C20)	15.87
heneicosane (C21)	7.85

Table 4.12: Peak area % of major components in the wax product from PP pyrolysis using a 5:100 zinc oxide catalyst to feed ratio at 450°C and 42 kPa (IP-08).

Liquid Component	Peak Area %
7-methyl-1-undecene (C12)	4.11
2-hexyl-1-dodecanol (C18)	9.46
E–3-octadecene (C18)	16.85
1,2,3,5-tetraisopropylcyclohexane (C18)	11.08
heneicosane (C21)	12.62

Table 4.13: Peak area % of major components in the wax product from PP pyrolysis using a 10:100 zinc oxide catalyst to feed ratio at 450°C and 42 kPa (IP-09).

Liquid Component	Peak Area %
2-hexyl-1-dodecanol (C18)	10.8
E-3-octadecene (C18)	20.68
1,2,3,5-tetraisopropylcyclohexane(C18)	15.97

Compared to the other plastic types, PP pyrolysis formed liquid and wax products with much higher proportions of components with short molecular chains. Examples of which are 1-undecane, 7-methyl (C_{12}) and 1-methyldodecanol (C_{13}) among others with similar carbon numbers, which had high peak area percentages in the liquid of IP-07, IP-08 and IP-09.

Regarding the classification of IP-07 products, more than 95 % of the components ranged from C_{12} to C_{27} (Table A11), indicating that the liquid may have similar properties to that of diesel (Kar et al., 2018). In comparison, the liquid from IP-08 (Table A12) contained more than 98 % of components in that range. HDPE plastic pyrolysis yielded liquid with 92.27 % (IP-04) and 91.39 % (IP-05) of components within the C_{12} to C_{27} range. It has been mentioned before that the polypropylene experiments in this work yielded the lowest relative liquid and wax products. The results from the chemical analysis however show that the polypropylene plastic should not be ruled out as a possible feed for pyrolysis process to generate liquid fuels. Although relatively low liquid + wax yields are produced, the quality of the products for certain applications may be higher than that of HDPE and LDPE pyrolysis.

Chemical analysis of the wax from IP-07 showed components such as E-3-eicosene (C_{20}), heneicosane (C_{21}) in larger proportions (components with a relatively low volatility) as compared to the liquid products. The use of the catalyst reduced the production of high carbon number molecules in the wax such as tetratetracontane (present in IP-07 but not in IP-08 or IP-09). The chemical analysis results of the polypropylene pyrolysis products also support the low liquid + wax yields produced. As mentioned before, high yields of gas were observed in the PP pyrolysis experiment (IP-07 to IP-09 on Figure 4.5). Product analysis showed that PP decomposes to form a variety of low carbon number components. Therefore, it is possible that a large quantity of the polymer decomposed to gaseous organic molecules.

4.5 Chemical analysis of liquid and wax products obtained from mixed plastic pyrolysis of LDPE, HDPE, and PP

Chemical analysis was performed on the liquid and wax products for all mixed plastic experiments. The chromatograph from the analysis of liquid from MP-01 is shown in Figure 4.12. Figure A3 in Appendix A contains the wax analysis chromatograph from MP-01. The peak area percentage for each component was obtained using automatic peak integration The analyses were conducted in triplicate and GC-MS peak area % was estimated within a repeatability of 0.1 - 0.5 %. The liquid and wax analysis results have been summarized in Figures 4.13 and 4.14 respectively.

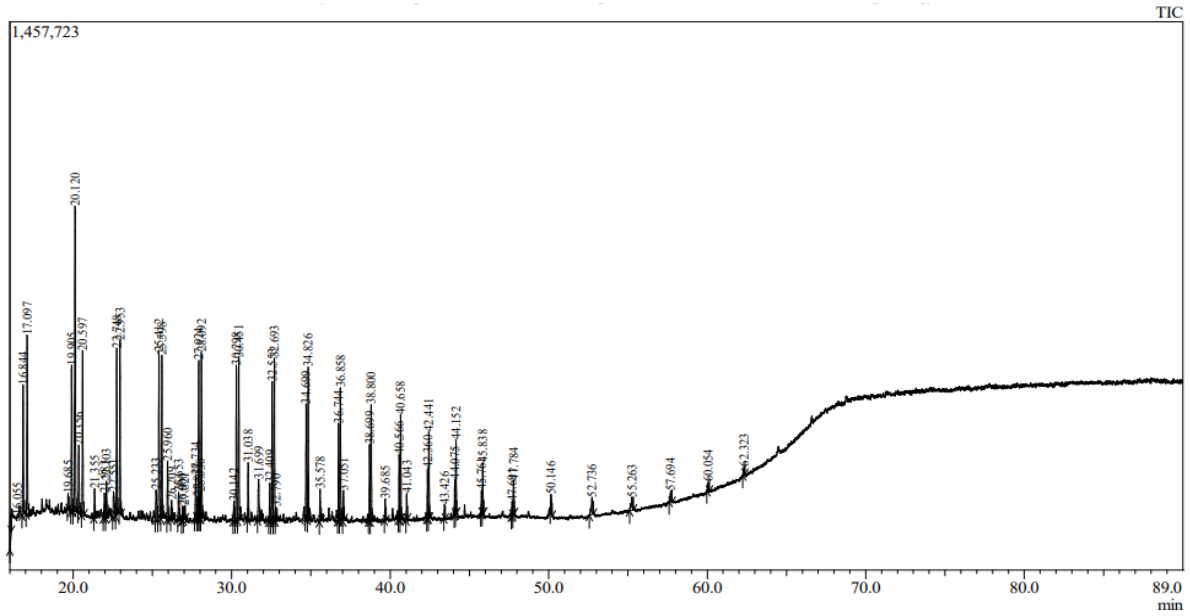

Figure 4.12: Chromatograph produced using GC-MS chemical analysis for the liquid product from uncatalysed pyrolysis of a feed mixture of 15 wt % LDPE, 45 wt % HDPE, and 40 wt % PP at 450°C and 42 kPa (MP-01) .

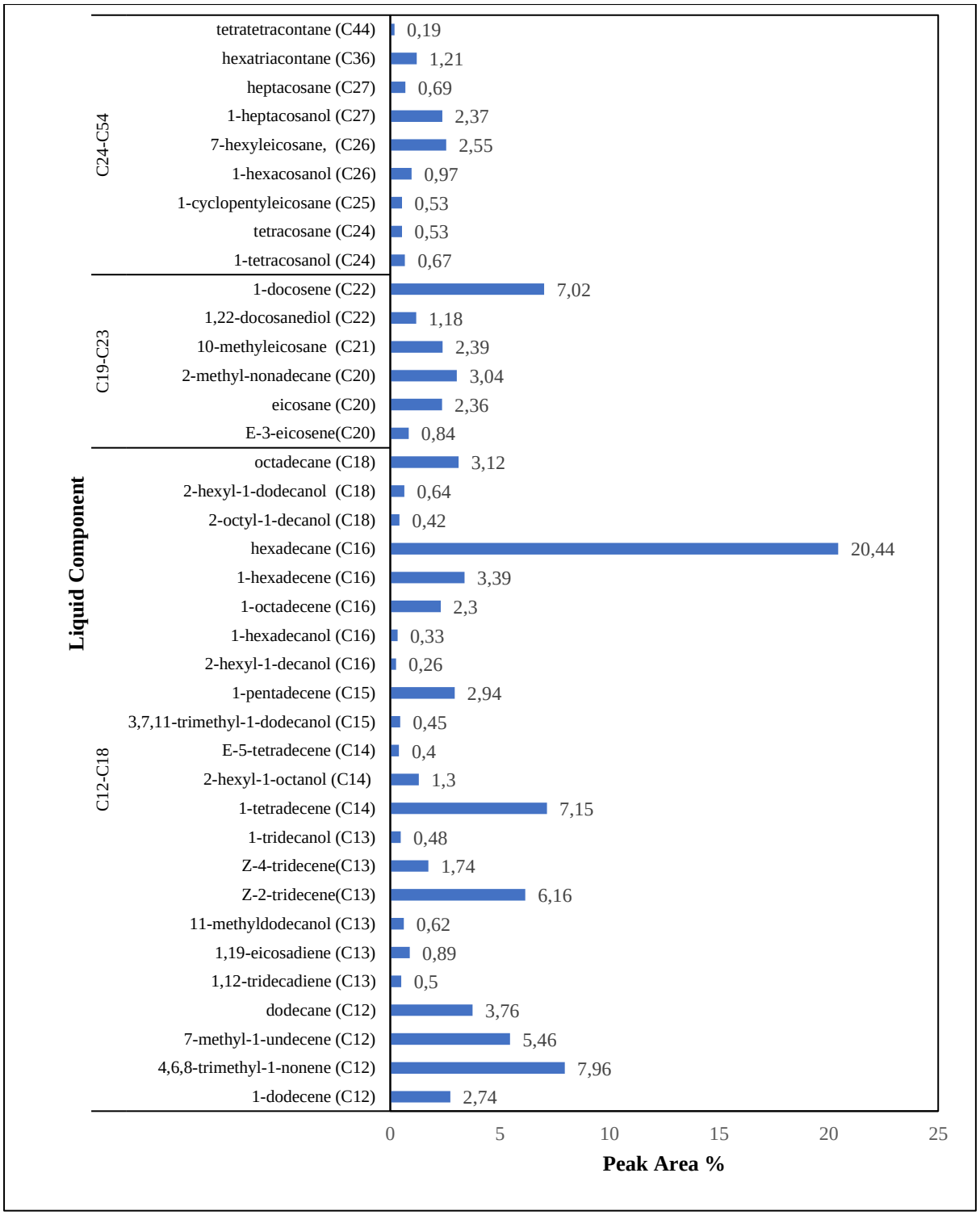

Figure 4.13: Comparison of peak area % of various components in the liquid product from uncatalysed pyrolysis of a feed mixture of 15 wt % LDPE, 45 wt % HDPE, and 40 wt % PP at 450°C and 42 kPa (MP-01).

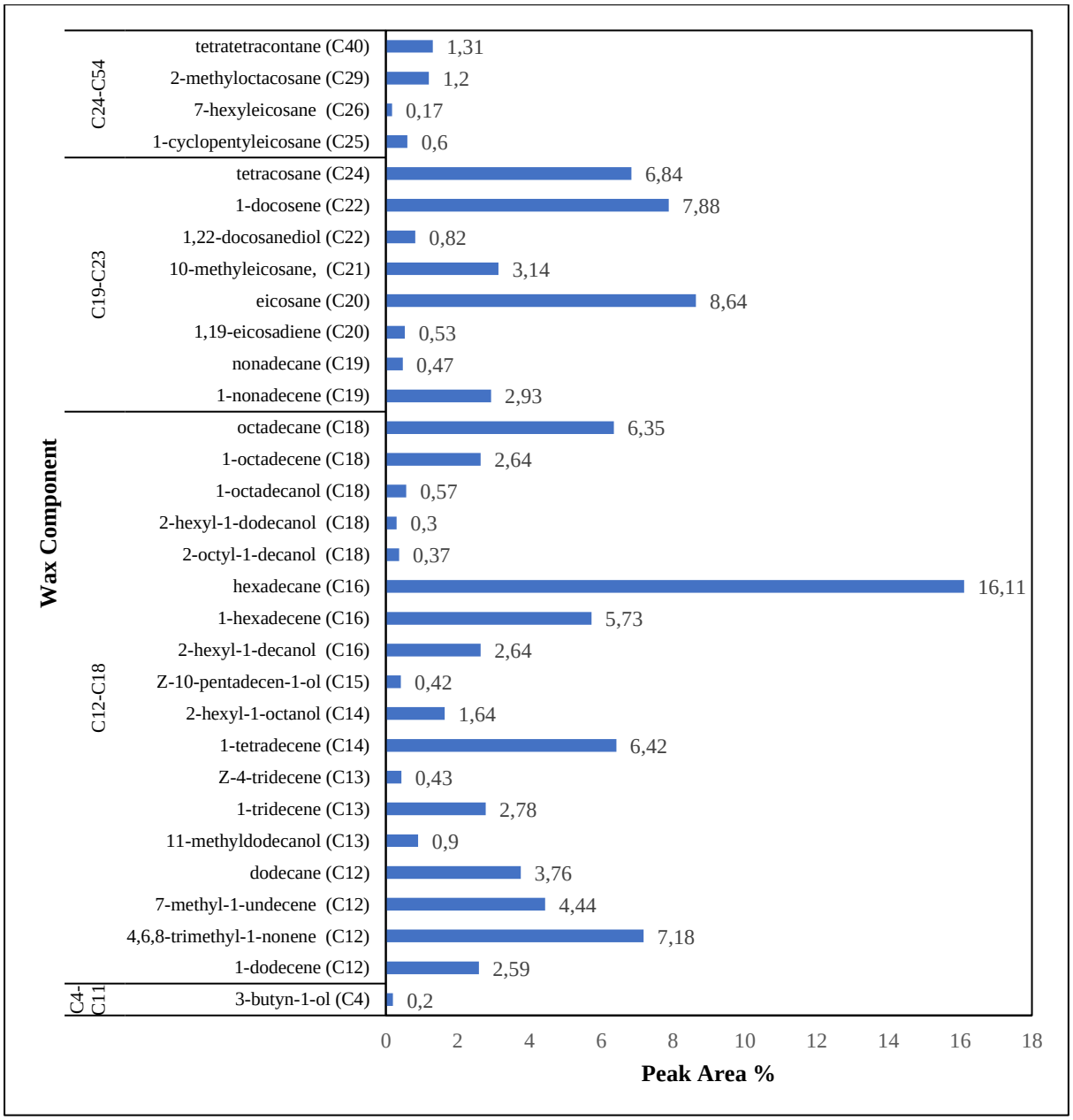

Figure 4.14: Comparison of peak area % of various components in the wax product from uncatalyzed pyrolysis of a feed mixture of 15 wt % LDPE, 45 wt % HDPE, and 40 wt % PP at 450°C and 42 kPa (MP-01).

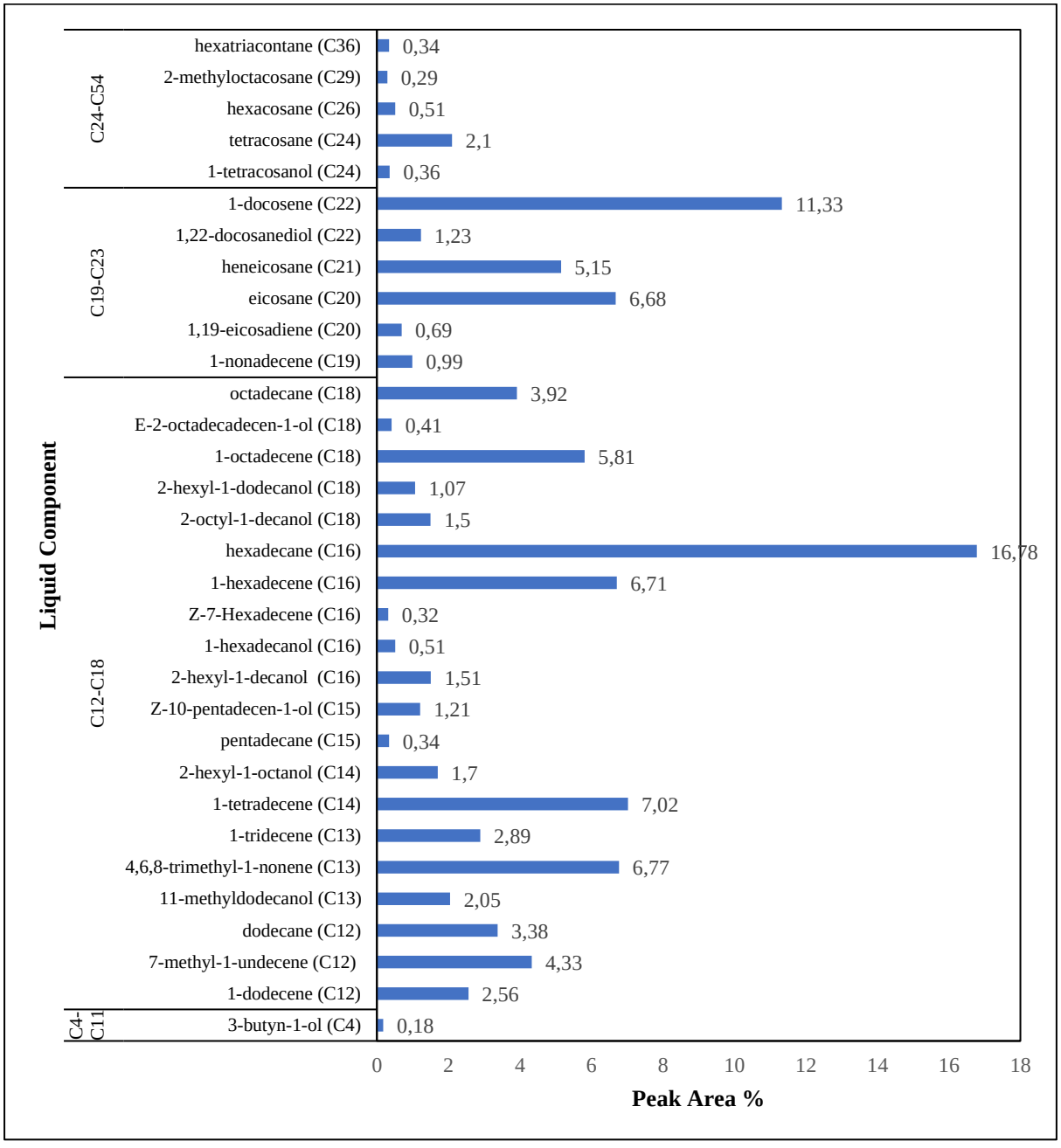

Figure 4.15: Comparison of peak area % of various components in the liquid product from the pyrolysis of a feed mixture of 15 wt % LDPE, 45 wt % HDPE, and 40 wt % PP using a 5:100 zinc oxide catalyst to feed ratio at 450°C and 42 kPa (MP-02).

According to the analysis results in Figure 4.13, the liquid product contained a large proportion of relatively short chained molecules such as hexadecane (20.44 %), 4,6,8-trimethyl-1-nonene (7.96 %), and 7-methyl-1-undecene (5.46 %). The relative peak area percentage of these shorter chained components were lower in the wax analysis (Figure 4.14) as compared to the liquid

analysis in Figure 4.15. The wax product contained 16.11 % hexadecane, 7.18 % of 4,6,8-trimethyl-1-nonene, and 4.44 % of 7-methyl-1-undecene. Evidence of this trend is also shown in the chromatograms. Figure A3 (wax) shows that there are more distinct peaks towards the end of the analysis (higher temperatures required for low volatility component). tetratetracontane in the wax product (1.31 %), corresponded to the peaks with retention time 66.571, 68.758, and 71.276 minutes, and was present in a relatively higher amount compared to the proportion in the liquid product (0.19 % tetratetracontane).

According to Figure 4.13, more than 98.6 % of the components in the liquid of MP-01 fell within the diesel carbon number range of C_{12} to C_{27}. As mentioned before, the PP experiments yielded more than 98 % of components within the diesel carbon number range. The relatively high composition of polypropylene in the MP-01 feed (40 wt % PP) may have contributed to the high quality of pyrolysis liquid.

In MP-02 a 5:100 zinc oxide catalyst to feed ratio was utilized. Liquid from the catalysed experiment showed that relatively high carbon number components such as tetratetracontane (C_{44}) were not formed. Instead, more of the relatively shorter chained components such as 2-methyloctacosane (C_{29}) were produced. The peak area percentage of 1-hexadecene (C_{16}) increased to 6.71 % compared to the uncatalysed experiment value of 3.39 % (MP-01). The catalyst also influenced the production of a C_4 component (3-butyn-1-ol) which was not present in the liquid from the uncatalysed experiment. Additional components such as Z-10-pentadecen-1-ol, and E-2-octadecene-1-ol (C18) were also detected in the liquid from the catalysed experiment. This indicates that some oxygen was present in the reactor. According to Figure 4.6, MP-02 produced the highest total liquid and wax yield (81.7 wt %). In addition to this, more than 99.19 % of the components in the liquid product were within the diesel carbon range of C_{12} to C_{27}. This shows that the experiment produces both a high liquid + wax yield, and components with desirable properties (desirable carbon number range). Similar results were obtained for MP-03 (10:100 zinc oxide catalyst to feed ratio) as presented in Tables A17 and A18 with high concentrations of C_{16} found in the liquid product. C_{22} and C_{26} were found to be in high concentrations in the wax product, accumulatively at approximately 10 % and 14 % respectively.

Plastic pyrolysis experiments MP-04, MP-05 and MP-06 tested feed plastic with a composition of 32.3 wt % LDPE, 33,18 wt % PP, and 34.52 wt % HDPE. Tables A19 to A21 (Appendix A) show the liquid analysis results for the MP-04 (uncatalysed), MP-05 (catalysed) and MP-06

(catalysed) runs respectively. The wax analysis results for MP-04 to MP-06 are shown in Tables A22 and A24 respectively. The analysis data from A19 to A24 has been summarised in Tables 4.16 to 4.18.

Table 4.14: Peak area % of major components in the liquid product from uncatalysed pyrolysis of a feed mixture of 32.30 wt % LDPE, 34.52 wt % HDPE, and 33.10 wt % PP at 450°C and 42 kPa (MP-04).

Liquid Component	Peak Area %
4,6,8-trimethyl-1-nonene (C12)	7.97
7-methyl-1-undecene (C12)	4.94
1-hexadecene (C16)	9.66
hexadecane (C16)	13.62

Table 4.15: Peak area % of major components in the liquid product from the pyrolysis of a feed mixture of 32.30 wt % LDPE, 34.52 wt % HDPE, and 33.10 wt % PP using a 5:100 zinc oxide catalyst to feed ratio at 450°C and 42 kPa (MP-05).

Liquid Component	Peak Area %
4,6,8-trimethyl-1-nonene (C12)	8.55
7-methyl-1-undecene (C12)	6.47
hexadecane (C16)	16.46
octadecane (C18)	11.07

Table 4.16: Peak area % of major components in the liquid product from the pyrolysis of a feed mixture of 32.30 wt % LDPE, 34.52 wt % HDPE, and 33.10 wt % PP using a 10:100 zinc oxide catalyst to feed ratio at 450°C and 42 kPa (MP-06).

Liquid Component	Peak Area %
hexadecane (C16)	16.9
octadecane (C18)	11.37
1-docosene (C22)	13.55

Table 4.17: Peak area % of major components in the wax product from uncatalysed pyrolysis of a feed mixture of 32.30 wt % LDPE, 34.52 wt % HDPE, and 33.10 wt % PP at 450°C and 42 kPa (MP-04).

Liquid Component	Peak Area %
2-methyl 2-methylundecane (C12)	13.04
hexadecane (C16)	8.57
octadecane (C18)	29.25

Table 4.18: Peak area % of major components in the wax product from the pyrolysis of a feed mixture of 32.30 wt % LDPE, 34.52 wt % HDPE, and 33.10 wt % PP using a 5:100 zinc oxide catalyst to feed ratio at 450°C and 42 kPa (MP-05).

Liquid Component	Peak Area %
1-dodecene (C12)	11.23
2-methyl 2-methylundecane (C12)	14.78
octadecane (C18)	25.9

Table 4.19: Peak area % of major components in the wax product from the pyrolysis of a feed mixture of 32.30 wt % LDPE, 34.52 wt % HDPE, and 33.10 wt % PP using a 10:100 zinc oxide catalyst to feed ratio at 450°C and 42 kPa (MP-06).

Liquid Component	Peak Area %
hexadecane (C16)	12.01
octadecane (C18)	24.61
1-docosene (C22)	13.65

According to Tables 4.16 to 4.20, the major constituents of the liquid and wax products consisted of molecules with carbon numbers C_{12}-C_{22}. MP-04 displayed many components that were also found in MP-01 to MP-03. Some of these components are 1-dodecene, hexadecane, and 1-hexadecene. The analysis results do however show that relatively shorter chained molecules are less common in MP-04 to MP-06 as compared to MP-01 to MP-03. Hexadecane made up 20.44 % in MP-01 liquid compared to its proportion of 13.62 % in MP-04 liquid. The

reason for this may be due to the increase in LDPE in the feed (32.3 wt % in MP-04 to MP-05). As mentioned before, the LDPE which usually consists of branched polymer chains was found to be more difficult to pyrolyze (requires more energy). Hence, molecules with relatively high carbon numbers are produced. According to the data, 92.62 % of components in the MP-04 liquid fall within the C_{12} to C_{27} category. Components such as tetratetracontane (4 %), nonacosane (1.26 %), and octacosane (2.18 %) form 7.44 % of components which have a carbon number higher than 27. In MP-02 (15 wt % LDPE) it was found that 99.19 % of components fell within the diesel carbon number range. The increase in the composition of LDPE in the feedstock is therefore the likely reason for the increase in components with higher carbon numbers in the pyrolysis products.

The use of catalyst in MP-05 (Table A20) increased the peak area percentage of components such as 1-hexacosanol and 2-hexyl-1-decanol. Furthermore, other components such as 1-heneicosanol, 1-octadecanol, and 2-hexyl-1-octanol were produced. These were not present in the liquid product from the uncatalysed reaction. The use of catalyst in MP-05 influenced the production of components with the hydroxyl group. The proportion of components in the diesel carbon number range also increased to 97.95 % when compared to the uncatalysed pyrolysis liquid (92.62 %). The use of the 10:100 catalyst to feed ratio (MP-06) produced compositions similar to MP-05 and unique, significant influence of the increased catalyst ratio on chain lengths and types of products formed, was not observed.

Plastic pyrolysis experiments MP-07 to MP-09 considered feed plastic with a composition of 65 wt % LDPE, 15 wt % PP, and 20 wt % HDPE. Tables A25 to A27 (Appendix A) present the liquid analysis results for MP-07 (uncatalysed), MP-08 (catalysed) and MP-09 (catalysed) runs respectively. The wax analysis results for MP-07 to MP-09 are presented in Tables A28 to A30 respectively. The major constituents observed in A25 to A30 is presented in Tables 4.22 to 4.27.

Table 4.20: Peak area % of major components in the liquid product from uncatalysed pyrolysis of a feed mixture of 65 wt % LDPE, 20 wt % HDPE, and 15 wt % PP at 450°C and 42 kPa (MP-07).

Liquid Component	Peak Area %
hexadecane (C16)	10.14
heneicosane (C21)	20.04

Table 4.21: Peak area % of major components in the liquid product from the pyrolysis of a feed mixture of 65 wt % LDPE, 20 wt % HDPE, and 15 wt % PP using a 5:100 zinc oxide catalyst to feed ratio at 450°C and 42 kPa (MP-08).

Liquid Component	Peak Area %
hexadecane (C16)	5.08
1-nonadecene (C19)	7.14
heneicosane (C21)	21.46

Table 4.22: Peak area % of major components in the liquid product from the pyrolysis of a feed mixture of 65 wt % LDPE, 20 wt % HDPE, and 15 wt % PP using a 10:100 zinc oxide catalyst to feed ratio at 450°C and 42 kPa (MP-09).

Liquid Component	Peak Area %
1-pentadecene (C15)	6.24
1-nonadecene (C19)	7.17
heneicosane (C21)	21.56

Table 4.23: Peak area % of major components in the wax product from uncatalysed pyrolysis of a feed mixture of 65 wt % LDPE, 20 wt % HDPE, and 15 wt % PP at 450°C and 42 kPa (MP-07).

Liquid Component	Peak Area %
tridecane (C13)	8.26
heneicosane (C21)	27.23
dotriacontane (C32)	7.98

Table 4.24: Peak area % of major components in the wax product from the pyrolysis of a feed mixture of 65 wt % LDPE, 20 wt % HDPE, and 15 wt % PP using a 5:100 zinc oxide catalyst to feed ratio at 450°C and 42 kPa (MP-08).

Liquid Component	Peak Area %
1-dodecene (C12)	11.23
2-methyl 2-methylundecane (C12)	14.78
octadecane (C18)	25.9

Table 4.25: Peak area % of major components in the wax from the pyrolysis of a feed mixture of 65 wt % LDPE, 20 wt % HDPE, and 15 wt % PP using a 10:100 zinc oxide catalyst to feed ratio at 450°C and 42 kPa (MP-09).

Liquid Component	Peak Area %
nonadecane (C19)	6.13
heneicosane (C21)	22.17
dotriacontane (C32)	6.94

Results from the previous set of experiments (MP-04 to MP-06) showed that an increase in LDPE composition in the feed resulted in pyrolysis products with higher carbon numbers. The results for experiments MP-07 to MP-09 seem to align with this trend. According to the data (Table A25 in Appendix A), MP-07 produced significant proportions of tetrapentacontane (C_{54}). Components with carbon numbers higher than 44 were not present in the liquid product of experiments MP-01 to MP-06. The wax product of MP-07 (Table A28) contained hexacontane which has a carbon number of C_{60}. According to Table 4.25, dotriacontane (C_{32})

formed one of the major constituents in the wax of MP-07. These results support the hypothesis that the increase of LDPE content in the pyrolysis feed yields products with relatively high carbon number molecules.

Throughout the liquid and wax analysis of all experiments, low volatility components were more common in the wax products compared to the liquid products. In effect, more of the components in the liquid fall within the diesel carbon number range. The use of catalyst in MP-08 produced a higher proportion of components with lower carbon numbers. The peak area percentage of components such as tetrapentacontane (C_{54}) decreased while the proportions of relatively shorter-chained components such as heneicosane (C_{21}) increased to 21.46 % (Table A26).

Further increase of the catalyst to feed ratio (10:100) in MP-09 produced liquid in which no tetrapentacontane was detected. The heneicosane peak area percentage increased slightly to 21.56 %. Short-chained components such as pentadecene also showed slight increases in peak area percentage. The use of the 10:100 catalyst to feed ratio therefore did not cause significant changes in the wax product composition, compared to the analysis results from MP-08, and slight decreases in heavier constituents were observed in comparison to the products from the uncatalysed run, MP-07.

4.6 Chemical analysis of emissions released from pure plastic pyrolysis of LDPE, HDPE, and PP

The proportions of emission components in IP-01 to IP-09 were analysed using gas chromatography-mass spectrometry. Since gas sampling was done instantaneously while the pyrolysis reaction proceeded, and the analysis time per injection was extensive, it was not possible to conduct multiple injections of the same gas sample to determine repeatability. It is however assumed that the repeatability in analysis would fall within a similar range of the liquid/wax samples of 0.1-0.5 % in peak area %, assuming a homogenous mixture was sampled. As mentioned previously, this work did not include the standard sample calibration of each emission component hence relative changes of the quantity of a particular component or carbon number class can be observed. In effect, this is useful to evaluate the influence of operational parameters on the production of different VOCs. GC-MS software was used to obtain the peak area % for each component. The total % of component classified as VOCs in the gas product stream, have also been estimated. Figure 4.16 shows the emission analysis results for IP-01. For product composition comparison purposes, especially emissions data,

these experiments were also replicated on a smaller scale, using the commercial pyrolyzer in conjunction with the GC-MS. The results are presented Figures A21 to A29 in Appendix A.

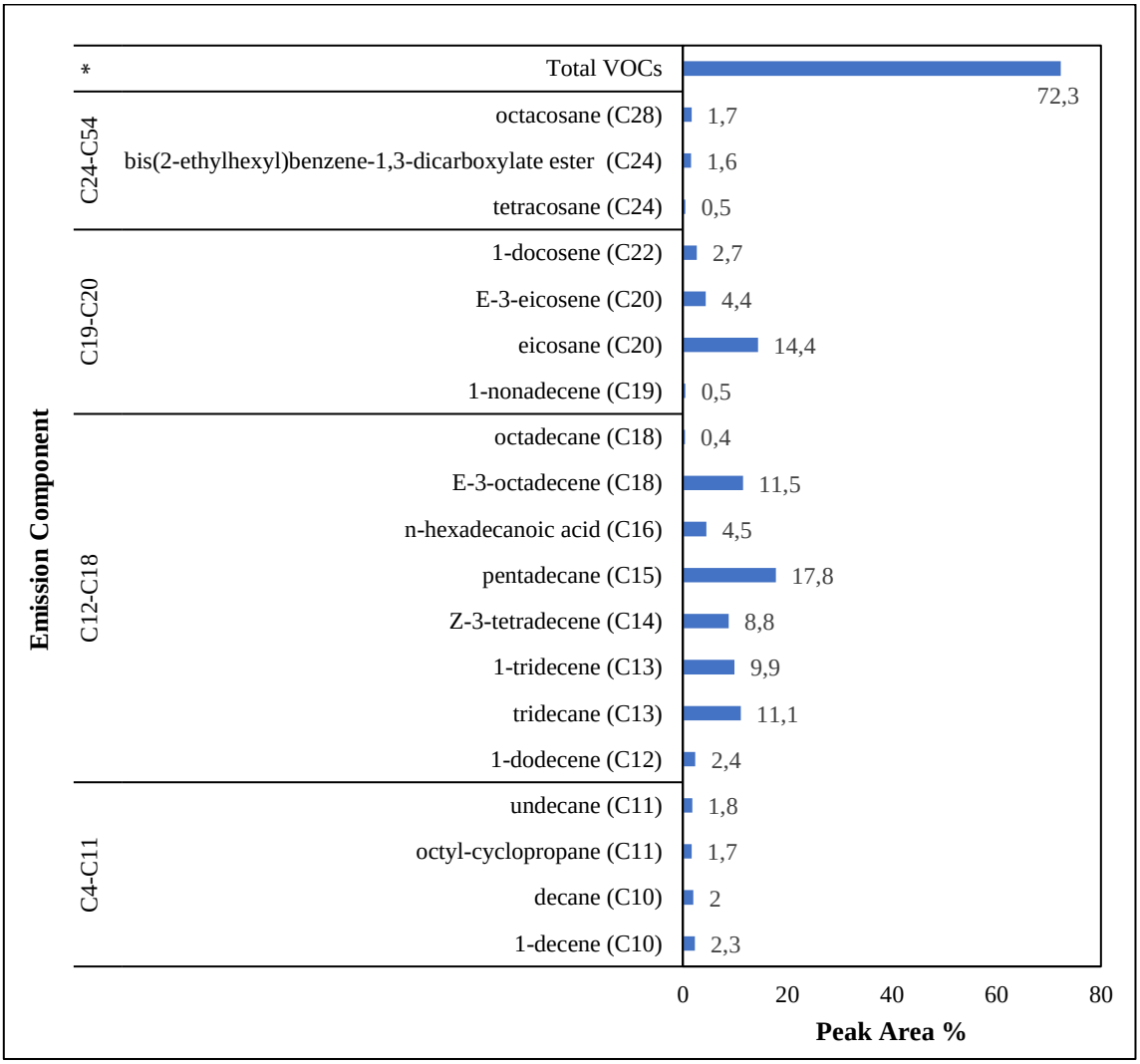

Figure 4.16: Comparison of peak area % of various components in the emissions from uncatalyzed LDPE pyrolysis at 450°C and 42 kPa (IP-01).

Upon analysis of Figure 4.16, one can observe that many VOCs such as 1-tridecene, 1-decene, and 3-tetradecene were produced in the uncatalysed LDPE pyrolysis (IP-01). The figure also indicates 'total VOCs' which is a summation of the peak area percentage of VOC emissions from the gas phase sample. IP-01 produced emissions with 72.3 % VOCs. The balance of hydrocarbons in the gas phase are not strictly classified as VOCs as they do not pose a significant threat to an individual's health or the environment. In the commercial pyrolyzer

measurements, Figure A21 shows that the components detected fall within a similar carbon number range to those determined by the bench-top lab-scale device, however the major constituent detected was C_{26} (1-hexacosanol). This is likely due to the vaporized liquid/wax produced during the pyrolysis in the commercial pyrolyzer chamber. A small quantity of C_8 hydrocarbons were also detected which were not observed in the bench-top IP-01 run. The C_8 compounds may have resulted from the secondary cracking of the pyrolysis liquid/gas within the commercial pyrolyzer chamber.

Many of the VOCs identified in this work were also detected in other studies where polyethylene pyrolysis was conducted. One example of which is the polyethylene geomembrane research performed by Valentin et al. (2022). In that work, gas chromatography-mass spectrometry was used to identify volatile organic compounds in geomembranes obtained from various companies. Some of these VOCs were 1-nonadecene, 1-docosene, and hexadecane. These components were also found in many of the emission analyses in the current work. IP-01 shows relatively high proportions of low carbon number components such as tridecane (C_{13}), 1-tridecene (C_{13}), and 3-tetradecene (C_{14}). The low carbon number hydrocarbons were expected to occur in abundance since this was the analysis of the gas phase components unlike the relatively higher carbon number components which were found in the liquid and wax product results of IP-01.

Figures A4 and A5 in Appendix A show the emission results for IP-02 (5:100 catalyst to feed ratio) and IP-03 (10:100 catalyst to feed ratio) respectively. A summary of the major constituents is presented in Tables 4.28 and 4.29.

Table 4.26: Peak area % of major components in the emissions from LDPE pyrolysis using a 5:100 zinc oxide catalyst to feed ratio at 450°C and 42 kPa (IP-02).

Liquid Component	Peak Area %
2-butyl-1-octanol (C12)	17.2
1-tetradecene (C14)	16.2
pentadecane (C15)	9.7
hexadecane (C16)	21.6
1-hexadecene (C16)	12.7
Total VOCs	67.2

Table 4.27: Peak area % of major components in the emissions from LDPE pyrolysis using a 10:100 zinc oxide catalyst to feed ratio at 450°C and 42 kPa (IP-03).

Liquid Component	Peak Area %
2-butyl-1-octanol (C12)	9.3
pentadecane (C15)	8.6
1-pentadecanol (C15)	10.2
octadecane (C18)	9
1-nonadecene (C19)	14.3
heneicosane (C21)	17.7
Total VOCs	32.6

The use of catalyst caused a decrease in the 1-tridecene content to 0.6 % in IP-02, compared to IP-01 (9.9 %, uncatalysed). 1-docosene decreased from 2.7 % to 0.8 %. The total VOC peak area changed from 72.3 wt % to 67.2 wt %. However, a few of the individual VOC component peak area percentages increased. 1-nonadecene increased from 0.5 % (IP-01) to 2 % (IP-02). Production of new VOC components such as 1-octadecene and 5-octadecene were identified in the catalysed experiment (5:100). The use of the catalyst caused a decrease in production of VOCs such as 1-tridecene and 1-docosene. In IP-02 a larger proportion of low carbon number components were formed (below C_{20}) compared to IP-01. The previous analyses of the liquid and wax pyrolysis products showed that the use of catalyst increased the cracking of large hydrocarbon molecular chains into shorter chains. This trend is also evident in the emissions of IP-01 and IP-02. Production of long chained components such as eicosane (C_{20}) reduced from 14.4 % in IP-01, to 0.5 % in IP-02. 1-docosene reduced from 2.7 wt % to 0.8 wt %. There was no production of relatively high carbon number components such as octacosane (C_{28}) in the catalysed process.

The use of the 10:100 zinc oxide catalyst to feed ratio (IP-03) significantly reduced the VOC emissions to 32.6 % of the gas phase sample. The use of the catalyst produced low carbon number molecules such as 1-nonene (C_9), 2,4-dimethyl-heptene (C_9), and 1-octene (C_8) in small quantities (Figure A5).

In the LDPE pyrolysis emission analyses, two significant trends are observed. Firstly, the use of the zinc oxide catalyst in the LDPE pyrolysis applications could significantly reduce the quantity of VOC emissions. This is evident since the total VOC emissions reduced when a

5:100 catalyst to feed ratio was used in IP-02. Furthermore, increasing the amount of catalyst (10:100 catalyst to feed) reduced the VOC emissions to a value of 32.6 % in IP-03. This is less than half of the VOC emissions of the uncatalysed LDPE pyrolysis VOC emissions. The second trend is that the use of the catalyst reduces production of components with relatively high carbon numbers in the gas phase. The reduction in VOC emissions would directly decrease the impact of a process on the environment. The zinc oxide catalyst may therefore be an essential tool to reduce the quantity of VOC emissions in LDPE pyrolysis.

In the commercial pyrolyzer experiments (A22-A23), higher carbon number components were detected in the gas phase. This may be due to incomplete interaction with the catalyst in the small vessel or inefficient heat transfer.

Figures A6 to A8 indicate the emission results for IP-04 to IP-06. A summary of the major constituents of the emissions have been presented in Tables 4.30 to 4.32.

Table 4.28: Peak area % of major components in the emissions from uncatalyzed HDPE pyrolysis at 450°C and 42 kPa (IP-04).

Liquid Component	Peak Area %
2-butyl-1-octanol (C12)	26.1
2-hexyl-1-decanol (C16)	32.3
1-nonadecene (C19)	10.6
heneicosane (C21)	14.7
Total VOCs	82.1

Table 4.29: Peak area % of major components in the emissions from HDPE pyrolysis using a 5:100 zinc oxide catalyst to feed ratio at 450°C and 42 kPa (IP-05).

Liquid Component	Peak Area %
2-butyl-1-Octanol (C12)	29.7
tridecane (C13)	26.9
hexadecane (C16)	20.4
Total VOCs	69.2

Table 4.30: Peak area % of major components in the emissions from HDPE pyrolysis using a 10:100 zinc oxide catalyst to feed ratio at 450°C and 42 kPa (IP-06).

Liquid Component	Peak Area %
2-butyl-1-octanol (C12)	42
tridecane (C13)	24.4
hexadecane (C16)	17.6
Total VOCs	74

Many chemical components in the LDPE pyrolysis emissions were also observed in the HDPE pyrolysis emissions. Some of these components are 1-nonene, 1-dodecene, and 1-decene. IP-04 yielded a total VOC emission in the gas product of 82.1 %. This is relatively higher than the VOC emissions in the gas product of the LDPE pyrolysis experiments. Large proportions of 2-butyloctanol, 2-hexyldecanol, and 1-nonadecene were identified. Small amounts of higher carbon number components such as 1-heptacosanol (C_{27}) and 1-hexacosanol (C_{26}) were formed.

The comparison of IP-04 (uncatalysed) and IP-05 (5:100 catalyst to feed ratio) shows that the use of the zinc oxide catalysed caused a reduction in the total VOC emissions. The VOC emissions for IP-05 was 69.2 %. The VOC emissions therefore decreased by approximately 16.0 %. Similar trends to the LDPE pyrolysis experiments were found in HDPE pyrolysis. Relatively high carbon number component such as octacosanol (C_{28}), 1-heptacosanol (C_{27}), and 1-hexacosanol (C_{26}) which were observed in the IP-04 emissions, were not present in the IP-05 emissions. All emission component carbon numbers from IP-05 were below C_{24}. The quantities of relatively short chained molecules such as 2-butyloctanol increased from 26.1 % to 29.7 % (Tables 4.30 and 4.31). High amounts of tridecane (26.9 %) were identified in the IP-05 emissions. hexadecane (C_{16}) quantity increased from 4.8 % in IP-04 to 20.4 % in IP-05, likely due the increased production of relatively low carbon number components.

There were a few significant findings in IP-06 (10:100 catalyst to feed ratio) such as the increase in the VOC production (74 % total VOCs) as compared to the experiment with the 5:100 catalyst to feed ratio (69.2 % total VOCs). A similar trend was observed when considering the total gas yields for the HDPE pyrolysis process, reported in section 4.4. For IP-05, a gas yield of 8.4 wt % was obtained. IP-06 yielded 17.56 wt % gas (Figure 4.5). The increase in catalyst usage increased the production of gas. The analysis of the gas stream

indicates that the production of VOCs was also increased. It is therefore essential to consider the trade-off between yields of desirable products and the minimization of VOC emissions. Chemical analysis shows that the VOC emissions were lowest for HDPE pyrolysis when a catalyst to feed ratio of 5:100 was used. The total liquid + wax yield for the 5:100 experiment (78.2 wt %) was also marginally higher than that of the 10:100 experiment (72.3 wt % yield). The 5:100 catalyst to feed ratio has therefore been proven effective in decreasing gas yields, decreasing the reaction time, increasing desirable product yields, and decreasing VOC emissions for HDPE pyrolysis.

In the commercial pyrolyzer experiments (A24-A26), the emissions detected were abundant in the C_{20}-C_{35} range. This was likely detected from the vaporized liquid and wax products from commercial pyrolyzer device. A significant quantity of C_8 hydrocarbons detected in IP-06 on the pyrolyzer, which were not observed in the bench-top IP-06 run. Again, it is assumed that these C8s have resulted from the secondary cracking of the pyrolysis liquid/gas within the commercial pyrolyzer chamber.

Figures A9 to A11 in Appendix A indicate the emission analysis results for IP-07 to IP-09. A summary of the major constituents of the emissions have been presented in tables 4.33 to 4.35.

Table 4.31: Peak area % of major components in the emissions from uncatalyzed PP pyrolysis at 450°C and 42 kPa (IP-07).

Liquid Component	Peak Area %
2,4-dimethyl-1-heptene (C9)	21.6
2-butyl-1-octanol (C12)	16.0
1-tetradecene (C14)	10.6
1-hexadecene (C16)	12.1
Total VOCs	83.3

Table 4.32: Peak area % of major components in the emissions from PP pyrolysis using a 5:100 zinc oxide catalyst to feed ratio at 450°C and 42 kPa (IP-08).

Liquid Component	Peak Area %
cyclotetradecane (C14)	9.1
pentadecane (C15)	14.3
heptadecane (C17)	12
E-3-eicosene(C20)	11.9
E-9-eicosene(C20)	9.9
Total VOCs	35.6

Table 4.33: Peak area % of major components in the emissions from PP pyrolysis using a 10:100 zinc oxide catalyst to feed ratio at 450°C and 42 kPa (IP-09).

Liquid Component	Peak Area %
2-butyl-1-octanol (C12)	11.1
2-hexyl-1-octanol (C14)	9
tetradecane (C12)	12
heptadecane (C17)	9.6
E-3-eicosene(C20)	7.3
Total VOCs	61.1

Many of the VOCs produced in PP pyrolysis (IP-07 to IP-09) such as 1-tridecene and 1-nonadecene were present in LDPE and HDPE pyrolysis. Many components from the emissions of the uncatalysed PP pyrolysis experiment were hydrocarbons with chain lengths ranging from C_8 to C_{21}. Components such as n-tetracosanol (C_{24}) were detected in small quantities (Figure A9). The large proportion of low carbon number components such as 2-butyloctanol (Table 4.33) were expected in the gas phase. The emission analysis showed a total VOC production of 83.3 % in experiment IP-07. Comparing the VOC emissions of PP pyrolysis to LDPE and HDPE pyrolysis, it can be observed that polypropylene pyrolysis without catalyst produced the highest percentage of VOCs in the emissions. More importantly, the uncatalysed experiment (IP-07) produced the second highest gas yield (19.2 wt %) in the set of IP-01 to IP-09. Higher gas yields with large VOC fractions will naturally increase the VOC management

requirements. It is unlikely that these processes would be able to easily abide with the laws and regulations for VOC emissions in South Africa without comprehensive mitigation strategies.

Comparison of Figure A9 and A10 shows that the use of zinc oxide catalyst in a 5:100 ratio significantly decreased the production of VOCs to 35.6 % (IP-08). The use of the catalyst in IP-08 produced a wider variety of low carbon number components such as 3-tetradecene, 1-undecanol, and 4,8-dimethylnonanol which were not detected in the uncatalysed experiment. The trend observed in the HDPE pyrolysis experiments, in which VOC emissions decreased with a 5:100 catalyst to feed ratio and thereafter increased with the 10:100 ratio, was also observed in PP pyrolysis.

A high proportion of C_8 and C_9 particles/compounds were detected in the commercial pyrolyzer experiments (A27-A29). Since the PP was easier to pyrolyze in general, and the liquid and wax constituents have lower carbon numbers, it is likely that these C_8 and C_9 hydrocarbons, which are VOCs, are resultant from secondary cracking. Although secondary cracking was not readily observed to occur in the bench scale laboratory experiments, it must be considered in commercial applications as it would result in lighter fugitive emissions that would need to be accounted for.

Hence the optimum catalyst to-feed ratio to reduce total VOC emissions varies depending on the plastic feed and must therefore be carefully controlled to reduce the amount of VOC emissions produced in the LDPE, HDPE, and PP pyrolysis processes.

4.7 Chemical analysis of emissions released from mixed plastic pyrolysis comprised of LDPE, HDPE, and PP

GC-MS analyses were performed on the emissions of the mixed plastic pyrolysis processes (MP-01 to MP-09). Data such as the peak area percentage of emission components and the total VOC content of the emissions have been determined. The emission results for MP-01 to MP-03 are shown in Figures A12 to A14 in Appendix A. The major constituents of these emissions have been summarised in Tables 4.36 to 4.38. Figures A30 to A38 in Appendix A indicate the analyses results obtained from the GC-MS pyrolyzer experiments, used for comparison purposes.

Table 4.34: Peak area % of major components in the emissions from uncatalysed pyrolysis of a feed mixture of 15 wt % LDPE, 45 wt % HDPE, and 40 wt % PP at 450°C and 42 kPa (MP-01).

Component	Peak Area %
pentadecanol (C15)	12.9
2-hexyl-1-decanol (C16)	34.1
hexadecane (C16)	13.3
1-nonadecene (C19)	12.4
heneicosane (C21)	11.9
Total VOCs	66.1

Table 4.35: Peak area % of major components in the emissions from the pyrolysis of a feed mixture of 15 wt % LDPE, 45 wt % HDPE, and 40 wt % PP using a 5:100 zinc oxide catalyst to feed ratio at 450°C and 42 kPa (MP-02).

Component	Peak Area %
2-butyl-1-octanol (C12)	9.4
tridecane (C13)	9.1
hexadecane (C15)	20
1-hexadecene (C16)	14.4
7-hexyleicosane (C21)	8.1
Total VOCs	79.4

Table 4.36: Peak area % of major components in the emissions from the pyrolysis of a feed mixture of 15 wt % LDPE, 45 wt % HDPE, and 40 wt % PP using a 10:100 zinc oxide catalyst to feed ratio at 450°C and 42 kPa (MP-03).

Component	Peak Area %
2-butyl-1-octanol (C12)	9.6
1-hexadecene (C16)	22.1
hexadecane (C16)	36.9
10-methyl-eicosane (C20)	8.5
Total VOCs	89.6

According to the Table 4.36 for MP-01, the uncatalysed pyrolysis experiment produced emissions with a 66.1 % VOC content. Major components found in these emissions were 2-hexyldecanol, hexadecane, and 1-nonadecene. Many of these emissions such as 1-nonadecene and hexadecane were present in pure plastic pyrolysis experiments with LDPE and HDPE. The results were also similar to the VOC studies performed by Valentin et al. (2022).

The emission results for MP-02 indicated the influence of a 5:100 zinc oxide catalyst to feed ratio on the pyrolysis process. According to Table 4.37, the addition of the catalyst increased the total VOC emissions proportion from 66.1 % to 79.4 %. It is important to note that the feed contained a larger proportion of HDPE and PP. These two materials have a relatively lower energy requirement for polymer cracking as compared to the LDPE material used in this work. Hence, the quantity of VOC emissions is strongly influenced by the behaviour of HDPE and PP materials in the pyrolysis processes. As observed previously in the individual plastic pyrolysis experiments results, the usage of catalyst in polypropylene pyrolysis increases the gas yields thereby increasing the VOC emissions. According to the data presented in Figures A13 and A14, high carbon number molecules such as dotriacontane (C_{32}), octacosanol (C_{28}), and 1-heptacosanol (C_{27}) were not present in the catalysed experiments. This result indicates that the use of the catalyst in MP-02 increased the conversion of plastic polymer to relatively low carbon number emission components as compared to MP-01. The further increase in catalyst usage (10:100 ratio in experiment MP-03), summarized in Table 38, significantly increased the VOC emissions to 89.6 % (Figure 4.30) which again correlates with the composition of the feed being high in HDPE and PP proportion.

The results of the emissions detected from these runs correlate reasonably well with the findings from the commercial pyrolyzer measurements of the corresponding mixtures presented in Figures A30-A32 with respect to abundant components of the same carbon number.

Figures A15 to A17 present the emission analysis results for MP-04 to MP-06. The peak area % of the major constituents of these emissions have been summarised in Tables 4.39 to 4.41.

Table 4.37: Peak area % of major components in the emissions from uncatalysed pyrolysis of a feed mixture of 32.30 wt % LDPE, 34.52 wt % HDPE, and 33.18 wt % PP at 450°C and 42 kPa (MP-04).

Component	Peak Area %
cyclododecane (C12)	8.3
pentadecane (C15)	9.1
hexadecane (C16)	10.5
eicosane (C20)	13.6
Total VOCs	65.8

Table 4.38: Peak area % of major components in the emissions from the pyrolysis of a feed mixture of 32.30 wt % LDPE, 34.52 wt % HDPE, and 33.18 wt % PP using a 5:100 zinc oxide catalyst to feed ratio at 450°C and 42 kPa (MP-05).

Component	Peak Area %
1-tetradecene (C14)	10.1
1-pentadecene (C15)	14.4
hexadecane (C16)	32.4
Total VOCs	76.5

Table 4.39: Peak area % of major components in the emissions of from the pyrolysis of a feed mixture of 32.30 wt % LDPE, 34.52 wt % HDPE, and 33.18 wt % PP using a 10:100 zinc oxide catalyst to feed ratio at 450°C and 42 kPa (MP-06).

Component	Peak Area %
2-hexyl-1-octanol (C14)	8.9
hexadecane (C16)	16.9
octadecane (C18)	8.5
10-methyleicosane, (C21)	10.8
1-docosene (C22)	11
Total VOCs	73.2

In MP-04 to MP-06 a feed of 32.3 wt % LDPE, 33.18 wt % PP, and 34.52 wt % HDPE was used. A total VOC production of 65.8 % of the total emissions (Table 4.39) was detected in MP-04 (uncatalysed experiment). Major components present were eicosane (C_{20}), hexadecane (C_{16}), and 1-octadecene (C_{18}).

Production of VOC emissions increased to 76.5 % (from 65.8 % for uncatalysed) when a 5:100 zinc oxide catalyst to feed ratio was used (Table 4.3). Similar to the other mixed plastic pyrolysis experiments, there was a higher production of relatively low carbon number components when the catalyst was used as compared to the uncatalysed process. Low carbon number components such as 3,7 dimethyldecane, 4-tetradecene, and tridecane formed in the experiment MP-05 (Figure A16), while C_{14}-C_{22} components were observed to be abundant in the emissions from the experiment MP-06. As mentioned before, there is a trade-off between the yields of desirable liquid/wax products and the minimization of VOC emissions. MP-04, MP-05, and MP-06 produced liquid + wax yields of 74.3 wt %, 76.6 wt %, and 75.4 wt % respectively. Although the addition of the catalyst increased the liquid + wax yield to 76.6 wt % in MP-05, the VOC emissions increased to 76.5 wt %. The catalyst ratio of 10:100 (MP-06) decreased the liquid + wax yield marginally to 75.4 wt %. This shows that in some cases, manipulating the catalyst to feed ratio may decrease the yield of desirable products but reduce the impact of the process on the environment to an extent.

Comparing MP-04, MP-05, and MP-06, it can be observed that the experiment MP-06 had both a reasonable yield and production of VOC emissions. Experiment MP-04 has the lowest liquid + wax yield and the lowest VOC emissions. MP-05 has the highest liquid + wax yield, however the VOC emissions were also the highest out of the three experiments. Note again, that the deviations between the liquid/wax yields of these particular runs are within 2.5 % and hence likely insignificant.

Again, the emissions detected from these runs correlate reasonably well with the findings from the commercial pyrolyzer measurements of the corresponding mixtures presented in Figures A33-A35 with respect to abundant components of the same carbon number. C_9s were detected in a small proportion in MP-05 for the commercial pyrolyzer experiments.

Figures A18 to A20 present the emission analysis results for MP-07 to MP-09. The peak area percentage of the major constituents of these emissions have been summarised in Tables 4.42 to 4.44.

Table 4.40: Peak area % of major components in the emissions from uncatalysed pyrolysis of a feed mixture of 65 wt % LDPE, 20 wt % HDPE, and 15 % PP at 450°C and 42 kPa (MP-07).

Liquid Component	Peak Area %
hexadecane (C16)	21.5
1-hexadecene (C16)	14.8
hexadecanoic acid (C16)	18.1
Total VOCs	76.9

Table 4.41: Peak area % of major components in the emissions from the pyrolysis of a feed mixture of 65 wt % LDPE, 20 wt % HDPE, and 15 wt % PP using a 5:100 zinc oxide catalyst to feed ratio at 450°C and 42 kPa (MP-08).

Liquid Component	Peak Area %
1-hexadecene (C16)	13.5
hexadecane (C16)	22.7
hexadecanoic acid (C16)	11.6
octadecane (C18)	9.4
Total VOCs	73.5

Table 4.42: Peak area % of major components in the emissions from the pyrolysis of a feed mixture of 65 wt % LDPE, 20 wt % HDPE, and 15 wt % PP using a 10:100 zinc oxide catalyst to feed ratio at 450°C and 42 kPa (MP-09).

Liquid Component	Peak Area %
1-hexadecene (C16)	19.1
hexadecane (C16)	25.7
octadecane (C18)	14.7
Total VOCs	74.5

Experiments MP-07 to MP-09 included uncatalysed and catalysed plastic pyrolysis processes using a feed of 65 wt % LDPE, 15 wt % PP, and 20 wt % HDPE. The uncatalysed experiment produced many emission components that were previously detected in experiments MP-01 to

MP-07. Some of these emission components are 1-hexadecene, tridecane, and 1-octadecene (Figure A18).

Table 4.42 shows that a total of 76.9 % VOCs were produced in the pyrolysis emissions for the uncatalysed process (MP-07). According to Table 4.43, there was a reduction of VOC emissions by 3.4 % when a 5:100 zinc oxide catalyst to feed ratio was used as compared to the uncatalysed process. The reason for this may be due to the major content of the LDPE in MP-07 to MP-09. According to the pure LDPE plastic pyrolysis experiments (IP-01 to IP-03), the VOC emissions decreased when a catalyst was used as compared to the uncatalysed pyrolysis experiment. The emission analysis results in MP-07 to MP-09 shows similar trends to the LDPE pyrolysis experiments due to the major proportion of LDPE (65 wt %) in the feed mixture. Figure A20 data which is summarized in Table 4.44 present the emission results for the catalysed process using a 10:100 catalyst to feed ratio. The data showed that increasing the quantity of catalyst in the pyrolysis process did not drastically influence the pyrolysis emissions (1 % increase in total VOCs in comparison to the MP-08 run).

The emissions detected from these runs were found to be in the C_{12} to C_{19} range which correlates reasonably well with the findings from the commercial pyrolyzer measurements of the corresponding mixtures presented in Figures A36-A38.

4.8 Gate to gate assessment (GGA) of the plastic pyrolysis process

The methodology for the preliminary GGA was described in section 3.5. This method has been applied to the lab-scale process for 15 g of feed as informed by the experimental study presented. The factors considered in this lab-scale assessment would find analogous counterparts in a similar to-scale process. Hence this preliminary GGA of the lab-scale process, would serve as a useful basis for the future to-scale GGA. In the preceding sections Stage 1 and parts of Stage 2 of the results of the GGA methodology has been presented. That is, for Stage 1, through literature review and interrogation, relevant information was collected and the process with scalable industrial significance was selected, namely the semi-batch pyrolysis of mixed plastic using zinc oxide catalyst. For Stage 2, the process of the pyrolysis on the lab scale has been detailed above, however the preceding and subsequent process steps are described in the following sections. A generic flow diagram was developed and is presented in Figure 4.17. For this GGA, feed compositions and process conditions are considered as variables, hence the mass and energy balances for each run considered are functions of these

parameters. This was done to compare the effect of these variations in process conditions, on the impact of the pyrolysis process.

Figure 4.17 describes the input and output data for the pyrolysis process. Data such as the indirect and direct CO_2 and VOC emissions, electricity usage, water usage, cleaning agent consumption and transportation fuel consumption were calculated for the process based on experimental data from this work and literature data.

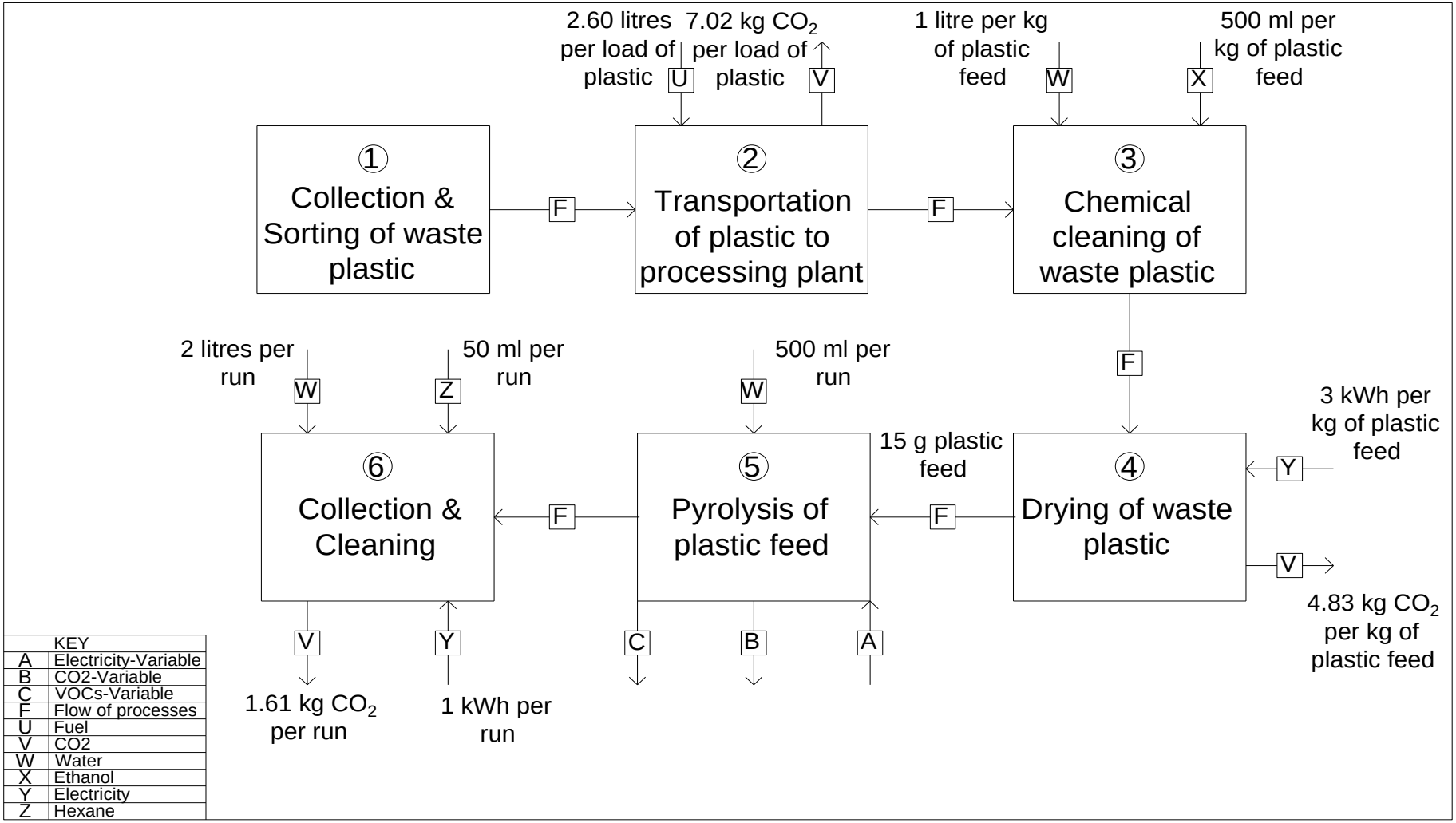

Figure 4.17: Life cycle gate-to-gate analysis for the laboratory-scale plastic pyrolysis process.

4.8.1 Collection, sorting, and transportation

According to the GGA in Figure 4.17, Step 1 in the process requires collection and sorting of the feed material. Collection and sorting are assumed to be performed manually by waste pickers for example, at their cost. For this reason, no significant inputs and outputs were considered for the LCIA.

Step 2, in the GGA, indicates that the waste plastic is transported from the waste collection site to the plastic pyrolysis plant. There are two main inventory factors associated with this step. The first of which is the fuel usage by the transportation. The waste pyrolysis plant was assumed to be within a 10 km radius of the waste plastic site. The transportation vehicle, for example a 1-ton capacity van, would need to travel from the plant site to the waste site, load the plastic, and thereafter travel back to the plant site. This would be 20 km travelled in total. Sample calculation B2 (Appendix B) illustrates the calculation of the fuel usage (2.60 litres). The CO_2 released from the diesel consumption is the second inventory factor to consider. The average emission factor of 2.7 kg CO_2 per litre of diesel consumed was obtained from literature (AutoSmart, 2014). The amount of CO_2 released into the atmosphere was calculated to be 7.02 kg for each roundtrip made.

4.8.2 Chemical cleaning of waste plastic

Step 3 in the LCA accounted for the cleaning of the waste plastic. For this purpose, 1 litre of water and 500 ml of ethanol was used per kg of plastic on the lab scale. A portion of the water can be re-used in a moving-bed was scenario for example. The ethanol assists in removing the wash water from the plastic and can also be reused with the addition of a small make-up flow. This degree of cleaning can be an important step as it aides in removing impurities from the feed and hence prevents the contamination of the final pyrolysis product produced, which increases its quality.

4.8.3 Drying of waste plastic

The drying process (Step 4) involves the use of a laboratory-scale dryer (Ugolini, 2018). Since ethanol is used to clean the waste plastics, the drying time is relatively short. It was assumed that the waste plastic is placed inside the dryer for 15 minutes. This time is fixed for up to 10 times the scale of the original feed batch size. Sample Calculation B3 in Appendix A indicates the procedure to calculate the electricity usage for drying. Approximately 3 kWh is used per

kg of waste plastic feed. The usage of energy for drying indicates an indirect release of carbon dioxide from coal-burning power plants. The calculation revealed that approximately 4.83 kg of CO_2 is indirectly released per kg of waste plastic. Solar drying could be considered in to-scale operation to reduce cost and decrease carbon impact.

4.8.4 Pyrolysis of plastic feed: electricity usage, CO_2 emissions, and VOCs

Tables 4.45 and 4.46 provide the electricity usage data for each pyrolysis experiment. Additionally, the energy usage per gram of product is described.

Table 4.43: Electricity usage for the plastic pyrolysis step for individual plastic pyrolysis experiments at 450°C and 42 kPa.

Experiment	Mass of liquid + wax (g)	Process Duration (h)	Energy Usage (kWh)				Energy Usage per gram of product (kWh per gram of liquid + wax)
			Heating Mantle (0.3 kW)	Vacuum Pump (0.3 kW)	Water Circulator/cooler (0.3 kW)	Total	
IP-01	10.46	27.67	8.30	8.30	8.30	24.90	2.38
IP-02	11.74	13.75	4.12	4.12	4.12	12.36	1.05
IP-03	11.68	10.83	3.25	3.25	3.25	9.75	0.84
IP-04	12.89	4.83	1.45	1.45	1.45	4.35	0.34
IP-05	11.74	3.33	1.00	1.00	1.00	3.00	0.26
IP-06	10.93	3.16	0.95	0.95	0.95	2.85	0.26
IP-07	10.76	2.91	0.87	0.87	0.87	2.61	0.24
IP-08	10.83	2.75	0.82	0.82	0.82	2.46	0.23
IP-09	10.81	2.33	0.70	0.70	0.70	2.10	0.19

Table 4.44: Electricity usage for the plastic pyrolysis step for mixed plastic pyrolysis experiments at 450°C and 42 kPa.

Experiment	Mass of liquid + wax (g)	Process Duration (h)	Energy Usage (kWh)				Energy Usage per gram of product (kWh per gram of liquid + wax)
			Heating Mantle (0.3 kW)	Vacuum Pump (0.3 kW)	Water Circulator (0.3 kW)	Total	
MP-01	10.20	13.90	4.17	4.17	4.17	12.51	1.23
MP-02	12.32	7.83	2.35	2.35	2.35	7.05	0.57
MP-03	10.55	7.16	2.15	2.15	2.15	6.45	0.61
MP-04	11.18	15.95	4.78	4.78	4.78	14.34	1.28
MP-05	11.53	12.75	3.82	3.82	3.82	11.46	0.99
MP-06	11.33	12.40	3.72	3.72	3.72	11.16	0.99
MP-07	12.03	17.75	5.32	5.32	5.32	15.96	1.33
MP-08	11.92	15.66	4.70	4.70	4.70	14.10	1.18
MP-09	11.76	15.41	4.62	4.62	4.62	13.86	1.18

The results show that there is a significant decrease in energy usage with the pyrolysis of HDPE or PP (Table 4.45) in comparison to LDPE. The mixed plastic pyrolysis experiments (Table 4.46) indicated similar trends to the pure plastic pyrolysis experiments. In mixed plastic pyrolysis, the process duration increased as the amount of LDPE in the pyrolysis feed composition was increased. This results in a higher usage of energy. Pyrolysis experiments with 65 wt % LDPE (MP-07 to MP-09) showed energy usage results ranging from 13.86 kWh to 15.96 kWh. In comparison, pyrolysis experiments with relatively low amounts of LDPE (15 wt % LDPE in MP-01 to MP-03) showed electricity usage results ranging from 6.45 kWh to 12.51 kWh.

Accounting for the electricity usage per unit mass of liquid + wax produced provides information on which set of pyrolysis conditions (feedstock composition) produces the most product using the least amount of energy (lowest cost). IP-01 (Table 4.45) indicates the largest

energy usage per gram of product obtained for the uncatalysed LDPE pyrolysis (2.38 $\frac{kWh}{g}$). Moreover, this experiment had the highest total energy usage (24.90 kWh) and lowest liquid + wax mass (10.46 g) yielded. IP-04 to IP-06 (pure HDPE pyrolysis) resulted in significantly lower energy usage per gram of product with values ranging from 0.26 $\frac{kWh}{g}$ to 0.34 $\frac{kWh}{g}$. The HDPE pyrolysis experiments yielded product masses ranging from 10.93 g to 12.89 g. These product masses were higher than those obtained in the LDPE pyrolysis experiments and is an additional factor in the reduction of the energy usage per gram of product obtained. IP-09 (10:100 zinc oxide catalysed PP pyrolysis) had the lowest energy usage per gram of product obtained in the pure plastic pyrolysis experiments (0.19 $\frac{kWh}{g}$).

The results from the pure plastic pyrolysis experiments are useful in predicting the behaviour of the mixed plastic pyrolysis experiments. Feeds with low quantities of LDPE and high quantities of PP should have the lowest energy usage per gram of liquid and wax product produced as indicated in the runs of MP-01 to MP-09. According to the data in Table 4.44, the lowest energy usage values, ranging 0.57 $\frac{kWh}{g}$ to 1.23 $\frac{kWh}{g}$, were obtained in experiments MP-01 to MP-03, which had a low proportion of LDPE (15 wt %) and a high proportion of PP (40 wt %). The results showed that the high energy usage per gram of product values were obtained by MP-07 to MP-09 which had a high feed proportion of LDPE (65 wt %). These high values were due to the relatively long process durations required for the cracking of LDPE. It is also clear that interactions between the mixed plastic waste components during catalytic pyrolysis cause an increase in energy usage per gram of useful product. For example, the energy usage per gram for the catalysed pure LDPE pyrolysis with the 5:100 and 10:100 catalyst to feed ratios are 1.05 and 0.84 $\frac{kWh}{g}$, respectively while that of the LDPE (65 wt %) mixture are approximately 1.18 $\frac{kWh}{g}$. This is significant as it highlights that the design and kinetics for mixed plastic pyrolysis waste cannot be easily inferred from pure plastic pyrolysis behaviour alone.

Tables 4.45 and 4.46 indicate the indirect CO_2 emission results for the pure and mixed plastic pyrolysis experiments respectively. Additionally, the CO_2 emissions per gram of liquid and wax product obtained are presented. This corresponds to the 'B' parameter in Figure 4.17. CO_2 was not detected in the pyrolysis gas by the GC-MS. For this reason, the gate-to-gate assessment did not consider these emissions. It is assumed that with strict control of the vacuum

in the system, that negligible quantities of CO_2 would be emitted as there should be minimal combustion occurring in the pyrolysis reactor.

Table 4.45: Indirect CO_2 emissions of the plastic pyrolysis processes for the individual plastic experiments at 450°C and 42 kPa.

Experiment	Mass of liquid + wax (g)	Indirect CO_2 Emissions (kg CO_2)				Indirect CO_2 emissions per gram of liquid + wax product obtained (kg CO_2 per gram)
		Heating Mantle	Vacuum Pump	Water Circulator	Total	
IP-01	10.46	13.35	13.35	13.35	40.05	3.83
IP-02	11.74	6.63	6.63	6.63	19.89	1.69
IP-03	11.68	5.22	5.22	5.22	15.66	1.34
IP-04	12.89	2.33	2.33	2.33	6.99	0.54
IP-05	11.74	1.60	1.60	1.60	4.80	0.41
IP-06	10.93	1.52	1.52	1.52	4.56	0.42
IP-07	10.76	1.40	1.40	1.40	4.20	0.39
IP-08	10.83	1.32	1.32	1.32	3.96	0.36
IP-09	10.81	1.12	1.12	1.12	3.36	0.31

Table 4.46: Indirect CO_2 emissions of the plastic pyrolysis processes for the mixed plastic experiments at 450°C and 42 kPa.

Experiment	Mass of liquid + wax (g)	Indirect CO_2 Emissions (kg CO_2)				Indirect CO_2 emissions per gram of liquid + wax product obtained (kg CO_2 per gram)
		Heating Mantle	Vacuum Pump	Water Circulator	Total	
MP-01	10.20	6.70	6.70	6.70	20.10	1.97
MP-02	12.32	3.78	3.78	3.78	11.34	0.92
MP-03	10.55	3.45	3.45	3.45	10.35	0.98
MP-04	11.18	7.69	7.69	7.69	23.07	2.06
MP-05	11.53	6.15	6.15	6.15	18.45	1.60
MP-06	11.33	5.98	5.98	5.98	17.94	1.58
MP-07	12.03	8.56	8.56	8.56	25.68	2.14
MP-08	11.92	7.56	7.56	7.56	22.68	1.90
MP-09	11.76	7.44	7.44	7.44	22.32	1.90

The data indicates that the three major power consuming units contribute somewhat equally to the CO_2 emissions, if they are all assumed to be operating at capacity. In line with the power consumption, experiment IP-01 (Table 4.34) had the highest CO_2 emissions per gram of product obtained (3.83 $\frac{kg\ CO_2}{g}$). The lowest CO_2 emission values were obtained for experiment IP-09 (PP pyrolysis) (0.31 $\frac{kg\ CO_2}{g}$).

Naturally as shown in Table 4.46, the CO_2 emissions per gram of product increased as the amount of LDPE in the feed was increased in the mixed plastic experiments. The lowest CO_2 emissions per gram of product obtained for the mixed plastic experiments were indicated by MP-02 to MP-03 (0.92 $\frac{kg\ CO_2}{g}$ and 0.98 $\frac{kg\ CO_2}{g}$ respectively). The highest values were obtained in experiments MP-07 to MP-09 as these had the highest proportions of LDPE (65 wt %). These experiments indicated indirect CO_2 emissions ranging from 1.90 $\frac{kg\ CO_2}{g}$ to 2.14 $\frac{kg\ CO_2}{g}$.

The trends observed in VOC emissions have been discussed in detail in sections 4.6 and 4.7. Tables 4.47 and 4.48 summarize the total VOC content in emissions for the pure plastic and mixed plastic experiments respectively.

Table 4.47: VOC content of emissions in the individual plastic pyrolysis experiments at 450°C and 42 kPa.

Experiment	VOC Emissions (%)
IP-01	72.3
IP-02	67.2
IP-03	32.6
IP-04	82.1
IP-05	69.2
IP-06	74.0
IP-07	83.3
IP-08	35.6
IP-09	61.1

Table 4.48: VOC content of emissions in the mixed plastic pyrolysis experiments at 450°C and 42 kPa.

Experiment	VOC Emissions (%)
MP-01	66.1
MP-02	79.4
MP-03	89.6
MP-04	65.8
MP-05	76.5
MP-06	73.2
MP-07	76.9
MP-08	73.5
MP-09	74.5

4.8.5 Collection and cleaning

The collection and cleaning step has constant inputs and outputs for all the pyrolysis experiments (Figure 4.17, step 6). The small amount of char and spent catalyst was collected after cooling as a brittle, porous mass (1.5 g per run). This was disposed of as solid waste. It may be possible to reuse the mixture as catalyst in subsequent pyrolysis process runs, however this was not considered in this GGA. Approximately 2 litres of water were used to clean all pyrolysis equipment after each experiment. Additionally, 50 ml of hexane was needed for cleaning to dissolve the waxy residue in the glassware. The cleaning process also utilized a 1.5 kW water circulator and heater, which was used to heat the residue in the condensing tube. The same method indicated by Sample Calculation B3 was used to calculate the electricity usage and indirect CO_2 emissions of the cleaning process. The data indicates that 1kWh was used after every experiment. This indirectly contributes to 1.61 kg of CO_2 released for cleaning after every experiment.

CHAPTER FIVE: CONCLUSIONS

- Pyrolysis of plastic pellets, firstly of pure LDPE, HDPE, and PP, followed by mixed plastic, were performed experimentally. Sample analyses were further conducted for the products, namely, liquid, gas, and wax. In total, 18 experiments were conducted using a glass apparatus setup with analytical GC-MS devices for analyses of the products.
- In the case of the LDPE refuse bags which were measured as a test system, a 3:100 zinc oxide catalyst to feed ratio at 300°C increased the rate and reduced the energy requirements of the pyrolysis process. In addition, this experiment produced high combined yields of liquid and wax (>90 wt %). Additionally, these conditions may produce low char and gas yields.
- Uncatalysed HDPE pyrolysis resulted in a combined liquid and wax yield of 85.4 wt % which was the highest yield among the pure plastic feed runs. It was found that the inclusion of the catalyst for HDPE pyrolysis increased the production of gaseous products appreciably at the selected fixed pyrolysis temperature. Lower temperatures could be considered if this is used as a pure feed. This effect was not observed in the HDPE rich mixed plastic experiments as gaseous yields decreased significantly with a 5:100 catalyst to feed ratio.
- PP pyrolysis reactions exhibited the lowest process durations to reaction completion (less than 3 hours). However, these experiments produced significantly higher gas yields (> 17.7 wt %).
- The composition of the liquid and wax was found to change slightly when catalyst was employed, however this effect varied among feeds and conditions.
- Pyrolysis of the 40 wt % PP mixture resulted in more than 99 % of components in the liquid within the diesel carbon number range. Waste plastic with high proportions of PP would therefore produce significant liquid + wax yields with desirable product components which could be used for fuel blends and waxes.
- Mixture plastic pyrolysis behaviours were observed to align only broadly with pure plastic pyrolysis behaviour, correlating with their relative proportions in the feedstock for certain parameters. In the case of the compounded LDPE rich mixture, higher heating requirements were required for the catalysed mixed waste reaction, than the pure compounded LDPE experiments.

- The use of the 5:100 catalyst to feed ratio increased the liquid + wax yields for the feed mixture of 15 wt % compounded LDPE, 40 wt % PP, and 45 wt % HDPE. This trend was also observed with the feed mixture of 32.3 wt % compounded LDPE, 33.18 wt % PP, and 34.52 wt % HDPE. This catalyst specification (5:100) has proven to be the most effective in the majority of the experiments by reducing reaction times and increasing the combined liquid and wax yields. Zinc oxide may therefore be an economical and useful catalyst to enhance the plastic pyrolysis process.
- The feed mixture with 65 wt % compounded LDPE, 15 wt % PP, and 20 wt % HDPE may have significantly higher process durations due to the high energy requirement for the pyrolysis of the compounded LDPE plastic. In these mixtures the catalyst was not found to appreciably alter the liquid + wax yields but did significantly reduce the pyrolysis reaction time.
- Pyrolysis of the feed mixture of 32.30 wt % compounded LDPE, 33.18 wt % PP, and 34.52 wt % HDPE produced total VOCs composition in the gas phase ranging from 65.8 % to 76.5 %. The total VOCs was lowest in these mixed plastic pyrolysis runs as compared to the other sets. It was observed that the catalyst increased the total VOCs and the carbon number of the most abundant VOCs in the gas stream. This may be desirable from a process perspective, as it indicates that these higher carbon number (heavier) VOCs can be captured by condensation more easily than lighter fractions. The balance of hydrocarbons in the gas phase are not strictly classified as VOCs as they are not recognised as exposure hazards. The presence of carbon dioxide in the gas phase was not detected according to GC-MS analysis results. The emissions detected from the bench scale laboratory experiments correlated broadly with data obtained from the commercial pyrolyzer experiments conducted in this work.
- The pyrolysis reaction of 32.30 wt % LDPE, 33.18 wt % PP, and 34.52 wt % HDPE with a zinc oxide catalyst to feed ratio of 5:100 may be considered most efficient from the results of the trials in this work, due to its balanced trade-off between the high liquid + wax yield (76.6 wt %), reasonably low gas yield (14.5 wt %) and relatively lower VOC content in the gas stream (76.5 wt % VOCs) and process duration to completion (12 h 45 min).
- The preliminary life cycle gate to gate analysis indicated that the energy usage and indirect CO_2 emissions per gram of product was 0.99 $\frac{kWh}{g}$ and 1.60 $\frac{kg\ CO_2}{g}$ respectively for the pyrolysis of 32.30 wt % LDPE, 33.18 wt % PP, and 34.52 wt % HDPE with a

zinc oxide catalyst to feed ratio of 5:100 . In comparison to the other runs, these values were close to the midpoint of the entire range of values for these two factors.

- It was observed that the use of the 5:100 zinc oxide catalyst to feed ratio decreased the VOC composition of the gas phase in all pure plastic pyrolysis experiments. Additionally, the feed mixture of 65 wt % LDPE, 15 wt % PP, and 20 wt % HDPE has shown the same trend with a slight decrease of VOCs with catalyst.
- The composition analyses of the liquid products formed during pyrolysis generally indicated many hydrocarbons with chain lengths of C_{12} to C_{27}. This indicates that the products may have similar properties to that of diesel fuel and there is potential for blending. The liquid and wax products formed during pyrolysis could also be used in further thermal hydrocarbon cracking processes to produce lighter fractions and higher proportions of gas product fuel, if it is desired for a particular application.

CHAPTER SIX: RECOMMENDATIONS

All plastic pellet pyrolysis experiments were performed at 450°C due to time constraints and equipment limitations. Operational temperatures of 300°C, 350°C, and 400°C and higher temperatures should be explored to investigate the influence of temperature on product yields, VOC content in emissions, and process duration.

The utilized zinc oxide catalyst to feed ratios were 5:100 and 10:100. Intermediate ratios such as 2.5:100 and 7.5:100 should be investigated to provide a well-defined set of results which may indicate more favourable economic options regarding the reduced usage of catalyst.

All experiments were performed with at a vacuum pressure of approximately 42 kPa due to the equipment limitations. Tekade et al. (2020) indicated that a variation of operational pressures significantly influences the product yields. This influence could be investigated with a view to increase the yield of liquid and wax. Many literature sources have utilized nitrogen environments in plastic pyrolysis. This is another method of providing an inert environment for reactions. The experimental set-up could be re-designed for higher pressures to allow for a nitrogen inert environment. Then the effect of such pressure changes and environmental factors should be investigated on the product yields and emission compositions.

Mixed plastics are often contaminated with other materials such as foil liners, biomass and sand that are difficult to isolate. Such realistic waste plastic sources should be considered for pyrolysis testing as a means to provide an effective waste management strategy for such waste.

The reactor vessel is not completely insulated from the surrounding atmosphere. In this case, a lot of heat energy is wasted. Further study into heat integration of the pyrolysis process should be done.

REFERENCES

ACSMaterial, (2022a). 'ZSM-5-Zeolite Socony Mobil-5'. [Online]. Available at: https://www.acsmaterial.com/blog-detail/zsm-5-molecular-seive.html. [Accessed 07/10/2022].

ACS Material, (2022b). 'ZSM-5 Series Zeolite (MFI) Powder'. [Online]. Available at: https://www.acsmaterial.com/zsm-5-series-zeolite-powder.html. [Accessed 08/06/2022].

ACS Material, (2022c). 'Y-type Series Zeolites'. [Online]. Available at: https://www.acsmaterial.com/y-type-series-zeolites.html. [Accessed 08/06/2022].

ACS Material, (2022). 'ZSM-11'. [Online]. Available at: https://www.acsmaterial.com/zsm-11.html. [Accessed 08/06/2022].

ACS Material, (2022d). 'ZSM-5 Catalyst'. [Online]. Available at: https://www.acsmaterial.com/zsm-5-catalyst.html. [Accessed 08/06/2022].

Al Rayaan, M., 2022. The feasibility of adoption of catalytic removal of nitrate in Saudi Arabia's groundwater: A gate-to-gate environmental analysis. Clean Eng Technol 10, 100542.

Aladin, A., Modding, B., Syarif, T., Dewi, F.C., 2021. Effect of nitrogen gas flowing continuously into the pyrolysis reactor for simultaneous production of charcoal and liquid smoke. J Phys Conf Ser 1763, 012020.

Almadhi, A., Abdelhadi, A., Alyamani, R., 2023. Moving from Linear to Circular Economy in Saudi Arabia: Life-Cycle Assessment on Plastic Waste Management. Sustainability 15, 10450.

Altin, O., Eser, S., 2004. Carbon deposition from thermal stressing of petroleum fuels. ACS National Meeting Book of Abstracts 228.

Andooz, A., Eqbalpour, M., Kowsari, E., Ramakrishna, S., Ansari Cheshmeh, Z., 2023. A comprehensive review on pyrolysis from the circular economy point of view and its environmental and social effects. J Clean Prod 388, 136021.

Anuar Sharuddin, S.D., Abnisa, F., Wan Daud, W.M.A., Aroua, M.K., 2016. A review on pyrolysis of plastic wastes. Energy Convers Manag 115, 308–326.

Baena-González, J., Santamaria-Echart, A., Aguirre, J.L., González, S., 2020. Chemical recycling of plastic waste: Bitumen, solvents, and polystyrene from pyrolysis oil. Waste Management 118, 139–149.

Batool, M., Shah, A.T., Imran Din, M., Li, B., 2016a. Catalytic Pyrolysis of Low Density Polyethylene Using Cetyltrimethyl Ammonium Encapsulated Monovacant Keggin Units (C19H42N)4H3(PW11O39) and ZSM-5. J Chem 2016, 1–5.

Budsaereechai, S., Hunt, A.J., Ngernyen, Y., 2019b. Catalytic pyrolysis of plastic waste for the production of liquid fuels for engines. RSC Adv 9, 5844–5857.

Cao, C., 2017. Sustainability and life assessment of high strength natural fibre composites in construction. In: Advanced High Strength Natural Fibre Composites in Construction. Elsevier, pp. 529–544.

Capello, C., Wernet, G., Sutter, J., Hellweg, S., Hungerbühler, K., 2009. A comprehensive environmental assessment of petrochemical solvent production. Int J Life Cycle Assess 14, 467–479.

Cho, M., Jung, S., Kim, J., 2010. Pyrolysis of Mixed Plastic Wastes for the Recovery of Benzene, Toluene, and Xylene (BTX) Aromatics in a Fluidized Bed and Chlorine Removal by Applying Various Additives. Energy & Fuels 24, 1389–1395.

Conesa, J.A., Font, R., Fullana, A., Martín-Gullón, I., Aracil, I., Gálvez, A., Moltó, J., Gómez-Rico, M.F., 2009. Comparison between emissions from the pyrolysis and combustion of different wastes. J Anal Appl Pyrolysis 84, 95–102.

Curran, M.A., 2012. Life Cycle Assessment Handbook: A guide for enviornmentally sustainable products. John Wiley & Sons.

Davidson, M.G., Furlong, R.A., McManus, M.C., 2021. Developments in the life cycle assessment of chemical recycling of plastic waste – A review. J Clean Prod 293, 126163.

de Freitas Costa, A.F., Ferreira, C.C., da Paz, S.P.A., Santos, M.C., Moreira, L.G.S., Mendonça, N.M., da Costa Assunção, F.P., de Freitas, A.C.G. de A., Costa, R.M.R., de Sousa Brandão, I.W., da Costa, C.E.F., da Mota, S.A.P., de Castro, D.A.R., Duvoisin, S., Borges, L.E.P., Machado, N.T., Bernar, L.P., 2023. Catalytic Upgrading of Plastic Waste of Electric and Electronic Equipment (WEEE) Pyrolysis Vapors over Si–Al Ash Pellets in a Two-Stage Reactor. Energies (Basel) 16, 541.

EDL, (2021). 'LDPE Plastic Recycling Process'. [Online]. Available at: https://www.edlpackaging.com/blog/how-is-ldpe-film-recycled-after-its-used-for-secondary-packaging/#:~:text=How%20Does%20the%20LDPE%20Plastic,pellets%20for%20ease%20of%20handling. [Accessed 04/06/2024]

Fadillah, G., Fatimah, I., Sahroni, I., Musawwa, M.M., Mahlia, T.M.I., Muraza, O., 2021. Recent progress in low-cost catalysts for pyrolysis of plastic waste to fuels. Catalysts 11.

Fichana, D., 2005. Green engineering and gate-to gate life cycle assessments for pharmaceutical products.

Gaurh, P., Pramanik, H., 2020. In-situ production of valuable aromatics via pyrolysis of waste polypropylene using commercial catalyst zsm-5. Indian Journal of Chemical Technology 27, 144–152.

Gebre, S.H., Sendeku, M.G., Bahri, M., 2021. Recent Trends in the Pyrolysis of Non-Degradable Waste Plastics. ChemistryOpen 10, 1202–1226.

Gowrishankar, D., Kumar, G.D., Prithviraj, R., Sanjay, V., Hariharan, D., Vignesh, M., 2021. Synthesis and performance evaluation of fuel from waste plastics. International Journal of Vehicle Structures and Systems 13, 289–292.

Grewan, K., Trois, P.C., 2023. Published by IEA Bioenergy Review of Waste to Energy Policies in South Africa and International Comparisons Title of publication Subtitle of publication.

Güneş, Ç.E., Şengül, H., 2022. Cradle-to-gate life cycle assessment of a liquid pharmaceutical product through analysis of chemical production pathways. Clean Technol Environ Policy 24, 1741–1755.

Harussani, M.M., Sapuan, S.M., Rashid, U., Khalina, A., Ilyas, R.A., 2022. Pyrolysis of polypropylene plastic waste into carbonaceous char: Priority of plastic waste management amidst COVID-19 pandemic. Science of The Total Environment 803, 149911.

Infinita Lab, (2024). 'Recycling of High-Density Polyethylene'. [Online]. Available at: https://infinitalab.com/plastics/the-process-of-recycling-hdpe/. [Accessed 04/06/2024].

Jamradloedluk, J., Lertsatitthanakorn, C., 2014. Characterization and utilization of char derived from fast pyrolysis of plastic wastes. Procedia Eng 69, 1437–1442.

Jiménez-González, C., Kim, S., Overcash, M.R., 2000. Methodology for developing gate-to-gate Life cycle inventory information. Int J Life Cycle Assess 5, 153–159.

Jin, Q., Wang, X., Li, S., Mikulčić, H., Bešenić, T., Deng, S., Vujanović, M., Tan, H., Kumfer, B.M., 2019. Synergistic effects during co-pyrolysis of biomass and plastic: Gas, tar, soot, char products and thermogravimetric study. Journal of the Energy Institute 92, 108–117.

Kaminsky, W., 2021a. Chemical recycling of plastics by fluidized bed pyrolysis. Fuel Communications 8, 100023.

Kaminsky, W., 2021b. Chemical recycling of plastics by fluidized bed pyrolysis. Fuel Communications 8, 100023.

Kar, Y., Göksu, D.Ş., Yalman, Y., 2018. Characterization of light diesel fraction obtained from upgraded heavy oil. Egyptian Journal of Petroleum 27, 1301–1304.

Kleinekorte, J., Fleitmann, L., Bachmann, M., Kätelhön, A., Barbosa-Póvoa, A., von der Assen, N., Bardow, A., 2020. Life Cycle Assessment for the Design of Chemical Processes, Products, and Supply Chains. Annu Rev Chem Biomol Eng 11, 203–233.

Kulas, D.G., Zolghadr, A., Shonnard, D.R., 2022. Liquid-fed waste plastic pyrolysis pilot plant: Effect of reactor volume on product yields. J Anal Appl Pyrolysis 166, 105601.

Lee, N., Joo, J., Lin, K.A., Lee, J., 2021. Waste-to-Fuels: Pyrolysis of Low-Density Polyethylene Waste in the Presence of H-ZSM-11. Polymers (Basel) 13, 1198.

LibreTexts, (2022). ‘Alkyl Groups’. [Online]. Available at: https://chem.libretexts.org/Courses/Athabasca_University/Chemistry_350%3A_Organic_Chemistry_I/03%3A_Organic_Compounds-_Alkanes_and_Their_Stereochemistry/3.03%3A_Alkyl_Groups#:~:text=An%20alkyl%20group%20is%20formed,names%20provided%20in%20Table%203.3. [Accessed 09/10/2024].

López, A., de Marco, I., Caballero, B.M., Laresgoiti, M.F., Adrados, A., 2011a. Influence of time and temperature on pyrolysis of plastic wastes in a semi-batch reactor. Chemical Engineering Journal 173, 62–71.

López, A., de Marco, I., Caballero, B.M., Laresgoiti, M.F., Adrados, A., Aranzabal, A., 2011b. Catalytic pyrolysis of plastic wastes with two different types of catalysts: ZSM-5 zeolite and Red Mud. Appl Catal B 104, 211–219.

Luo, G., Suto, T., Yasu, S., Kato, K., 2000. Catalytic degradation of high density polyethylene and polypropylene into liquid fuel in a powder-particle fluidized bed. Polym Degrad Stab 70, 97–102.

Luo, S., Xiao, B., Hu, Z., Liu, S., 2010. Effect of particle size on pyrolysis of single-component municipal solid waste in fixed bed reactor. Int J Hydrogen Energy 35, 93–97.

Mahath, C.S., Mophin Kani, K., Dubey, B., 2019. Gate-to-gate environmental impacts of dairy processing products in Thiruvananthapuram, India. Resour Conserv Recycl 141, 40–53.

Martín-Lara, M.A., Piñar, A., Ligero, A., Blázquez, G., Calero, M., 2021. Characterization and use of char produced from pyrolysis of post-consumer mixed plastic waste. Water (Switzerland) 13, 1–20.

Miandad, R., Barakat, M.A., Aburiazaiza, A.S., Rehan, M., Nizami, A.S., 2016. Catalytic pyrolysis of plastic waste: A review. Process Safety and Environmental Protection 102, 822–838.

Miandad, R., Rehan, M., Barakat, M.A., Aburiazaiza, A.S., Khan, H., Ismail, I.M.I., Dhavamani, J., Gardy, J., Hassanpour, A., Nizami, A.S., 2019. Catalytic pyrolysis of plastic waste: Moving toward pyrolysis based biorefineries. Front Energy Res 7.

Morgan, A., Grigg, R., Ampomah, W., 2021. A Gate-to-Gate Life Cycle Assessment for the CO2-EOR Operations at Farnsworth Unit (FWU). Energies 14, 2499.

Muringayil Joseph, T., Azat, S., Ahmadi, Z., Moini Jazani, O., Esmaeili, A., Kianfar, E., Haponiuk, J., Thomas, S., 2024. Polyethylene terephthalate (PET) recycling: A review. Case Stud. Chem. Environ. Eng. 9.

Núñez-Cacho, P., Leyva-Díaz, J.C., Sánchez-Molina, J., van der Gun, R., 2020. Plastics and sustainable purchase decisions in a circular economy: The case of Dutch food industry. PLoS One 15, 1–17.

Osman, A.I., Farrell, C., Al-Muhtaseb, A.H., Al-Fatesh, A.S., Harrison, J., Rooney, D.W., 2020. Pyrolysis kinetic modelling of abundant plastic waste (PET) and in-situ emission monitoring. Environ Sci Eur 32, 112.

Papuga, S., Djurdjevic, M., Ciccioli, A., Vecchio Ciprioti, S., 2022. Catalytic Pyrolysis of Plastic Waste and Molecular Symmetry Effects: A Review. Symmetry (Basel). 15, 38.

Papuga, S., Gvero, P., Vukic, L., 2016. Temperature and time influence on the waste plastics pyrolysis in the fixed bed reactor. Thermal Science 20, 731–741.

Parvatker, A.G., Tunceroglu, H., Sherman, J.D., Coish, P., Anastas, P., Zimmerman, J.B., Eckelman, M.J., 2019. Cradle-to-Gate Greenhouse Gas Emissions for Twenty Anesthetic Active Pharmaceutical Ingredients Based on Process Scale-Up and Process Design Calculations. ACS Sustain Chem Eng 7, 6580–6591.

Phakedi, D., Ude, A.U., Oladijo, P.O., 2021. Co-pyrolysis of polymer waste and carbon-based matter as an alternative for waste management in the developing world. J Anal Appl Pyrolysis 155, 105077.

Pires, L., Vaz, M., Carolina, A., Oliveira, C. De, Falcon, L., Stella, M., Pimenta, S., Bessa, I.G., Wouters, J., Andrade, H.S., Pinto, C., 2021. Capture and Reuse of Carbon Dioxide (CO 2) for a Plastics Circular Economy : A Review. Processes 9.

Raveh-Amit, H., Lemont, F., Bar-Nes, G., Klein-BenDavid, O., Banano, N., Gelfer, S., Charvin, P., Bin Rozaini, T., Sedan, J., Rousset, F., 2022. Catalytic Pyrolysis of High-Density Polyethylene: Decomposition Efficiency and Kinetics. Catalysts 12, 140.

Rehan, M., Miandad, R., Barakat, M.A., Ismail, I.M.I., Almeelbi, T., Gardy, J., Hassanpour, A., Khan, M.Z., Demirbas, A., Nizami, A.S., 2017. Effect of zeolite catalysts on pyrolysis liquid oil. Int. Biodeterior. Biodegradation 119, 162–175.

Roy, P., Dutta, A., 2019. Life Cycle Assessment (LCA) in Municipal Waste Management Decision Making. In: Plastics to Energy. Elsevier, pp. 377–402.

Ryan, P.G., 2020. The transport and fate of marine plastics in South Africa and adjacent oceans. S Afr J Sci 116.

Salisu, A., Maigari, Y.S., 2021. Polystyrene and Its Recycling : a Review Msnkad Id 2141. Proc. Mater. Sci. Technol. Soc. Niger. Kaduna State Chapter 195–203.

Senthil Kumar, P., Bharathikumar, M., Prabhakaran, C., Vijayan, S., Ramakrishnan, K., 2017. Conversion of waste plastics into low-emissive hydrocarbon fuels through catalytic depolymerization in a new laboratory scale batch reactor. International Journal of Energy and Environmental Engineering 8, 167–173.

Serrano, D.P., Aguado, J., Escola, J.M., 2012. Developing Advanced Catalysts for the Conversion of Polyolefinic Waste Plastics into Fuels and Chemicals. ACS Catal 2, 1924–1941.

Sivagami, K., Kumar, K. V., Tamizhdurai, P., Govindarajan, D., Kumar, M., Nambi, I., 2022. Conversion of plastic waste into fuel oil using zeolite catalysts in a bench-scale pyrolysis reactor. RSC Adv. 12, 7612–7620.

Skone, T.J., James III, R.E., Cooney, G., Jamieson, M., Littlefield, J., Marriott, J., 2013. Gate-to-Gate Life Cycle Inventory and Model of CO2-Enhanced Oil Recovery.

Slimani, F., Hedir, A., Moudoud, M., Durmus, A., Amir, M., Megherbi, M., 2021. Prediction of long-term physical properties of low density polyethylene (LDPE) cable insulation materials by artificial neural network modeling approach under environmental constraints. Turkish Journal of Electrical Engineering and Computer Sciences 25, 2437–2449.

Sogancioglu, M., Yel, E., Ahmetli, G., 2017. Pyrolysis of waste high density polyethylene (HDPE) and low density polyethylene (LDPE) plastics and production of epoxy composites with their pyrolysis chars. J Clean Prod 165, 369–381.

Tekade, S.P., Gugale, P.P., Gohil, M.L., Gharat, S.H., Patil, T., Chaudhari, P.K., Patle, D.S., Sawarkar, A.N., 2020. Pyrolysis of waste polyethylene under vacuum using zinc oxide. Energy Sources, Part A: Recovery, Utilization and Environmental Effects 00, 1–15.

Valentin, L.A., Valentin, C.A., Kobelnik, M., Lins da Silva, J., 2022. Chemical characterization of polyethylene geomembranes by chromatography coupled to mass spectrometry using multivariate tools. Case Studies in Chemical and Environmental Engineering 5, 100174.

Van De Beld, B., Holle, E., Florijn, J., 2013. The use of pyrolysis oil and pyrolysis oil derived fuels in diesel engines for CHP applications. Appl Energy 102, 190–197.

Van der Vorst, G., Dewulf, J., Aelterman, W., De Witte, B., Van Langenhove, H., 2011. A Systematic Evaluation of the Resource Consumption of Active Pharmaceutical Ingredient Production at Three Different Levels. Environ Sci Technol 45, 3040–3046.

Veksha, A., Giannis, A., Oh, W. Da, Chang, V.W.C., Lisak, G., 2018. Upgrading of non-condensable pyrolysis gas from mixed plastics through catalytic decomposition and dechlorination. Fuel Processing Technology 170, 13–20.

Wernet, G., Hellweg, S., Hungerbühler, K., 2012. A tiered approach to estimate inventory data and impacts of chemical products and mixtures. Int J Life Cycle Assess 17, 720–728.

Xayachak, T., Haque, N., Parthasarathy, R., King, S., Emami, N., Lau, D., Pramanik, B.K., 2022. Pyrolysis for plastic waste management: An engineering perspective. J Environ Chem Eng 10, 108865.

Yadav, G., Singh, A., Dutta, A., Uekert, T., DesVeaux, J.S., Nicholson, S.R., Tan, E.C.D., Mukarakate, C., Schaidle, J.A., Wrasman, C.J., Carpenter, A.C., Baldwin, R.M., Román-Leshkov, Y., Beckham, G.T., 2023. Techno-economic analysis and life cycle assessment for catalytic fast pyrolysis of mixed plastic waste. Energy Environ Sci 16, 3638–3653.

Yamashita, K., Kumagai, K., Noguchi, M., Yamamoto, N., Ni, Y., Mizukoshi, A., Yanagisawa, Y., 2007a. VOC emissions from waste plastics during melting processes. IAQVEC 2007 Proceedings - 6th International Conference on Indoor Air Quality, Ventilation and Energy Conservation in Buildings: Sustainable Built Environment 2, 407–412.

Yamashita, K., Kumagai, K., Noguchi, M., Yamamoto, N., Ni, Y., Mizukoshi, A., Yanagisawa, Y., 2007b. VOC emissions from waste plastics during melting processes. IAQVEC 2007 Proceedings - 6th International Conference on Indoor Air Quality, Ventilation and Energy Conservation in Buildings: Sustainable Built Environment 2, 407–412.

Zhang, S., Xu, C., Xie, R., Yu, H., Sun, M., Li, F., 2023. Environmental assessment of fabric wet processing from gate-to-gate perspective: Comparative study of weaving and materials. Science of The Total Environment 857, 159495.

Appendix A: Plastic pyrolysis data

Table A1: Mass of pyrolysis product equipment before and after uncatalysed test experiment at 280°C and 42 kPa.

Apparatus	Mass Before Experiment (g) (U= ± 0.001 g)	Mass After Experiment (g) (U= ± 0.001 g)
Reactor	96.706	97.276
Spiral Condenser	154.778	167.828
Collection Flask	115.572	115.802

Table A2: Mass and yields of products for uncatalysed LDPE test experiment at 280^0C and 42 kPa.

Pyrolysis Product	Mass (g)	Yield (wt %)
Liquid	0.230 ± 0.002 g	1.5
Wax	13.050 ± 0.002 g	86.8
Total Liquid + Wax	13.280 ± 0.004 g	88.3
Char	0.570 ± 0.002 g	3.5
Gas	1.190 ± 0.007 g	7.9

Table A3: Peak area % of various components in the liquid product from LDPE pyrolysis using a 10:100 zinc oxide catalyst to feed ratio at 450°C and 42 kPa (IP-03).

Liquid Component	Peak Area %
1-dodecene (C12)	0.90
dodecane (C12)	3.43
1,12-tridecadiene (C13)	0.23
1-tridecene (C13)	6.46
tetradecane (C14)	10.59
1-pentadecene (C15)	6.80
Z-10-pentadecen-1-ol (C15)	0.62
cyclohexadecane (C16)	0.28
hexadecane (C16)	3.77
1-heptadecene (C17)	9.43
heptadecane (C17)	3.71
octadecane (C18)	3.83
18-nonadecen-1-ol (C19)	0.36
1-nonadecene (C19)	4.96
nonadecane (C19)	1.29
E-3-eicosene (C20)	0.19
E-5-eicosene (C20)	1.86
E-9-eicosene(C20)	0.22
1,19-eicosadiene (C20)	0.72
1-heneicosanol (C21)	5.89
heneicosane (C21)	24.44
docosane (C20)	0.58
1-tetracosanol (C24)	3.83
1-pentacosene (C25)	0.22
1-heptacosanol (C27)	1.07
1-heptacosene (C27)	0.30
tetratetracontane (C44)	2.01

Table A4: Peak area % of various components in the wax product from LDPE pyrolysis using a 10:100 zinc oxide catalyst to feed ratio at 450°C and 42 kPa (IP-03).

Wax Component	**Peak Area %**
1-dodecene (C12)	2.67
cyclododecane (C12)	0.34
1-tridecene (C13)	5.57
1-pentyl-2-propylcyclopentane (C13)	0.41
tridecane (C13)	7.93
tetradecane (C14)	9.44
1-pentadecene (C15)	6.05
2-hexyl-1-decanol (C16)	0.65
1-heptadecene (C17)	5.31
heptadecane (C17)	3.18
E-5-octadecene (C18)	0.34
octadecane (C18)	3.38
1-nonadecene (C19)	7.95
nonadecane (C19)	3.10
E-3-eicosene (C20)	0.39
1-heneicosanol (C21)	1.66
heneicosane (C21)	25.62
1-docosene (C22)	0.40
1-docosanol (C22)	1.20
1-tetracosanol (C24)	0.92
1-cyclopentyleicosane (C25)	0.31
pentacosane (C25)	2.03
hexacosane (C26)	3.09
1-heptacosanol (C27)	0.62
2-methylhexacosane (C27)	0.26
dotriacontane (C32)	0.75
tetracontane (C40)	6.41

Table A5: Peak area % of various components in the liquid product from uncatalysed HDPE pyrolysis at 450°C and 42 kPa (IP-04).

Liquid Component	**Peak Area %**
1-dodecene (C12)	3.14
dodecane (C12)	3.14
Z-2-tridecene (C13)	3.61
tridecane (C13)	3.36
1,12-tridecadiene (C13)	1.01
1-tetradecene (C14)	8.57
1-pentadecene (C15)	3.90
hexadecane (C16)	14.98
1-hexadecene (C16)	2.91
E-15-heptadecenal (C17)	3.67
1-octadecene (C18)	4.14
octadecane (C18)	1.68
eicosane (C20)	13.03
heneicosane (C21)	3.37
10-methyleicosane, (C21)	3.18
1-docosene (C22)	11.57
tetracosane (C24)	6.04
bis(2-ethylhexyl) isophthalate (C24)	0.73
hexacosane (C26)	0.27
octacosane (C28)	6.38
tetratetracontane (C44)	1.25
11,20-didecyltriacontane (C50)	0.10

Table A6: Peak area % of various components in the liquid product from HDPE pyrolysis using a 5:100 zinc oxide catalyst to feed ratio at 450°C and 42 kPa (IP-05).

Liquid Component	Peak Area %
1-dodecene (C12)	4.23
dodecane (C12)	3.82
1-tridecene (C13)	4.32
1,12-tridecadiene (C13)	2.08
tridecane (C13)	3.91
1-tetradecene (C14)	5.00
1,15-pentadecanediol (C15)	0.60
1-pentadecene (C15)	5.08
Z-10-pentadecen-1-ol (C15)	0.56
1-hexadecene (C16)	4.86
E-14-hexadecenal (C16)	4.18
hexadecane (C16)	3.8
E-15-heptadecenal (C17)	3.8
1-octadecanol (C18)	1.44
1-octadecene (C18)	4.64
octadecane (C18)	1.43
Z-18-nonadecen-1-ol (C19)	1.74
E-5-eicosene (C20)	0.19
eicosane (C20)	8.15
heneicosane (C21)	6.87
1-docosene (C22)	12.25
tetracosane (C24)	6.77
hexacosane (C26)	1.66
octacosane (C28)	6.27
2-methyloctacosane (C29)	0.49
tetratetracontane (C44)	1.85

Table A7: Peak area % of various components in the liquid product from HDPE pyrolysis using a 10:100 zinc oxide catalyst to feed ratio at 450°C and 42 kPa (IP-06).

Liquid Component	**Peak Area %**
dodecane (C12)	3.79
1-dodecene (C12)	4.00
1-tridecene (C13)	4.10
tridecane (C13)	3.67
1-tetradecene (C14)	9.21
1-hexadecene (C16)	8.20
hexadecane (C16)	18.40
E-15-heptadecenal (C17)	3.55
1-octadecanol (C18)	0.64
1-octadecene (C18)	3.68
octadecane (C18)	6.69
1-nonadecene (C19)	0.99
10-methyleicosane, (C21)	2.78
heneicosane (C21)	6.77
1-docosene (C22)	11.48
2-methyltetracosane (C25)	0.28
7-hexyleicosane (C26)	5.35
2-methyloctacosane (C29)	0.98
hexatriacontane (C36)	4.84
tetratetracontane (C44)	0.60

Table A8: Peak area % of various components in the wax product from uncatalysed HDPE pyrolysis at 450°C and 42 kPa (IP-04).

Wax Component	Peak Area %
1,12-tridecadiene (C13)	0.29
1-tridecene (C13)	3.18
tridecane (C14)	5.73
1-tetradecene (C14)	7.76
1,15-pentadecanediol (C15)	0.87
Z-10-pentadecen-1-ol (C15)	0.95
1-hexadecene (C16)	3.57
hexadecane (C16)	12.8
1-octadecanol (C18)	1.23
1-octadecene (C18)	7.03
E-2-Octadecadecen-1-ol (C18)	0.56
octadecane (C18)	5.69
18-nonadecen-1-ol (C19)	0.29
1-nonadecene (C19)	4.22
1,19-eicosadiene (C20)	0.81
eicosane (C20)	6.11
heneicosane (C21)	6.06
1-docosene (C22)	11.77
tetracosane (C24)	4.11
2-methyltetracosane (C25)	1.22
octacosane (C28)	8.76
2-methyloctacosane (C29)	1.34
tetratetracontane (C44)	5.63

Table A9: Peak area % of various components in the wax product from HDPE pyrolysis using a 5:100 zinc oxide catalyst to feed ratio at 450°C and 42 kPa (IP-05).

Wax Component	Peak Area %
dodecane (C12)	2.14
1,12-tridecadiene (C13)	0.20
Z-2-tridecene (C13)	6.63
1-tridecanol (C13)	0.23
tridecane (C13)	2.51
1-tetradecene (C14)	7.36
E-3-tetradecene (C14)	0.98
1,15-pentadecanediol (C15)	0.3
1-hexadecene (C16)	3.42
hexadecane (C16)	15.55
Z-1,9-hexadecadiene (C16)	0.19
E-15-heptadecenal (C17)	4.30
1-octadecene (C18)	5.93
E-2-octadecadecen-1-ol (C18)	0.31
octadecane (C18)	6.26
1-nonadecene (C19)	1.09
1,19-eicosadiene (C20)	0.28
1-eicosanol (C20)	0.78
2-methylnonadecane (C20)	5.99
1-docosene (C22)	6.01
2-methyltetracosane (C25)	0.78
7-hexyleicosane (C26)	9.12
hexacosane (C26)	10.06
heptacosane (C27)	5.21
2-methyloctacosane (C29)	2.10
hexatriacontane (C36)	2.25

Table A10: Peak area % of various components in the wax product from HDPE pyrolysis using a 10:100 zinc oxide catalyst to feed ratio at 450 00 and 42 kPa (IP-06).

Wax Component	**Peak Area %**
1-dodecene (C12)	2.99
dodecane (C12)	2.73
1-tridecene (C13)	3.01
tridecane (C13)	2.57
1-tetradecene (C14)	6.55
pentadecane (C15)	2.79
1-hexadecanol (C16)	0.78
1-hexadecene (C16)	6.26
hexadecane (C16)	7.68
E-15-heptadecenal (C17)	2.62
1-octadecanol (C18)	0.56
1-octadecene (C18)	2.79
octadecane (C18)	8.94
1-nonadecene (C19)	5.34
10-methyleicosane, (C21)	9.82
1-docosene (C22)	6.07
tetracosane (C24)	2.97
hexacosane (C26)	13.91
heptacosane (C27)	2.98
2-methyloctacosane (C29)	1.85
tetratetracontane (C44)	6.80

Table A11: Peak area % of various components in the liquid product from uncatalyzed PP pyrolysis at 450°C and 42 kPa (IP-07).

Liquid Component	Peak Area %
1-dodecene (C12)	1.30
7-methyl-1-undecene (C12)	40.47
3,7-dimethyldecane (C12)	0.40
dodecane (C12)	1.01
11-methyldodecanol (C13)	11.65
1-tridecene (C13)	1.05
tridecane (C13)	0.87
2-hexyl-1-octanol (C14)	1.98
Z-3-tetradecene (C14)	1.14
2,3,5,8-tetramethyldecane (C14)	1.41
pentadecane (C15)	0.59
2-hexyl-1-decanol (C16)	9.41
1-hexadecene (C16)	4.58
hexadecane (C16)	5.94
2-octyl-1-decanol (C18)	0.95
1-octadecene (C18)	0.73
1-nonadecanol (C19)	0.49
1-(ethenyloxy)octadecane (C20)	1.08
1-docosene (C22)	0.48
1-tetracosanol (C24)	2.41
1-hexacosanol (C26)	6.43
7-hexyleicosane (C26)	0.93
1-heptacosanol (C27)	4.52
eicosyloctyl ether (C28)	0.20

Table A12: Peak area % of various components in the liquid product from PP pyrolysis using a 5:100 zinc oxide catalyst to feed ratio at 450°C and 42 kPa (IP-08).

Liquid Component	**Peak Area %**
7-methyl-1-undecene (C12)	40.98
11-methyldodecanol (C13)	9.46
1-tridecene (C13)	1.37
tridecane (C13)	0.62
2-hexyl-1-octanol (C14)	5.98
2,3,5,8-tetramethyldecane (C14)	1.64
4,6-dimethyldodecane (C14)	0.84
tetradecane (C14)	0.55
Z-3-tetradecene (C14)	0.76
pentadecane (C15)	0.51
2-hexyl-1-decanol (C16)	21.00
hexadecane (C16)	0.53
Z-3-hexadecene (C17)	1.01
2-octyl-1-decanol (C18)	1.29
2-hexyl-1-dodecanol (C18)	5.80
1-octadecene (C18)	0.91
E-9-octadecene (C18)	0.87
2-octyl-1-dodecanol (C20)	0.86
E-3-eicosene (C20)	0.58
eicosane (C20)	0.49
10-methyleicosane, (C21)	1.19
1-docosene (C22)	0.75
1-cyclopentyleicosane (C22)	0.50
1-hexacosanol (C26)	1.08
tetratetracontane (C44)	0.44

Table A13: Peak area % of various components in the liquid product from PP pyrolysis using a 10:100 zinc oxide catalyst to feed ratio at 450°C and 42 kPa (IP-09).

Liquid Component	**Peak Area %**
7-methyl-1-undecene (C12)	35.54
8-methyl-1-undecene (C12)	0.49
dodecane (C12)	0.91
11-methyldodecanol (C13)	8.72
2-hexyl-1-octanol (C14)	3.99
Z-3-tetradecene (C14)	1.05
2,3,5,8-tetramethyldecane (C14)	0.77
4,6-dimethyldodecane (C14)	0.72
tetradecane (C14)	1.13
pentadecane (C15)	1.31
2-hexyl-1-decanol (C16)	20.95
Z-3-hexadecene (C16)	1.80
hexadecane (C16)	0.77
heptadecane (C17)	1.17
2-hexyl-1-dodecanol (C18)	4.79
E-3-octadecene (C18)	1.61
octadecane (C18)	0.75
E-3-eicosene (C20)	4.25
eicosane (C20)	2.03
1-docosene (C22)	1.95
1-tridecene (C22)	2.68
tetracosane (C24)	2.13
hexacosane (C26)	0.50

Table A14: Peak area % of various components in the wax product from uncatalyzed PP pyrolysis at 450 °C and 42 kPa (IP-07).

Wax Component	Peak Area %
1-methylcycloheptane (C8)	0.64
2,4-diethyl-1-heptanol (C11)	0.51
7-methyl-1-undecene (C12)	3.20
dodecane (C12)	1.30
11-methyldodecanol (C13)	0.47
1-tridecene (C13)	3.17
2-hexyl-1-octanol (C14)	2.59
Z-3-tetradecene (C14)	1.47
2,3,5,8-tetramethyldecane (C14)	0.38
tetradecane (C14)	4.02
1-pentadecene (C15)	2.62
pentadecane (C15)	2.72
2-hexyl-1-decanol (C16)	6.79
Z-3-hexadecene (C16)	2.29
hexadecane (C16)	2.95
heptadecane (C17)	2.65
1-heptadecene (C17)	2.00
2-hexyl-1-dodecanol (C18)	7.64
E-5-octadecene (C18)	0.36
1,2,3,5-tetraisopropylcyclohexane (C18)	10.64
2-octyl-1-decanol (C18)	0.64
1-nonadecene (C18)	1.87
1,19-eicosadiene (C20)	0.95
E-3-eicosene (C20)	15.87
E-9-eicosene(C20)	3.26
1-heneicosanol (C21)	1.02
heneicosane (C21)	7.85
1-docosanol (C22)	0.86
1-cyclopentyleicosane (C25)	4.02
hexacosane (C26)	2.25
tetratetracontane (C44)	2.97

Table A15: Peak area % of various components in the wax product from PP pyrolysis using a 5:100 zinc oxide catalyst to feed ratio at 450°C and 42 kPa (IP-08).

Wax Component	Peak Area %
1-dodecene (C12)	1.35
7-methyl-1-undecene (C12)	4.11
1-methyl-3-propylcyclooctane (C12)	0.35
dodecane (C12)	0.91
11-methyldodecanol (C13)	2.79
1-tridecene (C13)	2.91
1-pentyl-2-propylcyclopentane (C13)	0.36
2-hexyl-1-octanol (C14)	1.53
tetradecane (C14)	4.50
1-pentadecene (C15)	4.03
2,6,11-trimethyldodecane (C15)	0.56
2-hexyl-1-decanol (C16)	7.35
hexadecane (C16)	1.44
1-heptadecene (C17)	3.49
heptadecane (C17)	1.60
2-hexyl-1-dodecanol (C18)	9.46
E-3-octadecene (C18)	16.85
1,2,3,5-tetraisopropylcyclohexane (C18)	11.08
2-octyl-1-decanol (C18)	1.73
1-nonadecene (C19)	4.10
2-octyl-1-dodecanol (C20)	0.49
E-9-eicosene(C20)	1.77
heneicosane (C21)	12.62
1-docosanol (C22)	1.09
1-tetracosanol (C24)	0.97
1-hexacosanol (C26)	0.42
1-heptacosanol (C27)	0.58
octacosanol (C28)	0.63
pentatriacontane (C35)	0.94

Table A16: Peak area % of various components in the wax product from PP pyrolysis using a 10:100 zinc oxide catalyst to feed ratio at 450°C and 42 kPa (IP-09).

Wax Component	**Peak Area %**
1-dodecene (C12)	0.84
7-methyl-1-undecene (C12)	4.60
1-methyl-3-propylcyclooctane (C12)	2.30
dodecane (C12)	0.57
1-tridecene (C13)	2.09
2-hexyl-1-octanol (C14)	3.10
tetradecane (C14)	3.91
1-pentadecene (C15)	3.29
2,6,11-trimethyldodecane (C15)	0.56
2-hexyl-1-decanol (C16)	8.17
hexadecane (C16)	1.21
1-heptadecene (C17)	4.55
heptadecane (C17)	1.53
2-octyl-1-decanol (C18)	1.38
2-hexyl-1-dodecanol (C18)	10.80
E-3-octadecene (C18)	20.68
1,2,3,5-tetraisopropylcyclohexane(C18)	15.97
1-nonadecene (C19)	3.36
2-octyl-1-dodecanol (C20)	0.44
heneicosane (C21)	7.26
1-docosanol (C22)	1.47
1-tetracosanol3 (C24)	0.41

Table A17: Peak area % of various components in the liquid product from the pyrolysis of a feed mixture of 15 wt % LDPE, 45 wt % HDPE, and 40 wt % PP using a 10:100 zinc oxide catalyst to feed ratio at 450°C and 42 kPa (MP-03).

Liquid Component	Peak Area %
3-butyn-1-ol (C4)	0.18
1-dodecene (C12)	2.56
7-methyl-1-undecene (C12)	4.33
dodecane (C12)	3.38
4,6,8-trimethyl-1-nonene (C12)	6.77
11-methyldodecanol (C13)	2.05
1-tridecene (C13)	2.89
1-tetradecene (C14)	7.02
2-hexyl-1-octanol (C14)	1.70
pentadecane (C15)	0.34
Z-10-pentadecen-1-ol (C15)	1.21
2-hexyl-1-decanol (C16)	1.51
1-hexadecanol (C16)	0.51
Z-7-Hexadecene (C16)	0.32
1-hexadecene (C16)	6.71
hexadecane (C16)	16.78
2-octyl-1-decanol (C18)	1.50
2-hexyl-1-dodecanol (C18)	1.07
1-octadecene (C18)	5.81
E-2-octadecen-1-ol (C18)	0.41
octadecane (C18)	3.92
1-nonadecene (C19)	0.99
1,19-eicosadiene (C20)	0.69
eicosane (C20)	6.68
heneicosane (C21)	5.15
1,22-docosanediol (C22)	1.23
1-docosene (C22)	11.33
1-tetracosanol (C24)	0.36
tetracosane (C24)	2.10
hexacosane (C26)	0.51

Table A18: Peak area % of various components in the wax product from the pyrolysis of a feed mixture of 15 wt % LDPE, 45 wt % HDPE, and 40 wt % PP using a 10:100 zinc oxide catalyst to feed ratio at 450°C and 42 kPa (MP-03).

Wax Component	**Peak Area %**
3-butyn-1-ol (C4)	0.19
2-butyl- 1-octanol (C12)	5.96
7-methyl-1-undecene (C12)	3.23
dodecane (C12)	3.42
11-methyldodecanol (C13)	1.41
1-tridecene (C13)	2.65
1-tetradecene (C14)	2.97
2-hexyl-1-octanol (C14)	0.85
1-pentadecene (C15)	3.03
2-hexyl-1-decanol (C16)	0.91
1-hexadecanol (C16)	0.46
1-hexadecene (C16)	5.49
hexadecane (C16)	13.87
E-15-heptadecenal (C17)	2.24
2-octyl-1-decanol (C18)	0.41
2-hexyl-1-dodecanol (C18)	1.37
1-octadecanol (C18)	0.65
1-octadecene (C18)	2.53
octadecane (C18)	6.60
1,19-eicosadiene (C20)	0.51
1-eicosanol (C20)	0.81
eicosane (C20)	4.36
10-methyleicosane, (C21)	4.37
heneicosane (C21)	2.36
1,22-docosanediol (C22)	0.79
1-docosene (C22)	8.44
1-dodecene (C22)	2.51
tetracosane (C24)	1.28
1-cyclopentyleicosane (C25)	0.67
hexacosane (C26)	14.23
tetratetracontane (C44)	1.43

Table A19: Peak area % of various components in the liquid product from uncatalysed pyrolysis of a feed mixture of 32.30 wt % LDPE, 34.52 wt % HDPE, and 33.10 wt % PP at 450°C and 42 kPa (MP-04).

Liquid Component	Peak Area %
1-dodecene (C12)	1.90
4,6,8-trimethyl-1-nonene (C12)	7.97
7-methyl-1-undecene (C12)	4.94
1,12-tridecadiene (C13)	0.37
11-methyldodecanol (C13)	3.91
Z-2-tridecene (C13)	2.65
Z-4-tridecene (C13)	0.66
tridecane (C13)	2.93
1-tetradecene (C14)	3.06
cyclotetradecane (C14)	0.40
tetradecane (C14)	3.28
pentadecane (C15)	3.19
1-hexadecene (C16)	9.66
hexadecane (C16)	13.62
heptadecane (C17)	1.45
2-hexyl-1-decanol (C16)	2.39
1-octadecene (C18)	0.62
octadecane (C18)	4.47
nonadecane (C19)	2.20
1-nonadecene (C19)	7.30
1-eicosanol (C20)	3.33
E-3-eicosene (C20)	0.69
1,19-eicosadiene (C20)	0.92
eicosane (C20)	6.30
1-tetracosanol (C24)	0.86
1-hexacosanol (C26)	0.24
2-methylhexacosane (C27)	3.24
octacosane (C28)	2.18
nonacosane (C29)	1.26
tetratetracontane (C44)	4.00

Table A20: Peak area % of various components in the liquid product from the pyrolysis of a feed mixture of 32.30 wt % LDPE, 34.52 wt % HDPE, and 33.10 wt % PP using a 5:100 zinc oxide catalyst to feed ratio at 450°C and 42 kPa (MP-05).

Liquid Component	**Peak Area %**
3-butyn-1-ol (C4)	0.50
4,6,8-trimethyl-1-nonene (C12)	8.55
7-methyl-1-undecene (C12)	6.47
dodecane (C12)	3.90
3-methylundecane (C12)	1.63
1,19-eicosadiene (C13)	2.29
11-methyldodecanol (C13)	1.41
1-tetradecene (C14)	5.91
2-hexyl-1-octanol (C14)	2.22
2,3,5,8-tetramethyldecane (C14)	0.33
2-hexyl-1-decanol (C16)	5.91
1-hexadecene (C16)	2.66
hexadecane (C16)	16.46
E-15-heptadecenal (C17)	2.21
heptadecane (C17)	4.80
1-octadecanol (C18)	1.67
1-octadecene (C18)	2.63
octadecane (C18)	11.07
1-eicosanol (C20)	1.27
E-3-eicosene (C20)	0.92
eicosane (C20)	0.54
1-heneicosanol (C21)	0.51
1-docosene (C22)	13.20
1-cyclopentyleicosane (C25)	0.83
1-hexacosanol (C26)	0.54
octacosane (C28)	0.42
2-methyloctacosane (C29)	0.32
nonacosane (C29)	0.81

Table A21: Peak area % of various components in the liquid product from the pyrolysis of a feed mixture of 32.30 wt % LDPE, 34.52 wt % HDPE, and 33.10 wt % PP using a 10:100 zinc oxide catalyst to feed ratio at 450°C and 42 kPa (MP-06).

Component	**Peak Area %**
3-butyn-1-ol (C4)	0.51
4,6,8-trimethyl-1-nonene (C12)	8.78
7-methyl-1-undecene (C12)	6.65
dodecane (C12)	4.01
3-methylundecane (C12)	1.68
1,19-eicosadiene (C13)	2.35
11-methyldodecanol (C13)	1.45
1-tetradecene (C14)	6.07
2-hexyl-1-octanol (C14)	2.28
2,3,5,8-tetramethyldecane (C14)	0.34
2-hexyl-1-decanol (C16)	6.07
1-hexadecene (C16)	2.74
hexadecane (C16)	16.9
heptadecane (C17)	4.93
1-octadecanol (C18)	1.72
1-octadecene (C18)	2.70
octadecane (C18)	11.37
1-eicosanol (C20)	1.31
E-3-eicosene (C20)	0.95
eicosane (C20)	0.56
1-heneicosanol (C21)	0.52
1-docosene (C22)	13.55
1-cyclopentyleicosane (C25)	0.85
1-hexacosanol (C26)	0.55
2-methyloctacosane (C29)	0.33
nonacosane (C29)	0.83

Table A22: Peak area % of various components in the wax product from uncatalysed pyrolysis of a feed mixture of 32.30 wt % LDPE, 34.52 wt % HDPE, and 33.10 wt % PP at 450°C and 42 kPa (MP-04).

Liquid Component	Peak Area %
Z-3-undecene (C11)	0.30
1-dodecene (C12)	9.20
7-methyl-1-undecene (C12)	3.63
2-methylundecane (C12)	13.04
1-pentyl-2-propylcyclopentane (C13)	0.34
1-tetradecene (C14)	5.92
2-hexyl-1-octanol (C14)	0.75
2-hexyl-1-decanol (C16)	0.88
1-hexadecene (C16)	4.93
hexadecane (C16)	8.57
2-hexyl-1-dodecanol (C18)	0.70
1-octadecanol (C18)	2.31
1-octadecene (C18)	2.03
octadecane (C18)	29.25
1-nonadecene (C19)	1.35
1,19-eicosadiene (C20)	0.35
1-eicosanol (C20)	1.14
eicosane (C20)	1.32
heneicosane (C21)	2.19
1,22-docosanediol (C22)	0.60
1-docosene (C22)	3.88
1-cyclopentyleicosane (C25)	1.21
octacosane (C28)	1.95
hexatriacontane (C36)	2.54
tetratetracontane (C44)	1.63

Table A23: Peak area % of various components in the wax product from the pyrolysis of a feed mixture of 32.30 wt % LDPE, 34.52 wt % HDPE, and 33.10 wt % PP using a 5:100 zinc oxide catalyst to feed ratio at 450°C and 42 kPa (MP-05).

Liquid Component	**Peak Area %**
1-dodecene (C12)	11.23
7-methyl-1-undecene (C12)	4.19
dodecane (C12)	0.24
2-methylundecane (C12)	14.78
11-methyldodecanol (C13)	1.14
1-tetradecene (C14)	2.65
4,6-dimethyl-dodecane (C14)	0.31
2-hexyl-1-decanol (C16)	2.35
1-hexadecene (C16)	5.17
cyclohexadecane (C16)	0.38
hexadecane (C16)	7.82
E-15-heptadecenal (C17)	2.13
heptadecane (C17)	1.80
1-octadecanol (C18)	2.23
1-octadecene (C18)	2.28
9-octadecenal (C18)	0.37
1,2,3,5-tetraisopropyl-cyclohexane (C18)	0.32
octadecane (C18)	25.90
1-nonadecene (C19)	3.97
1,19-eicosadiene (C20)	0.42
E-3-eicosene (C20)	0.59
eicosane (C20)	1.21
1,22-docosanediol (C22)	0.58
1-docosene (C22)	1.95
1-cyclopentyleicosane (C25)	0.61
heptacosane (C27)	0.85
2-methyloctacosane (C29)	1.41
hexatriacontane (C36)	2.44
tetratetracontane (C44)	0.68

Table A24: Peak area % of various components in the wax product from the pyrolysis of a feed mixture of 32.30 wt % LDPE, 34.52 wt % HDPE, and 33.10 wt % PP using a 10:100 zinc oxide catalyst to feed ratio at 450°C and 42 kPa (MP-06).

Component	**Peak Area %**
2-methyldecane (C11)	0.33
7-methyl-1-undecene (C12)	2.11
2-methylundecane (C12)	14.45
11-methyldodecanol (C13)	0.54
1-pentyl-2-propylcyclopentane (C13)	0.39
1-tetradecene (C14)	3.03
2-hexyl-1-octanol (C14)	0.60
E-4-tetradecene, (C14)	0.54
1-pentadecanol (C15)	0.43
2-hexyl-1-decanol (C16)	0.93
1-hexadecene (C16)	5.65
hexadecane (C16)	12.01
E-15-heptadecenal (C17)	2.40
heptadecane (C17)	3.98
1-octadecanol (C18)	2.33
1-octadecene (C18)	2.52
octadecane (C18)	24.61
1-nonadecene (C19)	3.07
9-nonadecene (C19)	0.31
1-eicosanol (C20)	1.57
E-3-eicosene (C20)	0.49
E-5-eicosene (C20)	0.51
heneicosane (C21)	0.78
1-docosene (C22)	13.65
1-cyclopentyleicosane (C25)	0.57
2-methyltetracosane (C25)	0.45
hexatriacontane (C36)	1.26
tetratetracontane (C44)	0.49

Table A25: Peak area % of various components in the liquid product from uncatalysed pyrolysis of a feed mixture of 65 wt % LDPE, 20 wt % HDPE, and 15 wt % PP at 450 °C and 42 kPa (MP-07).

Liquid Component	Peak Area %
2,4-diethyl-1-heptanol (C11)	0.38
11-dodecenol (C12)	0.26
7-methyl-1-undecene (C12)	2.89
dodecane (C12)	3.44
1-cyclopentyleicosane (C13)	0.83
1-tridecene (C13)	2.98
2-hexyl-1-decanol (C16)	0.72
1-tetradecene (C14)	3.55
cyclotetradecane (C14)	0.41
tetradecane (C14)	3.79
1,15-pentadecanediol (C15)	0.59
1-dodecene (C15)	2.51
1-pentadecene (C15)	6.72
pentadecane (C15)	3.72
Z-10-pentadecen-1-ol (C15)	0.54
2-hexyl-1-dodecanol (C18)	2.87
hexadecane (C16)	10.14
1-heptadecene	5.51
1,2,3,5-tetraisopropylcyclohexane (C18)	0.28
1-nonadecene (C19)	6.02
nonadecane (C19)	7.69
1,19-eicosadiene (C20)	1.09
E-3-eicosene (C20)	0.31
1-heneicosanol (C21)	2.2
heneicosane (C21)	20.04
1,22-docosanediol (C22)	0.77
docosane (C22)	2.76
Z-9-tricosene, (C23)	0.18
1-tetracosanol (C24)	3.57
tetracosane (C24)	0.95
1-hexacosanol (C26)	0.37
11-(1-ethylpropyl)- heneicosane (C26)	0.18
1-heptacosene (C27)	0.58
dotriacontane (C32)	0.4
tetracontane (C40)	0.44
tetrapentacontane (C54)	0.31

Table A26: Peak area % of various components in the liquid product from the pyrolysis of a feed mixture of 65 wt % LDPE, 20 wt % HDPE, and 15 wt % PP using a 5:100 zinc oxide catalyst to feed ratio at 450 °C and 42 kPa (MP-08).

Liquid Component	Peak Area %
2,4-diethyl-1-heptanol (C11)	0.30
7-methyl-1-undecene (C12)	1.53
dodecane (C12)	0.33
11-methyldodecanol (C13)	0.90
1-tridecene (C13)	2.58
1-tetradecene (C14)	3.00
Z-3-tetradecene (C14)	2.02
cyclotetradecane (C14)	0.23
tetradecane (C14)	3.22
1-cyclopentyleicosane (C15)	0.82
1-pentadecene (C15)	6.21
cyclopentadecane (C15)	0.39
pentadecane (C15)	3.18
Z-10-pentadecen-1-ol (C15)	0.44
2-hexyl-1-decanol (C16)	1.02
hexadecane (C16)	5.08
1-heptadecene (C17)	5.65
heptadecane (C17)	3.37
1-heptadecanol (C17)	0.23
2-hexyl-1-dodecanol (C18)	2.12
1-octadecanol (C18)	0.17
octadecane (C18)	3.48
1-nonadecene (C19)	7.14
nonadecane (C19)	3.93
1,19-eicosadiene (C20)	0.62
E-3-eicosene (C20)	0.27
heneicosane (C21)	21.46
1-henicosene (C22)	0.22
1,22-docosanediol (C22)	0.73
1-docosanol (C22)	3.17
docosane (C22)	4.60
Z-9-tricosene (C23)	0.19
1-tetracosanol (C24)	1.21
tetracosane (C24)	3.46
1-hexacosanol (C26)	0.78
1-heptacosanol (C27)	1.53
1-heptacosene (C27)	0.56
dotriacontane (C32)	0.33
tetracontane (C40)	3.41
tetrapentacontane (C54)	0.14

Table A27: Peak area % of various components in the liquid product from the pyrolysis of a feed mixture of 65 wt % LDPE, 20 wt % HDPE, and 15 wt % PP using a 10:100 zinc oxide catalyst to feed ratio at 450°C and 42 kPa (MP-09).

Component	Peak Area %
2,4-diethyl-1-heptanol (C11)	0.30
7-methyl-1-undecene (C12)	1.54
dodecane (C12)	0.33
11-methyldodecanol (C13)	0.91
1-tridecene (C13)	2.59
1-tetradecene (C14)	3.01
Z-3-tetradecene (C14)	2.03
cyclotetradecane (C14)	0.23
tetradecane (C14)	3.23
1-cyclopentyleicosane (C15)	0.82
1-pentadecene (C15)	6.24
cyclopentadecane (C15)	0.39
pentadecane (C15)	3.19
Z-10-penta-1-decenol (C15)	0.44
2-hexyl-1-decanol (C16)	1.02
hexadecane (C16)	5.10
1-heptadecene (C17)	5.68
heptadecane (C17)	3.38
1-heptadecanol (C17)	0.23
2-hexyl-1-dodecanol (C18)	2.13
1-octadecanol (C18)	0.17
octadecane (C18)	3.50
1-nonadecene (C19)	7.17
nonadecane (C19)	3.95
1,19-eicosadiene (C20)	0.62
E-3-eicosene (C20)	0.27
heneicosane (C21)	21.56
1-henicosene (C22)	0.22
1,22-docosanediol (C22)	0.73
1-docosanol (C22)	3.19
docosane (C22)	4.62
Z- 9-tricosene (C23)	0.19
1-tetracosanol (C24)	1.22
tetracosane (C24)	3.48
1-hexacosanol (C26)	0.78
1-heptacosanol (C27)	1.53
1-heptacosene (C27)	0.57
tetracontane (C40)	3.43

Table A28: Peak area % of various components in the wax product from uncatalysed pyrolysis of a feed mixture of 65 wt % LDPE, 20 wt % HDPE, and 15 wt % PP at 450°C and 42 kPa (MP-07).

Liquid Component	Peak Area %
2,4-diethyl-1-heptanol (C11)	0.13
cyclododecane (C12)	0.57
11-methyldodecanol (C13)	0.46
1-tridecene (C13)	2.68
tridecane (C13)	8.26
2,6-dimethylundecane, (C13)	0.13
1-tetradecene (C14)	2.75
1,2,4,5-tetraethylcyclohexane (C14)	0.15
tetradecane (C14)	3.05
1-pentadecene (C15)	2.72
Z-10-penta1-1-decenol (C15)	0.3
pentadecane (C15)	2.74
2-hexyl-1-decanol (C16)	0.27
1-heptadecene (C17)	7.47
2-hexyl-1-dodecanol (C18)	0.88
octadecane (C18)	2.96
1-nonadecene (C19)	6.02
nonadecane (C19)	3.07
1,19-eicosadiene (C20)	0.21
E-3-eicosene (C20)	0.32
E-5-eicosene (C20)	0.64
E-9-eicosene(C20)	0.21
heneicosane (C21)	27.23
1-henicosene (C21)	0.36
1-docosene (C22)	2.67
1-docosenol (C22)	2.79
1-cyclopentyleicosane (C25)	0.49
2-cyclohexylnonadecane (C25)	0.17
pentacosane (C25)	2.82
1-hexacosanol (C26)	1.16
1-heptacosanol (C27)	2.19
dotriacontane (C32)	7.98
tetrapentacontane (C54)	5.82
hexacontane (C60)	0.30

Table A29: Peak area % of various components in the wax product from the pyrolysis of a feed mixture of 65 wt % LDPE, 20 wt % HDPE, and 15 wt % PP using a 5:100 zinc oxide catalyst to feed ratio at 450°C and 42 kPa (MP-08).

Liquid Component	Peak Area %
cyclododecane (C12)	0.30
dodecane (C12)	2.85
11-methyldodecanol (C13)	0.34
1-tridecene (C13)	2.33
9-tricosene, Z- (C13)	0.18
tridecane (C13)	3.51
1-tetradecene (C14)	2.48
tetradecane (C14)	2.44
1-pentadecene (C15)	2.51
pentadecane (C15)	2.27
2-hexyl-1-decanol (C16)	0.69
hexadecane (C16)	2.56
1-heptadecene (C17)	7.4
1-heptadecanol (C17)	0.19
2-octyl-1-decanol (C18)	0.34
2-hexyl-1-dodecanol (C18)	0.41
1-nonadecene (C19)	6.89
nonadecane (C19)	5.53
1,19-eicosadiene (C20)	1.06
E-3-eicosene (C20)	0.33
E-5-eicosene (C20)	0.26
1-heneicosanol (C21)	0.28
heneicosane (C21)	22.05
1-henicosene (C21)	0.21
1-docosene (C22)	2.30
1-docosanol (C22)	1.86
1-tetracosanol (C24)	1.61
tetracosane (C24)	3.28
1-cyclopentyleicosane (C25)	0.52
2-cyclohexylnonadecane (C25)	0.21
pentacosane (C25)	2.59
1-hexacosanol (C26)	2.02
1-heptacosanol (C27)	2.85
1-octacosanol (C28)	0.19
dotriacontane (C32)	7.00
tetrapentacontane (C44)	8.15

Table A30: Peak area % of various components in the wax product from the pyrolysis of a feed mixture of 65 wt % LDPE, 20 wt % HDPE, and 15 wt % PP using a 10:100 zinc oxide catalyst to feed ratio at 450°C and 42 kPa (MP-09).

Component	Peak Area %
11-methyldodecanol (C13)	0.47
1-tridecene (C13)	1.85
tridecane (C13)	2.61
1-tetradecene (C14)	2.12
tetradecane (C14)	2.32
1-pentadecene (C15)	4.90
pentadecane (C15)	2.26
2-hexyl-1-decanol (C16)	0.55
hexadecane (C16)	3.59
1-heptadecene (C17)	5.18
2-hexyl-1-dodecanol (C18)	1.32
E-5-octadecene (C18)	0.39
1,2,3,5-tetraisopropylcyclohexane (C18)	0.74
octadecane (C18)	2.71
1-nonadecene (C19)	5.20
nonadecane (C19)	6.13
E-3-eicosene (C20)	0.28
1-heneicosanol (C21)	0.78
heneicosane (C21)	22.17
1-henicosene (C21)	0.38
1-dodecene (C22)	1.75
1-docosanol (C22)	4.30
Z- 9-tricosene (C23)	0.67
1-tetracosanol (C24)	1.84
tetracosane (C24)	3.21
1-cyclopentyleicosane (C25)	0.77
pentacosane (C25)	4.36
1-hexacosanol (C26)	2.53
1-heptacosanol (C27)	4.25
1-octacosanol (C28)	0.81
1-nonacosene (C29)	0.55
dotriacontane (C32)	6.94
tetrapentacontane (C54)	2.05

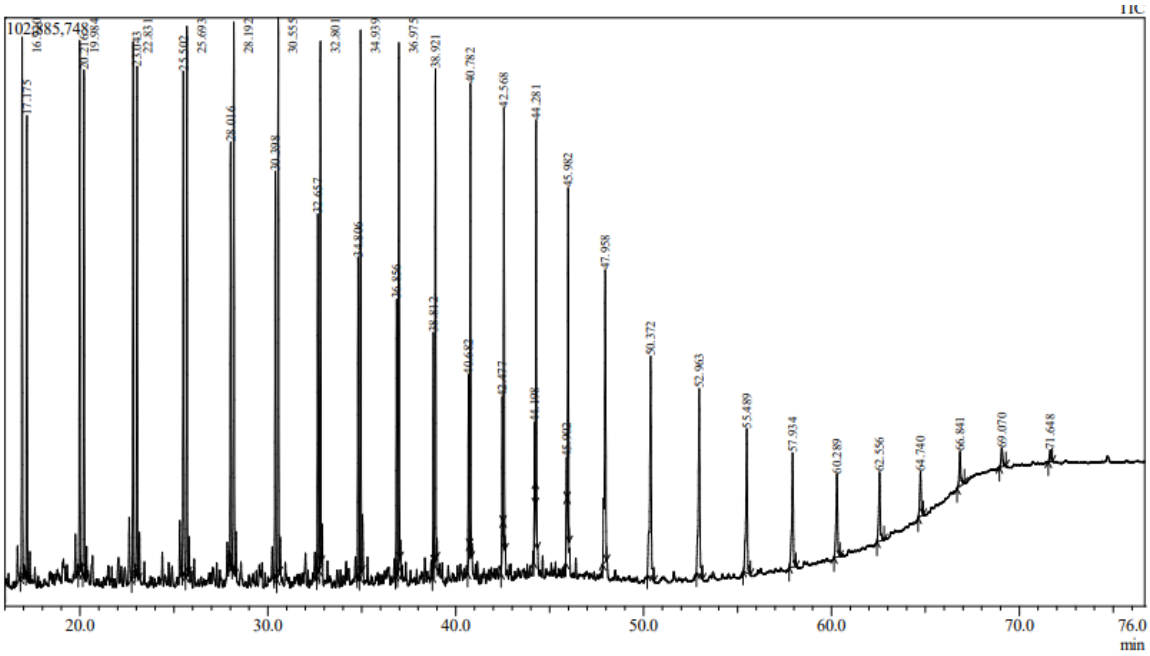

Figure A1: Chromatograph produced using GC-MS chemical analysis for the liquid product from uncatalyzed LDPE pyrolysis at 450°C and 42 kPa (IP-01).

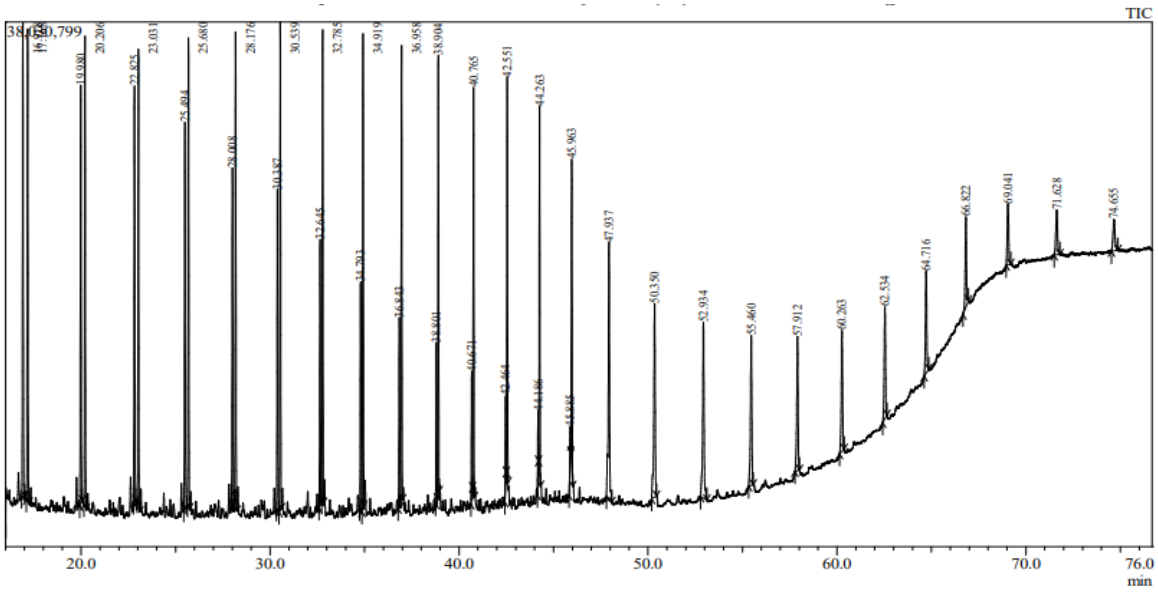

Figure A2: Chromatograph produced using GC-MS chemical analysis for the wax product from uncatalyzed LDPE pyrolysis at 450°C and 42 kPa (IP-01).

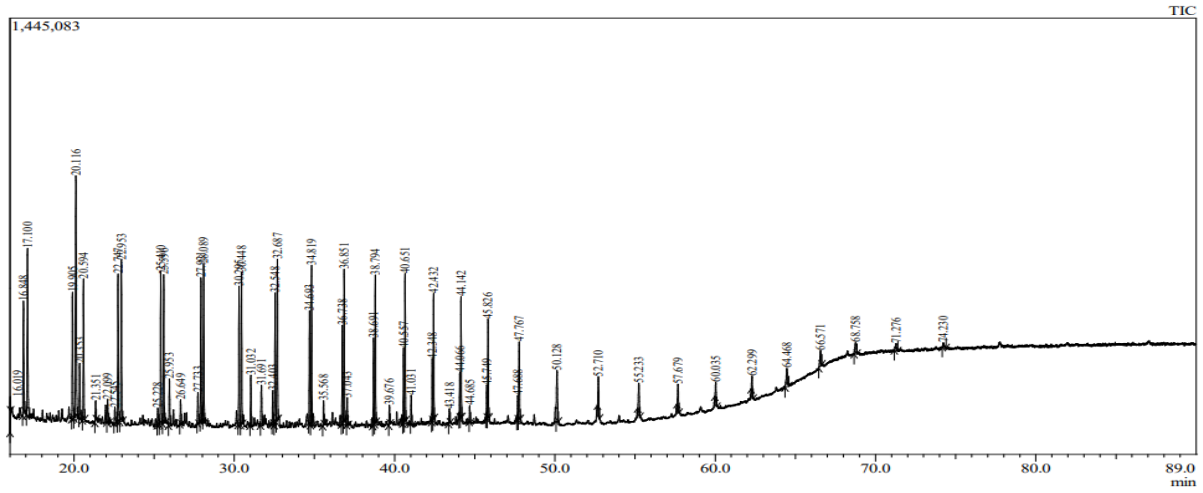

Figure A3: Chromatograph produced using GC-MS chemical analysis for the wax product from uncatalysed pyrolysis of a feed mixture of 15 wt % LDPE, 45 wt % HDPE, and 40 wt % PP at 450°C and 42 kPa (MP-01) .

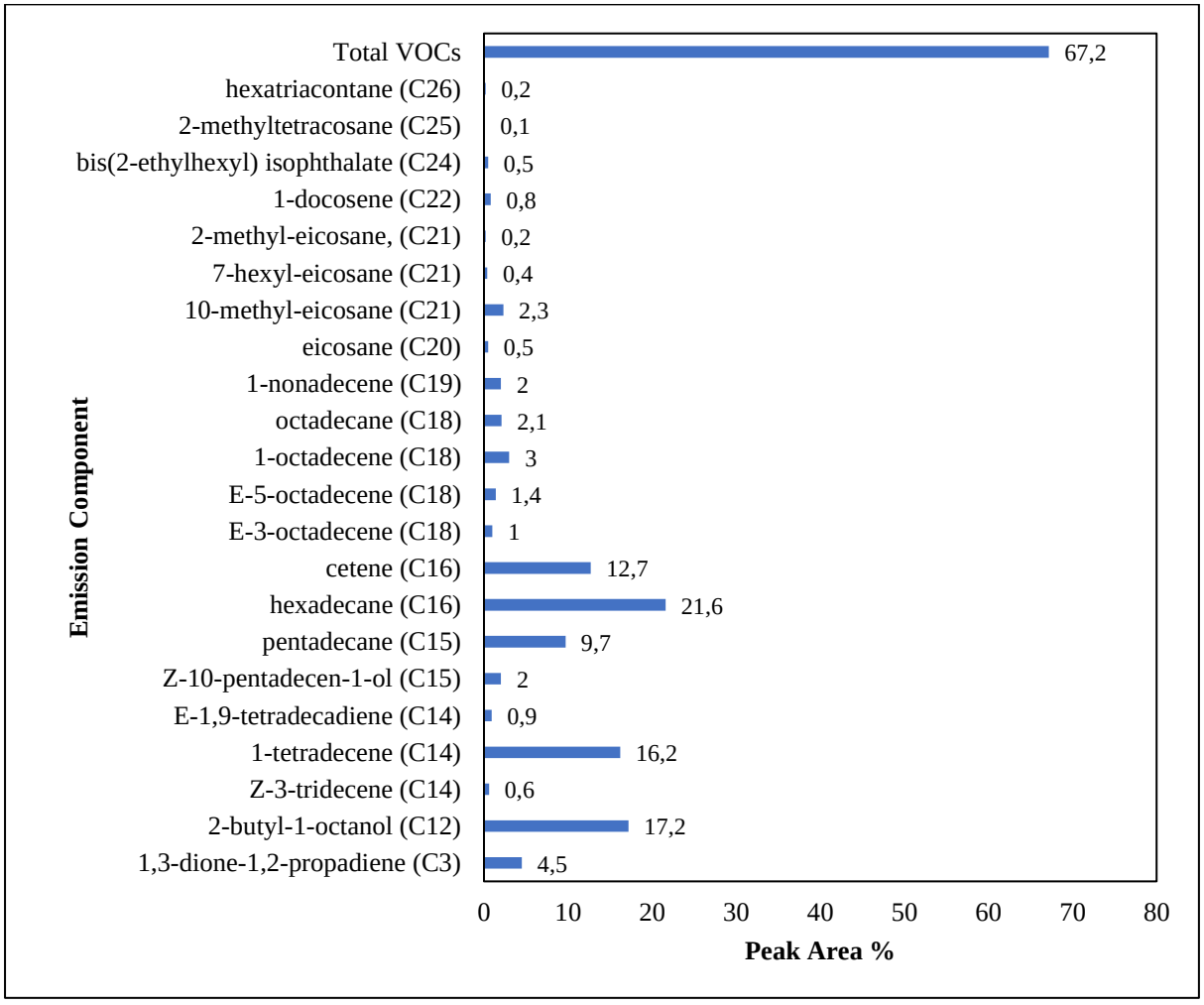

Figure A4: Comparison of peak area % of various components in the emissions from LDPE pyrolysis using a 5:100 zinc oxide catalyst to feed ratio at 450°C and 42 kPa (IP-02).

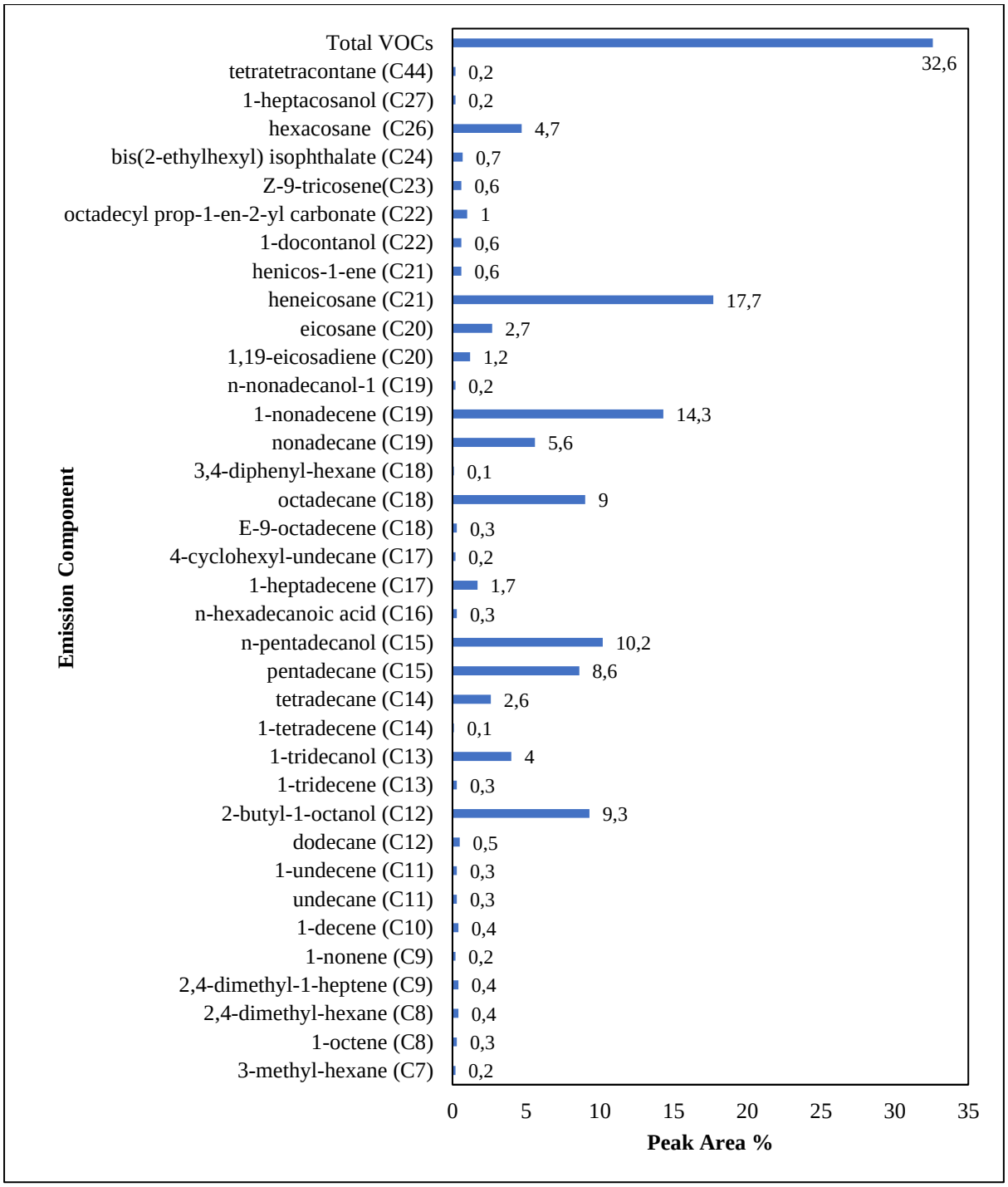

Figure A5: Comparison of peak area % of various components in the emissions from LDPE pyrolysis using a 10:100 zinc oxide catalyst to feed ratio at 450°C and 42 kPa (IP-03).

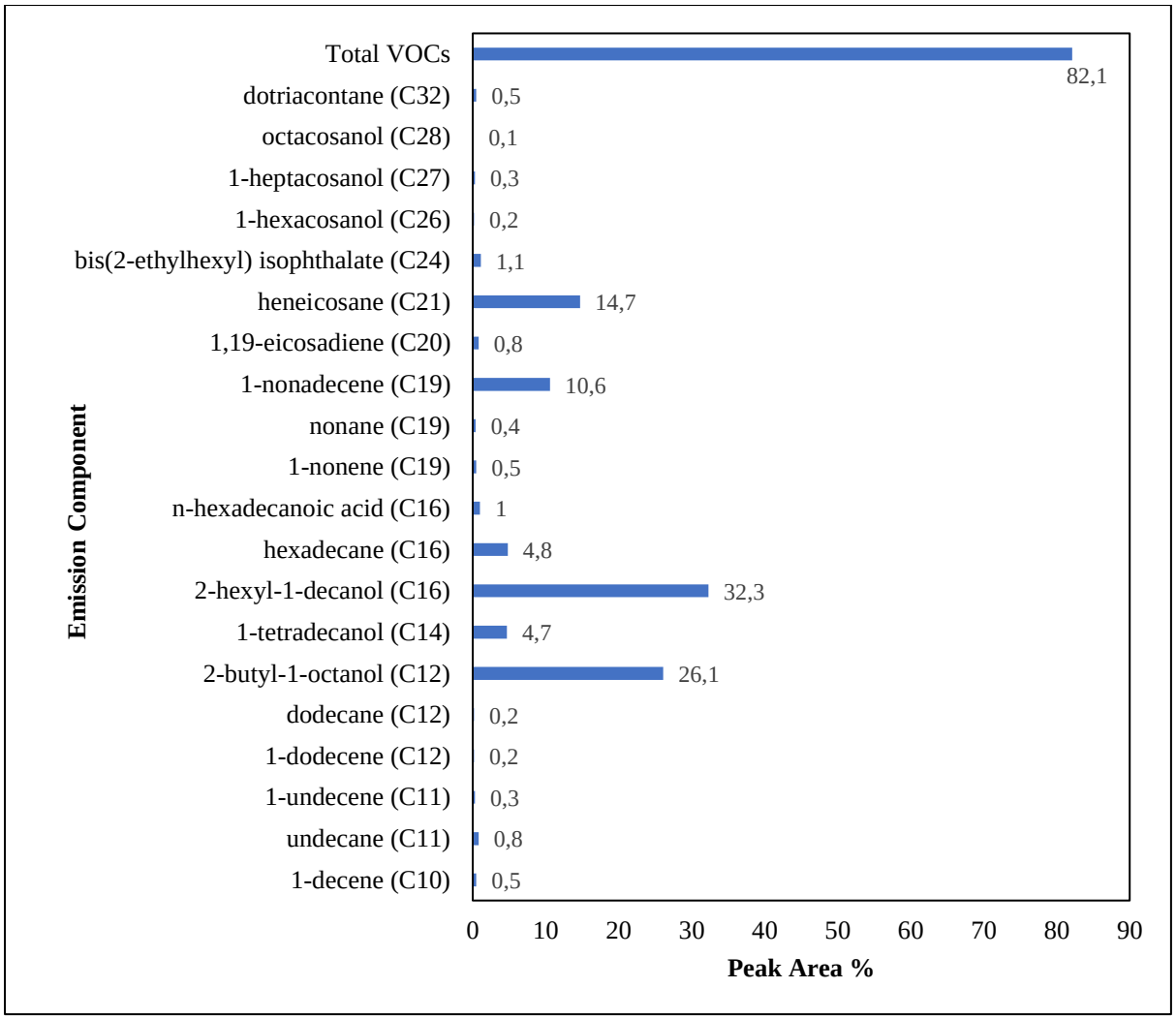

Figure A6: Comparison of peak area % of various components in the emissions from uncatalysed HDPE pyrolysis at 450°C and 42 kPa (IP-04).

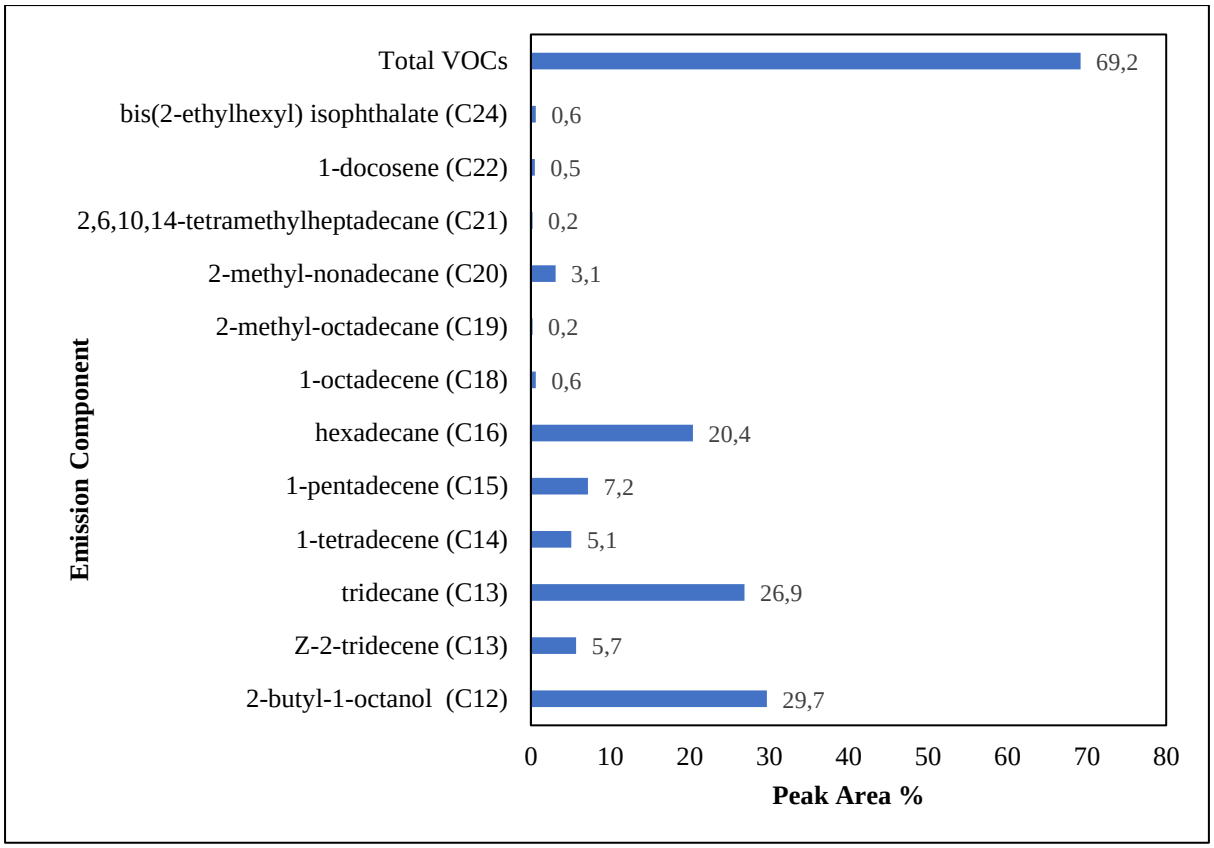

Figure A7: Comparison of peak area % of various components in the emissions from HDPE pyrolysis using a 5:100 zinc oxide catalyst to feed ratio at 450°C and 42 kPa (IP-05).

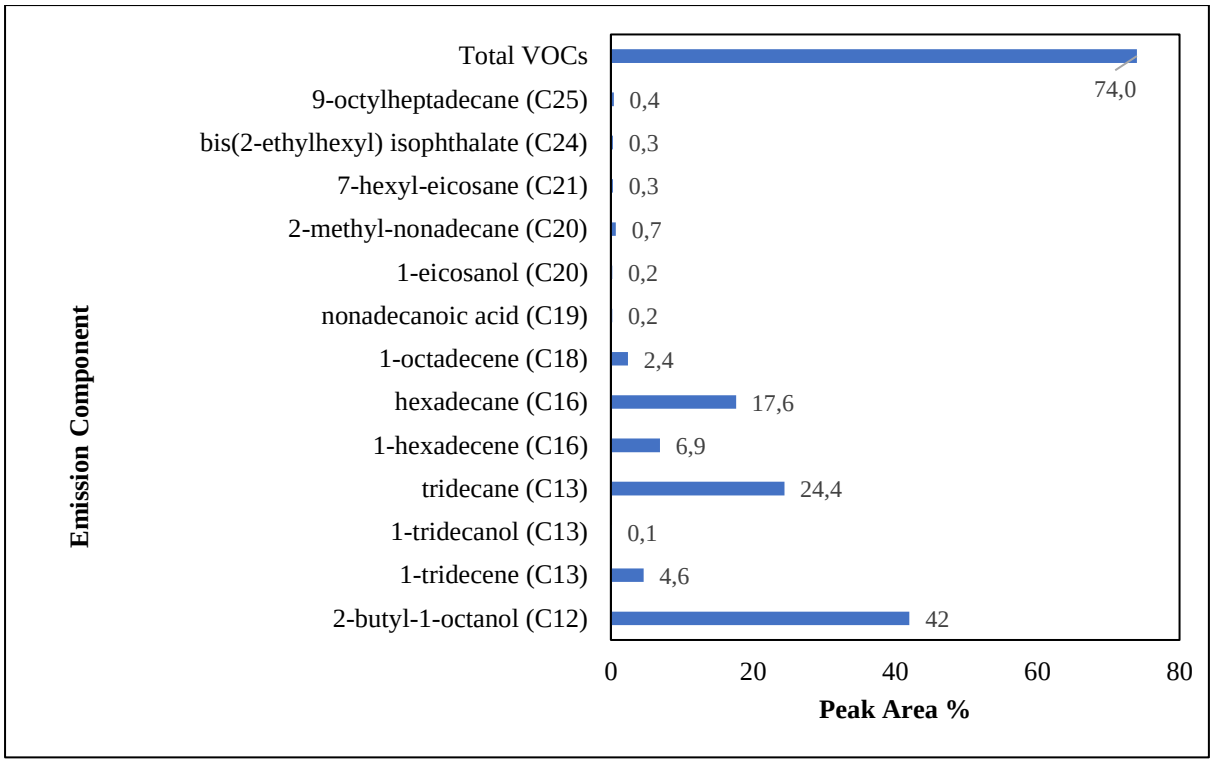

Figure A8: Comparison of peak area % of various components in the emissions from HDPE pyrolysis using a 10:100 zinc oxide catalyst to feed ratio at 450°C and 42 kPa (IP-06).

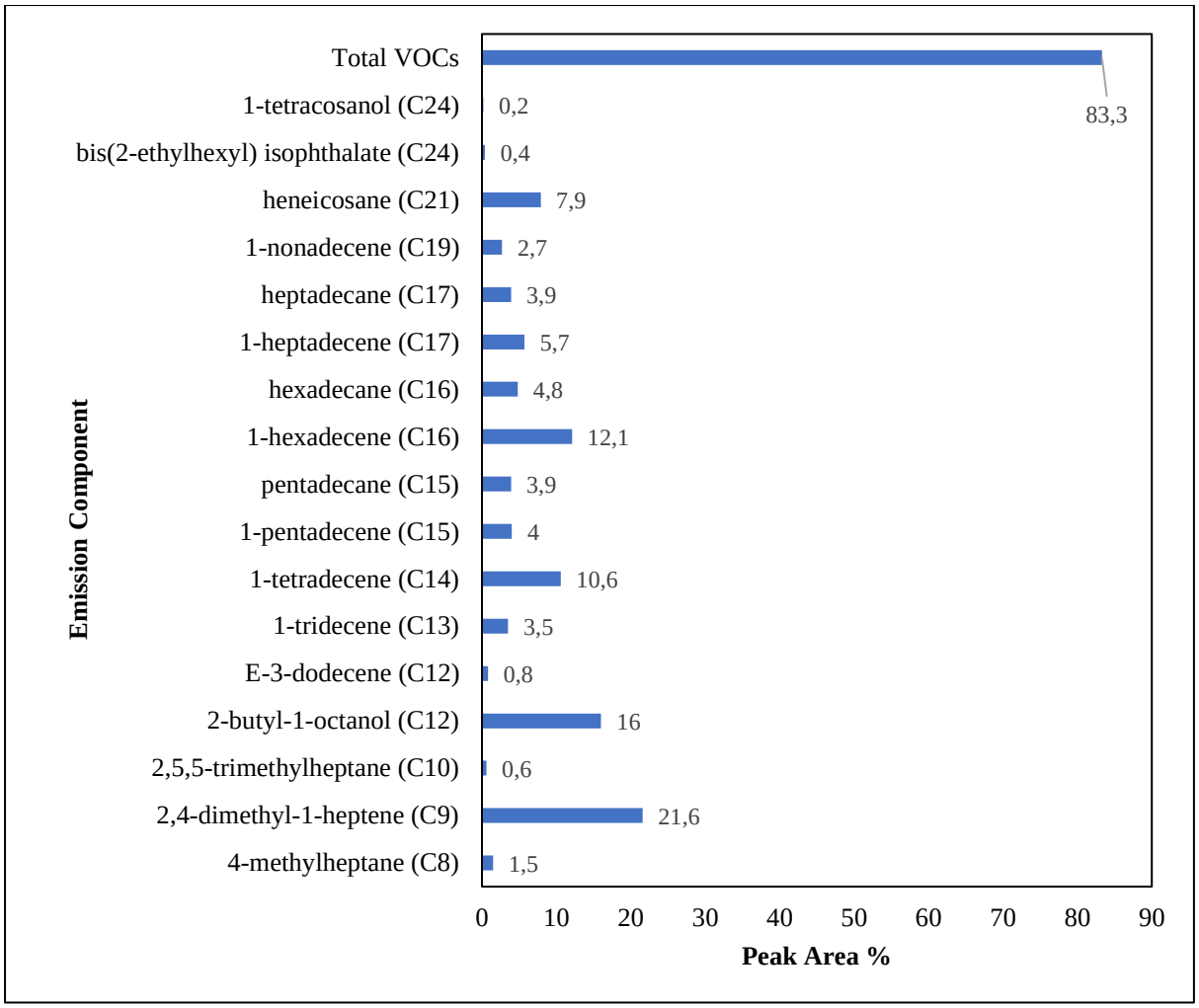

Figure A9: Comparison of peak area % of various components in the emissions from uncatalyzed PP pyrolysis at 450°C and 42 kPa (IP-07).

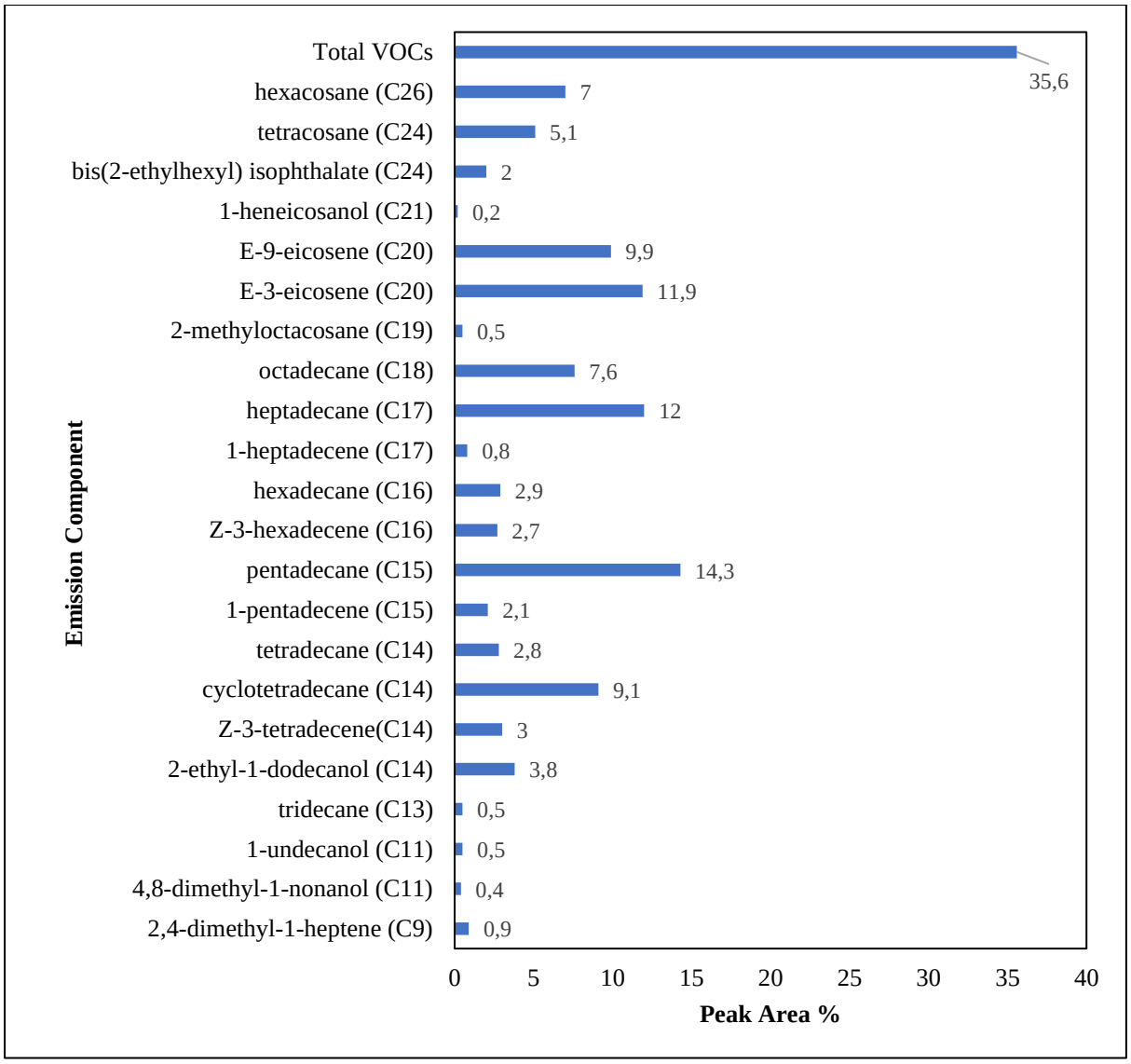

Figure A10: Comparison of peak area % of various components in the emissions from PP pyrolysis using a 5:100 zinc oxide catalyst to feed ratio at 450°C and 42 kPa (IP-08).

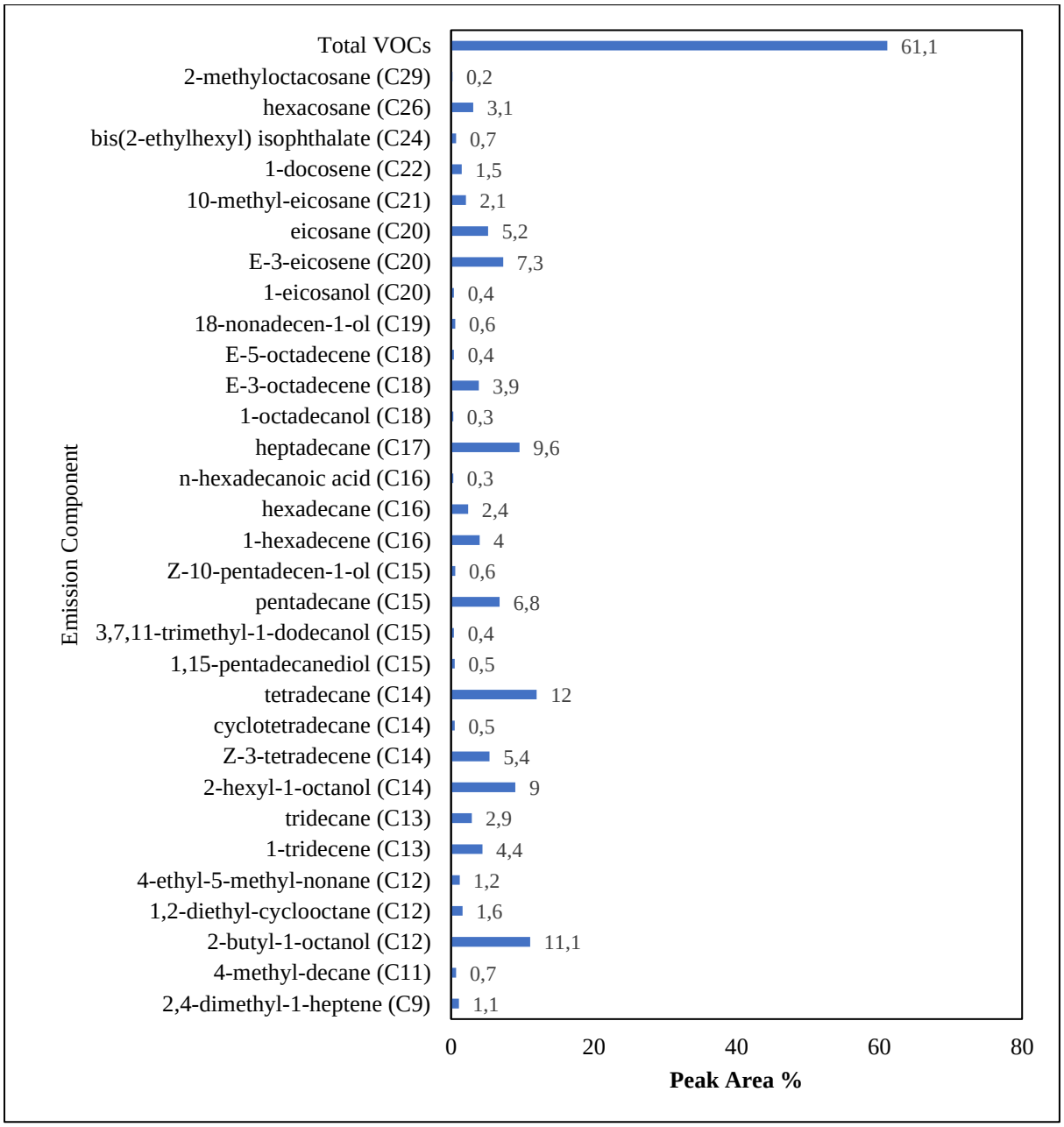

Figure A11: Comparison of peak area % of various components in the emissions from PP pyrolysis using a 10:100 zinc oxide catalyst to feed ratio at 450°C and 42 kPa (IP-09).

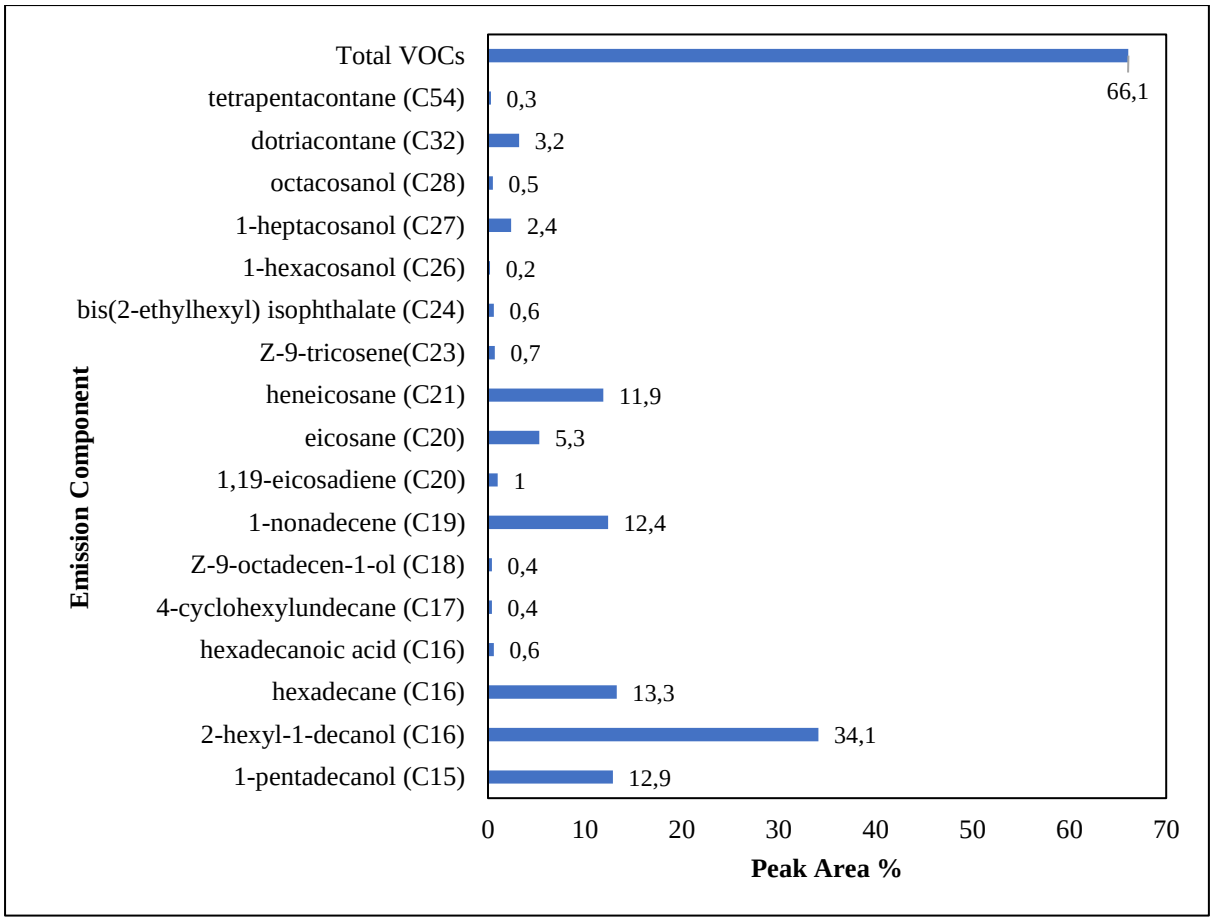

Figure A12: Comparison of peak area % of various components in the emissions from uncatalysed pyrolysis of a feed mixture of 15 wt % LDPE, 45 wt % HDPE, and 40 wt % PP at 450°C and 42 kPa (MP-01).

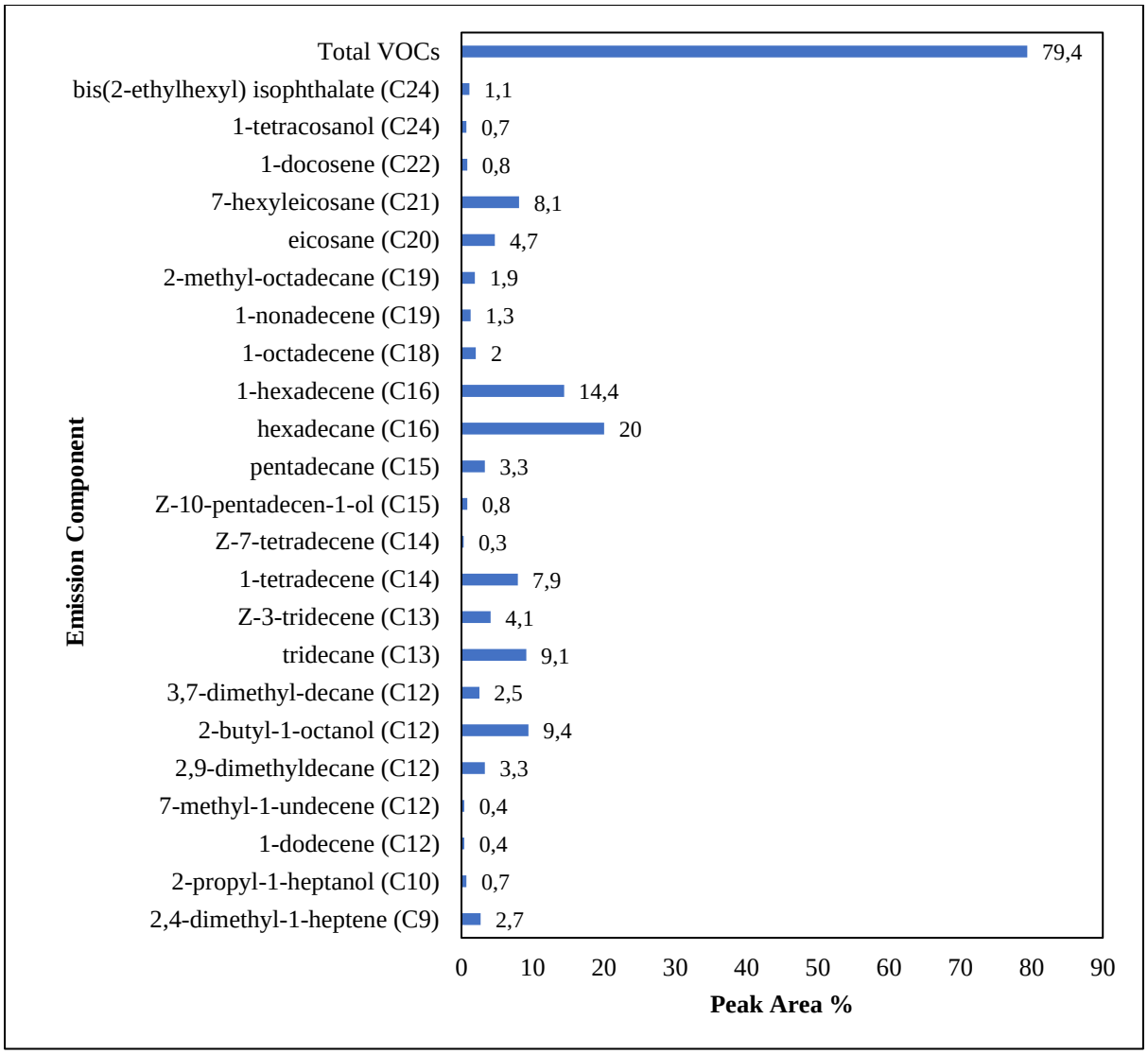

Figure A13: Comparison of peak area % of various components in the emissions from the pyrolysis of a feed mixture of 15 wt % LDPE, 45 wt % HDPE, and 40 wt % PP using a 5:100 zinc oxide catalyst to feed ratio at 450°C and 42 kPa (MP-02).

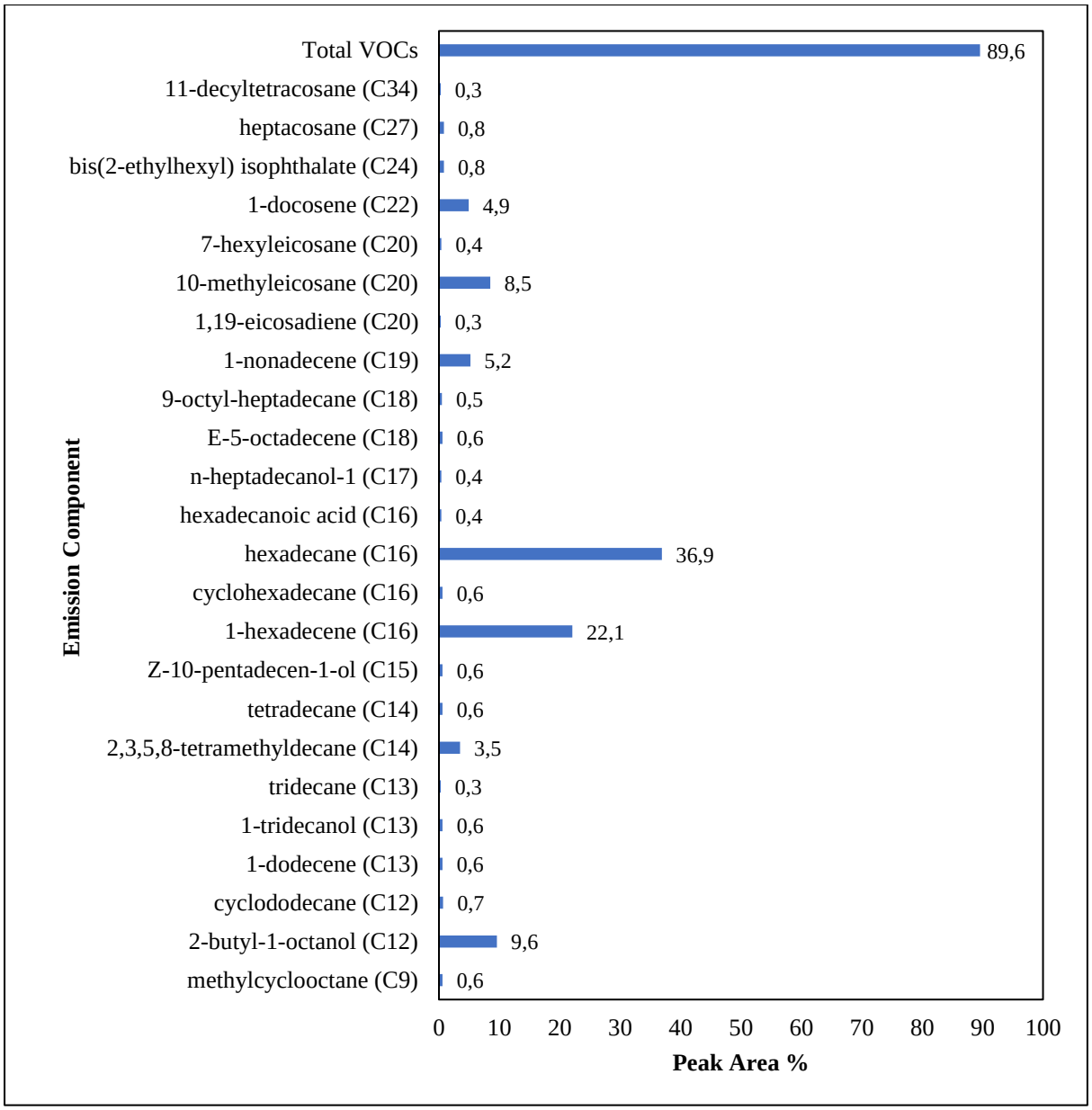

Figure A14: Comparison of peak area % of various components in the emissions from the pyrolysis of a feed mixture of 15 wt % LDPE, 45 wt % HDPE, and 40 wt % PP using a 10:100 zinc oxide catalyst to feed ratio at 450°C and 42 kPa (MP-03).

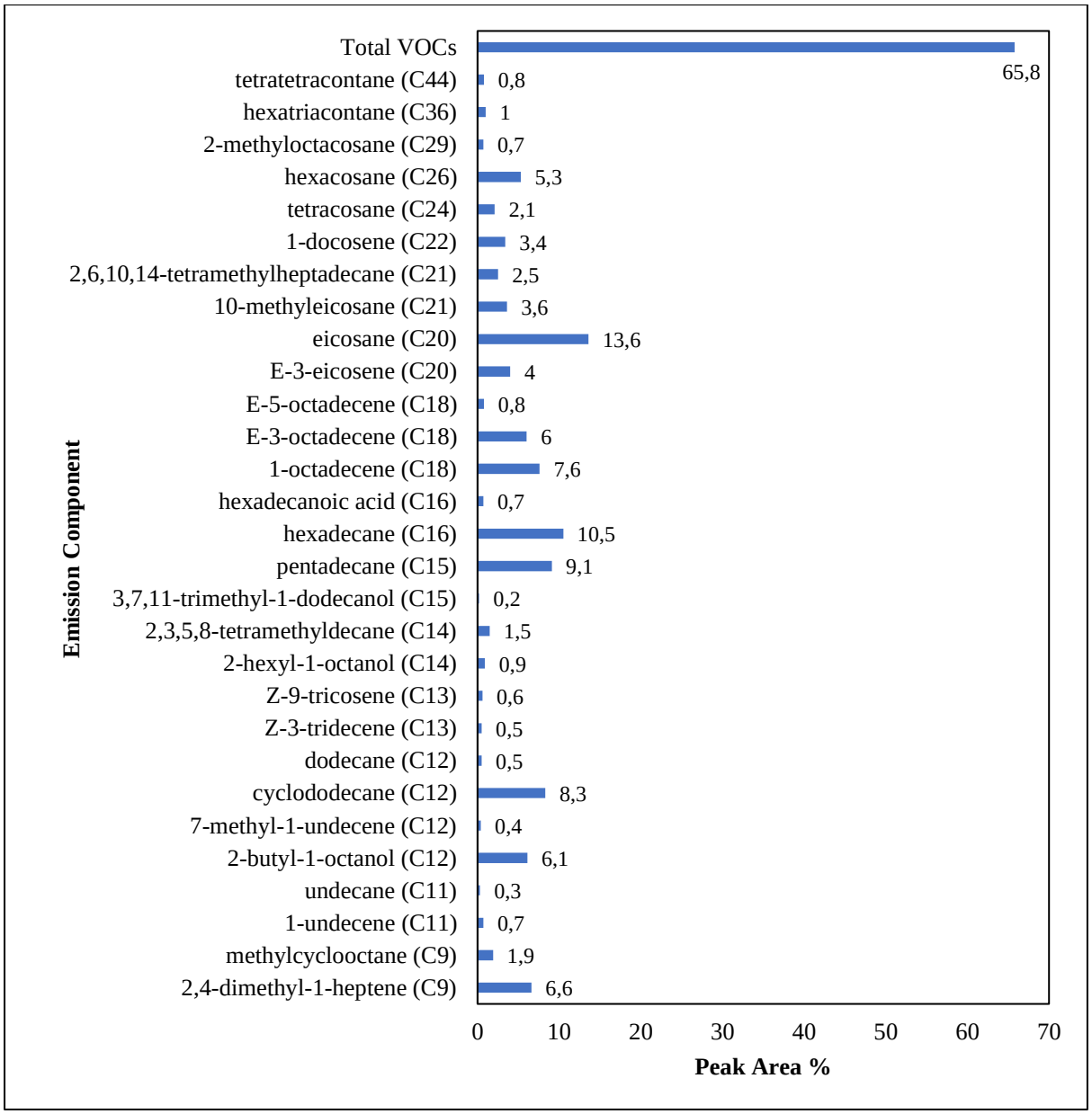

Figure A15: Comparison of peak area % of various components in the emissions from uncatalysed pyrolysis of a feed mixture of 32.30 wt % LDPE, 34.52 wt % HDPE, and 33.10 wt % PP at 450°C and 42 kPa (MP-04).

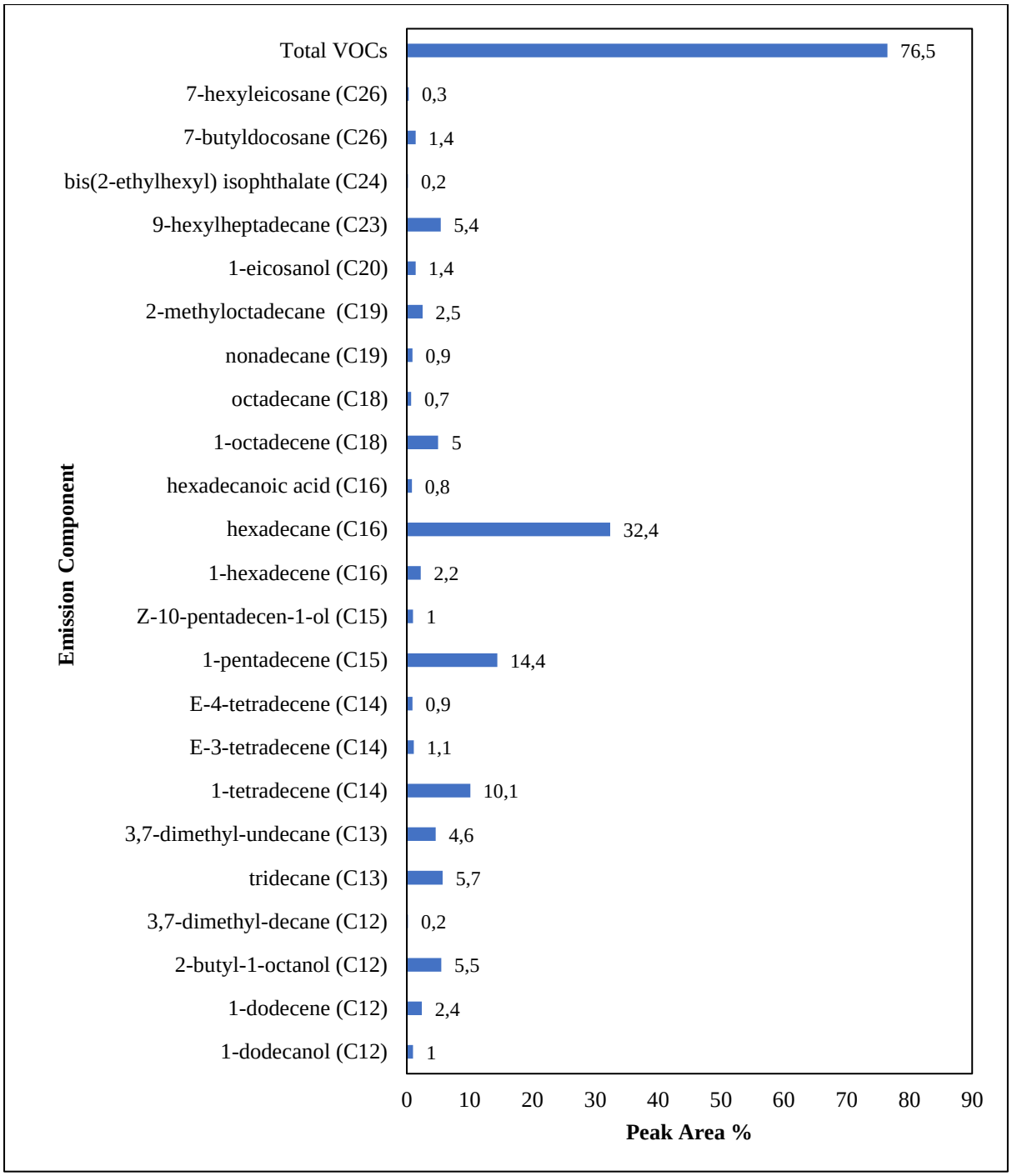

Figure A16: Comparison of peak area % of various components in the emissions from the pyrolysis of a feed mixture of 32.30 wt % LDPE, 34.52 wt % HDPE, and 33.10 wt % PP using a 5:100 zinc oxide catalyst to feed ratio at 450°C and 42 kPa (MP-05).

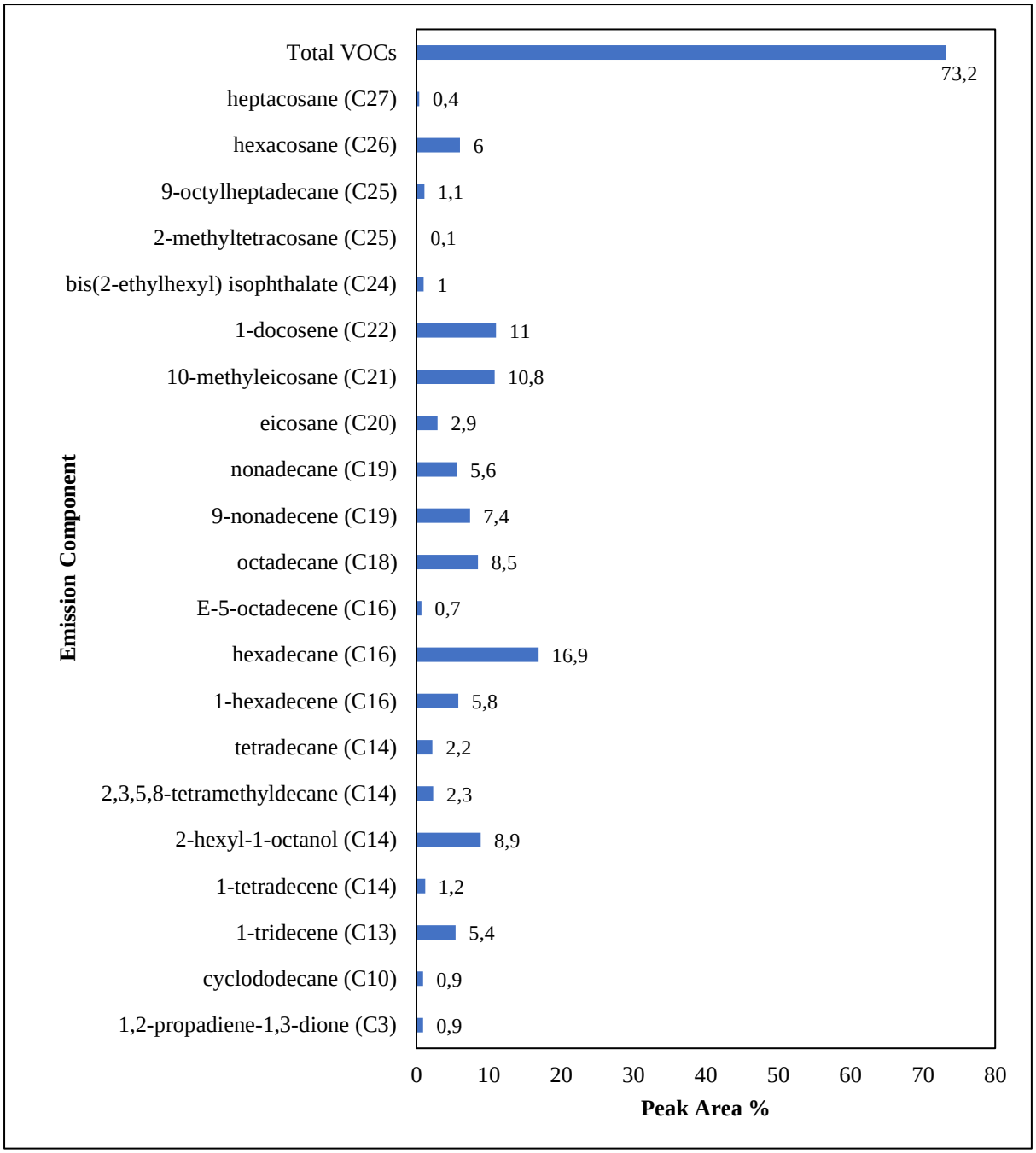

Figure A17: Comparison of peak area % of various components in the emissions from the pyrolysis of a feed mixture of 32.30 wt % LDPE, 34.52 wt % HDPE, and 33.10 wt % PP using a 10:100 zinc oxide catalyst to feed ratio at 450°C and 42 kPa (MP-06).

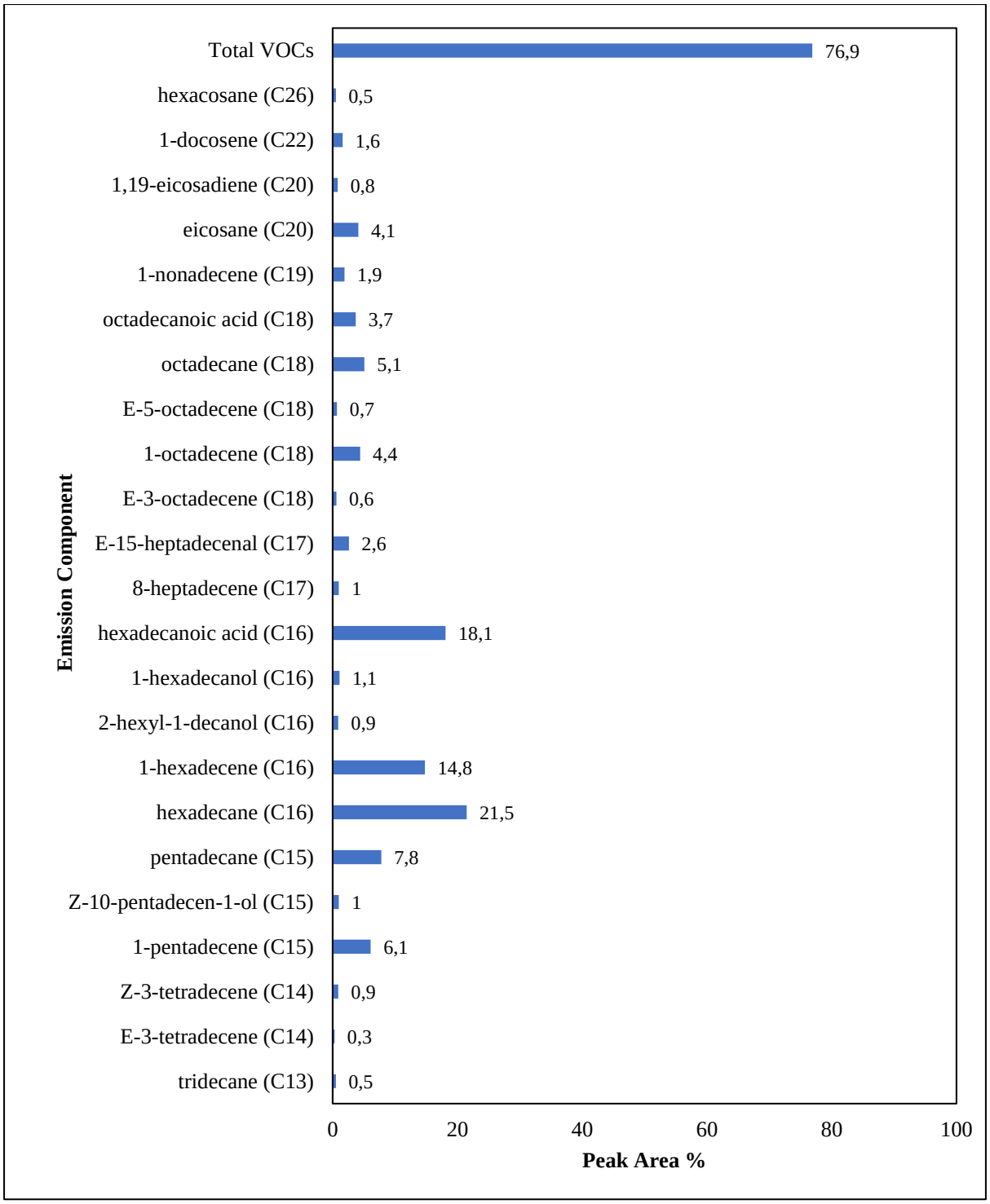

Figure A18: Comparison of peak area % of various components in the emissions from uncatalysed pyrolysis of a feed mixture of 65 wt % LDPE, 20 wt % HDPE, and 15 wt % PP at 450°C and 42 kPa (MP-07).

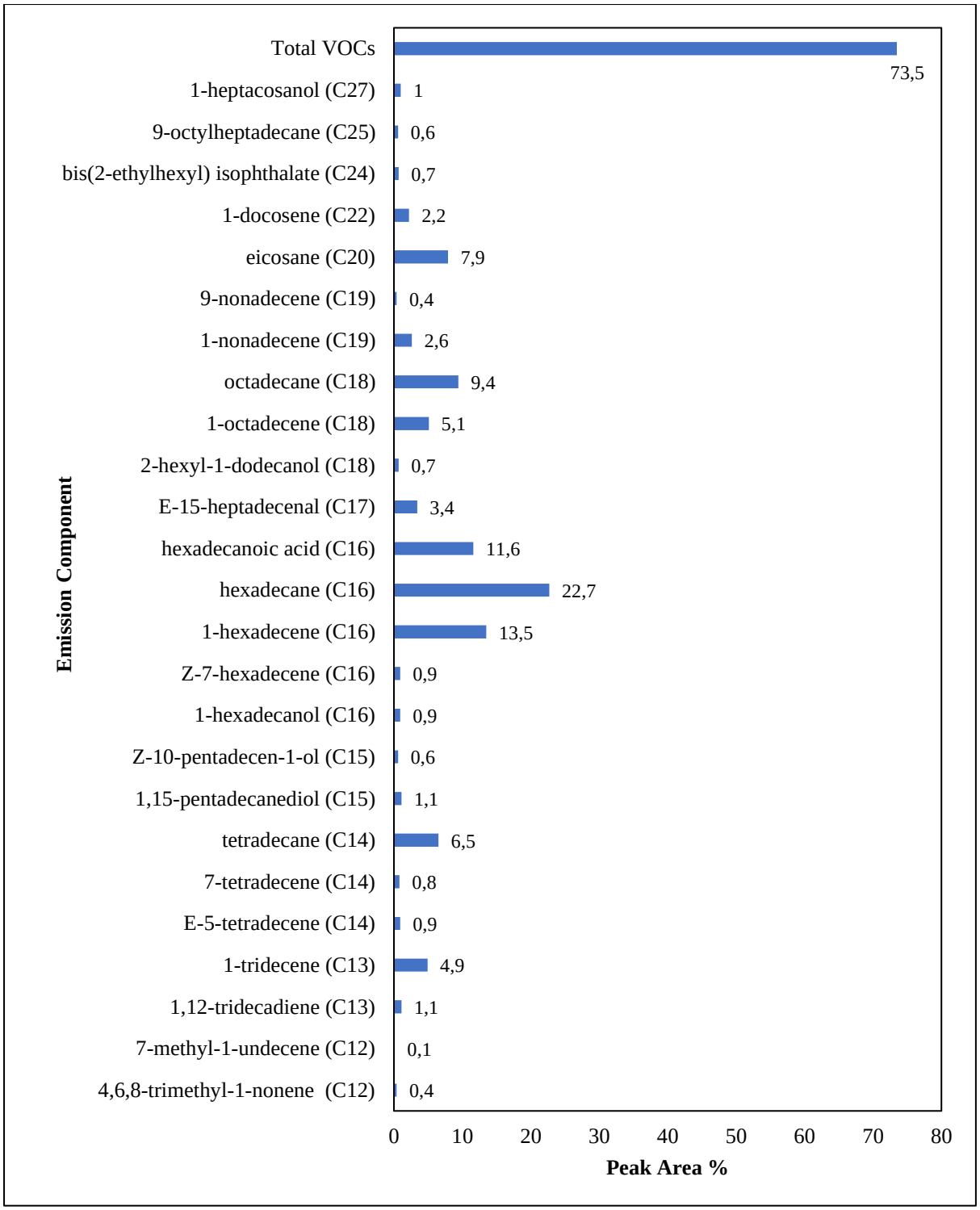

Figure A19: Comparison of peak area % of various components in the emissions from the pyrolysis of a feed mixture of 65 wt % LDPE, 20 wt % HDPE, and 15 wt % PP using a 5:100 zinc oxide catalyst to feed ratio at 450°C and 42 kPa (MP-08).

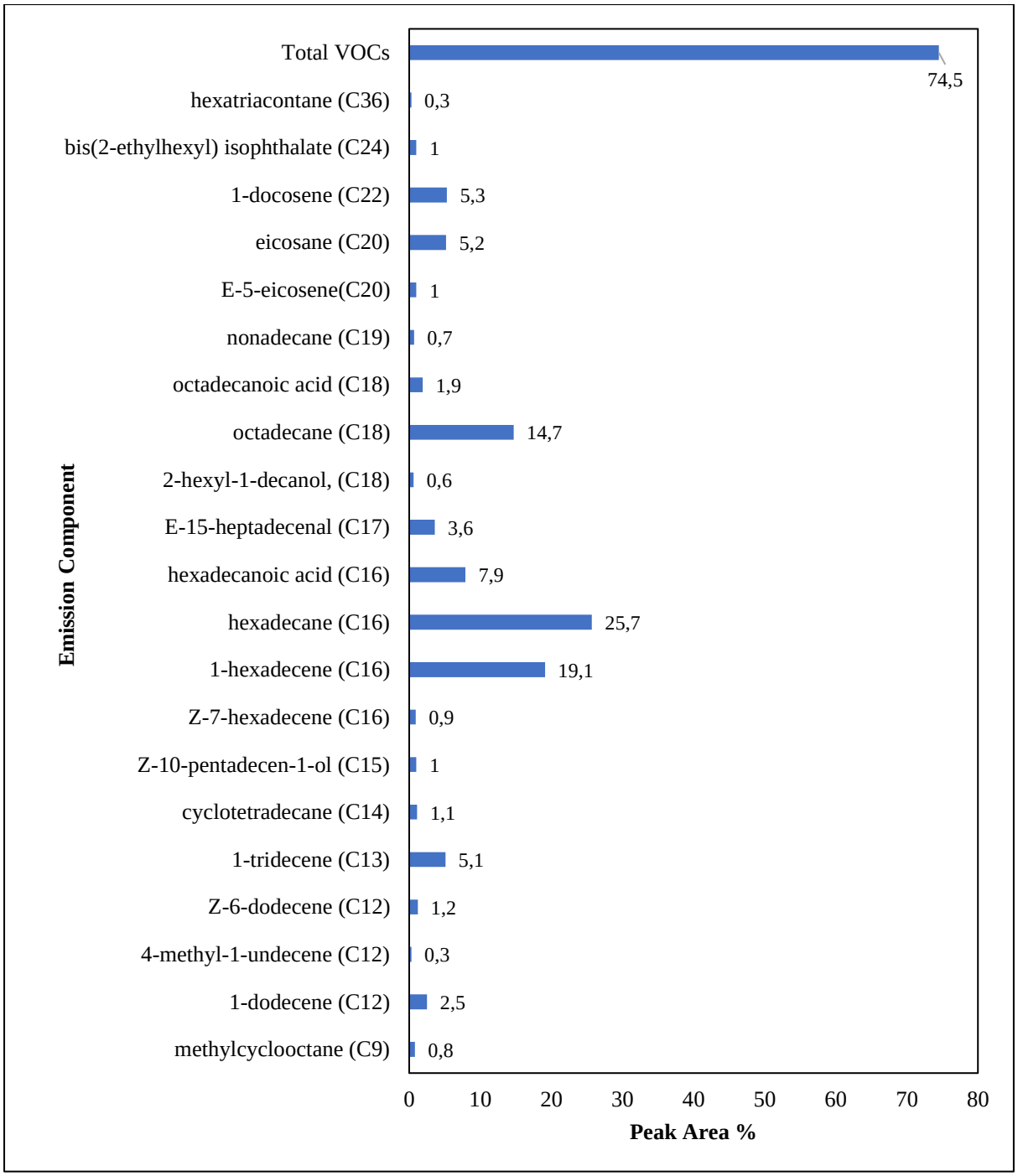

Figure A20: Comparison of peak area % of various components in the emissions from the pyrolysis of a feed mixture of 65 wt % LDPE, 20 wt % HDPE, and 15 wt % PP using a 10:100 zinc oxide catalyst to feed ratio at 450°C and 42 kPa (MP-09).

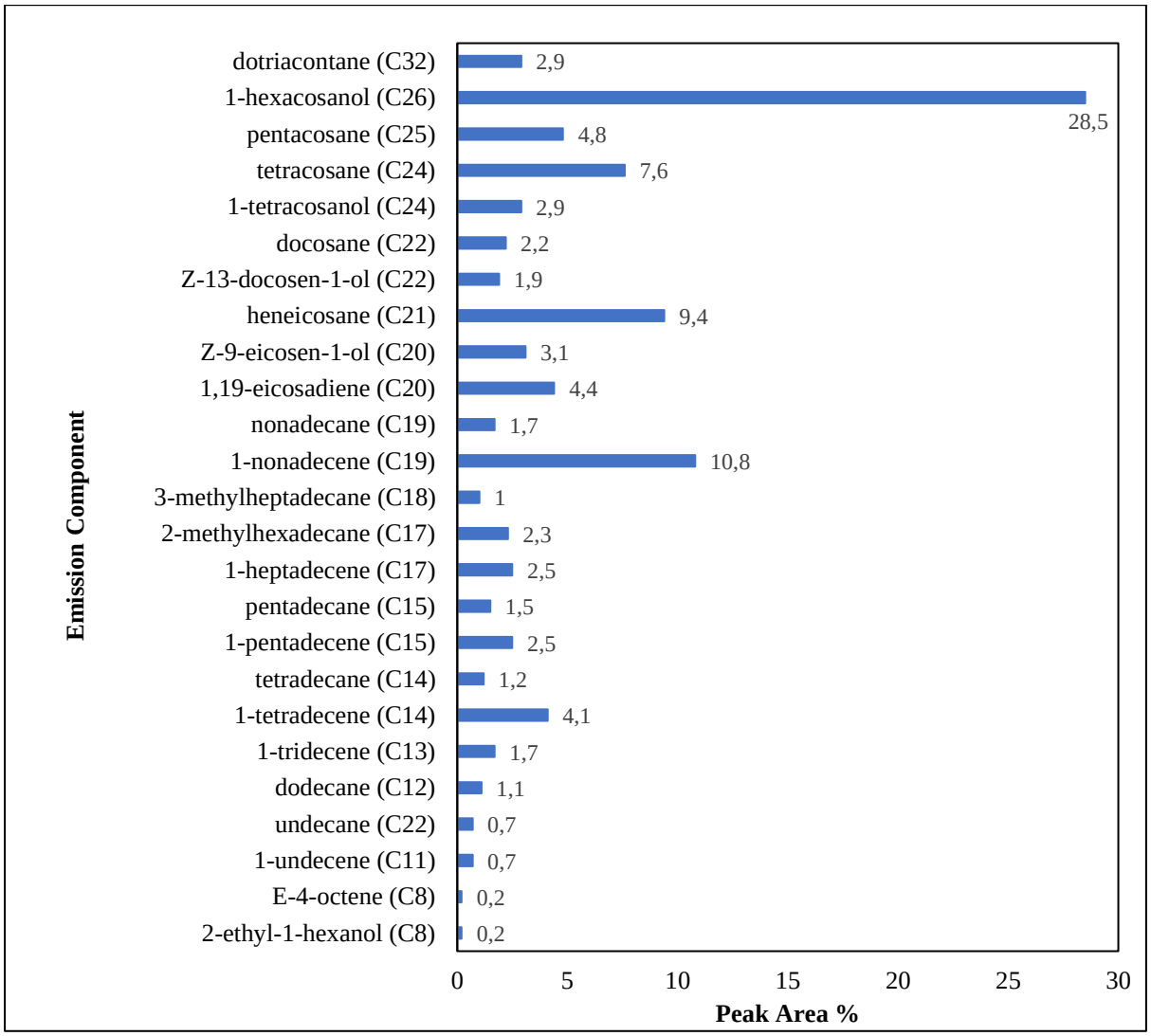

Figure A21: Comparison of peak area % of various components in the pyrolyzer emissions of IP-01.

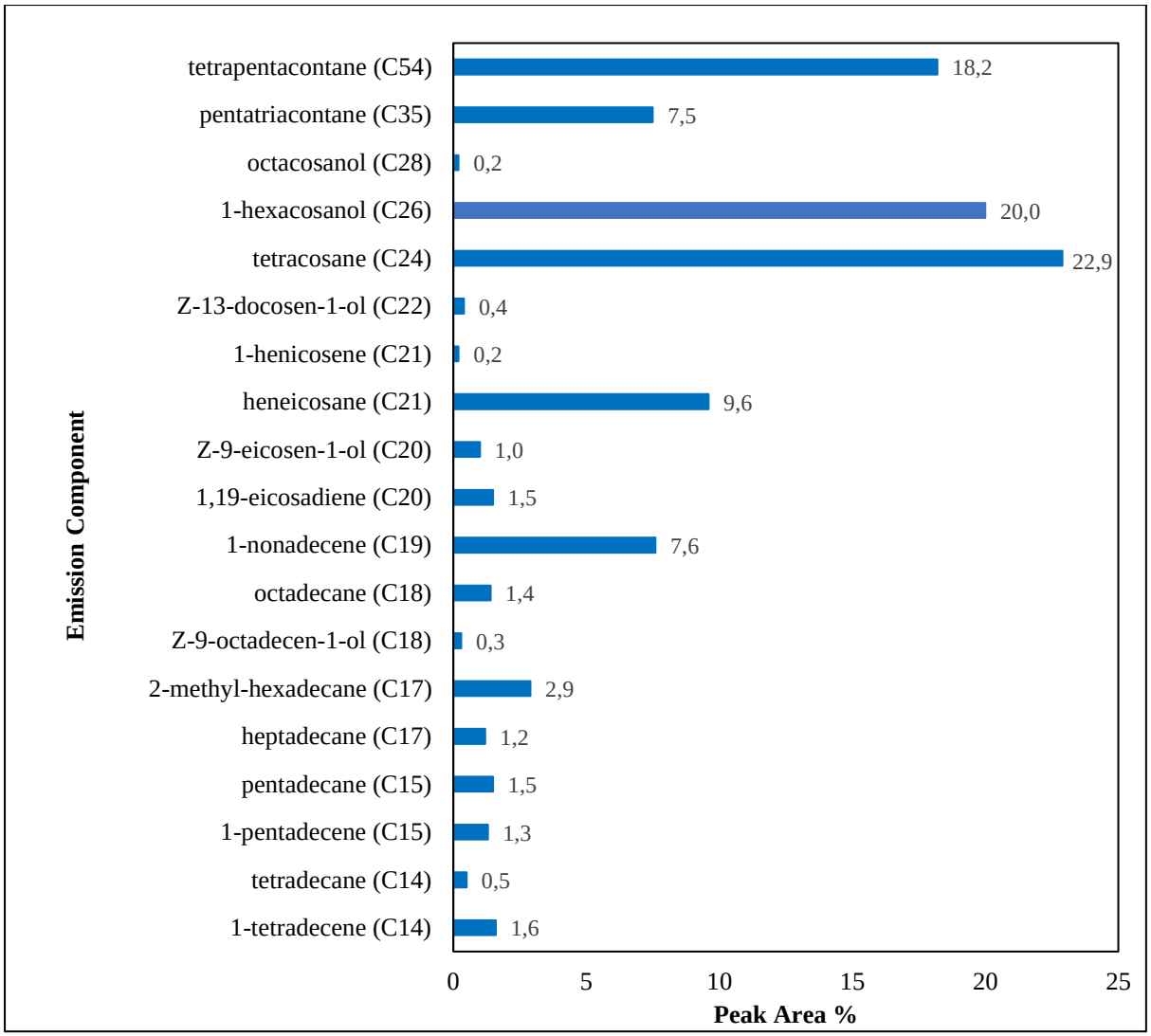

Figure A22: Comparison of peak area % of various components in the pyrolyzer emissions of IP-02.

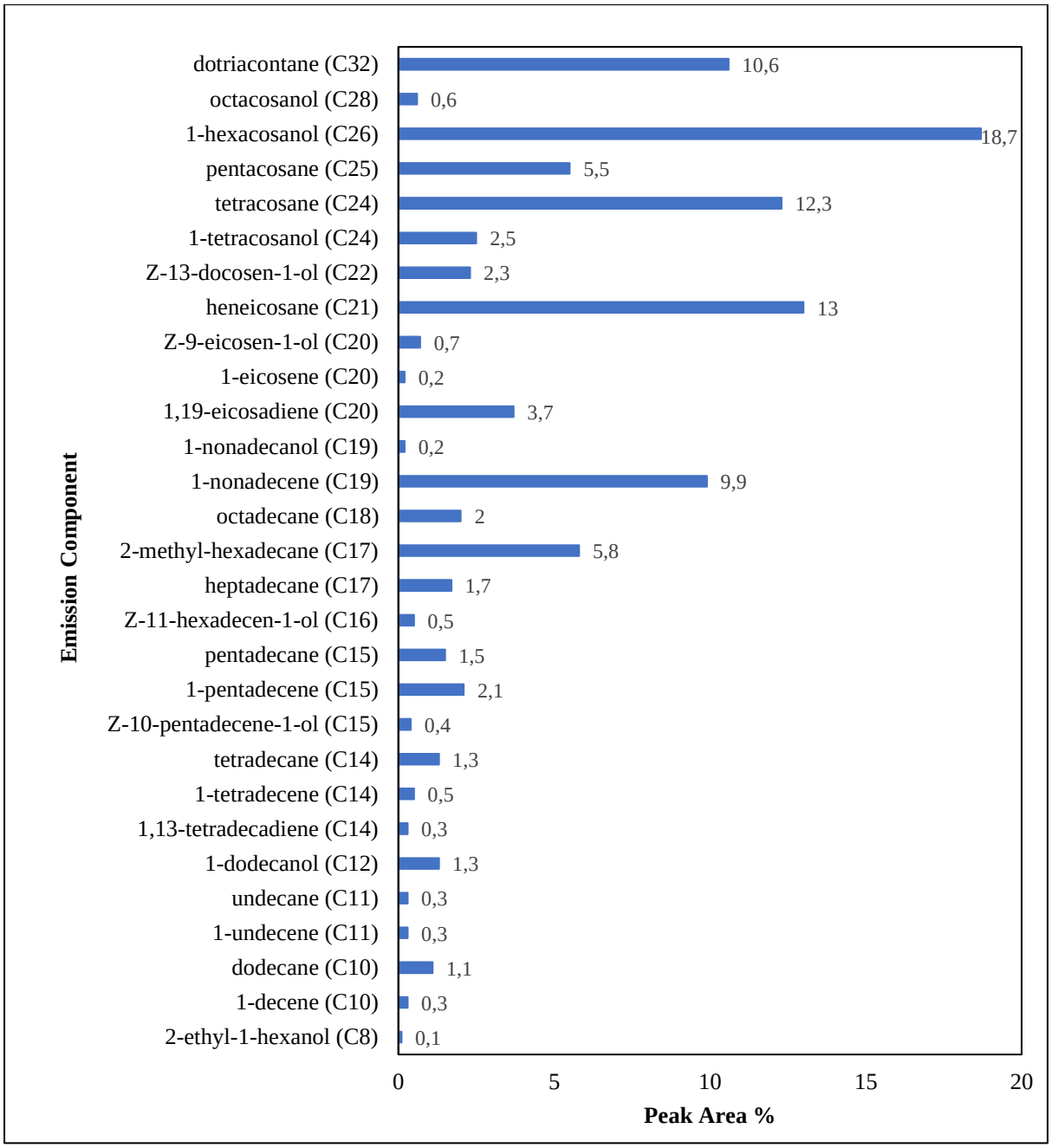

Figure A23: Comparison of peak area % of various components in the pyrolyzer emissions of IP-03.

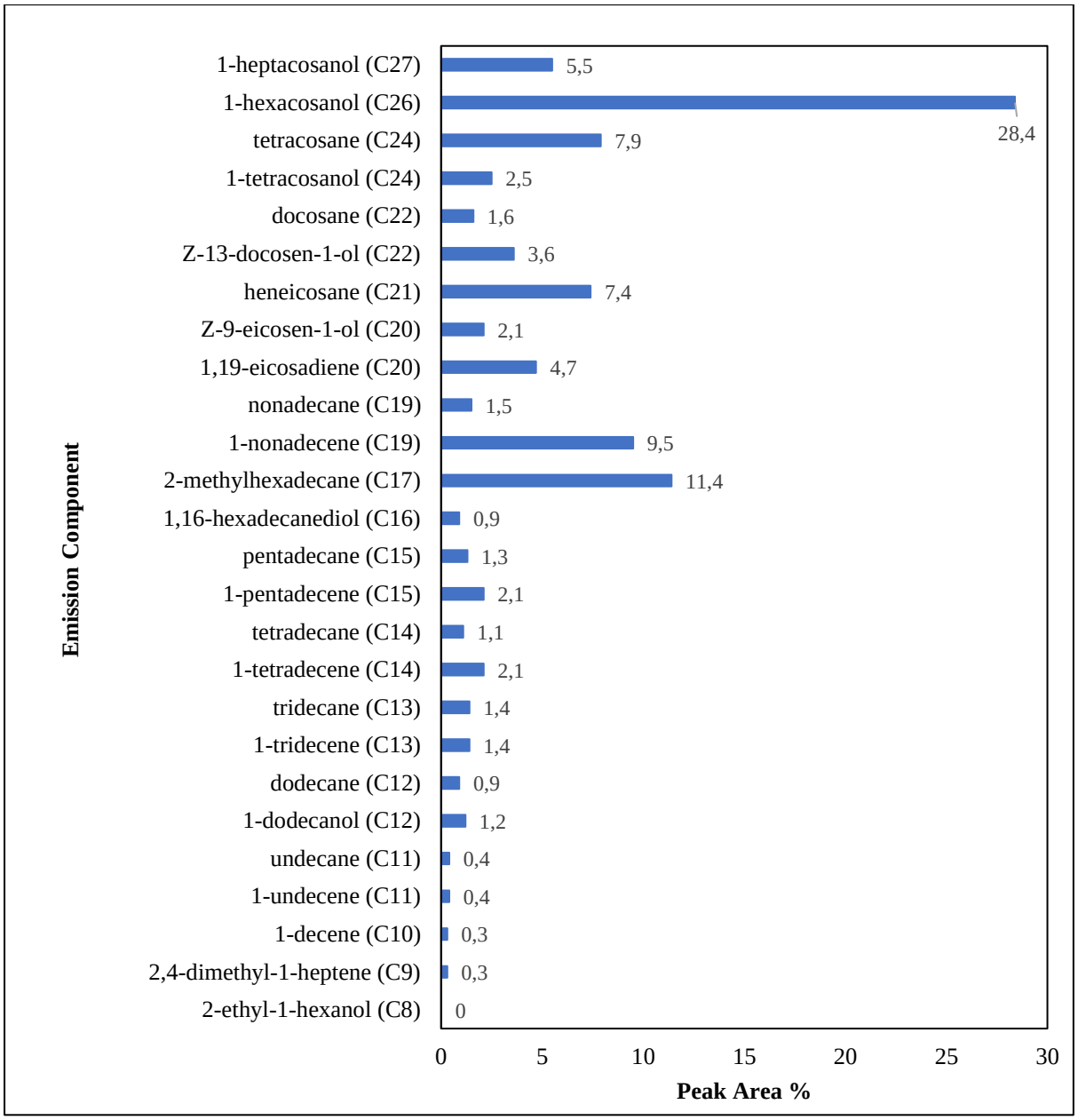

Figure A24: Comparison of peak area % of various components in the pyrolyzer emissions of IP-04.

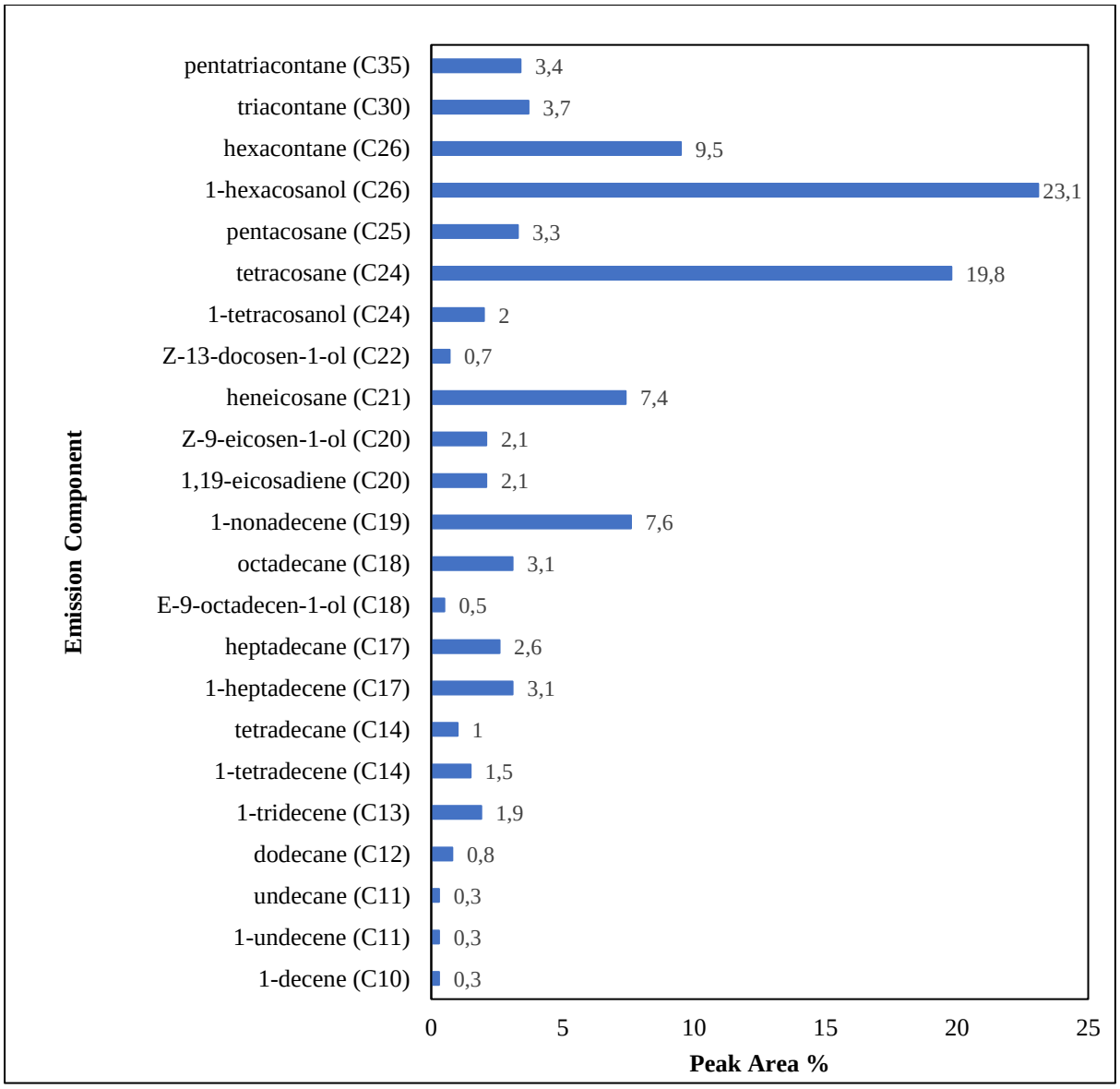

Figure A25: Comparison of peak area % of various components in the pyrolyzer emissions of IP-05.

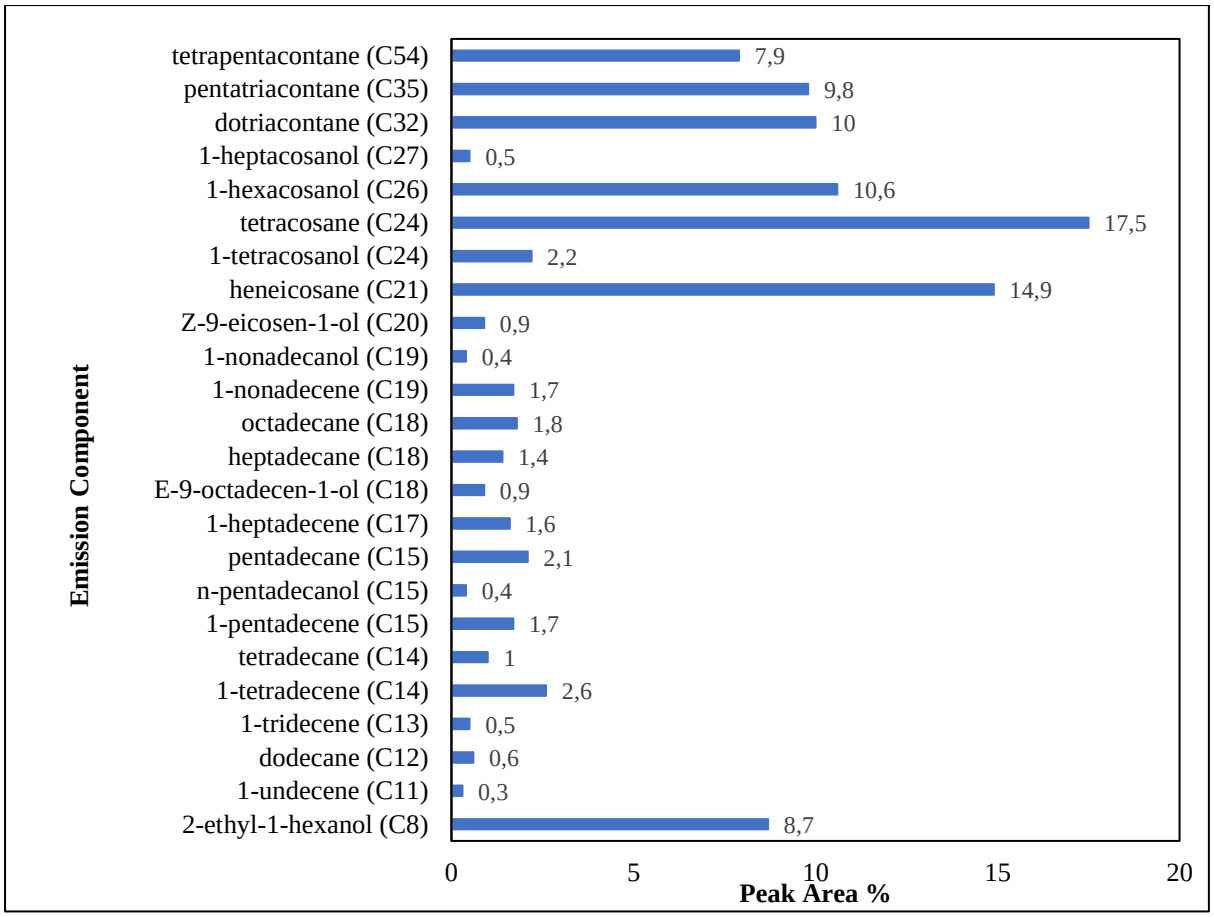

Figure A26: Comparison of peak area % of various components in the pyrolyzer emissions of IP-06.

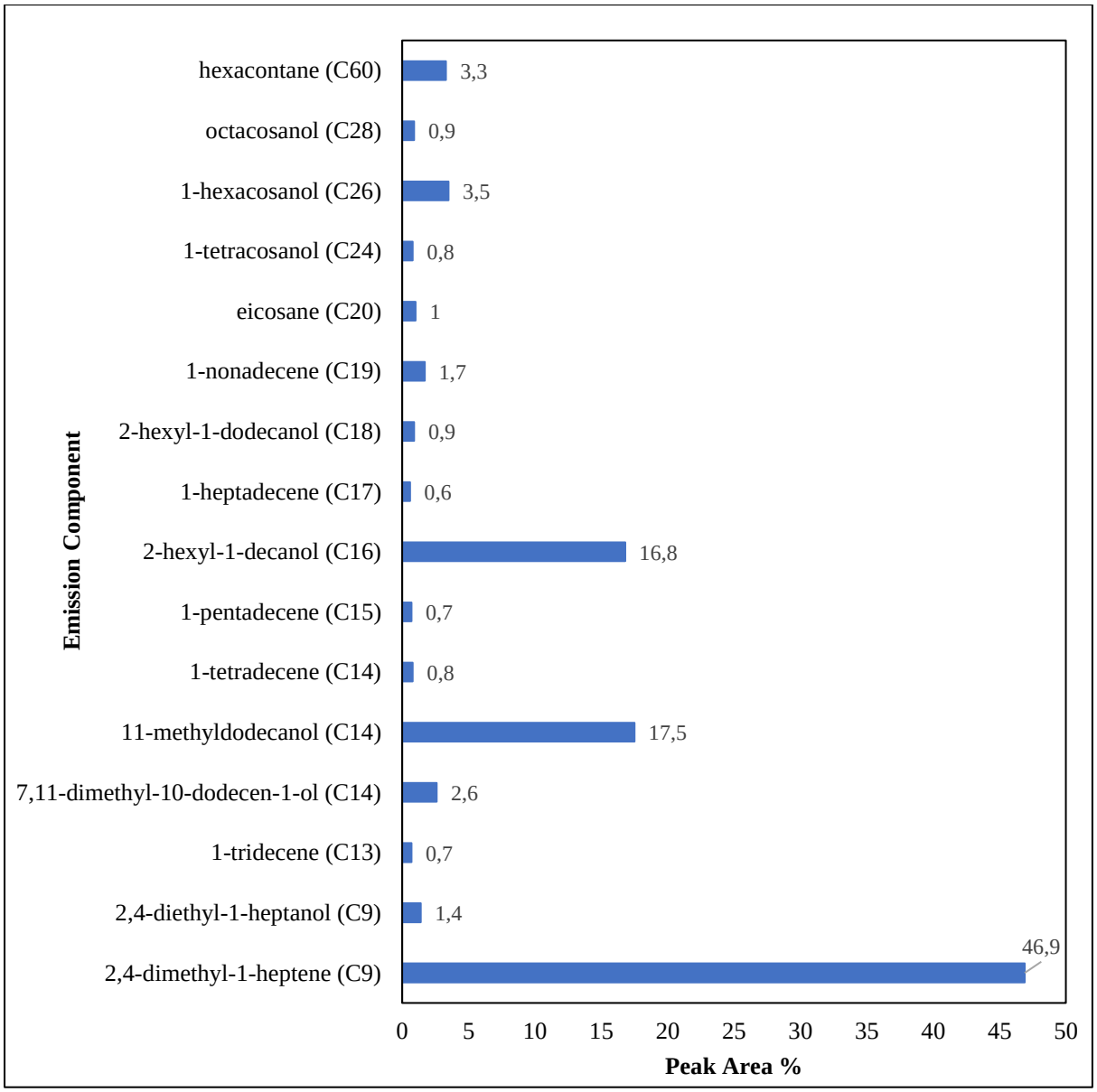

Figure A27: Comparison of peak area % of various components in the pyrolyzer emissions of IP-07.

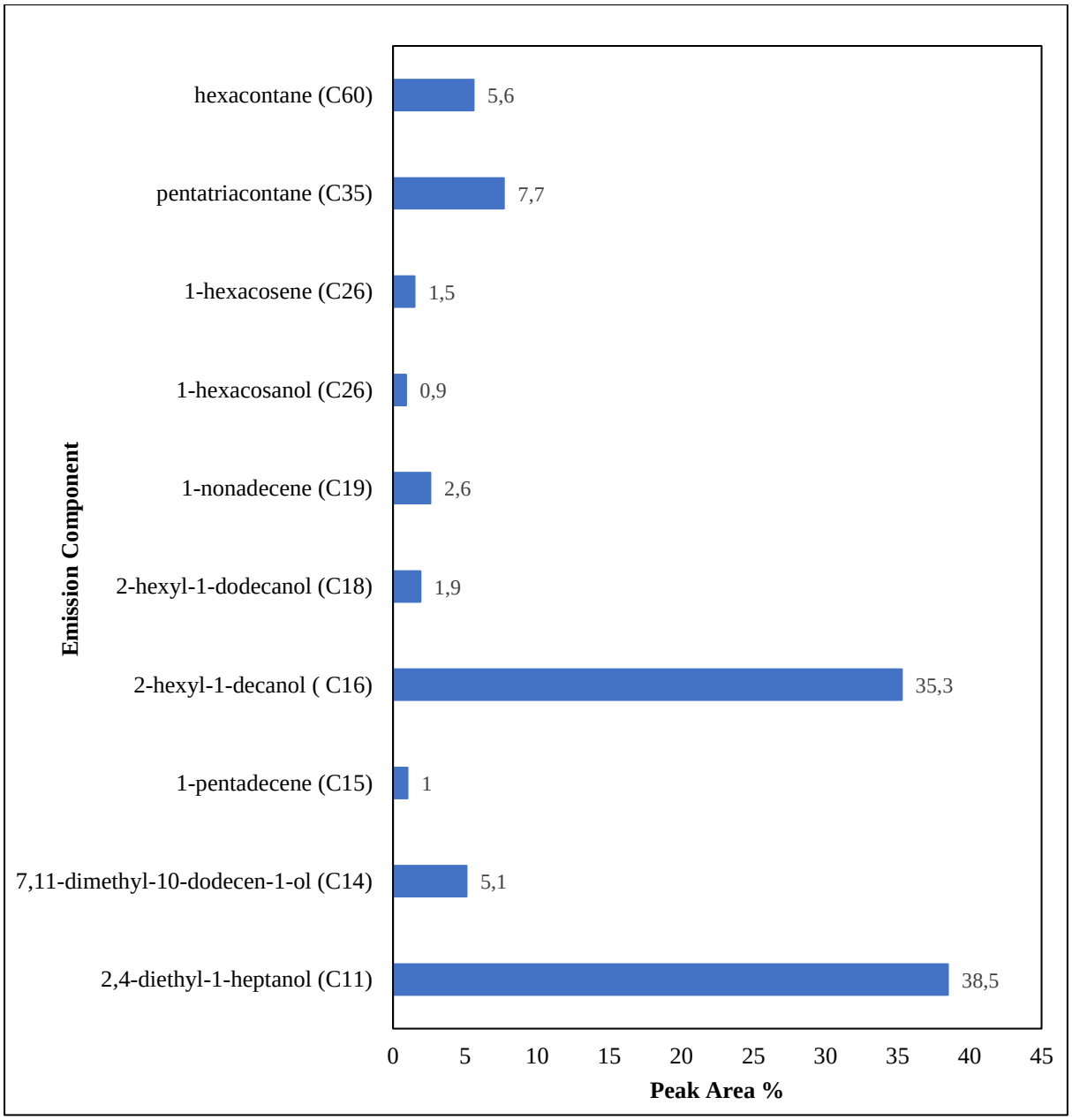

Figure A28: Comparison of peak area % of various components in the pyrolyzer emissions of IP-08.

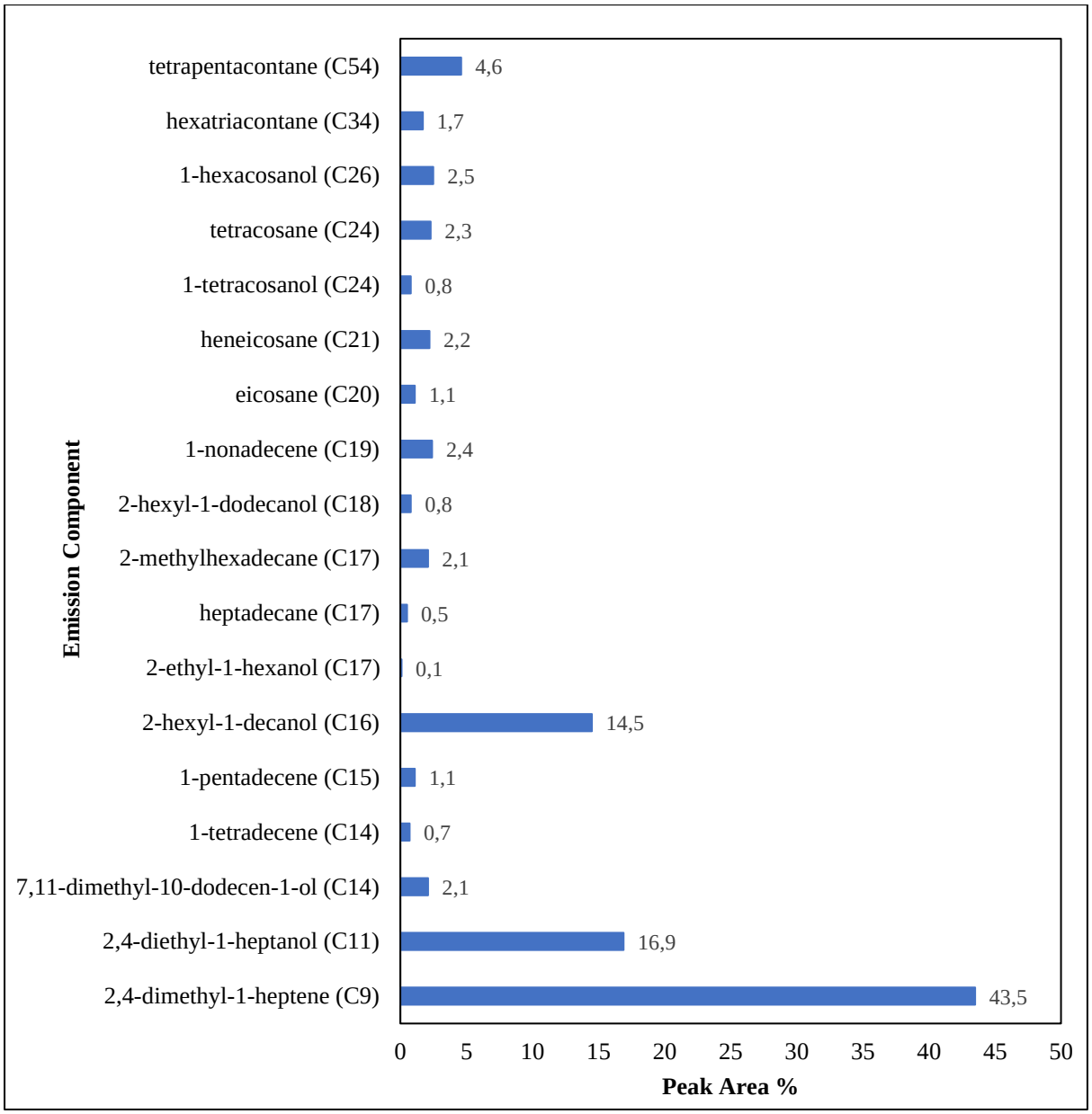

Figure A29: Comparison of peak area % of various components in the pyrolyzer emissions of IP-09.

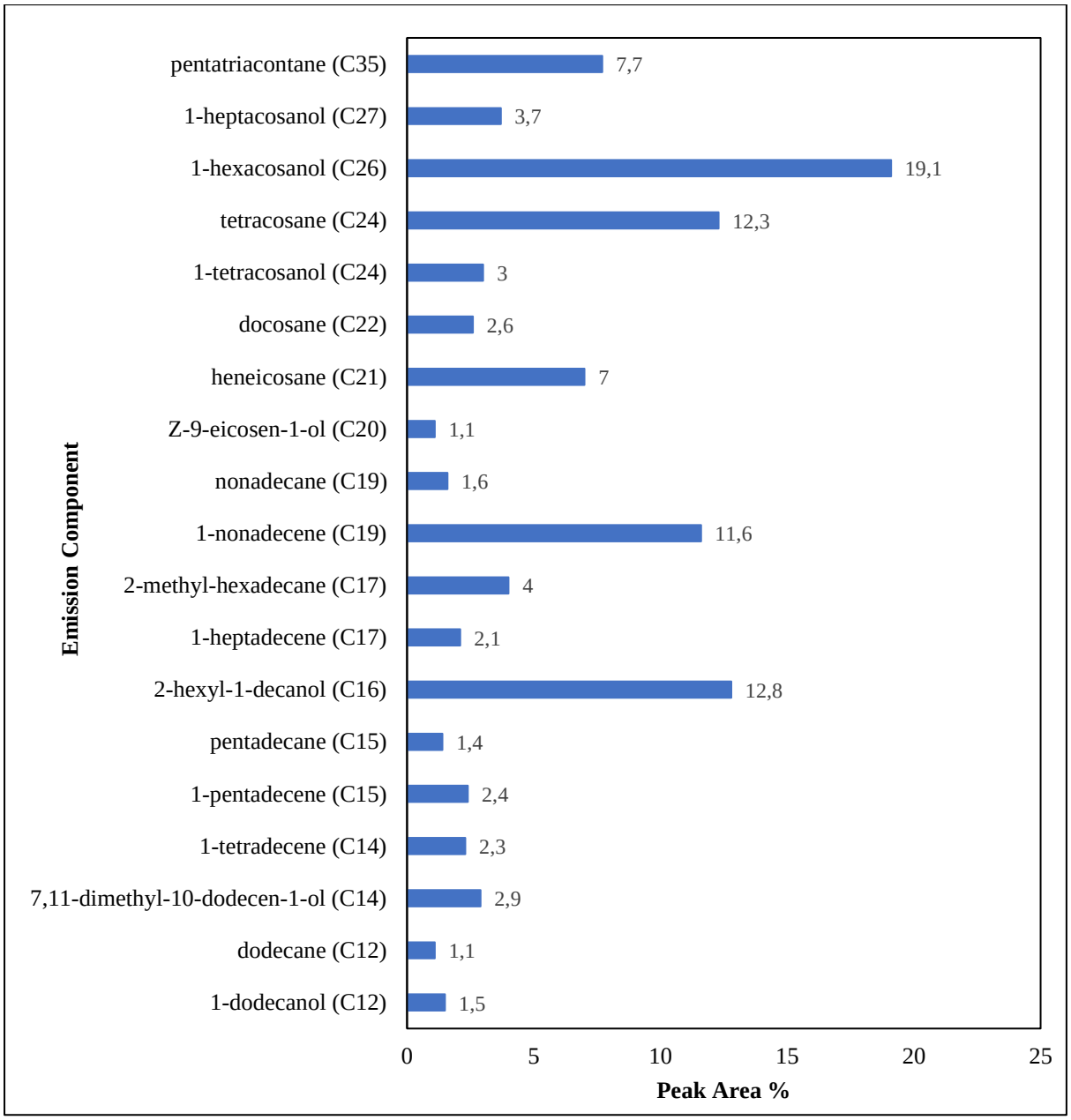

Figure A30: Comparison of peak area % of various components in the pyrolyzer emissions of MP-01.

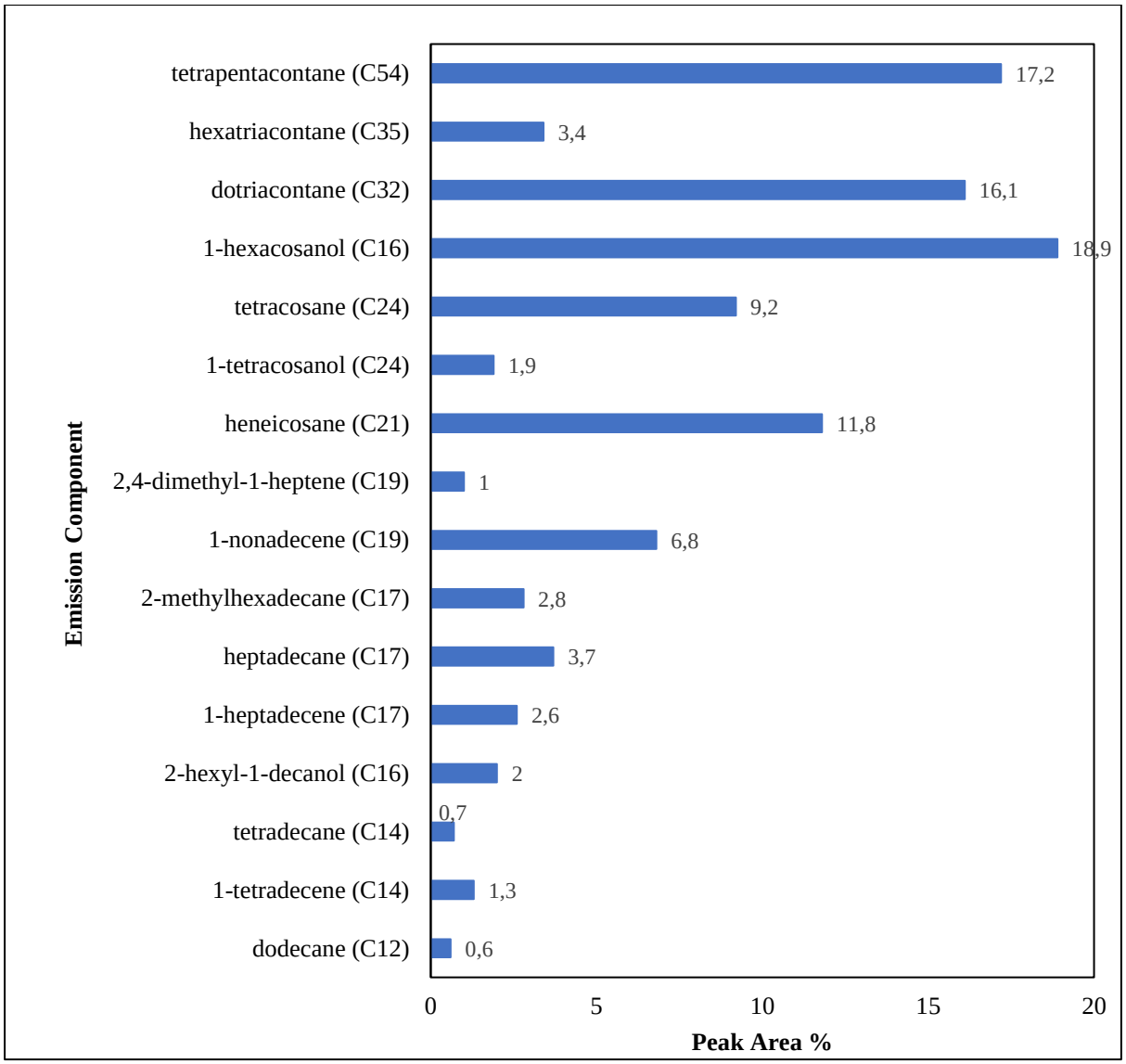

Figure A31: Comparison of peak area % of various components in the pyrolyzer emissions of MP-02.

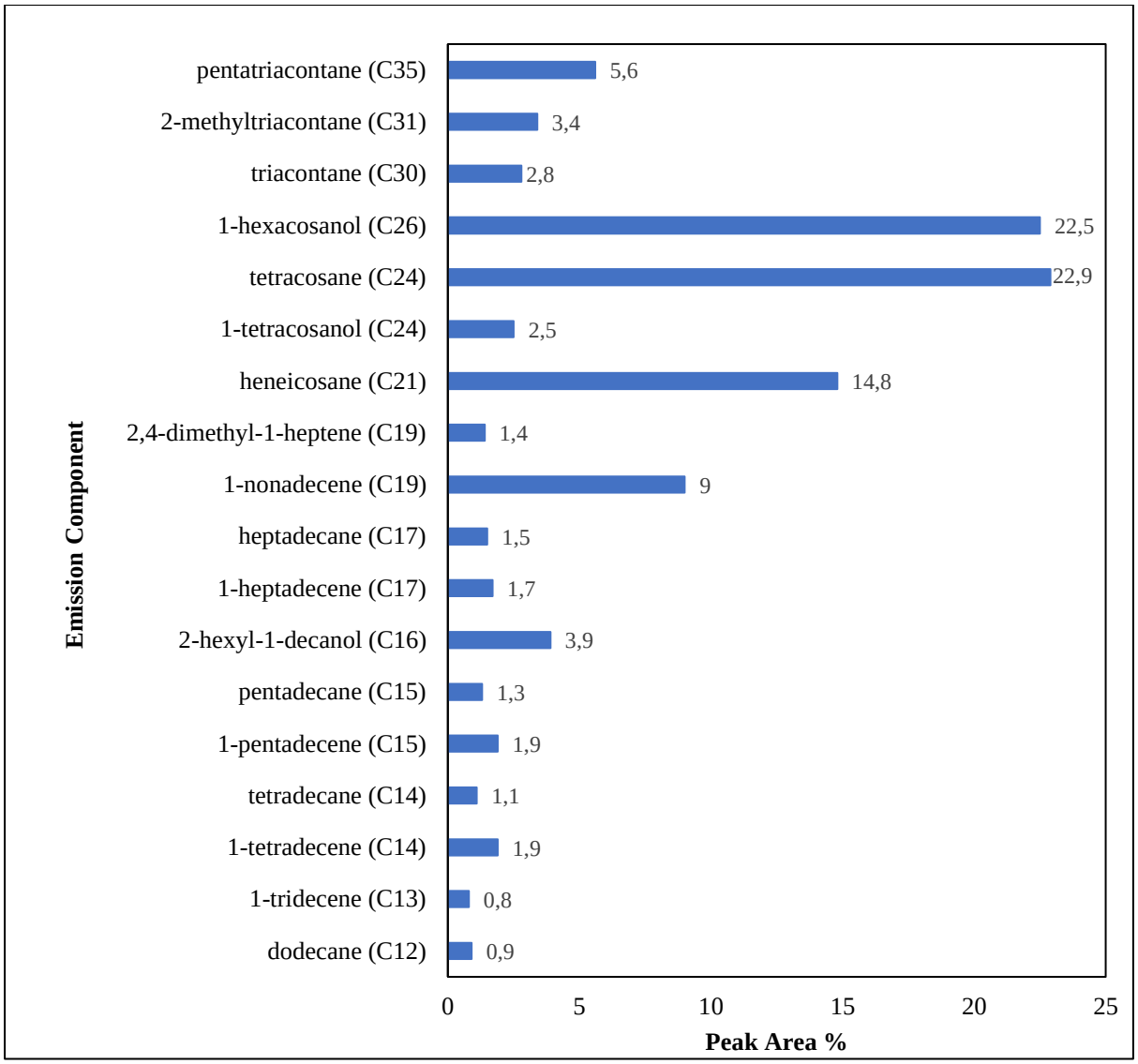

Figure A32: Comparison of peak area % of various components in the pyrolyzer emissions of MP-03.

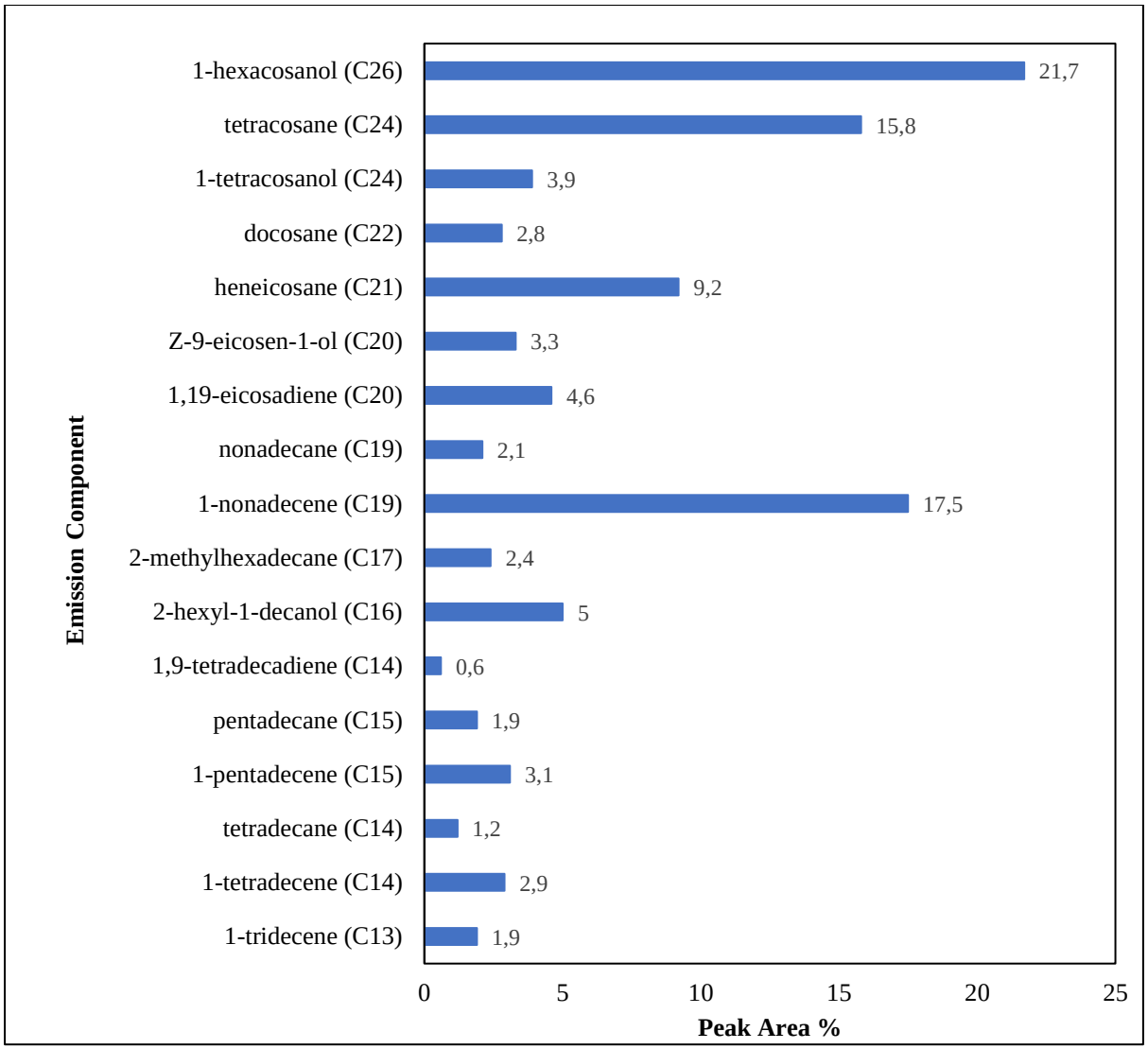

Figure A33: Comparison of peak area % of various components in the pyrolyzer emissions of MP-04.

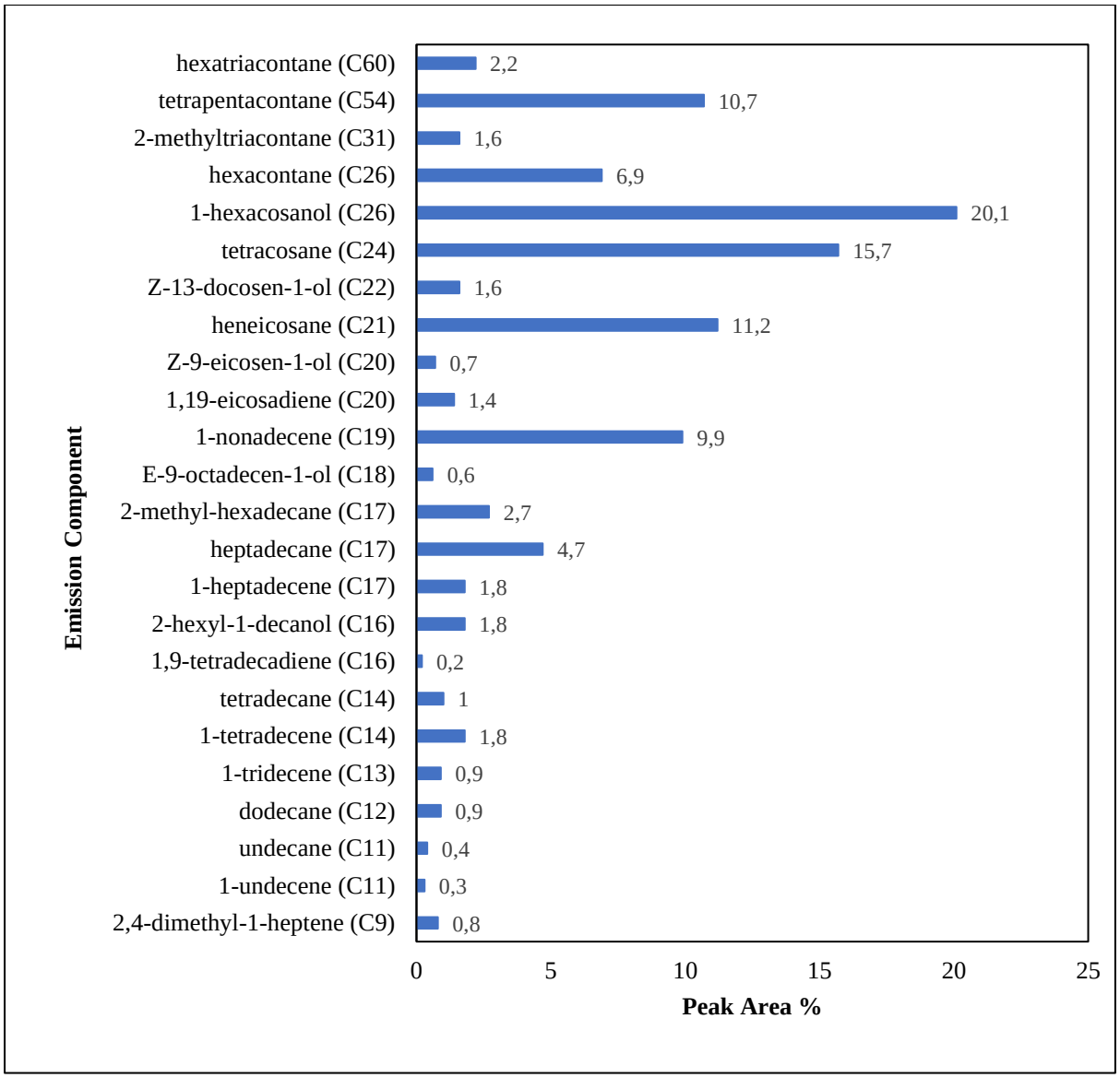

Figure A34: Comparison of peak area % of various components in the pyrolyzer emissions of MP-05.

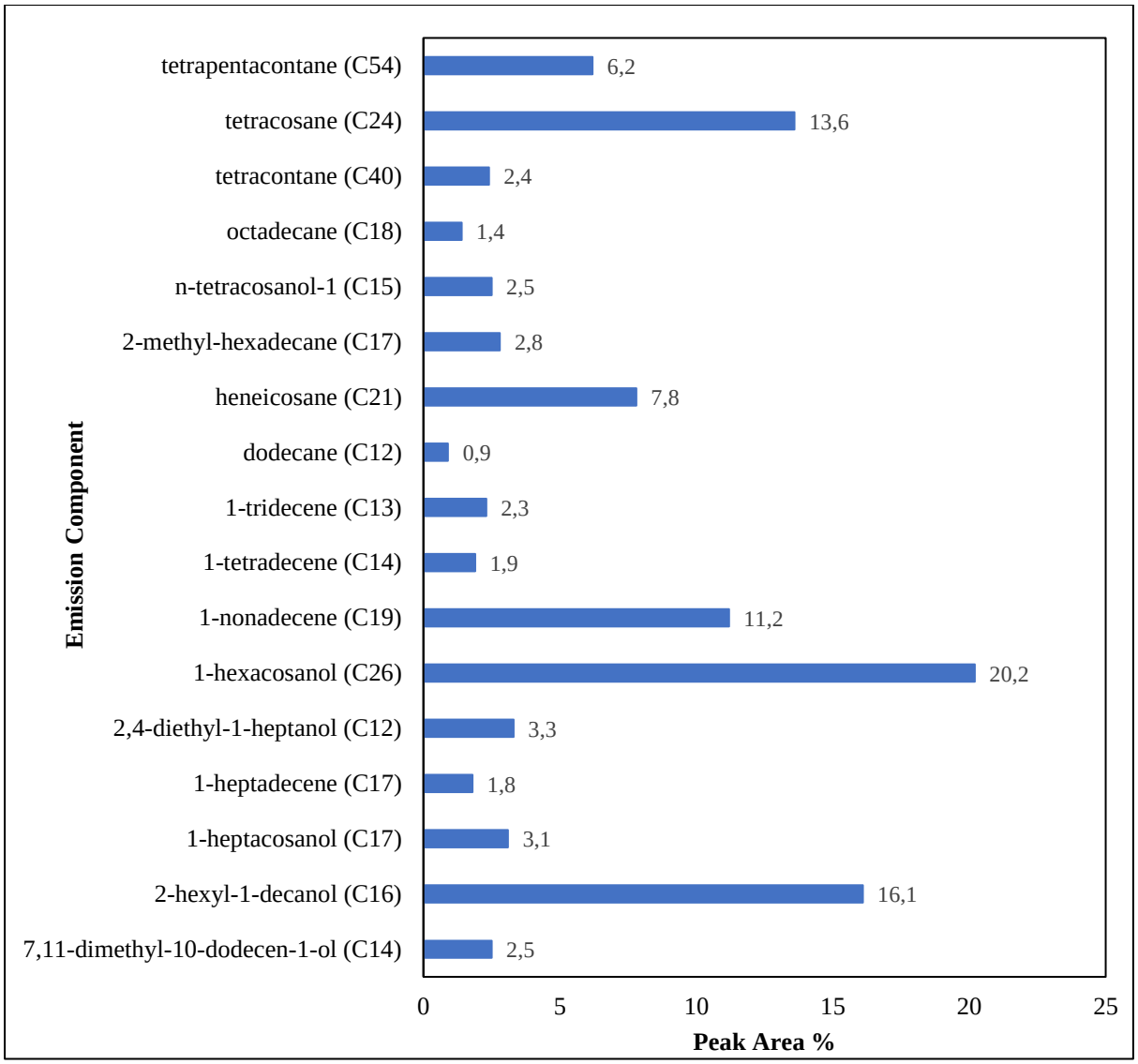

Figure A35: Comparison of peak area % of various components in the pyrolyzer emissions of MP-06.

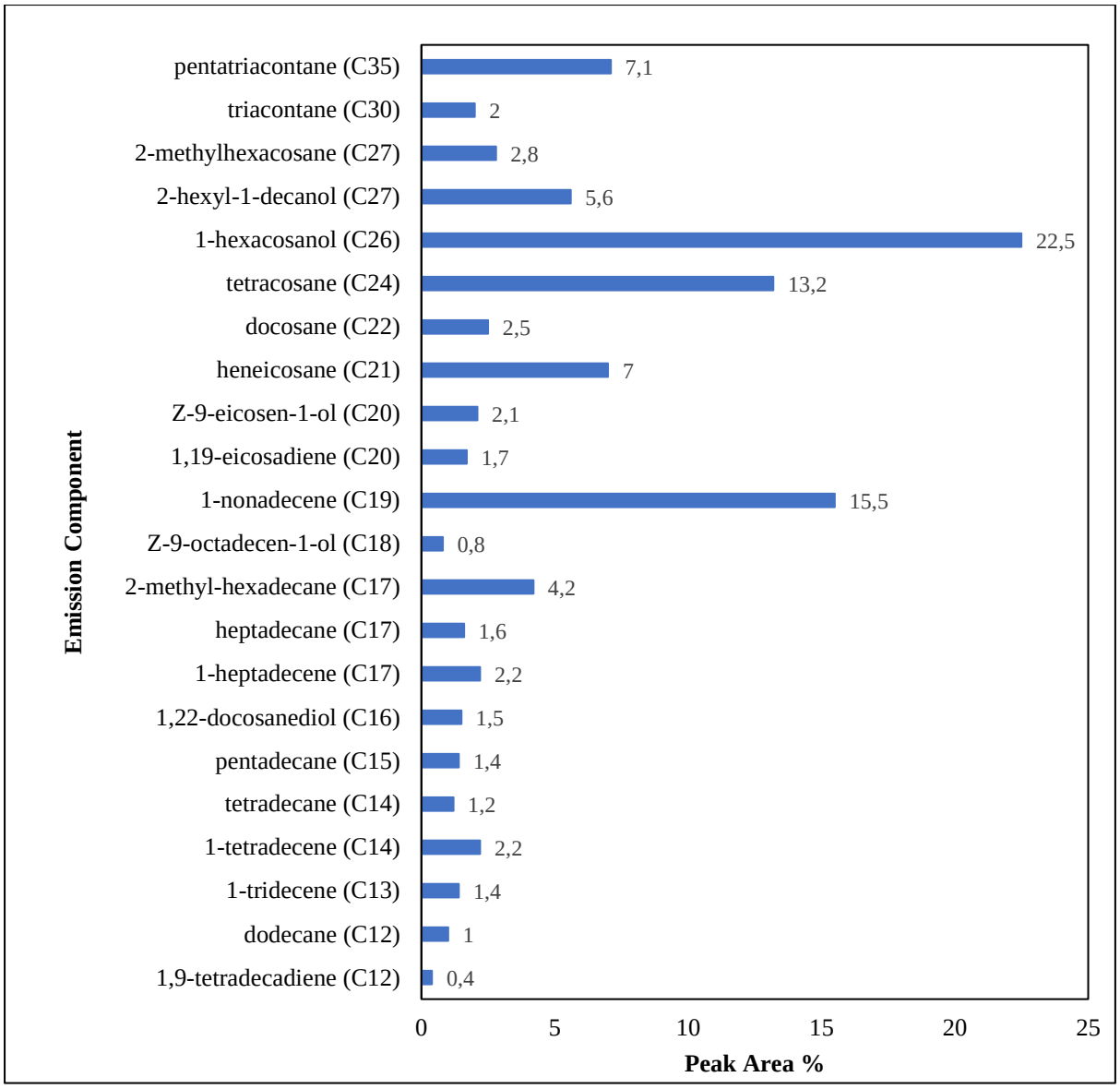

Figure A36: Comparison of peak area % of various components in the pyrolyzer emissions of MP-07.

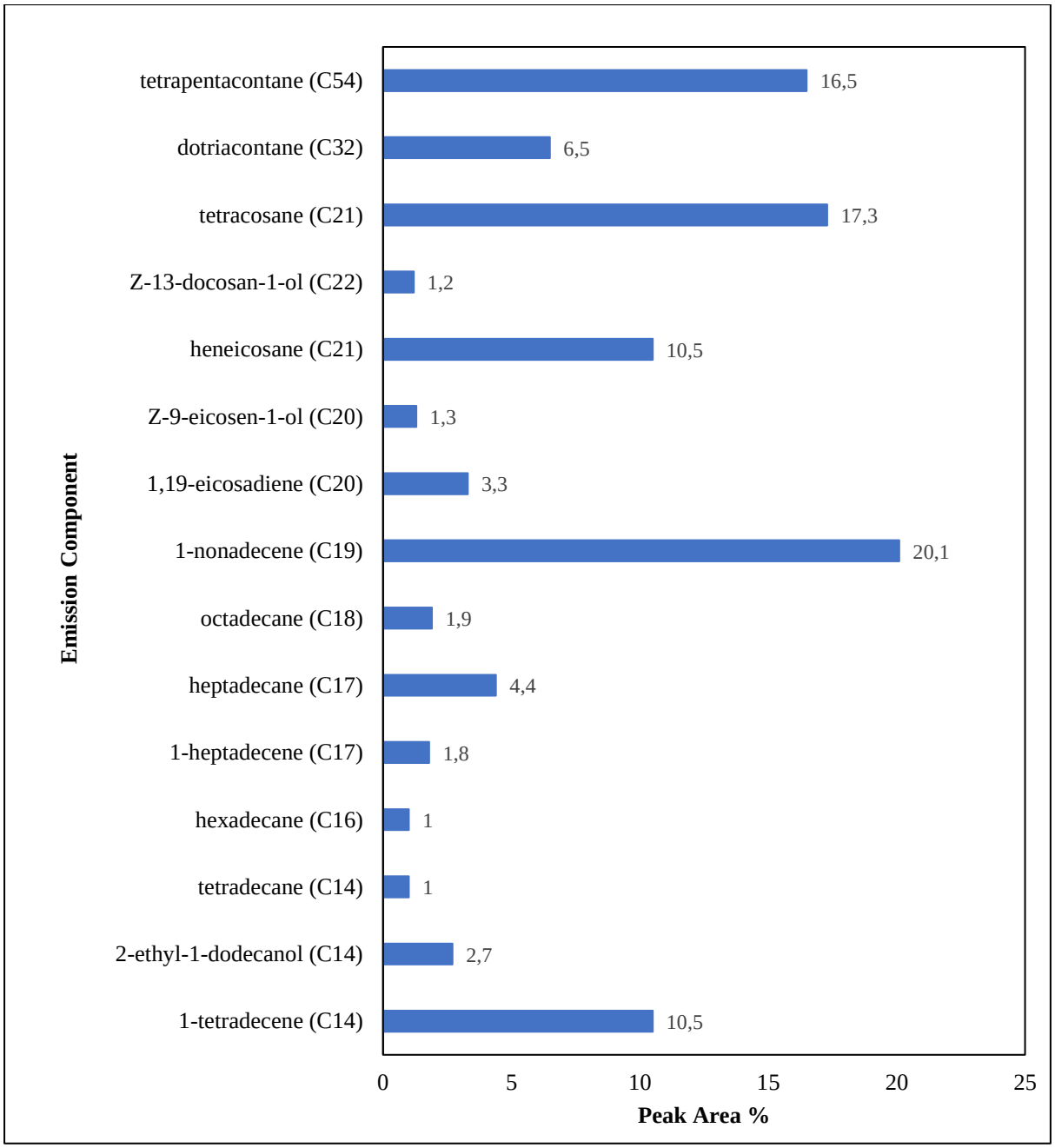

Figure A37: Comparison of peak area % of various components in the pyrolyzer emissions of MP-08.

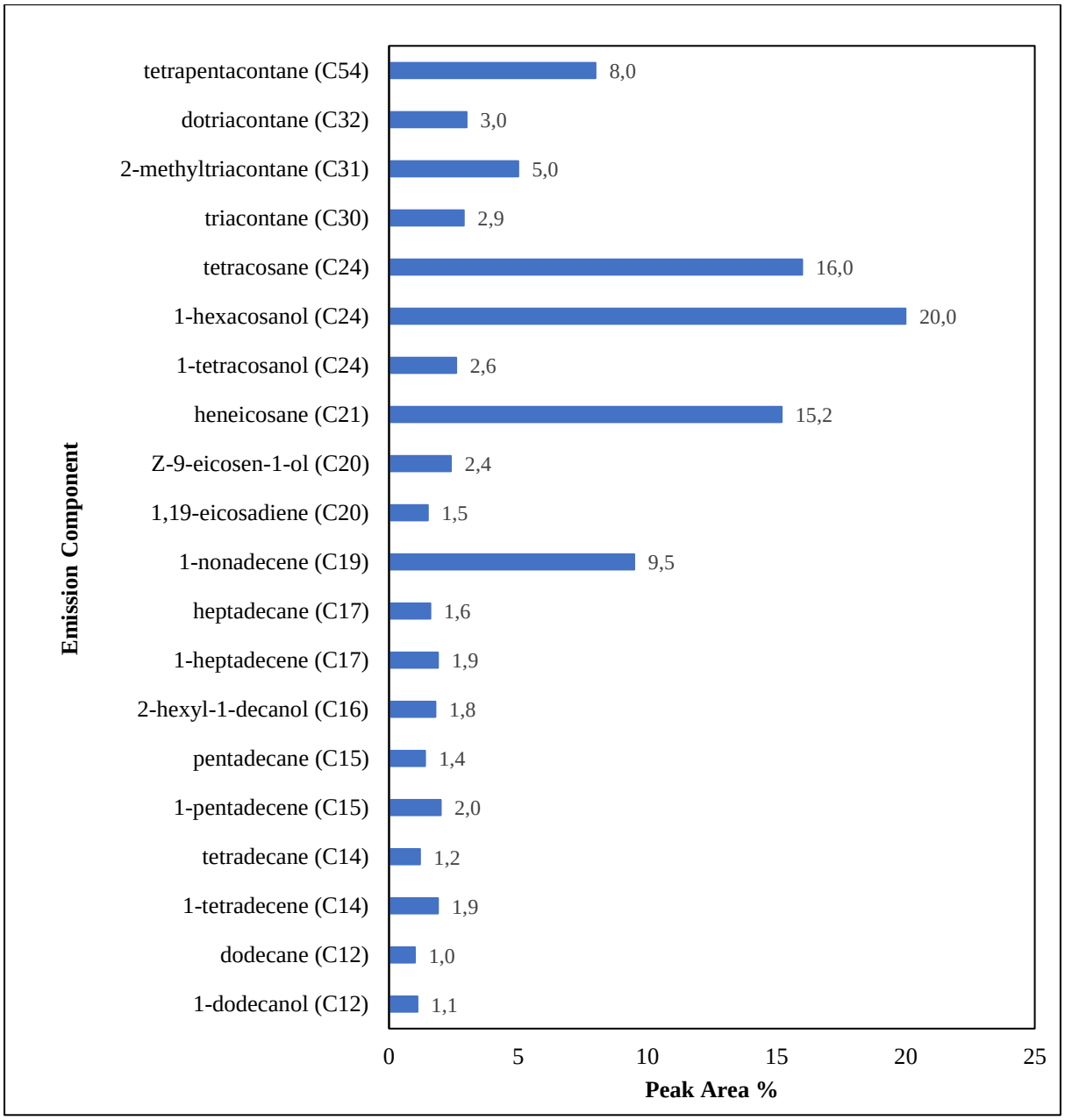

Figure A38: Comparison of peak area % of various components in the pyrolyzer emissions of MP-09.

Appendix B: Sample calculations

Sample Calculation B1: Product mass and yield calculation

The mass readings of the apparatus in table A1 were used to calculate the mass and yield of pyrolysis products listed in table A2.

The mass of liquid product was calculated using equation (3.1):

$m_{liquid} = m_{collection\ flask,\ final} - m_{collection\ flask,\ initial}$

$m_{liquid} = 115.802\ g - 115.572\ g$

$m_{liquid} = 0.230\ g$

The mass of wax was calculated using equation (3.2):

$m_{wax} = m_{spiral\ condenser,\ final} - m_{spiral\ condenser,\ initial}$

$m_{wax} = 167.828\ g - 154.778\ g$

$m_{wax} = 13.050\ g$

The mass of char was calculated using equation (3.3) for an uncatalysed process:

$m_{char,\ uncatalysed} = m_{reactor,\ final} - m_{reactor,\ \mathbf{initial}}$

$m_{char,\ uncatalysed} = 97.276\ g - 96.706\ g$

$m_{char,\ uncatalysed} = 0.570\ g$

Using the mass balance equation (3.5), the mass of gas formed was calculated as follows:

$m_{feed} = m_{liquid} + m_{wax} + m_{char} + m_{gas}$

$m_{gas} = 15.040\ g - 0.230\ g - 13.050\ g - 0.570\ g$

$m_{gas} = 1.190\ g$

The yield calculation for liquid was calculated using equation (3.6):

Pyrolysis Product Yield (wt %) = $\frac{m_{product}}{m_{feed}}$ x 100

Pyrolysis Product Yield (wt %) = $\frac{m_{liquid}}{m_{feed}}$ x 100

Pyrolysis Product Yield (wt %) = $\frac{0.230\ g}{15.040\ g}$ x 100

Pyrolysis Product Yield (wt %) = 1.5 wt %

The product yields for the wax, char, and gas were calculated using the same procedure as shown above.

Sample Calculation B2: Calculation of fuel usage and CO_2 emissions of vehicle

Distance from plant to waste site = 10 km

Distance to obtain plastic and deliver to plant = 10 km x 2 = 20 km

Fuel efficiency for a light duty truck = 7.69 km per litre

From equation (3.7):

Amount of fuel used = $\frac{Distance\ Travelled\ (km)}{Fuel\ efficiency\ (\frac{km}{litre})}$

= $\frac{20\ km}{7.69\frac{km}{litre}}$

= 2.60 litres (diesel)

Transport CO_2 Emissions = Amount of fuel used x Vehicle CO_2 Emission Factor

= 2.60 litres x 2.7 $\frac{kg\ CO_2}{litre}$

= 7.02 kg CO_2 released

Sample Calculation B3: Laboratory-scale dryer electricity usage and indirect CO_2 emissions

The laboratory-scale dryer was reported to have a power rating of 12 kW.

Equation (3.9) was used to calculate the electricity usage of the dryer:

Electricity Usage (kWh) = Energy Requirement (kW) x Duration (h)

= 12 kW x 0.25 h

= 3 kWh

The indirect CO_2 emission was calculated using the CO_2 Emission Factor and the Electricity Usage.

From equation (3.8):

CO_2 Emissions from Electricity Usage (kg CO_2) = Electricity Usage (kWh) x CO_2 Emission Factor (kg CO_2 per kWh)

= 3 kWh x 1.609 $\frac{kg\ CO_2}{kWh}$

= 4.83 kg CO_2 released

Sample Calculation B4: Calculation of plastic pyrolysis electricity usage

Electricity Usage Calculation for IP-02:

Mass of liquid + wax = 11.74 g

Process duration = 13.75 h

Power ratings for heating mantle, vacuum pump, and water circulator are 0.3 kW, 0.3 kW, and 0.3 kW respectively.

Electricity Usage for heating mantle:

From equation (3.9):

Electricity Usage (kWh) = Energy Requirement (kW) x Duration (h)

= 0.3 kW x 13.75 h

= 4.12 kWh

Similarly, the energy usage for the vacuum pump and water circulator was 4.12 kWh and 20.62 kWh respectively.

Total Energy Usage = Heating Mantle Energy Usage + Vacuum Pump Energy Usage + Water Circulator Energy Usage

= 4.12 kWh + 4.12 kWh + 4.12 kWh

= 12.36 kW

Energy Usage per gram of product = $\frac{Total\ Energy\ Usage}{Total\ liquid + wax\ obtained\ from\ experiment}$

= $\frac{12.36\ kW}{11.74\ g}$

=1.05 kWh per gram of liquid + wax product obtained

Sample Calculation B5: Calculation of indirect CO_2 emissions of the plastic pyrolysis process

For IP-02, using equation (3.8):

CO_2 Emissions from Electricity Usage (kg CO_2) = Electricity Usage (kWh) x CO_2 Emission Factor (kg CO_2 per kWh)

= 12.36 kWh x 1.609 $\frac{kg\ CO_2}{kWh}$

= 19.89 kg CO_2 released

CO_2 Emissions per gram of liquid + wax product = $\frac{Indirect\ CO_2\ Emissions}{Total\ liquid + wax\ obtained\ from\ experiment}$

= $\frac{19.89\ kg\ CO_2}{11.74\ g}$

=1.69 kg CO_2 per gram of liquid + wax product obtained

Appendix C: Descriptions of plastic pyrolysis processes obtained from literature

Pyrolysis of waste polyethylene under vacuum using zinc oxide (Tekade et al., 2020)

In the work of Tekade et al. (2020), pyrolysis experiments were implemented using separate feedstocks of LDPE and HDPE. Initially, uncatalysed experiments were performed using a heating rate of 10°C/min. Thereafter a zinc oxide catalyst was used in the pyrolysis process. The experiments included runs with catalyst to feed ratios of 3:100, 5:100. 10:100, and 15:100. A vacuum pressure of 50 kPa was used for both the uncatalysed and catalysed experiments. A round bottom flask served as the reactor for the experiment. The vapour from the reactor was cooled in a condenser (ice and water mixture at 6°C used as cooling fluid). The cooled liquid dripped into a collection flask. GC-MS was used to perform chemical analysis of the liquid products.

Waste-to-fuels Pyrolysis of Low-Density Polyethylene Waste in the Presence of H-ZSM-11 (Lee et al., 2021)

Lee et al., (2021) implemented LDPE plastic pyrolysis experiments using a zeolite catalyst H-ZSM-11. Pyrolysis experiments were performed at temperatures ranging from 500°C to 900°C with and without the use of catalyst. A split-hinge tube furnace served as the reactor. A heating rate of 10°C/min was used. Nitrogen gas was used to inert the closed environment. Pyrolysis liquid and gas yields were obtained. Chemical analysis was performed on the liquid and gas products.

Catalytic pyrolysis of low-density polyethylene using cetyltrimethyl ammonium encapsulated monovacant kegging units C19H42N4H3 (PW11O3) and ZSM-5 (Batool et al., 2016)

In the work of Batool et al., (2016), plastic pyrolysis was performed using a feedstock of LDPE. Initially, thermal pyrolysis experiments were implemented. Thereafter, catalysts such as CTA-POM and ZSM-5 were used in the LDPE pyrolysis experiments. Nitrogen gas was used to inert the atmosphere. A heating rate of 5°C per minute was used. Product yields were obtained for the pyrolysis liquid, gas, and the residue which remained in the reactor once the reaction was completed.

Catalytic pyrolysis of High-Density Polyethylene: Decomposition Efficiency and Kinetics (Raveh-Amit et al., 2022)

In Raveh-Amit et al., (2022), catalysts such as zeolite Y, ZSM-5 (SiO_2/Al_2O_3 Ratio of 25), and ZSM-5 (SiO_2/Al_2O_3 Ratio of 800) were used in high-density polyethylene plastic pyrolysis processes. A catalyst to feed ratio of 0.1:10 was used for the catalysed pyrolysis experiments. Pyrolysis experiments were implemented at 450°C and 525°C. Yields were obtained for the pyrolysis condensables, gas, and char.

In-situ production of valuable aromatics via pyrolysis of waste polypropylene using commercial catalyst ZSM-5(Gaurh and Pramanik, 2020)

(Gaurh and Pramanik, 2020) performed pyrolysis experiments using a feedstock of polypropylene plastic. According to literature, pyrolysis runs were implemented at temperatures ranging from 500°C to 800°C. Nitrogen gas was used to inert the atmosphere. Initially, uncatalysed experiments were performed. Thereafter, ZSM-5 catalyst was utilized in the pyrolysis experiments.

Chemical recycling of plastics by fluidized bed pyrolysis (Kaminsky, 2021b)

Kaminsky et al., (2021) provided emission data from various fluidized bed plastic pyrolysis experiments using polyethylene, polypropylene, mixed plastics, and a mixture of polyethylene and polypropylene. In many cases, nitrogen was used to inert the atmosphere. The mixed plastic (denoted as plastic B) contained 65 wt % polyolefin, 25 wt % PS, 1.2 wt % PVC, 1.5 wt % PET. The review was performed for a wide range of process temperatures. Data such as product yields and product gas compositions were extracted from the literature.

Pyrolysis of Mixed Plastic Wastes for the Recovery of Benzene, Toluene, and Xylene (BTX) Aromatics in a Fluidized Bed and Chlorine Removal by Applying Various Additives (Cho et al., 2010)

In the work of Cho et al., (2010), pyrolysis experiments were implemented in a fluidized bed reactor. The feed plastic was composed of polyethylene, polypropylene, polystyrene, PMMA, and PET. The pyrolysis reaction temperatures ranged from 660°C to 780°C. Various catalysts such as CaO and $Ca(OH)_2$ were used in the pyrolysis reactions. GC-MS was used to determine the composition of the gas phase product. Chemical analysis was also performed on the pyrolysis oil.